

# Portal Effective Theories

A framework for the model independent description  
of light hidden sector interactions

Chiara Arina<sup>\*a</sup>, Jan Hajer<sup>†a,b</sup>, and Philipp Klose<sup>‡a,c</sup>

<sup>a</sup>Centre for Cosmology, Particle Physics and Phenomenology,  
Université catholique de Louvain, Louvain-la-Neuve B-1348, Belgium

<sup>b</sup>Department of Physics, Universität Basel, Klingelbergstraße 82, CH-4056 Basel, Switzerland

<sup>c</sup>Albert Einstein Center for Fundamental Physics, Institute for Theoretical Physics,  
Universität Bern, Sidlerstraße 5, CH-3012 Bern, Switzerland

## Abstract

We present a framework for the construction of *portal effective theories* (PETs) that couple effective field theories of the Standard Model (SM) to light hidden messenger fields. Using this framework we construct electroweak and strong scale PETs that couple the SM to messengers carrying spin zero, one half, or one. The electroweak scale PETs encompass all portal operators up to dimension five, while the strong scale PETs additionally contain all portal operators of dimension six and seven that contribute at leading order to quark-flavour violating transitions. Using the strong scale PETs, we define a set of portal currents that couple hidden sectors to QCD, and construct portal chiral perturbation theories ( $\chi$ PTs) that relate these currents to the light pseudoscalar mesons. We estimate the coefficients of the portal  $\chi$ PT Lagrangian that are not fixed by SM observations using non-perturbative matching techniques and give a complete list of the resulting one- and two-meson portal interactions. From those, we compute transition amplitudes for three golden channels that are used in hidden sector searches at fixed target experiments: i) charged kaon decay into a charged pion and a spin zero messenger, ii) charged kaon decay into a charged lepton and a spin one half messenger, and iii) neutral pion decay into a photon and a spin one messenger. Finally, we compare these amplitudes to specific expressions for models featuring light scalar particles, axion-like particles, heavy neutral leptons, and dark photons.

---

\*chiara.arina@uclouvain.be

†jan.hajer@unibas.ch

‡pklose@itp.unibe.ch

# Contents

<b>1</b>	<b>Introduction</b>	<b>6</b>
<b>2</b>	<b>Quantum chromodynamics</b>	<b>10</b>
2.1	Electroweak interactions . . . . .	14
2.2	Flavour symmetry . . . . .	19
2.3	Four-quark operators . . . . .	20
<b>3</b>	<b>Portal interactions between the SM and hidden sectors</b>	<b>22</b>
3.1	Portal effective theories . . . . .	22
3.1.1	Power counting . . . . .	23
3.1.2	Mixing between SM and messengers fields . . . . .	24
3.2	Electroweak scale portal effective theories . . . . .	24
3.2.1	Minimal bases of portal operators . . . . .	24
3.2.2	External current description . . . . .	26
3.2.3	Electroweak symmetry breaking . . . . .	28
3.3	Portals at the strong scale . . . . .	29
3.3.1	Operator list . . . . .	31
3.3.2	QCD portal currents . . . . .	35
<b>4</b>	<b>Chiral perturbation theory</b>	<b>38</b>
4.1	Flavour symmetry . . . . .	40
4.2	Power counting . . . . .	41
4.3	Construction of the portal $\chi$ PT Lagrangian . . . . .	43
4.3.1	Weak current contributions . . . . .	48
4.3.2	Flavour-singlet current contributions . . . . .	50
4.3.3	Stress-energy tensor . . . . .	51
4.4	Matching of $\chi$ PT to QCD . . . . .	52
4.4.1	Scale dependence of the external currents . . . . .	53
4.4.2	$\chi$ PT realizations of QCD operators . . . . .	54
4.4.3	Determination of selected parameters . . . . .	57
4.5	Transition to the physical vacuum . . . . .	62
4.6	Expanded Lagrangian . . . . .	63
<b>5</b>	<b>Portal interactions of the light pseudoscalar mesons</b>	<b>67</b>
5.1	One- and two-meson interactions . . . . .	67
5.2	Flavour-blind hidden sectors . . . . .	73
<b>6</b>	<b>Meson interactions of hidden sector models</b>	<b>78</b>
6.1	Charged kaon decay to charged pions and hidden scalars . . . . .	79
6.1.1	Single scalar portal current contributions . . . . .	79
6.1.2	Relevant interactions . . . . .	80
6.1.3	Partial decay width . . . . .	82
6.1.4	Flavour-blind hidden sectors . . . . .	83
6.1.5	Explicit portal currents for specific hidden sector models . . . . .	84

6.2	Charged kaon decay to charged leptons and hidden fermions . . . . .	89
6.2.1	Relevant interactions . . . . .	89
6.2.2	Partial decay width . . . . .	90
6.2.3	Explicit portal currents for specific hidden sector models . . . . .	90
6.3	Neutral pion decay to photons and hidden vectors . . . . .	91
6.3.1	Relevant portal current contributions . . . . .	91
6.3.2	Partial decay width . . . . .	92
6.3.3	Explicit portal currents for specific hidden sector models . . . . .	93
<b>7</b>	<b>Conclusion</b>	<b>93</b>
<b>A</b>	<b>Construction of portal effective theories</b>	<b>97</b>
A.1	Naive dimensional analysis . . . . .	97
A.2	Reduction techniques . . . . .	98
A.3	Standard Model equations of motions . . . . .	100
A.3.1	EOMs at the electroweak scale . . . . .	100
A.3.2	EOMs at the strong scale . . . . .	100
A.3.3	Quark EOM including external currents . . . . .	101
<b>B</b>	<b>Electroweak scale portal operators</b>	<b>102</b>
B.1	Redundant portal operators with messenger field up to spin one . . . . .	102
B.2	Rarita-Schwinger and Fierz-Pauli fields . . . . .	103
<b>C</b>	<b>Portal operators at the strong scale</b>	<b>104</b>
C.1	Scalar portal . . . . .	105
C.2	Fermionic portal . . . . .	106
C.3	Vector portal . . . . .	107
<b>D</b>	<b>Expansion of the <math>\chi</math>PT building blocks</b>	<b>108</b>
D.1	Standard model meson phenomenology at NLO . . . . .	109
D.2	Mixing between mesons and scalar messengers . . . . .	112
D.3	Trilinear Standard Model vertices used in the $K^\pm \rightarrow \pi^\pm s_i$ decay . . . . .	113

## List of Figures

1	The PET framework . . . . .	7
2	Procedure to derive the PET Lagrangian coupling mesons to messengers . . . .	9
3	Feynman diagrams describing charged current and magnetic-dipole interactions	15
4	Feynman diagrams describing four-quark interactions . . . . .	17
5	Large $n_c$ scaling of four-quark operators . . . . .	18
6	The two possible types of strong scale quark-flavour violating diagrams . . . .	29
7	One-loop portal Feynman diagrams . . . . .	33
8	Quantum numbers of the light scalar meson nonet . . . . .	39
9	Energy scales appearing in portal $\chi^{\text{PT}}$ . . . . .	48
10	Feynman diagrams for the $K^\pm \rightarrow \pi^\pm s_i$ process. . . . .	80
11	Feynman diagrams for the $K^\pm \rightarrow \ell^\pm \xi_a$ process. . . . .	89
12	Feynman diagram for the $\pi^0 \rightarrow \gamma v^\mu$ process. . . . .	91

## List of Tables

1	Colour singlets and quark multilinears . . . . .	22
2	Portal SMEFT operators involving messengers with spin 0, $1/2$ , and 1 . . . . .	25
3	Portal SMEFT currents . . . . .	26
4	Leading portal LEFT operators . . . . .	31
5	Subleading portal LEFT operators . . . . .	32
6	Portal LEFT currents . . . . .	37
7	Small parameters appearing in portal $\chi^{\text{PT}}$ . . . . .	41
8	Impact of flavour traces on the $\delta$ -counting of an operator. . . . .	43
9	NDA and large $n_c$ scaling of selected coefficients . . . . .	47
10	Four-quark currents and parameters . . . . .	49
11	Order in $\delta$ at which we evaluate the LERs . . . . .	55
12	Portal SMEFT operators involving messengers with spin $3/2$ and 2 . . . . .	103

## List of Acronyms

**ALP** axion-like particle

**BSM** beyond the Standard Model

**CKM** Cabibbo-Kobayashi-Maskawa

**$\chi$ PT** chiral perturbation theory

**CS** Chern-Simons

**DM** dark matter

**DOF** degree of freedom

**EFT** effective field theory

**EM** electromagnetic

**EOM** equation of motion

**EW** electroweak

**EWSB** electroweak symmetry breaking

**GD** gluon dynamics

**GM** Gell-Mann

**HEFT** Higgs effective field theory

**HNL** heavy neutral lepton

**HQET** heavy quark effective theory

**LEC** low energy coefficient

**LEFT** light effective field theory

**LER** low energy realisation

**LHC** Large Hadron Collider

**LO** leading order

**MC** Maurer-Cartan

**$\overline{\text{MS}}$**  modified minimal subtraction

**NDA** naive dimensional analysis

**NGB** Nambu-Goldstone boson

**NLO** next-to-leading order

**NNLO** next-to-next-to-leading order

**NP** new physics

**NRQCD** non-relativistic quantum chromo-  
dynamics

**PET** *portal effective theory*

**PI** partial integration

**PNGB** pseudo Nambu-Goldstone boson

**QCD** quantum chromodynamics

**QED** quantum electrodynamics

**SCET** soft-collinear effective theory

**SM** Standard Model

**SMEFT** Standard Model effective field the-  
ory

**SUSY** supersymmetry

**2HDM** two Higgs-doublet model

**UV** ultraviolet

**VEV** vacuum expectation value

**WZW** Wess-Zumino-Witten

**YM** Yang-Mills

# 1 Introduction

The search for physics beyond the Standard Model (BSM) is one of the most pursued research avenues in modern high-energy physics. Models of BSM physics can be constructed from the top down by postulating a novel set of first principles, as *e.g.* in grand unified [1–3] or supersymmetric [4–7] theories, or from the bottom up by augmenting the SM with new particles and interactions that address specific hints for BSM physics, such as *e.g.* heavy neutral leptons (HNLs) generating neutrino masses [8–15], axions addressing the strong CP problem [16–20] or little Higgs models addressing the hierarchy problem [21–24]. The new particles predicted in both approaches are constrained to be relatively heavy or rather weakly coupled in order to be consistent with bounds from past and current collider and intensity experiments, respectively.

Effective field theories (EFTs) describe physics at a specific energy scale, with the impact of physics at other scales being contained within the free parameters of the theory [25, 26]. They can be used to describe the impact of new physics (NP) at energy scales well above the characteristic energy scale of the EFT while remaining agnostic about the specific realisation of NP in nature. EFTs are constructed by identifying the relevant fields and symmetries that determine the physics one intends to characterise. The theory then contains all available operators constructed from these fields. In particular, EFTs typically contain an infinite tower of higher dimensional, non-renormalisable operators that capture the impact of the heavy degrees of freedom (DOFs). At the electroweak (EW) scale, there are two EFTs that encompass the entire SM and that are commonly used to include heavy NP [27]: Standard Model effective field theory (SMEFT), which is composed of all the SM fields including the Higgs doublet and restricted by the SM gauge group [28–32], and Higgs effective field theory (HEFT), which lifts the restriction on the Higgs boson to be part of a doublet [33–36]. EFTs at lower energies, which encompass only a part of the SM, account for the impact of the heavy SM DOFs via their higher dimensional operators. Examples include light effective field theory (LEFT), which describes the interactions of the SM after integrating out its heavy particles [37–40],  $\chi$ PT, which encompasses the interactions of light hadrons [41–47], heavy quark effective theory (HQET) [48–53] and non-relativistic quantum chromodynamics (NRQCD) [54, 55], which capture the interactions of the hadrons containing heavy quarks, and soft-collinear effective theory (SCET), which describes physics of highly energetic particles, appearing for instance in jets [56–62].

These EFTs do not include the large class of SM extensions that feature new feebly interacting particles, such as axion-like particles (ALPs), light scalar particles, dilatons, HNLs, and novel gauge bosons, with masses at or below the energy scale of the EFT. In this paper, we address this gap by developing a framework for constructing PETs, which couple SM DOFs to light hidden messenger particles. To satisfy all existing experimental bounds, see *e.g.* [63–65], the latter can couple only very weakly to the SM fields. Besides the high intensity data sets of CMS [66–68], ATLAS [69] and LHCb [70–76], and the high luminosity runs of the Large Hadron Collider (LHC) [77], which are optimised for such searches, these particles could be produced in large quantities via meson decays in fixed target experiments such as NA62 [78–84], KOTO [85], SeaQuest [86], or SHiP [63]. If the messenger particles are unstable and decay predominantly into SM particles via the suppressed portal interactions, they are long-lived and can also be searched for in dedicated long-lived particle experiments [87], such as MATHUSLA [88], FASER [89] and CODEX-b [90].

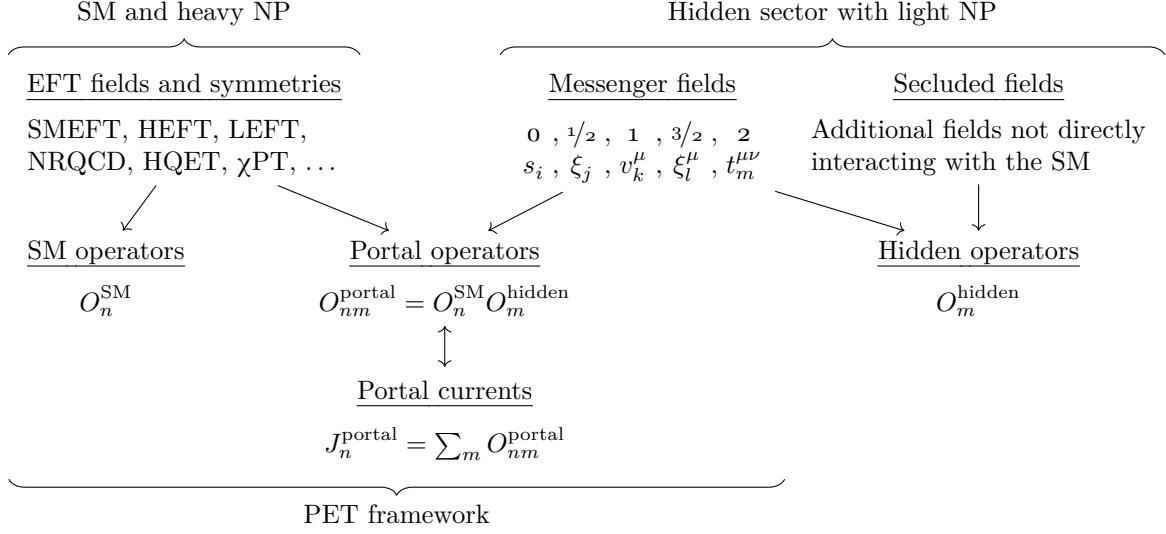


Figure 1: The PET framework extends a given EFT of the SM by combining its operators with portal operators that couple the SM DOFs to messenger fields that are dynamic at the relevant energy scale. The portal operators  $O_{nm}^{\text{portal}}$  can be collected into a set of portal currents  $J_n^{\text{portal}}$  that allow for a spurion analysis and for *e.g.* model-independent bounds. Here  $n$  and  $m$  symbolically label SM and hidden sector operators, respectively, so that  $\mathcal{L}_{\text{portal}} = O_n^{\text{SM}} J_n^{\text{portal}}$ . The PET framework is independent from additional secluded particles that do not interact directly with the SM fields.

By extending the existing EFTs of the SM, the PETs encompass all portal operators that conform with the symmetries of the relevant EFT, and can be used to constrain the coupling of the SM to light hidden sectors while remaining largely agnostic about the internal structure of the hidden sector. The hidden sector can in general contain an arbitrary number of secluded fields that do not couple directly to the SM but interact among themselves and with the messenger fields. This setup, which is illustrated in figure 1, describes both heavy and light new particles, since heavy particles with masses well above the characteristic energy of the EFT are captured by infinite towers of SM, portal, and hidden operators. Our comprehensive approach builds on previous works, in which SM particles are coupled to specific hidden particles, see *e.g.* [91–95], and is closely related to EFTs describing non-relativistic dark matter (DM) interactions [96–104].

To demonstrate the power of the PET framework, we construct a number of PETs and highlight the connections between them. Extending SMEFT, we first construct EW scale PETs that couple the SM to a light messenger field of spin  $0, 1/2$ , or  $1$  and encompass all available non-redundant portal operators up to dimension five. To connect these portal SMEFTs to PETs that describe the interactions of hidden fields at the strong scale, where many high intensity experiments search for feebly interacting particles, we subsequently construct portal LEFTs, which additionally encompass quark-flavour violating portal operators up to dimension seven. These additional operators capture leading order (LO) contributions to hidden sector induced, strangeness-violating kaon decays. Since the perturbative description of quantum chromodynamics (QCD) breaks down at low energies, it is not possible to compute transition amplitudes for meson decays using standard perturbative methods in QCD, however,  $\chi$ PT

provides an appropriate framework. In order to supply a complete toolkit for the computation of hidden sector induced meson transitions, we construct portal  $\chi$ PTs, which couple the light pseudoscalar mesons to a messenger of spin 0,  $1/2$ , or 1, and match them to the corresponding portal LEFTs. For this matching, we adapt to our framework a number of well-established non-perturbative techniques used to match  $\chi$ PT to QCD in the SM, as in *e.g.* [105–112].

Throughout this work, we encode the coupling to hidden sectors in terms of external currents, as depicted in figure 1. We use these currents to derive the coupling of  $\chi$ PT with the messenger particles via a spurion analysis, where we require that the  $\chi$ PT path integral changes like the QCD path integral under transformations of the external currents. Besides simplifying the spurion analysis, the external current approach has two advantages: First, it clarifies the discussion, as most of our work is independent of the specific content of the external currents. Second, this formulation makes it easier to generalise our framework. For instance, inclusive amplitudes do not encode any detailed information about the individual hidden sector particles. Therefore, we expect that, when computing such amplitudes, it is possible to integrate out the hidden fields entirely. In the resulting effective theory, the impact of hidden sectors would be encoded via an infinite tower of external current interactions, where the currents are space-time dependent functions of hidden sector parameters rather than being functionals of the hidden fields. These currents can then serve as a source or drain of energy, angular momentum, or other conserved quantum numbers, which, after matching the effective theory to the full theory, should exactly mimic the impact of the hidden sector fields on inclusive scattering amplitudes.<sup>1</sup> This means that the currents could be used to efficiently parameterise and therefore constrain the coupling to arbitrary hidden sectors in an extremely model independent way.

## Organisation and novel contributions

Figure 2 visualises the structure of this paper, which is organised as follows. In section 2, we summarise aspects of QCD at low energies that are pertinent to the discussion in the remainder of this work. In particular, we focus on the axial anomaly, the large  $n_c$  expansion, and the impact of higher dimensional operators that result from integrating out the heavy SM particles. We use the readers familiarity with the topic to introduce a notation that lends itself to the transition from QCD to  $\chi$ PT. In section 3, we construct portal SMEFTs and LEFTs that couple the SM to a single messenger field. Furthermore, we construct the corresponding hidden currents and specify the interaction Lagrangian that couples the currents to the SM fields. In section 4, we use the external current approach to derive the coupling of  $\chi$ PT to hidden sectors captured by the portal LEFTs. In section 5, we list the  $\chi$ PT portal interactions in terms of mesons and hidden fields, starting from the  $\chi$ PT Lagrangian derived in section 4. In section 6, we use the interactions derived in the previous section to compute smoking gun processes for meson decays into hidden fields, which are relevant for intensity experiments such as NA62 and KOTO. We additionally connect our results to characteristic BSM models, such as ALPs, scalar portal models, HNLs and dark photons. Section 7 concludes the paper with a discussion of the results and an outlook to prospective future work. Further details about the derivation of the main results of this paper are given in appendices A to D.

---

<sup>1</sup> This approach is inspired by a technique from non-equilibrium quantum field theory, where the impact of an external bath is captured by the von Neumann density matrix in the path integral, see *e.g.* [Section 3.2 in 113], and this density matrix can be recast as an infinite tower of external current interactions.



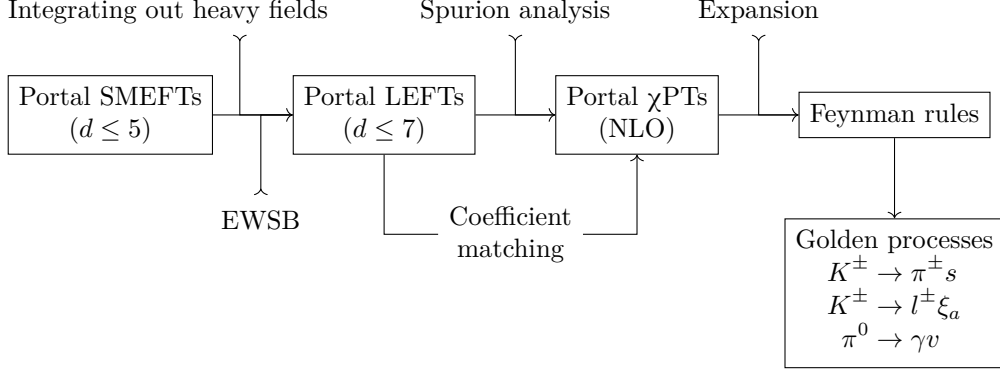


Figure 2: Overview of our procedure to derive the PET Lagrangian that couples the light mesons to messengers of spin 0,  $1/2$ , or 1. In the final step, we apply the Feynman rules extracted from the portal Lagrangian to compute universal amplitudes for the three golden processes.

In the following list we summarise the main new results that we present throughout this paper.

## Section 2

- We generalise the standard large  $n_c$  counting formula to also capture diagrams that contain higher-dimensional four-quark operators generated by virtual  $W$ -boson exchanges at the EW scale.
- We construct an alternative basis for the four-quark operators that contains four independent octet operators and one 27-plet operator. Compared to the standard basis, *cf.* (2.36), which consists of six operators, this basis simplifies the matching between  $\chi$ PT and QCD.

## Section 3

- We develop the PET framework and define the procedure for constructing general PETs.
- We construct EW scale PETs that couple SMEFT to a light messenger particle with spin 0,  $1/2$ , or 1, which is neutral under the unbroken SM gauge group  $G_{\text{SM}} = \text{SU}(3)_c \times \text{SU}(2)_L \times \text{U}(1)_Y$ . These PETs encompass all available portal operators up to dimension five, and are embedded into 21 portal currents. We further derive the shape of the EW portal Lagrangian after electroweak symmetry breaking (EWSB) in the unitary gauge, which is sufficient for computations at tree level.
- We construct strong scale PETs that couple LEFT to a light messenger particle with spin 0,  $1/2$ , or 1 that is neutral with respect to the broken SM gauge group  $G_{\text{sm}} = \text{SU}(3)_c \times \text{U}(1)_{\text{EM}}$ . These PETs contain all available portal operators up to dimension five and additionally encompass all LO quark-flavour violating portal operators up to dimension seven.
- We embed the portal LEFTs into ten external portal currents  $J \in \{S_\omega, \Theta, M, L^\mu, R^\mu, T^{\mu\nu}, \Gamma, \mathfrak{H}_s, \mathfrak{H}_l, \mathfrak{H}_r\}$  that parameterise the coupling of the messenger particles to QCD.

## Section 4

- We derive the coupling of  $\chi$ PT to the scalar current  $S_\omega$ . The SM does not contain an external current that couples to QCD like  $S_\omega$ , and hence this term is usually not included in SM  $\chi$ PT. Our result generalises the  $\chi$ PT Lagrangian in [106], where the authors derived the coupling of a light Higgs boson to  $\chi$ PT, which interacts with QCD via an operator  $hG_{\mu\nu}G^{\mu\nu}$  that is encompassed in  $S_\omega$ .
- Using the spurion technique, we derive the coupling of  $\chi$ PT to the four external currents  $\boldsymbol{\Gamma}$ ,  $\mathfrak{H}_l$ ,  $\mathfrak{H}_r$  and  $\mathfrak{H}_s$ . The coupling of  $\chi$ PT to *constant* currents  $\boldsymbol{\Gamma}$  and  $\mathfrak{H}_x$  is well-understood [42, 114–117]. Here, we generalise the description to account for *spacetime dependent* external currents.
- The EW sector of the portal  $\chi$ PT Lagrangian contains 27 coefficients  $\kappa$ , 21 of which are not fixed completely by SM observations. We estimate the two coefficients  $\kappa_\Gamma$  and  $\kappa_\Gamma^M + \kappa_\Gamma^{M'}$ , that measure the strength of the chromomagnetic current interactions, the seven coefficients  $\kappa_\omega^x$ , which measure the strength of the scalar current interactions, and the 13 coefficients  $\kappa_y^x$ , that measure the coupling of  $\chi$ PT to the hidden currents  $\boldsymbol{H}_x$  and  $\mathfrak{H}_x$ . The authors of [106] have estimated four out of the seven coefficients  $\kappa_\omega^x$ . Here, we adapt their strategy to also estimate the remaining three coefficients. Similarly, the coefficients  $\kappa_y^x$  are known in the large  $n_c$  limit [107, 108, 110–112]. Here, we adapt the strategies used in [106–108, 112] in order to obtain improved estimates for the  $\kappa_y^x$  that incorporate corrections beyond the large  $n_c$  limit.

## Section 5

- We expand the  $\chi$ PT Lagrangian in the meson matrix  $\boldsymbol{\Phi}$ , and present a complete list of one- and two-meson interactions that couple  $\chi$ PT to generic hidden sectors.

## Section 6

- We compute the most general LO transition amplitudes for three smoking-gun processes with hidden particles, relevant for searches at fixed target experiments such as NA62 and KOTO. Specifically, we consider the following meson decays:  $K^\pm \rightarrow \pi^\pm s_i$ ,  $K^\pm \rightarrow \ell^\pm \xi_a$ , and  $\pi^0 \rightarrow \gamma v$ , where  $s_i$ ,  $\xi$ , and  $v^\mu$  are a spin 0, spin  $1/2$ , and spin 1 hidden field, respectively.

## 2 Quantum chromodynamics

QCD is a  $SU(n_c)$  gauge theory, where  $n_c = 3$  is the number of colours. It depends on  $n_c^2 - 1 = 8$  gluons  $G_\mu$  as gauge fields and features  $n_f$  massive quark flavours  $f$ . Using the QCD gauge coupling  $g_s$ , we define the fine-structure constant and its inverse as

$$\alpha_s = \frac{g_s^2}{4\pi} , \quad \omega = \frac{2\pi}{\alpha_s} . \quad (2.1)$$

The inverse fine-structure constant  $\omega$  is the natural parameter for describing the dependence of the gauge coupling on the renormalisation scale  $\mu$ . In the modified minimal subtraction ( $\overline{\text{MS}}$ ) scheme, it obeys the particularly simple renormalization group equation [118, 119]

$$\frac{d\omega}{dt} = \beta_s , \quad \beta_s = \beta_0 + \mathcal{O}\left(\frac{1}{\omega}\right) , \quad \beta_0 = \frac{11}{3}n_c - \frac{2}{3}n_f , \quad (2.2)$$

where  $t = \ln \mu/\Lambda$  is the logarithm of the renormalisation scale, and  $\beta_0$  is the LO coefficient of the  $\beta$ -function. In this scheme, the heavier quark flavours have to be integrated out when they become inactive, so that  $n_f$  ranges from six above the top mass to three below the charm mass. At low energies, this prescription reveals an infrared divergence for the coupling strength at  $[120\text{--}128]^2$

$$A_{\text{QCD}}^{\overline{\text{MS}}}(\omega) = (343 \pm 12_{\text{lat}}) \text{ MeV} , \quad (2.3)$$

which invalidates the perturbative expansion in the gauge coupling. Working with  $\omega$  simplifies the inclusion of flavour invariant external currents introduced in section 3. For the same reason, it is also convenient to normalise the gluon fields such that the covariant quark derivative  $D^\mu = \partial^\mu - i G^\mu$  is independent of  $g_s$ . Then, the kinetic part of the QCD Lagrangian is

$$\mathcal{L}_Q^{\text{kin}} = \mathcal{L}_Q^\omega + i q^\dagger \not{D} q + i \bar{q} \not{D} \bar{q}^\dagger , \quad \mathcal{L}_Q^\omega = -\omega \Upsilon(x) , \quad \Upsilon(x) = (4\pi)^{-2} \langle G_{\mu\nu} G^{\mu\nu} \rangle_c , \quad (2.4)$$

where angle brackets  $\langle \circ \rangle_c$  indicate a trace in colour space, and the gauge singlet  $\Upsilon(x)$  is normalised such that the gauge coupling does not explicitly appear in the anomalous contribution to the trace of the improved stress-energy tensor  $\mathcal{T}$  introduced below. Following [appendix J of 129], we use two distinct left-handed Weyl fermions  $q$  and  $\bar{q}$  to describe each Dirac fermion  $(q, \bar{q}^\dagger)$ .<sup>3</sup> The kinetic Lagrangian is invariant under global flavour rotations

$$q_a \rightarrow \mathbf{V}_a^b q_b , \quad \bar{q}^{\dot{a}} \rightarrow \bar{q}^{\dot{b}} \bar{\mathbf{V}}_{\dot{b}}^{\dot{a}} , \quad (\mathbf{V}, \bar{\mathbf{V}}) \in G_{LR} = \text{U}(n_f)_L \times \text{U}(n_f)_R , \quad (2.5)$$

where  $n_f = 3$  is the number of active quark flavours below the charm mass and boldface symbols indicate matrices in flavour space. Lower (un-)dotted indices denote objects that transform as members of the fundamental representations of  $\text{U}(n_f)_L$  and  $\text{U}(n_f)_R$ , respectively, while upper indices denote objects that transform as members of the anti-fundamental representations.<sup>4</sup>

Various mechanisms, either spontaneously or explicitly, break the  $G_{LR}$  symmetry of the kinetic Lagrangian. First, the finite vacuum expectation values (VEVs) of the light and strange quark condensates [128, 130–137]

$$\Sigma_{\text{ud}} = -\frac{1}{2} \langle 0 | \bar{u}u + \bar{d}d | 0 \rangle_{2\text{GeV}}^{\overline{\text{MS}}} + \text{h.c.} = (272 \pm 5_{\text{lat}})^3 \text{ MeV}^3 , \quad (2.6a)$$

$$\Sigma_s = -\langle 0 | \bar{s}s | 0 \rangle_{2\text{GeV}}^{\overline{\text{MS}}} + \text{h.c.} = (296 \pm 11_{\text{lat}})^3 \text{ MeV}^3 , \quad (2.6b)$$

spontaneously break  $G_{LR}$  to the global vector symmetry  $G_V \cong \text{U}(n_f)_V$  by causing the QCD vacuum to change under the action of the axial quotient group  $\text{U}(n_f)_A \cong G_{LR}/G_V$ . In mass-independent renormalisation schemes, the ratio

$$\frac{\Sigma_s}{\Sigma_{\text{ud}}} = 1.29 \pm 0.16_{\text{lat}} \quad (2.7)$$

<sup>2</sup> We label the errors of quantities calculated on the lattice with the subscript *lat*.

<sup>3</sup> Note that the bar over the fermion does not denote a mathematical operation but is part of its definition.

<sup>4</sup> The index-notation is inspired by the (un-)dotted *Greek* indices used in supersymmetry (SUSY) to distinguish between left- and right-chiral *spinor* indices. In contrast to the SUSY notation, the *Latin* indices we use run over  $n_f$ -tuples in the (u, d, s) *flavour* space of QCD. We suppress flavour indices whenever the meaning is captured by the implicit boldface notation.

is scale independent [109, 138]. Second, the SM Higgs mechanism explicitly breaks the chiral symmetry by inducing the mass term

$$\mathcal{L}_Q^m = -\langle \mathbf{m} \mathbf{Q} \rangle_f + \text{h.c.} , \quad \mathbf{m} = \text{diag}(m_u, m_d, m_s, \dots) , \quad \mathbf{Q}_a^{\dot{a}} = q_a \bar{q}^{\dot{a}} , \quad (2.8)$$

where  $\langle \circ \rangle_f$  denotes a trace in flavour space and  $\mathbf{Q}$  is a scalar quark bilinear. The formulation of the mass term as a trace of matrices in flavour space is unusual in standard treatments of QCD, but it is convenient for understanding correspondences between QCD and  $\chi$ PT, and serves as preparation for the matching between these two theories, performed in section 4. Third, the axial anomaly explicitly breaks the global axial  $U(1)_A$  flavour symmetry that is part of  $U(n_f)_A$  [139–141]. In general, anomalies appear as a result of the transformation behaviour of the integration measure in the generating functional

$$\mathcal{Z}_Q[J] = \mathcal{N} \int \mathcal{D}\varphi \exp\left(i \int (\mathcal{L}_Q + O_i J_i) dx\right) , \quad (2.9)$$

where  $\varphi$  collectively denotes the QCD fields, the  $O_i$  are local, gauge-invariant operators composed of QCD fields, and the  $J_i$  are external currents. The axial anomaly is related to the topologically nontrivial vacuum structure of QCD, which also causes the existence of a further contribution to the QCD Lagrangian,

$$\mathcal{L}_Q^\theta = -\theta w(x) , \quad w = \frac{\langle \tilde{G}_{\mu\nu} G^{\mu\nu} \rangle_c}{(4\pi)^2} = \epsilon_{\mu\nu\rho\sigma} \frac{\partial^\mu \omega_0^{\nu\rho\sigma}}{(4\pi)^2} , \quad \omega_0^{\nu\rho\sigma} = \left\langle G^\nu G^{\rho\sigma} + \frac{2}{3} i G^\nu G^\rho G^\sigma \right\rangle_c , \quad (2.10)$$

where  $\tilde{G}_{\mu\nu} = \epsilon_{\mu\nu\rho\sigma} G^{\rho\sigma}/2$ , and  $\theta$  is the QCD vacuum angle [142, 143], which is experimentally constrained to be  $|\theta| \lesssim 10^{-10}$  [144]. Although the topological charge density  $w(x)$  is a total derivative of the three-dimensional Chern-Simons (CS) term  $\omega_0^{\nu\rho\sigma}(x)$ , its contribution to the QCD action does not vanish, since the gluon fields remain finite at spatial infinity for field configurations with finite winding number  $n_w = \int w(x) d^4x$  [145, 146]. The axial anomaly manifests itself as a shift of the vacuum angle that results from the transformation of the path integral measure  $\mathcal{D}\varphi$  under  $U(1)_A$  flavour rotations. The typical energy scale associated with such a shift is measured by the topological susceptibility [147, 148]

$$\chi = \frac{\langle 0 | n_w^2 | 0 \rangle}{V} = -i \int \langle 0 | T w(x) w(0) | 0 \rangle d^4x = (66 \pm 13_{\text{lat}})^4 \text{ MeV}^4 , \quad (2.11)$$

where  $V$  is a spacetime volume element and  $T$  is the time ordering operator. The quark contribution to the topological susceptibility is governed by their condensates (2.6) and masses (2.8) [149, 150],

$$\frac{1}{\chi} = \frac{1}{\chi_0} + \frac{\langle \mathbf{m}^{-1} \rangle_f}{\Sigma_0} , \quad \Sigma_0 = \Sigma_{\text{ud}}|_{m_{\text{ud}} \rightarrow 0} = \Sigma_{\text{s}}|_{m_{\text{s}} \rightarrow 0} , \quad (2.12)$$

where  $\chi_0$  is the ‘quenched’ topological susceptibility obtained in a pure Yang-Mills (YM) theory without quark fields, and  $\Sigma_0$  is the value of the quark condensates in the chiral limit. Besides the perturbative expansion in the fine-structure constant that breaks down in the vicinity of

the QCD scale (2.3), one may also expand QCD in powers of  $n_c^{-1}$  [151], which corresponds to a semi-classical expansion in an effective theory of weakly interacting mesons and glueballs. The axial anomaly (2.10) vanishes at zeroth order in the large  $n_c$  limit [152], which restores the otherwise badly broken  $U(n_f)_A$  flavour symmetry. Including higher orders, the effect of the axial anomaly is therefore suppressed by factors of  $n_c^{-1}$ .

The large  $n_c$  expansion is defined such that the value of the QCD scale, which depends on the product  $n_c \omega^{-1}$ , remains finite as  $n_c$  goes to infinity [151, 153–155]. Therefore, the  $n_c$  enhancement of diagrams with additional closed colour loops balances with the suppression due to additional powers of the coupling  $\omega^{-1} \propto n_c^{-1}$ , and it can be shown that connected diagrams can scale at most as  $n_c^2$ , while disconnected diagrams scale like the product of their connected subdiagrams. The leading connected diagrams do not contain any closed quark loops or QCD  $\theta$  angle insertions. Diagrams with  $n_q$  quark loops and  $n_\theta$  vacuum angle insertions scale at most as [151, 153–155]

$$n_c^{2-n_q-n_\theta} . \quad (2.13)$$

Since the leading connected diagrams scale with a positive power of  $n_c$ , correlation functions for operators that can be decomposed into multiple gauge singlets are dominated by contributions from disconnected diagrams. Hence, renormalised QCD correlation functions obey the large  $n_c$  factorization rule

$$\langle 0|O_i O_j|0\rangle = \langle 0|O_i|0\rangle \langle 0|O_j|0\rangle (1 + \mathcal{O}(n_c^{-1})) , \quad (2.14)$$

where the  $O_i$  are local colour singlets that cannot be decomposed further into other colour singlets. This ‘vacuum saturation hypothesis’ can be used to match certain QCD observables with their  $\chi$ PT counterparts.

In addition to the flavour symmetry, the classical theory associated with the kinetic Lagrangian (2.4) is conformally invariant. The generators of the conformal Poincaré group can be expressed via the Hilbert stress-energy tensor

$$\mathcal{T}^{\mu\nu} = 2 \frac{\partial \mathcal{L}}{\partial g_{\mu\nu}} - g^{\mu\nu} \mathcal{L} , \quad (2.15)$$

which is divergenceless, symmetric, and traceless in the case of conformal theories.<sup>5</sup> The conformal invariance of QCD is broken, at the classical level, by the masses of the quarks (2.8), and, at the quantum level, by the conformal anomaly associated with the running of the gauge coupling (2.2), as it introduces an additional mass scale. Consequently, both terms contribute to the trace of the Hilbert stress-energy tensor [157–160],

$$\mathcal{T}_Q = -\mathcal{L}_Q^m + \frac{\beta_s}{\omega} \mathcal{L}_Q^\omega = (\langle \mathbf{m} \mathbf{Q} \rangle_f + \text{h.c.}) - \beta_s \mathcal{Y}(x) . \quad (2.16)$$

Notably, the dependence on the inverse fine-structure constant  $\omega$  cancels in this expression. In section 4, we use this trace relation to express  $\mathcal{Y}(x)$  as a linear combination of  $\chi$ PT operators.

---

<sup>5</sup> The equally conserved canonical stress-energy tensor associated with the Noether current of spacetime translations is generically neither symmetric nor traceless for conformal theories. This shortcoming can be overcome by adding model dependent improvement terms [156], which then must result in the same expression as the Hilbert stress-energy tensor.

Loop corrections associated with the quark masses generate another contribution to the trace of the stress-energy tensor,

$$\gamma_m(\langle \mathbf{m} \mathbf{Q} \rangle_f + \text{h.c.}) , \quad (2.17)$$

where  $\gamma_m$  is the anomalous dimension of the SM quark masses. However, we do not keep track of this subleading contribution.

**Summary** The complete QCD Lagrangian without EW contributions is constructed by adding gauge fixing and ghost Lagrangians to the kinetic (2.4), mass (2.8), and axial anomaly (2.10) terms, so that

$$\mathcal{L}_Q = \mathcal{L}_Q^{\text{kin}} + \mathcal{L}_Q^m + \mathcal{L}_Q^\theta + \mathcal{L}_Q^\xi + \mathcal{L}_Q^{\text{ghost}} , \quad (2.18)$$

where, for covariant gauges,

$$\mathcal{L}_Q^\xi = \frac{1}{\xi} \langle (\partial_\mu G^\mu)^2 \rangle_c , \quad \mathcal{L}_Q^{\text{ghost}} = 2 \langle \partial_\mu \bar{c} D^\mu c \rangle_c , \quad (2.19)$$

with  $\xi$  being the gauge-fixing parameter while  $\bar{c}$  and  $c$  are the QCD ghost-fields.

## 2.1 Electroweak interactions

Besides the quarks and gluons, the SM at low energies contains an EW sector consisting of the photon field, the charged electron and muon fields, and the left-handed SM neutrino fields. QCD couples to the photons  $A^\mu$  via the left- and right-handed vector current interactions

$$\mathcal{L}_Q^v = -\langle I_A^\mu \mathbf{Q}_\mu \rangle_f - \langle \mathbf{r}_A^\mu \bar{\mathbf{Q}}_\mu \rangle_f , \quad \mathbf{r}_A^\mu = I_A^\mu = \mathbf{v}_A^\mu , \quad \mathbf{v}_A^\mu = e \mathbf{q} A^\mu , \quad (2.20)$$

where  $\mathbf{q} = \text{diag}(2, -1, -1)/3$  is the quark-charge matrix,

$$\mathbf{Q}^{\mu b}_a = q_a \sigma^\mu q^{b\dagger} , \quad \bar{\mathbf{Q}}^{\mu \dot{b}}_{\dot{a}} = \bar{q}_{\dot{a}}^\dagger \bar{\sigma}^\mu \bar{q}^{\dot{b}} , \quad (2.21)$$

are left- and right-handed vectorial quark bilinears, and sans-serif boldface font indicates traceless matrices. The electromagnetic (EM) currents are parity blind ( $\mathbf{v}_A^\mu = I_A^\mu = \mathbf{r}_A^\mu$ ), traceless, diagonal, and couple identically to the down and strange quarks,

$$\mathbf{v}_A^\mu = \text{diag}(\mathbf{v}_{Au}^\mu, \mathbf{v}_{Ad}^\mu, \mathbf{v}_{As}^\mu) , \quad \mathbf{v}_{Ad}^\mu = \mathbf{v}_{As}^\mu = -2\mathbf{v}_{Au}^\mu , \quad (2.22)$$

where individual fermion flavours are indicated by upright font. The split of the parity blind EM current into a left- and right-handed current simplifies the generalisation to other spin 1 currents. However, we will drop this distinction and use  $\mathbf{v}_A^\mu$  when considering the phenomenology of the hidden messengers in sections 5 and 6.

The impact of diagrams at the EW scale with virtual exchanges of the heavy SM fields that have been integrated out can be captured at the strong scale by introducing an infinite tower of higher dimensional operators. As their mass-dimensions are larger than four, these

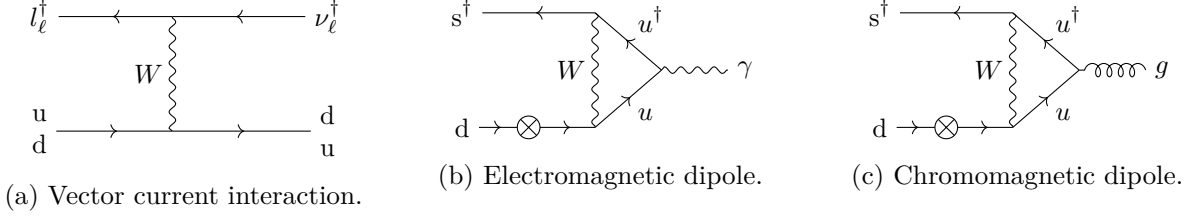


Figure 3: Processes that generate higher dimensional operators at the strong scale with two quarks. Panel (a) shows the tree level diagram that describes the charged current interaction (2.24). Panels (b) and (c) show the 1-loop photon and gluon diagrams that describe the dipole interactions (2.28). The cross indicates a mass insertion that can appear at either external fermion leg. Up type quarks are collectively denoted by  $u = u, c, t$ .

operators are suppressed by powers of<sup>6</sup>

$$\epsilon_{\text{SM}} = \frac{\partial^2}{\Lambda_{\text{SM}}^2}, \quad \partial^2 \lesssim m_c^2, \quad \Lambda_{\text{SM}} = 4\pi v, \quad (2.23)$$

which measures the ratio between the EW and low energy momentum scales, where  $v = (\sqrt{8}G_F)^{-1/2} = (174.10358 \pm 0.00004_{\text{exp}}) \text{ GeV}$  is the Higgs VEV [144].<sup>7</sup> Since the renormalisable strong and EM interactions conserve quark flavour, the higher dimensional operators contribute at LO to flavour violating processes such as kaon decays. LO transitions that violate flavour by one unit,  $\Delta f = \pm 1$ , are generated by operators with mass dimension five and six.

At tree level, the contribution depicted in figure 3a and its Hermitian conjugate induce the leptonic charged current interactions that couple quarks to charged leptons and neutrinos,

$$\mathcal{L}_Q^W = -\langle l_W^\mu \mathbf{Q}_\mu \rangle_f, \quad l_W^\mu = -v^{-2} (V_{ud} \lambda_u^d + V_{us} \lambda_u^s) \sum_{\ell=e,\mu} l_\ell^\dagger \bar{\sigma}^\mu \nu_\ell + \text{h.c.}, \quad (2.24)$$

where the  $V_{ij}$  are elements of the Cabibbo-Kobayashi-Maskawa (CKM) matrix. We use the matrices

$$\lambda_a^b, \quad (\lambda_a^b)_i^j = \delta_{ai} \delta^{bj} \quad (2.25)$$

to construct an orthonormal basis in flavour space. The weak leptonic charged current is traceless, Hermitian, and has no neutral contributions, so that

$$l_{Wu}^\mu = l_{Wd}^{\mu\dagger}, \quad l_{Ws}^\mu = l_{Ws}^{\mu\dagger}, \quad (2.26)$$

while all remaining entries vanish. In order to prepare for the inclusion of the portal current interactions in section 3, it is convenient to absorb the charged current interaction into the left-handed external current

$$l^\mu = l_A^\mu + l_W^\mu, \quad (2.27)$$

<sup>6</sup> The relevant operators in this paper are generated by contributions with virtual  $W$ -boson exchanges, so that they are suppressed by factors  $\partial^2 g_w^2 / m_W^2$  that involve the mass of the  $W$ -boson  $m_W$  rather than the Higgs VEV. We write the ratio of scales in terms of  $v^2 = 2m_W^2 / g_w^2$  to simplify the shape of the equations that appear throughout this paper.

<sup>7</sup> The subscript exp indicates an experimental error.

so that the vector current Lagrangian (2.20) accounts for both EM and weak charged current interactions.

At one-loop, the contributions depicted in figures 3b and 3c with a virtual  $W$ -boson exchange and a light quark mass insertion at one of the external legs further induce the electro- and chromomagnetic-dipole interactions between two quarks and a gauge boson [161]

$$\mathcal{L}_Q^\tau = -\Lambda_{\text{SM}}^{-2} \langle \boldsymbol{\tau}^{\mu\nu} \mathbf{Q}_{\mu\nu} \rangle_f + \text{h.c.} , \quad \mathcal{L}_Q^\gamma = -\Lambda_{\text{SM}}^{-2} \langle \boldsymbol{\gamma}_G \tilde{\mathbf{Q}} \rangle_f + \text{h.c.} , \quad (2.28)$$

where the tensorial and scalar quark bilinears are

$$\mathbf{Q}_{\mu\nu a}^{\dot{a}} = q_a \sigma_{\mu\nu} \bar{q}^{\dot{a}} , \quad \tilde{\mathbf{Q}}_a^{\dot{a}} = q_a \sigma_{\mu\nu} G^{\mu\nu} \bar{q}^{\dot{a}} . \quad (2.29)$$

The tensorial EM-dipole current and the scalar electro- and chromomagnetic-dipole currents are

$$\boldsymbol{\tau}^{\mu\nu} = \frac{1}{3} F^{\mu\nu} \boldsymbol{\gamma}_A , \quad \boldsymbol{\gamma}_V = m \left( \lambda_s^{\text{d}} \sum_{u=\text{u,c,t}} c_u^V V_{su}^\dagger V_{ud} + \text{h.c.} \right) , \quad (2.30)$$

where the indices  $V = G, A$  denote either gluon or photon contributions and the  $c_u^V$  are known Wilson coefficients [161]. In the following, we abbreviate the chromomagnetic-dipole current by  $\boldsymbol{\gamma} = \boldsymbol{\gamma}_G$ . The dipole currents are strangeness violating, but not necessarily Hermitian. The only nonvanishing contributions are

$$\boldsymbol{\gamma}_d^s , \quad \boldsymbol{\gamma}_s^{\text{d}} , \quad \boldsymbol{\tau}^{\mu\nu s}_{\text{d}} , \quad \boldsymbol{\tau}^{\mu\nu \text{d}}_s . \quad (2.31)$$

The operator  $\tilde{\mathbf{Q}}$  also has nonvanishing condensates

$$\Sigma_{G\text{ud}} = -\frac{1}{2} \langle 0 | \tilde{\mathbf{Q}}_{\text{u}}^{\text{u}} + \tilde{\mathbf{Q}}_{\text{d}}^{\text{d}} | 0 \rangle_{2\text{GeV}}^{\overline{\text{MS}}} + \text{h.c.} = (434 \pm 4_{\text{lat}})^5 \text{ MeV}^5 , \quad (2.32\text{a})$$

$$\Sigma_{Gs} = -\langle 0 | \tilde{\mathbf{Q}}_s^s | 0 \rangle_{2\text{GeV}}^{\overline{\text{MS}}} + \text{h.c.} = (425 \pm 14_{\text{lat}})^5 \text{ MeV}^5 , \quad (2.32\text{b})$$

which are estimated using QCD sum rules [162–165] or lattice computations [166].<sup>8</sup> Their ratios with the VEV of light quark condensate (2.6a) are

$$\frac{\Sigma_{G\text{ud}}}{\Sigma_{\text{ud}}} = (875 \pm 31_{\text{lat}})^2 \text{ MeV}^2 , \quad \frac{\Sigma_{Gs}}{\Sigma_s} = (731 \pm 73_{\text{lat}})^2 \text{ MeV}^2 . \quad (2.33)$$

Note that the ratio between the two quark-gluon condensates

$$\frac{\Sigma_{Gs}}{\Sigma_{G\text{ud}}} = 0.90 \pm 0.15_{\text{lat}} . \quad (2.34)$$

is consistent with one.





Figure 4: Processes that generate higher dimensional operators at the strong scale with four quarks. The tree level diagram (a) generates the operators  $O_1$  and  $O_2$  in (2.36a), while the penguin diagram in (b) generates the operators  $O_3$  to  $O_6$  in (2.36b) and (2.36c). Up-type quarks are collectively denoted by  $u = u, c, t$ .

**Four-quark interactions** The diagrams in figure 4 depict the contributions that generate four-quark interactions of the shape [167–170]

$$\mathcal{L}_Q^h = -\frac{V_{su}^\dagger V_{ud}}{v^2} \sum_{i=1}^6 c_i O_i + \text{h.c.} , \quad (2.35)$$

where  $|V_{su}^\dagger V_{ud}| = 0.2186 \pm 0.00008$  [144] and the  $c_i$  are known Wilson coefficients [161]. After neglecting EM penguin diagrams, which are suppressed by at least one power of  $\alpha_{\text{EM}}$ , there are six four-quark operators that violate quark-flavour by one unit [171],

$$O_1 = s^\dagger \bar{\sigma}^\mu u \ u^\dagger \bar{\sigma}_\mu d , \quad O_2 = s^\dagger \bar{\sigma}^\mu d \ u^\dagger \bar{\sigma}_\mu u , \quad (2.36a)$$

$$O_3 = s^\dagger \bar{\sigma}^\mu d \ q^\dagger \bar{\sigma}_\mu q , \quad O_4 = s^\dagger \bar{\sigma}^\mu q \ q^\dagger \bar{\sigma}_\mu d , \quad (2.36b)$$

$$O_5 = s^\dagger \bar{\sigma}^\mu d \ \bar{q} \sigma_\mu \bar{q}^\dagger , \quad O_6 = s^\dagger \bar{q}^\dagger \ \bar{q} d . \quad (2.36c)$$

Since these operators are necessarily neutral, they can only violate quark-flavour by mediating  $d \leftrightarrow s$  transitions and thereby violate strangeness,  $\Delta s = \pm 1$ . The operators  $O_1$  and  $O_2$  (2.36a) are generated by the tree-level diagram shown in figure 4a, while the operators  $O_3$  to  $O_6$  (2.36b) and (2.36c) are generated by one-loop penguin diagrams as shown in figure 4b. Although the penguin operators are suppressed by loop-factors, the operator  $O_6$  is enhanced at low energies due to chirality effects, so that it contributes at LO to certain transitions. For a more detailed discussion, see section 4.4. We organise the four-quark operators (2.36) according to their chirality structure into a scalar-scalar and two vector-vector interaction terms

$$\mathcal{L}_Q^h = -v^{-2} \left( \mathfrak{h}_{sab}^{\dot{a}b} Q_{\dot{a}}^{\dagger a} Q_b^{\dot{b}} + \mathfrak{h}_{raa}^{bb} Q_{\mu b}^a \bar{Q}^{\mu \dot{a}}_{\dot{b}} + \mathfrak{h}_{lac}^{bd} Q_{\mu b}^a Q^{\mu c}_d \right) , \quad (2.37)$$

where the parameters  $\mathfrak{h}_s$ ,  $\mathfrak{h}_r$ , and  $\mathfrak{h}$  are four-index tensors in flavour space, which we indicate using symbols in Fraktur font. Comparing this formulation of the four-quark Lagrangian with

<sup>8</sup> For simplicity, we indicate errors for values estimated using QCD sum rules with the same label as errors for values calculated on the lattice.

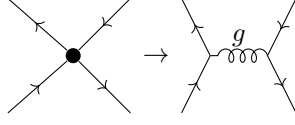


Figure 5: Replacement used to determine the number of closed colour loops in QCD diagrams with four-quark operators. Diagrams with a given number of four-quark vertices contain the same number of colour loops as diagrams where each four-quark vertex is replaced by the subdiagram with gluon exchange that is depicted on the right-hand side.

the operators listed in equation (2.36), the parameters are given as

$$\mathfrak{h}_s = V_{su}^\dagger V_{ud} c_6 \sum_{u=u,d,s} \lambda_s^u \otimes \lambda_u^d + \text{h.c.} , \quad \mathfrak{h}_r = V_{su}^\dagger V_{ud} c_5 \lambda_s^d \otimes \mathbf{1} + \text{h.c.} , \quad (2.38a)$$

$$\mathfrak{h}_l = V_{su}^\dagger V_{ud} \left( c_1 \lambda_s^u \otimes \lambda_u^d + c_2 \lambda_s^d \otimes \lambda_u^u + c_3 \lambda_s^d \otimes \mathbf{1} + c_4 \sum_{u=u,d,s} \lambda_s^u \otimes \lambda_u^d \right) + \text{h.c.} , \quad (2.38b)$$

where  $\otimes$  denotes a tensor product.

Connected diagrams with four-quark vertices in Lagrangian (2.37) are not included in standard derivations of the large  $n_c$  power counting rule (2.13) [151, 153, 155]. To generalise this counting rule to diagrams with a finite number of four-quark vertices, we use the replacement shown in figure 5 in order to map a given set of diagrams with four-quark vertices onto an equivalent set of pure QCD diagrams without four-quark vertices. This replacement is chosen such that the resulting diagram always contains the same number of closed colour loops as its corresponding original four-quark diagram. The overall large  $n_c$  scaling of the diagram differs from the scaling of the original diagram in two ways: First, the two three-point vertices in the pure QCD diagrams are associated with a total prefactor of  $\omega^{-1} \propto n_c^{-1}$ , whereas the four quark vertices scale as  $\omega^0 \propto 1$ , so that the four-quark diagrams are enhanced by one relative factor of  $n_c$  for each four-quark vertex. Second, the number of quark loops in the pure QCD diagrams can be lower than the number of quark loops in the original four-quark diagrams, even though both diagrams contain the same number of closed colour loops. Hence, the leading contribution to the infinite series of diagrams with exactly  $n_h$  four-quark insertions and an arbitrary number of colour loops is given by the subset for which the equivalent pure QCD diagram contains exactly one quark loop. Applying the standard counting formula (2.13), we find that the leading four-quark diagrams scale as

$$n_c^{1-n_\theta+n_h} , \quad n_h > 0 . \quad (2.39)$$

Further, the leading diagrams with  $n_h$  four-quark insertions, as well as  $n_q$  simple QCD quark loops *in addition* to the quark loops associated with the four-quark vertices, scale as

$$n_c^{1-n_q-n_\theta+n_h} , \quad n_h > 0 , \quad (2.40)$$

which extends the usual scaling behaviour (2.13).

**Summary** The EW interactions induce the EW correction to the QCD Lagrangian (2.18)

$$\mathcal{L}_Q^{\text{EW}} = \mathcal{L}_Q^\gamma + \mathcal{L}_Q^\tau + \mathcal{L}_Q^v + \mathcal{L}_Q^h , \quad (2.41)$$

which is given by the Lagrangians (2.20), (2.28), and (2.35), where Lagrangian (2.20) includes the full current (2.27). The EW interactions in Lagrangians (2.24), (2.28), and (2.35) also generate additional contributions to the trace of the Hilbert stress-energy tensor (2.16). After using the quark field equation of motion (EOM) in the presence of external currents in equation (A.23), the EW contribution becomes

$$\mathcal{T}_Q^{\text{EW}} = \mathcal{L}_Q^\gamma + \mathcal{L}_Q^\tau - \mathcal{L}_Q^W + 2\mathcal{L}_Q^h. \quad (2.42)$$

## 2.2 Flavour symmetry

Under the flavour symmetry (2.5) of the kinetic Lagrangian (2.4), the quark bilinears (2.8), (2.21), and (2.29) transform as

$$Q \rightarrow VQ\bar{V}, \quad Q_\mu \rightarrow VQ_\mu V^\dagger, \quad Q_{\mu\nu} \rightarrow VQ_{\mu\nu}\bar{V}, \quad (2.43a)$$

$$\tilde{Q} \rightarrow V\tilde{Q}\bar{V}, \quad \bar{Q}_\mu \rightarrow \bar{V}^\dagger \bar{Q}_\mu \bar{V}. \quad (2.43b)$$

As a consequence, the QCD path integral (2.9)

$$\mathcal{Z}_Q = \mathcal{Z}_Q[\omega, \theta, \mathbf{m}, \mathbf{l}^\mu, \mathbf{r}^\mu, \mathbf{h}, \boldsymbol{\tau}^{\mu\nu}, \mathfrak{h}_s, \mathfrak{h}_r, \mathfrak{h}_l], \quad (2.44)$$

is invariant under global  $G_{LR}$  flavour rotations that transform the external currents as<sup>9</sup>

$$\theta \rightarrow \theta - i\langle \ln V\bar{V} \rangle_f, \quad \mathbf{m} \rightarrow \bar{V}^\dagger \mathbf{m} V^\dagger, \quad \mathfrak{h}_{sac}^{bd} \rightarrow V_a^u \bar{V}_y^b \mathfrak{h}_{su\dot{x}}^{yv} \bar{V}_{\dot{c}}^{\dagger\dot{x}} V_v^{\dagger d}, \quad (2.45a)$$

$$\mathbf{l}^\mu \rightarrow V \mathbf{l}^\mu V^\dagger, \quad \boldsymbol{\gamma} \rightarrow \bar{V}^\dagger \boldsymbol{\gamma} V^\dagger, \quad \mathfrak{h}_{rac}^{bd} \rightarrow V_a^u V_v^{\dagger b} \mathfrak{h}_{ru\dot{x}}^{vy} \bar{V}_{\dot{c}}^{\dagger\dot{x}} \bar{V}_{\dot{y}}^d, \quad (2.45b)$$

$$\mathbf{r}^\mu \rightarrow \bar{V}^\dagger \mathbf{r}^\mu \bar{V}, \quad \boldsymbol{\tau}^{\mu\nu} \rightarrow \bar{V}^\dagger \boldsymbol{\tau}^{\mu\nu} V^\dagger, \quad \mathfrak{h}_{lac}^{bd} \rightarrow V_a^u V_v^{\dagger b} \mathfrak{h}_{lu\dot{x}}^{vy} V_c^x V_y^{\dagger d}. \quad (2.45c)$$

Remarkably, the path-integral is additionally invariant under *local* flavour rotations that transform the left- and right-handed currents in (2.20) as

$$\mathbf{l}^\mu \rightarrow V \mathbf{l}^\mu V^\dagger + i V \partial^\mu V^\dagger, \quad \mathbf{r}^\mu \rightarrow \bar{V}^\dagger \mathbf{r}^\mu \bar{V} + i \bar{V}^\dagger \partial^\mu \bar{V}, \quad (2.46)$$

while the transformation behaviour of the other external currents is unaltered. This transformation law is analogous to that of gauge fields. To facilitate the construction of operators that are invariant under the action of  $G_{LR}$ , it is convenient to define covariant derivatives for the quark fields

$$D^\mu q = \partial^\mu q - i \mathbf{l}^\mu q, \quad D^\mu \bar{q}^\dagger = \partial^\mu \bar{q}^\dagger - i \mathbf{r}^\mu \bar{q}^\dagger, \quad (2.47)$$

as well as field-strength tensors for the left- and right-handed currents

$$\mathbf{l}^{\mu\nu} = \partial^\mu \mathbf{l}^\nu - \partial^\nu \mathbf{l}^\mu - i [\mathbf{l}^\mu, \mathbf{l}^\nu], \quad \mathbf{r}^{\mu\nu} = \partial^\mu \mathbf{r}^\nu - \partial^\nu \mathbf{r}^\mu - i [\mathbf{r}^\mu, \mathbf{r}^\nu]. \quad (2.48)$$

While the symmetry of the path integral with respect to (2.46) corresponds mathematically to a gauge symmetry, it is important to emphasise that  $\mathbf{l}^\mu$  and  $\mathbf{r}^\mu$  are not fields in a physical sense. In particular, while a gauge symmetry relates different field configurations that correspond to the *same* physical state, the local  $G_{LR}$  symmetry relates field configurations that correspond to *different* physical states.

---

<sup>9</sup> Being a function of the gauge coupling only, the inverse fine-structure constant  $\omega$  is invariant under flavour rotations.

### 2.3 Four-quark operators

The four-quark operators in Lagrangian (2.37) transform as singlets under  $U(3)_R$  [115]. For this reason, we suppress the right-handed indices of the external currents, and define

$$\mathbf{h}_{sa}^d = \frac{1}{n_f} \mathfrak{h}_{sa\dot{c}}^{\dot{c}d}, \quad \mathbf{h}_{ra}^b = \frac{1}{n_f} \mathfrak{h}_{ra\dot{c}}^{b\dot{c}}, \quad (2.49)$$

where the reduced parameters  $\mathbf{h}_s$  and  $\mathbf{h}_r$  transform under  $U(3)_L$  as

$$\bar{3} \otimes 3 = 8 \oplus 1. \quad (2.50)$$

The traceless octet contributions are given as

$$\mathbf{h}_s = \mathbf{h}_s - \frac{1}{n_f} h_s, \quad \mathbf{h}_r = \mathbf{h}_r - \frac{1}{n_f} h_r, \quad (2.51)$$

where  $h_r = \langle \mathbf{h}_r \rangle_f$  and  $h_s = \langle \mathbf{h}_s \rangle_f$ . The corresponding left-handed, traceless octet operators composed of the quark bilinears (2.8) and (2.21) are

$$\mathcal{O}_s = \mathbf{Q}^\dagger \mathbf{Q} - \frac{1}{n_f} \langle \mathbf{Q}^\dagger \mathbf{Q} \rangle_f, \quad \mathcal{O}_r = \mathbf{Q}^\mu \bar{\mathbf{Q}}_\mu - \frac{1}{n_f} \mathbf{Q}^\mu \bar{\mathbf{Q}}_\mu, \quad (2.52)$$

where  $Q_\mu = \langle \mathbf{Q}_\mu \rangle_f$  and  $\bar{Q}_\mu = \langle \bar{\mathbf{Q}}_\mu \rangle_f$ .

The purely left-handed vector-vector interaction parameter  $\mathfrak{h}_{ac}^{bd}$  transforms under  $U(3)_L$  as a member of

$$(\bar{3} \otimes 3) \otimes (\bar{3} \otimes 3) = (8 \oplus 1) \otimes (8 \oplus 1) = \underbrace{8 \oplus 1}_{\text{totally antisymmetric}} \oplus \underbrace{(27 \oplus 8 \oplus 1)}_{\text{totally symmetric}} \oplus \underbrace{(\bar{10} \oplus 10 \oplus 8)}_{\text{mixed symmetric}} \oplus 8, \quad (2.53)$$

where the parenthesis on the outermost right-hand side indicate the decomposition of the  $8 \otimes 8$  product. Furthermore, the symmetry of each representation under exchanges of the quark bilinears and quark spinors is indicated by curly braces above and below the expression, respectively. Since  $\mathfrak{h} \mathbf{Q}_\mu \mathbf{Q}^\mu$  is symmetric under exchange of the quark bilinears, only representations that are totally (anti-)symmetric under exchanges of the quark spinors can contribute to  $\mathfrak{h}$ . Therefore, the parameter  $\mathfrak{h}_{ac}^{bd}$  can be written as

$$\mathbf{h}_l = \mathbf{h}_l^+ + \frac{1}{n_8^-} \mathbf{h}_l^- \wedge \mathbf{1} + \frac{1}{n_8^+} \mathbf{h}_l^+ \odot \mathbf{1} + \frac{1}{n_1^-} \mathbf{h}_l^- \mathbf{1} \wedge \mathbf{1} + \frac{1}{n_1^+} \mathbf{h}_l^+ \mathbf{1} \odot \mathbf{1}, \quad (2.54)$$

where  $\wedge$  and  $\odot$  are (anti-)symmetrised tensor products and the symmetry prefactors are

$$n_8^\pm = \frac{n_f \pm 2}{4}, \quad n_1^\pm = \frac{n_f^2 \pm n_f}{2}. \quad (2.55)$$

The totally (anti-)symmetric singlet  $\mathbf{h}_l^\pm$ , octet  $\mathbf{h}_l^\pm$ , and 27-plet  $\mathbf{h}_l^+$  contributions are related to the complete tensor via<sup>10</sup>

$$h_l^+ = \mathfrak{h}_{(xy)}^{(xy)}, \quad \mathbf{h}_{l\ a}^{+b} = \mathfrak{h}_{(ax)}^{(bx)} - \frac{1}{n_f} \mathbf{1}_a^b h_l^+, \quad \mathbf{h}_{l\ ac}^{+bd} = \mathfrak{h}_{(ac)}^{(bd)} - \frac{1}{n_8^+} \mathbf{1}_{(a}^b \mathbf{h}_{c)}^{+d} - \frac{1}{n_1^+} \mathbf{1}_{(a}^b \mathbf{1}_{c)}^d h_l^+, \quad (2.56a)$$

$$h_l^- = \mathfrak{h}_{[xy]}^{[xy]}, \quad \mathbf{h}_{l\ a}^{-b} = \mathfrak{h}_{[ax]}^{[bx]} - \frac{1}{n_f} \mathbf{1}_a^b h_l^-. \quad (2.56b)$$

<sup>10</sup> (Anti-)symmetrised tensors are defined as  $2T^{[\mu\nu]} = T^{\mu\nu} - T^{\nu\mu}$  and  $2T^{(\mu\nu)} = T^{\mu\nu} + T^{\nu\mu}$ , respectively.

The totally (anti-)symmetric octet operators formed by the two traceless pairings of two left-handed quark bilinears (2.21) related to the octet parameter  $\mathfrak{h}$  (2.56) are

$$\mathcal{O}_l^\pm = \frac{1}{2n_8^\pm} \left[ \left( \mathbf{Q}^\mu \mathbf{Q}_\mu - \frac{1}{n_f} \mathbf{Q}^\mu \mathbf{Q}_\mu \right) \pm \left( \mathbf{Q}^\mu \mathbf{Q}_\mu - \frac{1}{n_f} \langle \mathbf{Q}^\mu \mathbf{Q}_\mu \rangle_f \right) \right], \quad (2.57)$$

while the (symmetric) 27-plet combination is

$$\mathfrak{D}_l^+ = \mathbf{Q}^\mu \odot \mathbf{Q}_\mu - \mathbf{1} \odot \mathcal{O}_l^+ - \frac{1}{2n_1^+} (\mathbf{Q}^\mu \mathbf{Q}_\mu + \langle \mathbf{Q}^\mu \mathbf{Q}_\mu \rangle_f) \mathbf{1} \odot \mathbf{1}. \quad (2.58)$$

Hence, the complete octet and 27-plet contributions to the four-quark Lagrangian (2.37) are

$$\mathcal{L}_Q^h = -v^{-2} \langle \mathbf{h}_s \mathbf{O}_s + \mathbf{h}_r \mathbf{O}_r + \mathbf{h}_l^- \mathbf{O}_l^- + \mathbf{h}_l^+ \mathbf{O}_l^+ \rangle_f - v^{-2} \langle \langle \mathfrak{h}_l^+ \mathfrak{D}_l^+ \rangle \rangle_f, \quad (2.59)$$

where the brackets  $\langle \langle \rangle \rangle_f$  denote the complete contraction of the totally symmetric tensors. Using the symmetry properties of the 27-plet term

$$-\mathfrak{h}_{l\text{su}}^{+\text{du}} = (n_f - 1) \mathfrak{h}_{l\text{sd}}^{+\text{dd}} = (n_f - 1) \mathfrak{h}_{l\text{ss}}^{+\text{ds}}, \quad -\mathfrak{D}_{l\text{su}}^{+\text{du}} = \mathfrak{D}_{l\text{sd}}^{+\text{dd}} + \mathfrak{D}_{l\text{ss}}^{+\text{ds}}, \quad (2.60)$$

the strangeness violating contributions listed in (2.36) can be extracted via

$$\mathcal{L}_Q^h|_{\Delta s=\pm 1} = -\frac{1}{v^2} (\mathbf{h}_{ss}^{\text{d}} \mathbf{O}_{sd}^{\text{s}} + \mathbf{h}_{rs}^{\text{d}} \mathbf{O}_{rd}^{\text{s}} + \mathbf{h}_l^{-\text{d}} \mathbf{O}_{l\text{d}}^{-\text{s}} + \mathbf{h}_l^{+\text{d}} \mathbf{O}_{l\text{d}}^{+\text{s}}) - 2 \frac{n_{27}}{v^2} \mathfrak{h}_{l\text{su}}^{+\text{du}} \mathfrak{D}_{l\text{du}}^{+\text{su}} + \text{h.c.}, \quad (2.61)$$

where the 27-plet symmetry prefactor is

$$n_{27} = \frac{2n_f - 1}{n_f - 1}. \quad (2.62)$$

In terms of the coefficients in Lagrangian (2.35) the octet and 27-plet coefficients are

$$\mathbf{h}_{l\text{s}}^{+\text{d}} = \frac{1}{4} V_{\text{su}}^\dagger V_{\text{ud}} (c_{12}^+ + (n_f + 2) c_{34}^+), \quad \mathbf{h}_{rs}^{\text{d}} = V_{\text{su}}^\dagger V_{\text{ud}} c_5, \quad \mathfrak{h}_{l\text{su}}^{+\text{du}} = \frac{1}{4} V_{\text{su}}^\dagger V_{\text{ud}} \frac{n_f + 1}{n_f + 2} c_{12}^+, \quad (2.63a)$$

$$\mathbf{h}_{l\text{s}}^{-\text{d}} = -\frac{1}{4} V_{\text{su}}^\dagger V_{\text{ud}} (c_{12}^- + c_{34}^-), \quad \mathbf{h}_{ss}^{\text{d}} = V_{\text{su}}^\dagger V_{\text{ud}} c_6, \quad c_{l\kappa}^\pm = c_l \pm c_\kappa. \quad (2.63b)$$

**Summary** The QCD Lagrangian at the strong scale can be written in the compact form

$$\begin{aligned} \mathcal{L}_Q = & \theta w - \omega \Upsilon - \langle (\mathbf{m} \mathbf{Q} + \text{h.c.}) + \mathbf{l}^\mu \mathbf{Q}_\mu + \mathbf{r}^\mu \overline{\mathbf{Q}}_\mu \rangle_f - \Lambda_{\text{SM}}^{-2} \langle \boldsymbol{\gamma} \tilde{\mathbf{Q}} + \boldsymbol{\tau}^{\mu\nu} \mathbf{Q}_{\mu\nu} + \text{h.c.} \rangle_f \\ & - v^{-2} \langle \mathbf{h}_s \mathbf{O}_s + \mathbf{h}_r \mathbf{O}_r + \mathbf{h}_l^- \mathbf{O}_l^- + \mathbf{h}_l^+ \mathbf{O}_l^+ \rangle_f - v^{-2} \langle \langle \mathfrak{h}_l^+ \mathfrak{D}_l^+ \rangle \rangle_f, \end{aligned} \quad (2.64)$$

where the gluon contributions are defined in (2.4) and (2.10), the nonet contributions are defined in (2.8), (2.21), and (2.29), the octet contributions are defined in (2.51) and (2.57), and the 27-plet contribution is defined in (2.58). All operators are also listed in table 1. Finally, the complete trace of the Hilbert stress-energy tensor (2.15) that includes both strong and EW contributions is

$$\begin{aligned} \mathcal{T}_Q = & \frac{\beta_s}{\omega} \mathcal{L}_Q^\omega - \mathcal{L}_Q^m + \mathcal{L}_Q^\tau + \mathcal{L}_Q^\gamma - \mathcal{L}_Q^W + 2\mathcal{L}_Q^h \\ = & -\beta_s \Upsilon(x) + \langle (\mathbf{m} \mathbf{Q} + \text{h.c.}) + \mathbf{l}_W^\mu \mathbf{Q}_\mu \rangle_f - \Lambda_{\text{SM}}^{-2} \langle \boldsymbol{\gamma} \tilde{\mathbf{Q}} + \boldsymbol{\tau}^{\mu\nu} \mathbf{Q}_{\mu\nu} + \text{h.c.} \rangle_f \\ & - 2v^{-2} \langle \mathbf{h}_s \mathbf{O}_s + \mathbf{h}_r \mathbf{O}_r + \mathbf{h}_l^- \mathbf{O}_l^- + \mathbf{h}_l^+ \mathbf{O}_l^+ \rangle_f - v^{-2} \langle \langle \mathfrak{h}_l^+ \mathfrak{D}_l^+ \rangle \rangle_f. \end{aligned} \quad (2.65)$$

	$\mathcal{V}$	$w$	$Q$	$Q_\mu$	$\bar{Q}_\mu$	$Q_{\mu\nu}$	$\tilde{Q}$	$O_s$	$O_r$	$O_l^-$	$O_l^+$	$\mathfrak{O}_l^+$
$\epsilon_{\text{SM}}$	0			1								
$d$	4		3			3	5		6			6
representation	1		$8 \oplus 1$			$8 \oplus 1$			8			27

Table 1: Colour singlets and quark multilinear operators at the strong scale. For each of them, we show respectively their order in  $\epsilon_{\text{SM}}$ , their mass dimension  $d$  and their flavour representation. The composite gluon operators  $\mathcal{V}$  and  $w$  are defined in (2.4) and (2.10), the quark bilinears  $Q$  are defined in (2.8), (2.21), and (2.29), and the quark quadrilinears  $O$  and  $\mathfrak{O}$  are defined in (2.51), (2.57), and (2.58). The corresponding external currents including their SM and BSM contribution are listed in table 6.

### 3 Portal interactions between the SM and hidden sectors

In this section, we present a framework for the construction of general *portal effective theories* (PETs), and use it to construct EW and strong scale PETs that couple SMEFT and LEFT to a light messenger of spin 0,  $1/2$ , or 1. The portal SMEFTs comprise all independent portal operators up to dimension five, and the portal LEFTs additionally encompass quark-flavour violating portal operators of dimension six and seven. The latter are necessary to capture quark-flavour violating transitions, which govern for instance hadronic kaon decays. We use the accidental symmetries of the portal SMEFTs to further constrain the shape of the corresponding portal LEFTs, so that these PETs should be understood as the low energy limit of the portal SMEFTs, in which the heavy SM DOFs have been integrated out.

For completeness, we provide in appendix B.2 a basis of independent portal operators with dimension five or less that couple SMEFT to hidden particles with spin  $3/2$  and 2.

#### 3.1 Portal effective theories

A PET is an EFT that couples SM DOFs to hidden sectors via messenger fields. The framework we present is generic and can be used to construct PETs by starting from any EFT that either encompasses or is derived from the SM, such as SMEFT, HEFT, LEFT, HQET, or  $\chi$ PT. The PET Lagrangian can be cast as

$$\mathcal{L} = \mathcal{L}_{\text{EFT}} + \mathcal{L}_{\text{portal}} + \mathcal{L}_{\text{hidden}} , \quad (3.1)$$

where the original EFT Lagrangian  $\mathcal{L}_{\text{EFT}}$  and the hidden Lagrangian  $\mathcal{L}_{\text{hidden}}$  depend only on SM and hidden fields, respectively. The portal Lagrangian  $\mathcal{L}_{\text{portal}}$  contains all available operators that couple the SM fields to the hidden messenger fields. Since we aim to capture the physics of the portal Lagrangian while remaining agnostic about the hidden sector, the hidden Lagrangian may be fully general. In particular, it can contain, in addition to the messenger field, *secluded* fields with arbitrary masses, quantum numbers, and interactions, that do not couple directly to the SM particles. This idea is schematically depicted in figure 1. We integrate out all hidden fields with masses well above the characteristic energy scale of the relevant EFT. This does not restrict the regime of applicability of the resulting PET, since the EFT by itself, even without being coupled to hidden sectors, already becomes invalid at energies well above its characteristic energy scale. The impact of the heavy particles is

captured by an infinite tower of higher dimensional operators in the EFT, portal, and hidden Lagrangians, which contain only the remaining light SM and hidden fields.

In the remainder of this section, we construct PETs that couple the SM to a single messenger field of spin 0,  $1/2$ , and 1. We begin by constructing EW scale PETs that extend SMEFT, and then use the resulting portal SMEFTs as a starting point to derive a corresponding set of strong scale PETs that extend LEFT. In the first step, we take the typical energy scale of SMEFT to be the Higgs VEV, and in the second step, we take the typical energy scale of LEFT to be around 1 GeV, which corresponds roughly the proton mass. When extending SMEFT, we assume that the messenger is a singlet under the full SM gauge group  $G_{\text{SM}} = \text{SU}(3)_c \times \text{SU}(2)_L \times \text{U}(1)_Y$  in order to remain consistent with the SMEFT setup, but for the PETs that extend LEFT we only assume that the messenger field is invariant under the broken SM gauge group  $G_{\text{sm}} = \text{SU}(3)_c \times \text{U}(1)_V$ . We do not assume that the portal SMEFTs respect any additional symmetries, such as gauge symmetries or a new parity of the hidden sector. In particular, we allow for both P and CP violating portal interactions. However, we use the accidental symmetries of the portal SMEFTs to constrain the shape of the corresponding portal LEFTs.

### 3.1.1 Power counting

The lack of evidence for light sectors at colliders and fixed target experiments [63–65] implies that any portal interaction has to be strongly suppressed. In order to reflect this suppression, we normalise all portal operators such that they contain at least one explicit degree of smallness  $\epsilon_i$ , independent of their mass dimension. Physically, these degrees of smallness can result from a wide variety of mechanisms that do not have to be connected to each other, such as the small breaking of an approximate symmetry of the theory. At the EW scale, unitarity implies that higher dimensional portal operators with mass dimension larger than four must be dimensionally suppressed by factors  $\epsilon_i^{d-4} = (v/f_i)^{d-4}$ , where  $f_i$  is some ultraviolet (UV) scale. For our purposes, it is not necessary to distinguish between the various degrees of smallness  $\epsilon_i$ . Therefore, we define the generic degree of smallness

$$\epsilon_{\text{UV}} = \max_i \epsilon_i = \frac{v}{f_{\text{UV}}} , \quad f_{\text{UV}} \gg v , \quad (3.2)$$

and only count powers of  $\epsilon_{\text{UV}}$  rather than distinguishing between various sources of smallness for the portal operators. Using this power counting, portal operators of mass-dimension three, four, and five are suppressed by a single factor of  $\epsilon_{\text{UV}}$ , while higher dimensional portal operators are suppressed by higher powers of  $\epsilon_{\text{UV}}$ , due to the required dimensional suppression.

When constructing the portal SMEFTs in section 3.2, we neglect portal operators with mass-dimension six or higher, and in the remainder of this work, we use these PETs as the starting point for the subsequent construction of the strong scale portal LEFT and  $\chi$ PT Lagrangians. This constraint restricts the types of hidden sectors we are able to describe. For one, some SM extensions couple to the SM only via operators of mass-dimension six or higher. For example, this is the case of fermionic DM models that couple to the SM via four-fermion interactions of dimension six, see *e.g.* [172, 173]. In addition, higher dimensional portal operators can mediate transitions that are not captured by lower dimensional portal operators. As we show in section 3.2, this is the case for baryon-number violating portal interactions, which

only appear starting at dimension six. However, we emphasise that these limitations are not a consequence of the PET approach as such, but merely a consequence of our choice to only account for portal operators up to dimension five. We leave the investigation of PETs with operators of dimension six or higher for future work.

### 3.1.2 Mixing between SM and messengers fields

Generically, the portal sector contains quadratic operators that mix neutral SM fields with hidden fields. Even though it is possible to diagonalise the portal Lagrangian such that these quadratic operators are effectively eliminated from the theory, this diagonalisation would induce two new types of portal operators: First, one would obtain portal operators that mirror SM interactions, except that one SM field is replaced by a messenger field. Second, one would obtain new portal operators that mirror *hidden sector* interactions involving the messenger fields, except that one messenger field is replaced by a neutral SM field. This second type of portal operator conflicts with our strategy of being agnostic about the internal structure of the hidden sector, as it introduces direct coupling between the secluded fields and the neutral SM fields. Listing all of the corresponding portal operators is impossible without making further assumptions about the hidden sector. Therefore, we do not diagonalise any of the quadratic portal interactions.

However, in principle, it is necessary to diagonalise the portal mixing in order to construct the proper asymptotic energy eigenstates of the theory. This can be avoided when performing perturbative calculations at fixed order in  $\epsilon_{UV}$ , since the undiagonalised fields approximately overlap with the asymptotic energy eigenstates of the theory in the limit of small  $\epsilon_{UV}$ . However, it may be necessary to re-sum the quadratic portal interactions in order to describe certain effects that cannot be captured by fixed-order computations in perturbation theory. For example, consider a type-I seesaw model in which the SM is augmented by a single HNL. In order to capture neutrino oscillations in this model, it is necessary to re-sum the mass-mixing between the SM neutrinos and the HNL. However, this does not affect the computation of  $S$ -matrix elements for microscopic scattering amplitudes, since these oscillations typically occur over macroscopic distances, *e.g.* over several kilometers in case of neutrinos produced in nuclear reactors [174].

## 3.2 Electroweak scale portal effective theories

We explicitly construct the EW scale PETs that couple SMEFT to a single messenger of spin 0,  $1/2$ , or 1, and give a complete basis of portal operators with mass dimension five or less for each resulting portal SMEFT. We then use these PETs to define a set of portal currents that parameterise the coupling of SMEFT to generic hidden sectors, and study the shape of the portal SMEFTs after EWSB.

### 3.2.1 Minimal bases of portal operators

In general, a naive listing of all possible portal operators with mass-dimension five or less will contain numerous redundant operators. In order to obtain a minimal set of independent portal operators for each type of messenger, we use the reduction techniques collected in appendix A. The resulting operator basis is presented in table 2. We consider three types of messengers:



	$d$	Higgs	Yukawa + h.c.	Fermions	Gauge bosons
	3	$s_i  H ^2$			
	4	$s_i s_j  H ^2$			
$s_i$		$s_i s_j s_k  H ^2$	$s_i q_a \bar{u}_b \tilde{H}^\dagger$		$s_i G_{\mu\nu}^a G_a^{\mu\nu}$
		$s_i D^\mu H^\dagger D_\mu H$	$s_i q_a \bar{d}_b H^\dagger$		$s_i W_{\mu\nu}^a W_a^{\mu\nu}$
	5	$s_i  H ^4$	$s_i \ell_a \bar{e}_b H^\dagger$		$s_i B_{\mu\nu} B^{\mu\nu}$
					$s_i G_{\mu\nu}^a \tilde{G}_a^{\mu\nu}$
					$s_i W_{\mu\nu}^a \tilde{W}_a^{\mu\nu}$
					$s_i B_{\mu\nu} \tilde{B}^{\mu\nu}$
$\xi_a$	4		$\xi_a \ell_b \tilde{H}^\dagger$		
$+$	5	$\xi_a \xi_b  H ^2$	$\xi_a^\dagger \bar{\sigma}^\mu \ell_b D_\mu \tilde{H}^\dagger$		$\xi_a \sigma^{\mu\nu} \xi_b B_{\mu\nu}$
$\text{h.c.}$					
$v^\mu$	4	$v_\mu v^\mu  H ^2$		$v^\mu q_a^\dagger \bar{\sigma}_\mu q_b$	
		$\partial_\mu v^\mu  H ^2$		$v^\mu \bar{u}_a^\dagger \sigma_\mu \bar{u}_b$	
		$v^\mu H^\dagger \vec{D}_\mu H$		$v^\mu \bar{d}_a^\dagger \sigma_\mu \bar{d}_b$	
				$v^\mu \ell_a^\dagger \bar{\sigma}_\mu \ell_b$	
				$v^\mu \bar{e}_a^\dagger \sigma_\mu \bar{e}_b$	

Table 2: List of all operators up to dimension five with SM fields and spin 0 ( $s_i$  with  $i = 1, 2$ ), spin  $1/2$  ( $\xi_a$  with  $a = 1, 2$ ) or spin 1 ( $v^\mu$ ) messengers. The first column specifies the spin of the messenger field, the second column denotes the dimension  $d$  of the operator and the remaining columns label the SM sectors the messengers interact with. The left-handed SU(2) doublets  $\ell_a = (\nu_a, e_a)^T$  and  $q_a = (u_a, d_a)^T$  and the right-handed singlets  $\bar{u}_a^\dagger$ ,  $\bar{d}_a^\dagger$ , and  $\bar{e}_a^\dagger$  are Weyl fermions.

**Spin 0 fields** can be either real (pseudo-)scalar or complex scalar fields. As we do not require portal interactions to conserve parity, pseudoscalar and scalar fields couple to SMEFT via the same set of portal interactions. Furthermore, a complex scalar couples to SMEFT in the same way as two real scalar fields. Therefore, we can account for all types of spin 0 messengers by considering how SMEFT couples to two real scalar fields  $s_1(x)$  and  $s_2(x)$ . These can interact with the SM fields via a minimal basis of 14 different operators with dimensions ranging from three to five. There are twelve additional redundant operators.

**Spin  $1/2$  fields** can be either Weyl, Majorana, or Dirac fermions. Without loss of generality, a Dirac fermion can be written as a combination of two left-handed Weyl fermions, while a Majorana fermion can be written as single left-handed Weyl fermion. Therefore, we can account for all types of fermionic messengers by considering how SMEFT couples to two left-handed Weyl fermions  $\xi_1(x)$  and  $\xi_2(x)$ . These can interact with the SM fields via a minimal basis of four portal operators of dimension four and five. Additionally, there are two redundant operators. Notice that the operator  $\xi_a \sigma^{\mu\nu} \xi_b B_{\mu\nu}$  is antisymmetric under exchange of  $a$  and  $b$ , so that it can only contribute if SMEFT couples to a Dirac fermion.

**Spin 1 fields** can be either vector or axial-vector fields. As we do not require portal interactions to conserve parity, both of these can couple to SMEFT via the same portal interactions, and we can account for both possibilities by considering how SMEFT couples

		$S_m^H$	$S_x$	$S_x$	$\Xi$	$V_H^\mu$	$V_x^\mu$	$\Xi_\mu$	$T_{\mu\nu}$
	spin		0		$1/2$		1	$3/2$	2
	$d$	2	0		$3/2$		1	$3/2$	2
	representation	1	1	$8 \oplus 1$	3	1	$8 \oplus 1$	3	1
flavour	symmetry						$V_\mu^\dagger = V_\mu$		
	DOFs	1	1	18	3	1	9	3	1

Table 3: Properties of the portal SMEFT currents. The first two rows list spin and mass dimension  $d$ , and the remaining rows list the representation and symmetries under flavour transformations as well as the resulting number of DOFs.

to a vector field  $v^\mu(x)$ . These can interact with the SM fields via a minimal basis of eight independent operators with mass-dimension four. Notably, there are no operators of dimension five. There are two additional redundant operators.

For the sake of completeness, we list the redundant operators in appendix B.1. If the internal structure of the hidden sector is known, it is potentially possible to discard further operators by using *e.g.* the EOMs for the messenger field. As discussed in section 3.1.2, this may involve other hidden sector fields besides the messenger. Here and in the following, we refrain from making such model dependent simplifications.

All of the above portal operators conserve baryon number, and portal operators with spin 0 and 1 messengers also conserve lepton number. Portal operators with spin  $1/2$  messengers can violate lepton number by one unit. Furthermore, portal operators with spin  $1/2$  messengers do not couple to either the SM quark fields or any of the right-handed charged lepton fields, and operators with spin 1 messengers only couple to pairs of quarks and leptons with identical chirality, so that they cannot serve as a separate source of chiral symmetry breaking. This becomes important when constructing strong scale PETs, since it implies that some strong scale portal operators are subdominant as a result of chiral suppression due to a light SM fermion mass insertion.

Further, we note that, although we have focused on the case in which SMEFT couples only to a single messenger field, the portal sector defined by the operators in table 2 already captures interactions between SMEFT and an arbitrary number of messengers with *identical spin*. For sets of messengers  $s_i$  or  $\xi_i$  or  $v_i^\mu$ , it is sufficient to iterate over all possible values for the index  $i$  in the portal operators. However, we do not account for the possibility of coupling SMEFT to multiple messengers with *different spin*.

### 3.2.2 External current description

It is convenient to collect all of the operators associated with the three messenger fields into a single portal Lagrangian (3.1). We separate the portal operators into a Higgs  $H$ , a Yukawa like  $Y$ , a fermionic  $F$ , and a gauge  $V$  sector

$$\mathcal{L}_{\text{portal}} = \mathcal{L}_{\text{EW}}^H + \mathcal{L}_{\text{EW}}^Y + \mathcal{L}_{\text{EW}}^F + \mathcal{L}_{\text{EW}}^V . \quad (3.3)$$

The individual Lagrangians are<sup>11</sup>

$$\mathcal{L}_{\text{EW}}^H = S_m^H |H|^2 + \frac{1}{2} S_\lambda^H |H|^4 + S_\kappa^H D^\mu H^\dagger D_\mu H + i V_H^\mu H^\dagger \overleftrightarrow{D}_\mu H , \quad (3.4a)$$

$$\mathcal{L}_{\text{EW}}^Y = \mathbf{S}_m^e \ell \bar{e} H^\dagger + \mathbf{S}_m^d q \bar{d} H^\dagger + \mathbf{S}_m^u q \bar{u} \tilde{H}^\dagger + \Xi \ell \tilde{H}^\dagger + \Xi_\mu \ell D^\mu \tilde{H}^\dagger + \text{h.c.} , \quad (3.4b)$$

$$\mathcal{L}_{\text{EW}}^F = \mathbf{V}_q^\mu q^\dagger \bar{\sigma}_\mu q + \mathbf{V}_\ell^\mu \ell^\dagger \bar{\sigma}_\mu \ell + \mathbf{V}_u^\mu \bar{u}^\dagger \sigma_\mu \bar{u} + \mathbf{V}_d^\mu \bar{d}^\dagger \sigma_\mu \bar{d} + \mathbf{V}_e^\mu \bar{e}^\dagger \sigma_\mu \bar{e} , \quad (3.4c)$$

$$\mathcal{L}_{\text{EW}}^V = (S_\omega^B B_{\mu\nu} + S_\theta^B \tilde{B}_{\mu\nu} + T_{\mu\nu}^B) B^{\mu\nu} + (S_\omega^W W_{\mu\nu} + S_\theta^W \tilde{W}_{\mu\nu}) W^{\mu\nu} + (S_\omega G_{\mu\nu} + S_\theta \tilde{G}_{\mu\nu}) G^{\mu\nu} . \quad (3.4d)$$

Lepton and quark doublets are written as left-handed Weyl fermions  $\ell_a = (\nu_a, e_a)^T$  and  $q_a = (u_a, d_a)^T$ , and the singlets as conjugated left-handed Weyl fermions  $\bar{u}_a^\dagger$ ,  $\bar{d}_a^\dagger$ , and  $\bar{e}_a^\dagger$ .<sup>3</sup> Table 3 summarises the properties of the scalar  $S$ , fermionic  $\Xi$ , and vectorial  $V^\mu$  portal currents. The *scalar current* of mass-dimension two that appears in the Higgs mass-like term in Lagrangian (3.4a) is

$$S_m^H = \epsilon_{\text{UV}} \left[ v c_i^{S_m^H} s_i + c_{ij}^{S_m^H} s_i s_j + c_{v^2}^{S_m^H} v^\mu v_\mu + c_{\partial v}^{S_m^H} \partial^\mu v_\mu + \frac{1}{v} \left( c_{ijk}^{S_m^H} s_i s_j s_k + c_{ab}^{S_m^H} \xi_a^\dagger \xi_b \right) \right] , \quad (3.5)$$

where the  $c_{\text{operator}}^{\text{current}}$  are dimensionless Wilson coefficients. The other (*pseudo*)-*scalar currents* of mass dimension zero in Lagrangians (3.4a), (3.4b), and (3.4d) are

$$S_x = \frac{\epsilon_{\text{UV}}}{v} c_i^{S_x} s_i , \quad \mathbf{S}_x = \frac{\epsilon_{\text{UV}}}{v} \mathbf{c}_i^{S_x} s_i , \quad (3.6)$$

where  $x$  symbolically labels the different scalar currents. The *left-handed fermionic currents* in Lagrangian (3.4b) are

$$\Xi = \epsilon_{\text{UV}} c_a^{\Xi} \xi_a , \quad \Xi^\mu = \epsilon_{\text{UV}} c_{\partial a}^{\Xi} \xi_a^\dagger \bar{\sigma}_\mu , \quad (3.7)$$

and the *vectorial currents* in Lagrangians (3.4a) and (3.4c) are

$$V_x^\mu = \epsilon_{\text{UV}} c_v^x v^\mu , \quad \mathbf{V}_x^\mu = \epsilon_{\text{UV}} \mathbf{c}_v^x v^\mu , \quad (3.8)$$

where the matrix valued vectorial currents and its Wilson coefficient are Hermitian. The *tensorial current* in Lagrangian (3.4d) is

$$T_{\mu\nu} = \frac{\epsilon_{\text{UV}}}{v} c_{ab}^T \xi_a^\dagger \sigma_{\mu\nu} \xi_b . \quad (3.9)$$

---

<sup>11</sup> The Higgs doublet is denoted by  $H$ , and its conjugate is  $\tilde{H} = -\frac{i}{2} \sigma_2 H^\dagger$ . We abbreviate  $|H|^2 = H^\dagger H$  and the antisymmetrised derivative is  $H^\dagger \overleftrightarrow{\partial}^\mu H = (\partial^\mu H)^\dagger H - H^\dagger \partial^\mu H$ . The  $G_a^\mu$  are the gluon fields, while  $W_a^\mu$  and  $B^\mu$  denote the EW gauge bosons. The field strength tensors are given as  $V_a^{\mu\nu} = \partial^\mu V_a^\nu - \partial^\nu V_a^\mu - i f_{abc} V_b^\mu V_c^\nu$ .

### 3.2.3 Electroweak symmetry breaking

After EWSB, the Higgs field  $H$  acquires a finite VEV  $v$ , which induces a shift in the currents. In unitary gauge, the portal Lagrangian (3.3) becomes<sup>12</sup>

$$\mathcal{L}_{\text{EWSB}}^H = \frac{1}{2} S_\kappa^H \partial_\mu h \partial^\mu h + \frac{1}{2} S_\lambda^H \left( v + \frac{h}{\sqrt{2}} \right)^4 \quad (3.10a)$$

$$+ \left( v + \frac{h}{\sqrt{2}} \right)^2 \left( \frac{1}{2} S_\kappa^H \left( W_\mu^+ W^{-\mu} + \frac{1}{2} Z^\mu Z_\mu \right) + V_H^\mu Z_\mu + S_m^H \right),$$

$$\mathcal{L}_{\text{EWSB}}^Y = \frac{1}{\sqrt{2}} (v + H) \left( \widehat{S}_m^{e\bar{e}} e \bar{e} + \widehat{S}_m^{d\bar{d}} d \bar{d} + \widehat{S}_m^{u\bar{u}} u \bar{u} - \Xi \nu \right) - \frac{\partial^\mu h}{\sqrt{2}} \Xi_\mu \nu + \text{h.c.}, \quad (3.10b)$$

$$\begin{aligned} \mathcal{L}_{\text{EWSB}}^F = & \widehat{V}_{qu}^\mu u^\dagger \bar{\sigma}_\mu u + \widehat{V}_{qd}^\mu d^\dagger \bar{\sigma}_\mu d + \widehat{V}_{u\bar{u}}^\mu \bar{u} \sigma_\mu \bar{u}^\dagger + \widehat{V}_{d\bar{d}}^\mu \bar{d} \sigma_\mu \bar{d}^\dagger \\ & + \widehat{V}_{\ell e}^\mu e^\dagger \bar{\sigma}_\mu e + \widehat{V}_{e\bar{e}}^\mu \bar{e} \sigma_\mu \bar{e}^\dagger + V_\ell^\mu \nu^\dagger \bar{\sigma}_\mu \nu, \end{aligned} \quad (3.10c)$$

$$\begin{aligned} \mathcal{L}_{\text{EWSB}}^V = & \left( S_\omega^Z \bar{Z}_{\mu\nu} + S_\theta^Z \widetilde{\bar{Z}}_{\mu\nu} + T_{\mu\nu}^Z \right) \bar{Z}^{\mu\nu} + \left( S_\omega^A A_{\mu\nu} + S_\theta^A \widetilde{A}_{\mu\nu} + T_{\mu\nu}^A \right) A^{\mu\nu} \\ & + (S_\omega G_{\mu\nu} + S_\theta \widetilde{G}_{\mu\nu}) G^{\mu\nu} + \left( S_\omega^{AZ} \bar{Z}_{\mu\nu} + S_\theta^{AZ} \widetilde{\bar{Z}}_{\mu\nu} \right) A^{\mu\nu} + 2 \left( S_\omega^W \bar{W}_{\mu\nu}^+ + S_\theta^W \widetilde{\bar{W}}_{\mu\nu}^+ \right) \bar{W}_-^{\mu\nu} \\ & - 2i \left( S_\omega^W \partial^{\nu\rho\sigma} - 2S_\theta^W \epsilon^{\mu\nu\rho\sigma} \partial_\mu \right) W_\nu^3 W_\rho^+ W_\sigma^- + 4S_\omega^W g^{\mu[\nu} g^{\rho]\sigma} (2W_\mu^3 W_\nu^3 + W_\mu^+ W_\nu^-), \end{aligned} \quad (3.10d)$$

where

$$\partial^{\mu\rho\sigma} = g^{\rho\sigma} (\partial_+ - \partial_-)^\mu + g^{\sigma\mu} (\partial_- - \partial_3)^\rho + g^{\mu\rho} (\partial_3 - \partial_+)^\sigma \quad (3.11)$$

and we have defined the new *scalar currents*

$$S_x^Z = c_w^2 S_x^W + s_w^2 S_x^B, \quad S_x^A = s_w^2 S_x^W + c_w^2 S_x^B, \quad S_x^{AZ} = 2c_w s_w (S_x^W - S_x^B), \quad (3.12)$$

as well as the new *tensorial currents*

$$T_{\mu\nu}^A = c_w T_{\mu\nu}^B, \quad T_{\mu\nu}^Z = -s_w T_{\mu\nu}^B, \quad (3.13)$$

that couple directly to the photon and  $Z$ -boson field strength tensors, with  $c_w$  and  $s_w$  denoting the (co-)sine of the EW mixing angle. In Lagrangians (3.10a) and (3.10c), we used a singular value decomposition in order to diagonalise the SM fermion mass matrices  $\mathbf{m}_{xy} = \mathbf{U}_x \mathbf{m}_x \mathbf{U}_y^\dagger$  via a unitary rotation of the SM fermion fields. The resulting mass-diagonal SM fermions couple to the rotated portal currents

$$\widehat{S}_m^{xy} = \mathbf{U}_y^\dagger \mathbf{S}_m^x \mathbf{U}_x, \quad \widehat{V}_{xy}^\mu = \mathbf{U}_y^\dagger \mathbf{V}_x^\mu \mathbf{U}_y. \quad (3.14)$$

Note that the CKM matrix  $\mathbf{V}_{\text{CKM}} = \mathbf{U}_d^\dagger \mathbf{U}_u$  and the Pontecorvo–Maki–Nakagawa–Sakata matrix that one obtains after diagonalising the neutrino to hidden sector mass mixing are the only combinations of the  $\mathbf{U}_x$  constrained by measuring SM or portal interactions in the broken phase. This implies that such observations cannot fully constrain the shape of the unrotated portal currents  $\mathbf{S}_m^x$  and  $\mathbf{V}_x$  that couple to the SM fermion gauge eigenstates. This may be of interest when trying to constrain the shape of the portal interactions at high temperatures or in the early universe with collider or fixed-target experiments.

<sup>12</sup> In unitary gauge, the Higgs field is given as  $H = (0, v + h/\sqrt{2})^T$ , and  $\tilde{H} = -(v + h/\sqrt{2}, 0)^T$ .

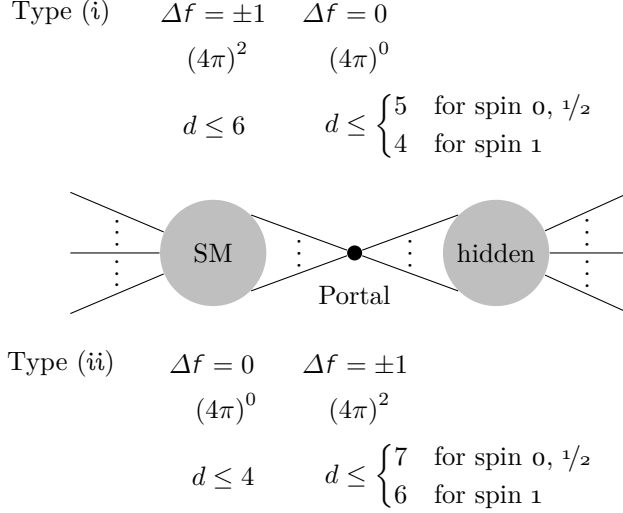


Figure 6: Schematic representation of the two possible types of quark-flavour violating diagrams at the strong scale, which we distinguish based on the sector in which the flavour violation is located. We assume that the relevant strong scale PET is the low energy limit of a corresponding EW scale portal SMEFT. The diagrams show the suppression due to NDA power counting and the dimension of the operators in the diagram. Type (i) diagrams contain a flavour *violating* SM sub-diagram that scales as  $(4\pi)^2$  and contains one  $d \leq 6$  Fermi theory operator, as well as one flavour conserving portal operator that scales as  $(4\pi)^0$  and has  $d \leq 5$ . Type (ii) diagrams contain a flavour *conserving* SM sub-diagram that scales as  $(4\pi)^0$  and contains only renormalisable  $d \leq 4$  operators, as well as one flavour violating portal operators that scales as  $(4\pi)^2$  and have  $d = 6, 7$  or  $5, 6$ . Type (i) diagrams with  $d = 5$  portal operators and type (ii) diagrams with  $d = 7$  portal operators can appear in strong scale PETs with spin 1 messengers that are derived from other EW scale PETs besides portal SMEFT. See also appendix A.1 and [175–178] for details on the NDA counting.

### 3.3 Portals at the strong scale

At the strong scale, which we define to be roughly the scale associated with the gluon dynamics (GD) contribution  $\sim 1$  GeV to the proton mass, the SM dynamics is captured by LEFT, which contains only the massless gauge bosons, electrons, muons, neutrinos, and the light quarks (u, d, and s). Starting from the previously constructed portal SMEFTs, we now derive the strong scale PETs that couple LEFT to a single messenger of spin 0,  $1/2$ , or 1. While we have only included portal operators of dimension  $d \leq 5$  in the portal SMEFTs, we now also include quark-flavour violating  $d \leq 7$  portal operators. These operators are generated by diagrams that include virtual  $W$ -boson exchanges and are necessary to capture quark-flavour violating transitions, such as decays of charged kaons into pions and hidden fields, at LO in  $\epsilon_{\text{SM}}$ .

To see why it is necessary to include the higher dimensional operators when constructing a general strong scale PET, consider a generic quark-flavour violating transition at the strong scale. Such a transition has to be suppressed by at least one degree of smallness  $\epsilon_{\text{UV}}$ , and another degree of smallness  $\epsilon_{\text{SM}} \equiv \partial^2/\Lambda_{\text{SM}}^2$ , cf. (2.23). At  $\mathcal{O}(\epsilon_{\text{UV}}\epsilon_{\text{EW}})$ , quark-flavour violating processes are described by the two types of diagram depicted in figure 6:

- (i) Diagrams with one quark-flavour *violating* dimension six SM charged current vertex and

one quark-flavour *conserving* strong scale portal vertex.

- (ii) Diagrams with a renormalisable quark-flavour *conserving* SM vertex and a quark-flavour *violating* strong scale portal vertex.

To fully capture quark-flavour violating transitions one has to include all portal operators that can appear in either type of diagram.

First, consider the set of portal operators that can appear in type (i) diagrams: The SM charged current interaction that appears in these diagrams is associated with a suppression factor  $\epsilon_{\text{SM}}$ . Since the overall diagram has to scale as  $\epsilon_{\text{UV}}\epsilon_{\text{SM}}$ , portal operators that contribute to the diagrams cannot have a higher mass-dimension than their EW scale counterparts, as this would imply further suppression by powers of  $\sqrt{\epsilon_{\text{SM}}}$ . Hence, to capture all type (i) diagrams, it is sufficient to include quark-flavour conserving portal operators with spin 0 or  $1/2$  messengers that are at most of dimension five and quark-flavour conserving portal operators with spin 1 messengers that are at most of dimension four. If the strong scale PET is the low energy limit of another EW scale PET besides SMEFT, dimension five portal operators with spin 1 messengers can also contribute to type (i) diagrams.

Next, consider the set of portal operator that can appear in type (ii) diagrams. Since these diagrams do not contain a SM four-fermion vertex, they can contain portal operators that are suppressed by a factor  $\epsilon_{\text{UV}}\epsilon_{\text{SM}}$  rather than just a factor  $\epsilon_{\text{UV}}$ . These portal operators are generated by diagrams in the EW scale theory that contain a virtual  $W$ -boson exchange, and they can have a mass-dimension that is at most the mass-dimension of the corresponding EW scale portal operators plus two. Therefore, to capture all type (ii) diagrams, one has to include quark-flavour violating portal operators with spin 0 and  $1/2$  messengers that are of dimension seven or less and quark-flavour violating portal operators with spin 1 messengers that are of dimension six or less. As in the case of type (i) diagrams, dimension seven portal operators with spin 1 messengers can also contribute to type (ii) diagrams, if the strong scale PET is the low energy limit of another EW scale PET besides SMEFT.

In order to be phenomenologically viable, any strong scale portal operators have to be invariant under the low energy SM gauge group  $G_{\text{sm}} = \text{SU}(3)_c \times \text{U}(1)_{\text{EM}}$ , but they do not have to be invariant under the complete SM gauge group  $G_{\text{SM}}$ , which also encompasses weak interactions mediated by the heavy  $W$ - and  $Z$ -bosons. In addition, our operators have to preserve the accidental symmetries obeyed by the relevant portal SMEFTs. This implies that all strong scale portal operators have to conserve baryon number and bosonic messenger fields have to conserve lepton number, while operators with spin  $1/2$  messengers can violate lepton number by one unit. In addition, the portal SMEFT interactions with spin  $1/2$  and 1 messenger fields do not mix SM fermions of different chirality, so that strong scale portal operators with chirality flips are suppressed by an additional factor of  $m_l/v \sim \sqrt{\epsilon_{\text{SM}}}$ , where  $m_l$  is the mass of the relevant light SM fermion. Portal SMEFT interactions with scalar messenger fields can induce a single chirality flip, so that only strong scale portal operators with at least two chirality flips are suppressed by such a factor of  $\sqrt{\epsilon_{\text{SM}}}$ .

In addition to the dimensional suppression associated with  $\epsilon_{\text{SM}}$ , the higher dimensional quark-flavour violating portal operators can also be suppressed by loop factors of  $(4\pi)^{-2}$ . We keep track of this suppression by using the  $4\pi$  power counting scheme of naive dimensional analysis (NDA) [175–178], see also appendix A.1 for a detailed explanation. Using NDA, the most suppressed type (i) diagrams with spin 0 and  $1/2$  messengers scale as  $(4\pi)^2 \epsilon_{\text{UV}}^3 \epsilon_{\text{SM}}$ , while

$d$	Scalar	Vector	Gauge
4	$s_i \bar{\psi}\psi$		
$s_i$	$s_i s_j \bar{\psi}\psi$		$s_i F_{\mu\nu} F^{\mu\nu}$
5			$s_i F_{\mu\nu} \tilde{F}^{\mu\nu}$ $s_i G_{\mu\nu} G^{\mu\nu}$ $s_i G_{\mu\nu} \tilde{G}^{\mu\nu}$
$\xi_a$	3	$\xi_a \nu$	
+			
h.c.	5		$\xi_a \bar{\sigma}_{\mu\nu} \nu F^{\mu\nu}$ $\xi_a \bar{\sigma}_{\mu\nu} \xi_b F^{\mu\nu}$
$v_\mu$	4	$v_\mu \psi^\dagger \bar{\sigma}^\mu \psi$	

(a) Type (i) quark-flavour conserving portal operators of dimension three, four, and five.

$d$	Two quarks	Quark dipole	Four fermions
	$s_i s_j s_k \bar{d}d$	$s_i F^{\mu\nu} \bar{d} \sigma_{\mu\nu} d$	
6	$\partial^2 s_i \bar{d}d$	$s_i G^{\mu\nu} \bar{d} \sigma_{\mu\nu} d$	
	$s_i \partial_\mu s_j d^\dagger \bar{\sigma}^\mu d$		
$s_i$	$s_i s_j s_k s_l \bar{d}d$		$s_i d^\dagger \bar{q}^\dagger \bar{q} d$ $s_i q^\dagger \bar{\sigma}^\mu q q^\dagger \bar{\sigma}_\mu q$ $s_i d^\dagger \bar{\sigma}^\mu d \bar{q} \sigma_\mu \bar{q}^\dagger$ $s_i e^\dagger \bar{\sigma}_\mu \nu u^\dagger \bar{\sigma}^\mu d$ $s_i \nu^\dagger \bar{\sigma}_\mu \nu d^\dagger \bar{\sigma}^\mu d$
7			
$\xi_a$	6	$\xi_a^\dagger \bar{\sigma}_\mu e d^\dagger \bar{\sigma}^\mu u$	
h.c.		$\xi_a^\dagger \bar{\sigma}_\mu \nu d^\dagger \bar{\sigma}^\mu d$	

(b) Type (ii) dimension six and seven quark-flavour violating portal operators.

Table 4: List of all LO strong scale portal operators up to dimension seven that couple LEFT to messenger fields of spin 0,  $1/2$ , or 1. Panel (a) shows operators that contribute to type (i) diagrams and panel (b) shows operators that contribute to type (ii) diagrams. See also figure 6 for more details. The first column specifies the spin of the messenger field, the second column contains the dimension  $d$  of the operators and the remaining columns label the SM sectors they interact with. A generic SM fermion is labelled by  $\psi = u, d, e, \nu$ , the down-type quarks are  $d = d, s$ , the leptons are  $e = e, \mu$  and  $\nu = \nu_e, \nu_\mu, \nu_\tau$ , and  $q$  runs over all three light quarks  $u, d$  and  $s$ .

the most suppressed type (i) diagrams with spin 1 messengers scale as  $(4\pi)^2 \epsilon_{UV} \epsilon_{SM}^2$ , see also figure 6. In both cases, the  $(4\pi)^2$  enhancement captures the fact that the leading strong-scale Fermi theory interactions are generated by tree-level diagrams at the EW scale. When applying NDA to strong scale PETs, we discard all quark-flavour violating dimension six and seven type (ii) operators that are even more suppressed than the most suppressed type (i) operators. For PETs with spin 0 and spin  $1/2$  messengers, dimension six operators without chiral suppression are suppressed by a relative factor of  $\sqrt{\epsilon_{SM}}$ , rather than  $\epsilon_{SM}$ , compared to the unsuppressed dimension five portal operators in these PETs. This means that they are enhanced by a relative factor of  $\epsilon_{SM}^{-1/2}$  compared to the most suppressed type (i) diagrams. Therefore, we only use NDA to discard operators that are either of dimension seven or of dimension six and chirally suppressed. For PETs with spin 1 messengers, we only use NDA to discard operators that are either of dimension six, or of dimension four or five and sufficiently chirally suppressed.

### 3.3.1 Operator list

We construct minimal bases of portal operators for each portal LEFT by combining the restrictions discussed in the previous section with the reduction techniques given in appendix A. The complete bases of both quark-flavour conserving and quark-flavour violating operators up to dimension seven are given in appendix C. Table 4a shows the subset of portal operators with dimension five or less. This subset mirrors the set of portal operators in the corresponding portal SMEFTs and contributes at LO to both quark-flavour conserving and violating transitions. In

$(4\pi)^{-n}$	Two Quarks	Quark Dipole	$(4\pi)^{-n}$	$\bar{d}d$	$d^\dagger d$	$d^\dagger V^{\mu\nu} d$
1	$s_i s_j \partial_\mu s_k$	$d^\dagger \bar{\sigma}^\mu d$	1		$v_\mu v^\mu v_\nu d^\dagger \bar{\sigma}^\nu d$	$v^\mu d^\dagger \bar{\sigma}^\nu G_{\mu\nu} d$ $v^\mu d^\dagger \bar{\sigma}^\nu \tilde{G}_{\mu\nu} d$
		$\partial_\nu s_i d^\dagger \bar{\sigma}_\mu V^{\mu\nu} d$ $\partial_\nu s_i d^\dagger \bar{\sigma}_\mu \tilde{V}^{\mu\nu} d$ $s_i s_j \bar{d} \bar{\sigma}_{\mu\nu} V^{\mu\nu} d + \text{h.c.}$		$v_\mu v^\mu \bar{d}d$ $\partial_\mu v^\mu \bar{d}d$ $\partial_\mu v_\nu \bar{d} \sigma^{\mu\nu} d$	$\partial_\nu v^\nu v_\mu d^\dagger \bar{\sigma}^\mu d$ $\partial_\mu v_\nu v^\nu d^\dagger \bar{\sigma}^\mu d$ $\partial_\nu v_\mu v^\nu d^\dagger \bar{\sigma}^\mu d$ $\partial^2 v_\mu d^\dagger \bar{\sigma}^\mu d$ $\epsilon^{\alpha\beta\mu\nu} \partial_\alpha v_\beta v_\nu d^\dagger \bar{\sigma}_\mu d$ $v^\mu v^\nu d^\dagger \bar{\sigma}_\mu D_\nu d$ $\partial_{(\nu} v_{\mu)} d^\dagger \bar{\sigma}^\mu D^{\nu} d$	$v^\mu d^\dagger \bar{\sigma}^\nu F_{\mu\nu} d$ $v^\mu d^\dagger \bar{\sigma}^\nu \tilde{F}_{\mu\nu} d$
2	$\partial^2 s_i \bar{d}d$ $s_i \partial_\mu s_j d^\dagger \bar{\sigma}^\mu d$		2			

(a) Scalar.

(b) Vector			
$LL \times LL$	$LR \times RL$	$RL \times RL$	$LL \times RL$
$\xi_a^\dagger \bar{\sigma}_\mu \xi_b$	$d^\dagger \bar{\sigma}^\mu d$	$\nu \xi_a^\dagger \bar{d}d$	$\nu D^\mu \xi_a d^\dagger \bar{\sigma}_\mu d$
$\bar{e} \sigma_\mu \xi_a^\dagger$	$d^\dagger \bar{\sigma}^\mu u$	$\xi_a \xi_b^\dagger \bar{d}d$	$\xi_a D^\mu \xi_b d^\dagger \bar{\sigma}_\mu d$
	$e^\dagger \xi_a^\dagger \bar{u}d$	$e \xi_a \bar{d}u$	$e D^\mu \xi_a d^\dagger \bar{\sigma}^\mu u$
		$\nu \bar{\sigma}^{\mu\nu} \xi_a \bar{d} \bar{\sigma}_{\mu\nu} d$	$\nu \bar{\sigma}^{\mu\nu} D_\nu \xi_a d^\dagger \bar{\sigma}_\mu d$
		$\xi_a \bar{\sigma}^{\mu\nu} \xi_b \bar{d} \bar{\sigma}_{\mu\nu} d$	$\xi_a \bar{\sigma}^{\mu\nu} D_\nu \xi_b d^\dagger \bar{\sigma}_\mu d$
		$e \bar{\sigma}^{\mu\nu} \xi_b \bar{d} \bar{\sigma}_{\mu\nu} u$	$e \bar{\sigma}^{\mu\nu} D_\nu \xi_a d^\dagger \bar{\sigma}^\mu u$

(c) Fermion

Table 5: List of all sub-leading quark-flavour changing strong scale operators up to dimension seven that couple LEFT to messenger fields of spin 0,  $1/2$ , or 1. Panel (a) shows the operators for spin 0 messenger fields, panel shows (c) those for spin  $1/2$  messengers, and panel (b) shows those for spin 1 messengers. All fermionic operators are suppressed by factors of  $(4\pi)^{-1}$ , and the suppression factor for the bosons are given in the tables. The notation is the same as in table 4.

the following we focus on the operators appearing only at the strong scale. Table 4b shows the relevant subset of higher dimensional portal operators that contribute to quark-flavour violating transitions at LO in  $\epsilon_{UV}$ ,  $\epsilon_{SM}$ , and the  $4\pi$  counting of NDA. The quark-flavour violating dimension six and seven operators that are sub-leading only due to  $4\pi$  loop suppression factors are given in table 5. As in the case of the portal SMEFTs, we consider three types of messenger field:

**Spin 0 fields** couple to LEFT via six operators of dimension five or less. In addition, there are eleven quark-flavour violating dimension six and seven operators that contribute at LO in both  $\epsilon_{SM}$  and  $4\pi$ . At dimension six, there are three leading two-quark operators

$$s_i s_j s_k \bar{d}d, \quad \partial^2 s_i \bar{d}d, \quad s_i \partial_\mu s_j d^\dagger \bar{\sigma}^\mu d, \quad (3.15)$$

and two leading two-quark dipole operators involving the EM and the gluonic field strength tensor

$$s_i \bar{d} \sigma_{\mu\nu} d F^{\mu\nu}, \quad s_i \bar{d} \sigma_{\mu\nu} d G^{\mu\nu}. \quad (3.16)$$



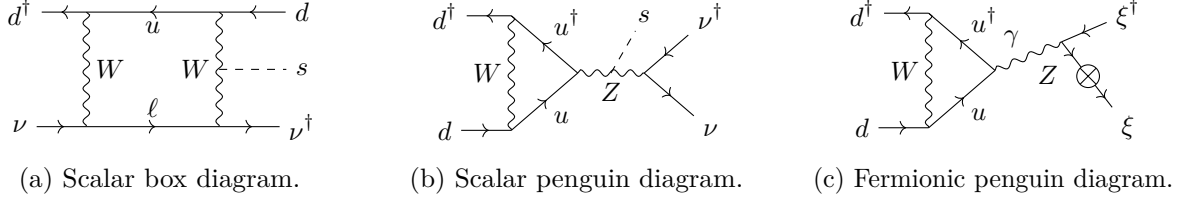


Figure 7: One-loop portal diagrams for some of the portal operators. Panels (a) and (b) depict contributions to the scalar portal operator (3.18b), where the scalar field can couple to any of the heavy EW bosons. Panel (c) depicts the contribution to the fermionic portal operator in (3.21).

At dimension seven, there is one leading two-quark operator

$$s_i s_j s_k s_l \bar{d} d \quad (3.17)$$

as well as five leading four-fermion operators

$$s_i q^\dagger \bar{\sigma}^\mu q \ q^\dagger \bar{\sigma}_\mu q \ , \quad s_i u^\dagger \bar{\sigma}^\mu d \ e^\dagger \bar{\sigma}_\mu \nu \ , \quad (3.18a)$$

$$s_i d^\dagger \bar{\sigma}^\mu d \ \bar{q} \sigma_\mu \bar{q}^\dagger \ , \quad s_i d^\dagger \bar{\sigma}^\mu d \ \nu^\dagger \bar{\sigma}_\mu \nu \ , \quad s_i d^\dagger \bar{q}^\dagger \ \bar{q} d \ . \quad (3.18b)$$

The semi-leptonic neutral current operator  $s_i d^\dagger \bar{\sigma}^\mu d \ \nu^\dagger \bar{\sigma}_\mu \nu$  is generated by the box- and penguin-type diagrams shown in figures 7a and 7b. These diagrams involve at least two heavy boson exchanges, so that one might expect all of them to be suppressed by an additional factor of  $\epsilon_{\text{SM}}$  due to the second heavy boson exchange. However, the analogous SM four-fermion operators  $d^\dagger \bar{\sigma}^\mu d \ \nu^\dagger \bar{\sigma}_\mu \nu$  scale as  $\epsilon_{\text{SM}} f(m_t^2/v^2)$ , with some function  $f(x) \sim 1$ , so that there is no additional suppression [Section XI.B of 179]. We expect that the same can occur in case of the portal operator  $s_i d^\dagger \bar{\sigma}^\mu d \ \nu^\dagger \bar{\sigma}_\mu \nu$ , and we therefore keep this operator as part of the portal Lagrangian. All of the operators mentioned above are listed in table 4.

The sub-leading dimension seven operators differ in their suppression. The four operators

$$s_i s_j \partial_\mu s_k d^\dagger \bar{\sigma}^\mu d \ , \quad \partial_\nu s_i d^\dagger \bar{\sigma}_\mu V^{\mu\nu} d \ , \quad \partial_\nu s_i d^\dagger \bar{\sigma}_\mu \tilde{V}^{\mu\nu} d \ , \quad s_i s_j \bar{d} \sigma_{\mu\nu} V^{\mu\nu} d + \text{h.c.} \ , \quad (3.19)$$

with  $V^{\mu\nu} \in \{F^{\mu\nu}, G^{\mu\nu}\}$  are suppressed by factors of  $(4\pi)^{-1}$ , and the operators

$$s_i \partial^2 s_j \bar{d} d \ , \quad \partial_\mu s_i \partial^\mu s_j \bar{d} d \ , \quad (3.20)$$

and their Hermitian conjugates are suppressed by factors of  $(4\pi)^{-2}$ . The above sub-leading dimension seven operators are listed in table 5a.

**Spin 1/2 fields** couple to LEFT via three operators of dimension five or less. In addition, there are two quark-flavour violating dimension six operators

$$\xi_a^\dagger \bar{\sigma}_\mu e \ d^\dagger \bar{\sigma}^\mu u \ , \quad d^\dagger \bar{\sigma}^\mu d \ \xi_a^\dagger \bar{\sigma}_\mu \nu \ , \quad (3.21)$$

and their Hermitian conjugates, which contribute at LO in both  $\epsilon_{\text{SM}}$  and  $4\pi$ . The second operator and its Hermitian conjugate can only be generated by penguin- and box-type diagrams

involving at least two heavy SM bosons. In analogy to the case of the scalar portal operators in (3.18b), we expect that the diagrams with a virtual top quark exchange inside the loop can scale as  $\epsilon_{\text{SM}} f(m_t^2/v^2)$ , so that there is no additional suppression compared to the first operator. All of the operators mentioned above are listed in table 4.

The sub-leading operators can be either of dimension six or seven, and they are suppressed by factors of  $(4\pi)^{-1}$  or  $(4\pi)^{-2}$ . At dimension six, there are ten operators

$$\bar{d}d \nu \xi_a, \quad \bar{d}d \nu^\dagger \xi_a^\dagger, \quad \bar{d}\bar{\sigma}_{\mu\nu}d \nu \bar{\sigma}^{\mu\nu} \xi_a, \quad \bar{d}u e \xi_a, \quad d^\dagger \bar{\sigma}^\mu u \bar{e} \sigma_\mu \xi_a^\dagger, \quad (3.22a)$$

$$\bar{d}d \xi_a \xi_b, \quad \bar{d}d \xi_a^\dagger \xi_b^\dagger, \quad \bar{d}\bar{\sigma}_{\mu\nu}d \xi_a \bar{\sigma}^{\mu\nu} \xi_b, \quad \bar{u}d e^\dagger \xi_a^\dagger, \quad \bar{d}\bar{\sigma}_{\mu\nu}u e \bar{\sigma}^{\mu\nu} \xi_b, \quad (3.22b)$$

that contain charged right-chiral SM fermion fields, so that they are suppressed by an additional factor of  $m_\psi/v \propto \sqrt{\epsilon_{\text{SM}}}$ , where  $m_\psi$  is the mass of the relevant right-chiral fermion, due to the associated chiral suppression. As a result, they effectively behave as dimension seven operators. Applying NDA, one finds that they are suppressed by factors of  $(4\pi)^{-1}$ . In addition, the operator

$$d^\dagger \bar{\sigma}^\mu d \xi_a^\dagger \bar{\sigma}_\mu \xi_b \quad (3.23)$$

and its Hermitian conjugate, generated by penguin diagrams shown in figure 7c, contain at least two SM gauge boson exchanges. At the EW scale, the hidden fermion only couples to photons and  $Z$ -bosons via the dipole-type operator  $\xi_a \bar{\sigma}^{\mu\nu} \xi_b B_{\mu\nu}$ . This coupling flips the chirality of the hidden fermion, so that a light mass-insertion is necessary to undo the flip. Therefore, the operator is suppressed by an additional factor of  $\sqrt{\epsilon_{\text{SM}}}$ , and it effectively counts as a dimension seven operator. Applying NDA, one also has to account for the  $4\pi$  suppression associated with the EW gauge couplings, so that the operator is suppressed by at least a factor of  $(4\pi)^{-2}$ .

Finally, at dimension seven, there are six derivative operators

$$d^\dagger \bar{\sigma}_\mu d \nu D^\mu \xi_a, \quad d^\dagger \bar{\sigma}^\mu u e D^\mu \xi_a, \quad d^\dagger \bar{\sigma}_\mu d \xi_a D^\mu \xi_b, \quad (3.24a)$$

$$d^\dagger \bar{\sigma}_\mu d \nu \bar{\sigma}^{\mu\nu} D_\nu \xi_a, \quad d^\dagger \bar{\sigma}^\mu u e \bar{\sigma}^{\mu\nu} D_\nu \xi_a, \quad d^\dagger \bar{\sigma}_\mu d \xi_a \bar{\sigma}^{\mu\nu} D_\nu \xi_b, \quad (3.24b)$$

and their Hermitian conjugates. We collect all of the above sub-leading operators in table 5.

**Spin 1 fields** couple to LEFT via one operator of dimension four, see table 4. Since there are no dimension five operators that couple spin 1 messengers to SMEFT, the resulting portal LEFT contains higher dimensional operators of dimension five and six, but not seven. None of them contributes at LO in the  $4\pi$  counting. The dimension six operators

$$v_\mu v^\mu v_\nu d^\dagger \bar{\sigma}^\nu d, \quad v^\mu d^\dagger \bar{\sigma}^\nu G_{\mu\nu} d, \quad v^\mu d^\dagger \bar{\sigma}^\nu \tilde{G}_{\mu\nu} d, \quad (3.25)$$

are suppressed by factors of  $(4\pi)^{-1}$ . The dimension five operators

$$v_\mu v^\mu \bar{d}d, \quad \partial_\mu v^\mu \bar{d}d, \quad \partial_\mu v_\nu \bar{d}\sigma_{\mu\nu}d \quad (3.26)$$

and their Hermitian conjugates are suppressed by a factor of  $\sqrt{\epsilon_{\text{SM}}}$  associated with each right-chiral light quark insertion, so that they effectively contribute like dimension six operators.

Applying the NDA rules, one finds that they are suppressed by factors of  $(4\pi)^{-2}$ . Finally, the dimension six operators

$$\begin{aligned} v^\mu F_{\mu\nu} d^\dagger \bar{\sigma}^\nu d, \quad \partial_\nu v^\nu v_\mu d^\dagger \bar{\sigma}^\mu d, \quad v^\mu v^\nu d^\dagger \bar{\sigma}_\mu D_\nu d, \quad \partial^2 v_\mu d^\dagger \bar{\sigma}^\mu d, \\ v^\mu \tilde{F}_{\mu\nu} d^\dagger \bar{\sigma}^\nu d, \quad \partial_\mu v_\nu v^\nu d^\dagger \bar{\sigma}^\mu d, \quad \epsilon^{\alpha\beta\mu\nu} \partial_\alpha v_\beta v_\nu d^\dagger \bar{\sigma}_\mu d, \quad \partial_{(\nu} v_{\mu)} d^\dagger \bar{\sigma}^\mu D^\nu d, \\ \partial_\nu v_\mu v^\nu d^\dagger \bar{\sigma}^\mu d. \end{aligned} \quad (3.27)$$

are also suppressed by factors of  $(4\pi)^{-2}$ . We collect all of the above operators in table 5.

### 3.3.2 QCD portal currents

In order to prepare for the derivation of the portal  $\chi$ PT Lagrangian in the following section, we embed the interactions encompassed by the portal LEFTs into appropriate portal currents, as we have done for the interactions of the portal SMEFTs. These currents contain the leading quark-flavour conserving and violating portal operators collected in table 4, but we neglect the subleading quark-flavour violating operators collected in table 5. Hence, the QCD sector of the portal Lagrangian is

$$\begin{aligned} \mathcal{L}_Q^{\text{portal}} = S_\theta w - S_\omega \mathcal{R} - \langle \mathbf{S}_m \mathbf{Q} + \mathbf{V}_l^\mu \mathbf{Q}_\mu + \mathbf{V}_r^\mu \overline{\mathbf{Q}}_\mu \rangle_f - \Lambda_{\text{SM}}^{-2} \langle \mathbf{S}_\gamma \tilde{\mathbf{Q}} + \mathbf{T}^{\mu\nu} \mathbf{Q}_{\mu\nu} + \text{h.c.} \rangle_f \\ - v^{-2} \langle \mathbf{S}_s \mathbf{O}_s + \mathbf{S}_r \mathbf{O}_r + \mathbf{S}_l^- \mathbf{O}_l^- + \mathbf{S}_l^+ \mathbf{O}_l^+ \rangle_f - v^{-2} \langle \langle \mathbf{S}_l^+ \mathbf{O}_l^+ \rangle \rangle_f, \end{aligned} \quad (3.28)$$

where the composite QCD gluon operators  $w$  and  $\mathcal{R}$  are defined in (2.4) and (2.10), the quark bilinears  $\mathbf{Q}$  are defined in (2.8), (2.21), and (2.29), and the quark quadrilinears  $\mathbf{O}$  and  $\mathbf{O}$  are defined in (2.51), (2.57), and (2.58).

The (pseudo-)scalar portal currents  $S_\theta$  and  $S_\omega$  couple to QCD in the same way as the  $\theta$  angle and the gluon coupling  $\omega$  in Lagrangians (2.4) and (2.10). They read

$$S_\omega = \frac{\epsilon_{\text{UV}}}{v} c_i^{S_\omega} s_i, \quad S_\theta = \frac{\epsilon_{\text{UV}}}{v} c_i^{S_\theta} s_i. \quad (3.29)$$

The (pseudo-)scalar portal current  $\mathbf{S}_m$  couples to QCD in the same way as the quark mass matrix in (2.8). It reads

$$\mathbf{S}_m = \epsilon_{\text{UV}} c_i^{S_m} s_i + \frac{\epsilon_{\text{UV}}}{v} c_{ij}^{S_m} s_i s_j + \frac{\epsilon_{\text{UV}}}{v^2} \left( c_{ijk}^{S_m} s_i s_j s_k + c_{\partial^2 i}^{S_m} \partial^2 s_i \right) + \frac{\epsilon_{\text{UV}}}{v^3} c_{ijkl}^{S_m} s_i s_j s_k s_l. \quad (3.30)$$

This current has to be uncharged, so that it obeys

$$\mathbf{S}_m = \mathbf{S}_m + \frac{1}{n_f} S_m, \quad \mathbf{S}_{m\text{d}}^{\text{u}} = \mathbf{S}_{m\text{u}}^{\text{d}} = \mathbf{S}_{m\text{s}}^{\text{u}} = \mathbf{S}_{m\text{u}}^{\text{s}} = 0. \quad (3.31)$$

The left- and right-handed vector portal currents  $\mathbf{V}_l^\mu$  and  $\mathbf{V}_r^\mu$  couple to QCD in the same way as the left- and right-handed EW currents in (2.20). They read

$$\mathbf{V}_l^\mu = \epsilon_{\text{UV}} c_v^L v^\mu + \frac{\epsilon_{\text{UV}}}{v^2} \left[ c_{ij}^L s_i \partial^\mu s_j + (\lambda_{\text{u}}^s c_{\text{us}i}^L e^\dagger \bar{\sigma}^\mu \nu s_i + \lambda_{\text{d}}^s c_{\text{ds}i}^L \nu^\dagger \bar{\sigma}^\mu \nu s_i \right. \quad (3.32a)$$

$$\left. + \lambda_{\text{u}}^s c_{\text{us}a}^L e^\dagger \bar{\sigma}^\mu \xi_a + \lambda_{\text{d}}^s c_{\text{ds}a}^L \nu^\dagger \bar{\sigma}^\mu \xi_a + \text{h.c.} \right],$$

$$\mathbf{V}_r^\mu = \epsilon_{\text{UV}} c_v^R v^\mu. \quad (3.32b)$$

The current  $\mathbf{V}_l^\mu$  is the only portal current that can carry charge due to the contributions generated by virtual  $W$ -boson exchanges, which implies

$$\mathbf{V}_{r\bar{d}}^{\mu u} = \mathbf{V}_{r\bar{u}}^{\mu d} = \mathbf{V}_{rs}^{\mu u} = \mathbf{V}_{ru}^{\mu s} = 0 , \quad \mathbf{V}_{l,r}^\mu = \mathbf{V}_{l,r}^\mu + \frac{1}{n_f} \mathbf{V}_{l,r}^\mu . \quad (3.33)$$

$\mathbf{V}_r^\mu$  and  $\mathbf{V}_l^\mu$  are also Hermitian, so that

$$\mathbf{V}_{l,r\bar{d}}^{\mu s} = (\mathbf{V}_{l,r\bar{s}}^{\mu d})^\dagger , \quad \mathbf{V}_{l\bar{u}}^{\mu d} = (\mathbf{V}_{l\bar{d}}^{\mu u})^\dagger , \quad \mathbf{V}_{l\bar{u}}^{\mu s} = (\mathbf{V}_{l\bar{s}}^{\mu u})^\dagger . \quad (3.34)$$

The dipole portal currents  $\mathbf{T}_\tau^{\mu\nu}$  and  $\mathbf{S}_{\gamma_V}$  couple to QCD in the same way as the dipole currents in Lagrangian (2.28). They read

$$\mathbf{T}_\tau^{\mu\nu} = -\frac{1}{3} F^{\mu\nu} \mathbf{S}_{\gamma_A} , \quad \mathbf{S}_{\gamma_V} = \epsilon_{UV} (\lambda_s^d c_{i\bar{s}d}^{\gamma_V} + \lambda_d^s c_{i\bar{d}s}^{\gamma_V}) s_i . \quad (3.35)$$

The chromomagnetic and tensor currents  $\mathbf{S}_{\gamma_G}$  and  $\mathbf{T}_\tau^{\mu\nu}$  are uncharged and strangeness violating, but not necessarily Hermitian. Hence, the only non-vanishing contributions are

$$\mathbf{S}_{\gamma_G\bar{d}}^s , \quad \mathbf{S}_{\gamma_G\bar{s}}^d , \quad \mathbf{T}_{\tau\bar{d}}^{\mu\nu s} , \quad \mathbf{T}_{\tau\bar{s}}^{\mu\nu d} . \quad (3.36)$$

Finally, the four-quark portal currents mirror the four-quark interactions in Lagrangian (2.59). They read

$$\mathbf{S}_s = h_{si} \frac{\epsilon_{UV}}{v} s_i , \quad \mathbf{S}_r = h_{ri} \frac{\epsilon_{UV}}{v} s_i , \quad (3.37a)$$

$$\mathbf{S}_l^- = h_{ai} \frac{\epsilon_{UV}}{v} s_i , \quad \mathbf{S}_l^+ = h_{si} \frac{\epsilon_{UV}}{v} s_i , \quad \mathfrak{S}_l^+ = \mathfrak{h}_{si} \frac{\epsilon_{UV}}{v} s_i , \quad (3.37b)$$

where the four-quark portal sector parameters  $a_{x1,2} = a_x(c_{l1,2})$  and Wilson coefficients  $c_{l1,2}$  are defined such that they mirror the SM four-quark parameters (2.51) and (2.56) and Wilson coefficients (2.35). It is convenient to define  $a_{x0} = a_x(c_{l0})$  and  $c_{l0} = c_l$ , so that the generic objects  $a_{xi}$  and  $c_{li}$  with  $i = 0, 1, 2$  can be used to collectively refer to the complete set of both SM and portal sector parameters and Wilson coefficients.

Combining the SM and BSM contributions (*cf.* table 6) to the external currents, we define the complete external currents

$$\Theta = \theta + S_\theta , \quad \mathbf{M} = \mathbf{m} + \mathbf{S}_m , \quad \mathbf{R}^\mu = \mathbf{r}^\mu + \mathbf{V}_r^\mu , \quad \mathbf{T}^{\mu\nu} = \mathbf{\tau}^{\mu\nu} + \mathbf{T}_\tau^{\mu\nu} , \quad (3.38a)$$

$$\Omega = \omega + S_\omega , \quad \mathbf{\Gamma} = \mathbf{\gamma} + \mathbf{S}_\gamma , \quad \mathbf{L}^\mu = \mathbf{l}^\mu + \mathbf{V}_l^\mu , \quad (3.38b)$$

and<sup>13</sup>

$$\mathbf{H}_s = h_s + \mathbf{S}_s , \quad \mathbf{H}_r = h_r + \mathbf{S}_r , \quad (3.39a)$$

$$\mathbf{H}_l^- = h_l^- + \mathbf{S}_l^- , \quad \mathbf{H}_l^+ = h_l^+ + \mathbf{S}_l^+ , \quad \mathfrak{H}_l^+ = \mathfrak{h}_l^+ + \mathfrak{S}_l^+ . \quad (3.39b)$$

---

<sup>13</sup> We emphasise that the use of  $h$  and  $H$  for both the Higgs field and the four quark current can not lead to conflicts as these currents only appear at energy scales at which the Higgs field has been integrated out.

		$\Omega$	$\Theta$	$M$	$\Gamma$	$H_s$	$H_r$	$H_l^-$	$H_l^+$	$\mathfrak{H}_l^+$	$L^\mu$	$R^\mu$	$T^{\mu\nu}$
contribution	SM	$\omega$	$\theta$	$m$	$\gamma$	$h_s$	$h_r$	$h_l^-$	$h_l^+$	$\mathfrak{h}_l^+$	$l^\mu$	$r^\mu$	$\tau^{\mu\nu}$
	BSM	$S_\omega$	$S_\theta$	$S_m$	$S_\gamma$	$S_s$	$S_r$	$S_l^-$	$S_l^+$	$\mathfrak{S}_l^+$	$V_l^\mu$	$V_r^\mu$	$T_\tau^{\mu\nu}$
spin		0									1	2	
$\epsilon_{\text{SM}}$		0			1						0	1	
$d$		0	1	1	0			0		1	3		
flavour	representation	1	$8 \oplus 1$	8	8			27		$8 \oplus 1$	8		
	symmetry	$V_\mu^\dagger = V_\mu$											
	DOFs	1	18	16	16			54		9	16		
$\Delta s = \pm 1$		0	4	4	4			4		2	4		

Table 6: List of all external currents interacting with QCD at the strong scale including both SM and BSM contributions. The first three rows list their spin, the order in  $\epsilon_{\text{SM}}$  at which they contribute and their mass dimension  $d$ . Rows four, five, and six list their representations and symmetries under flavour rotations as well as the resulting DOFs. The last row counts the number of strangeness violating DOFs, which are the only relevant DOFs for currents starting contribute at order  $\epsilon_{\text{SM}}$ .

Using these complete external currents in place of the SM external currents, one obtains the corresponding complete interaction Lagrangians

$$\mathcal{L}_Q^\theta \rightarrow \mathcal{L}_Q^\Theta, \quad \mathcal{L}_Q^\omega \rightarrow \mathcal{L}_Q^\Omega, \quad \mathcal{L}_Q^m \rightarrow \mathcal{L}_Q^M, \quad \mathcal{L}_Q^v \rightarrow \mathcal{L}_Q^V, \quad (3.40a)$$

$$\mathcal{L}_Q^\gamma \rightarrow \mathcal{L}_Q^\Gamma, \quad \mathcal{L}_Q^\tau \rightarrow \mathcal{L}_Q^T, \quad \mathcal{L}_Q^h \rightarrow \mathcal{L}_Q^H, \quad (3.40b)$$

where the original Lagrangians are given in (2.18), (2.35), and (2.41). Hence, the complete external current sector of QCD including both SM and hidden contributions is

$$\begin{aligned} \mathcal{L}_Q = & \Theta w - \Omega \Upsilon - \langle M Q + L^\mu Q_\mu + R^\mu \bar{Q}_\mu \rangle_f - \Lambda_{\text{SM}}^{-2} \langle \Gamma \tilde{Q} + T^{\mu\nu} Q_{\mu\nu} + \text{h.c.} \rangle_f \\ & - v^{-2} \langle H_s O_s + H_r O_r + H_l^- O_l^- + H_l^+ O_l^+ \rangle_f - v^{-2} \langle \mathfrak{H}_l^+ \mathfrak{O}_l^+ \rangle_f, \end{aligned} \quad (3.41)$$

where the external currents are defined in (3.38) and (3.39) and summarised in table 6. All of them receive contributions from the SM. However, without NP, the currents  $\Theta$ ,  $\Omega$ ,  $M$ ,  $H$ ,  $H_x$ , and  $\mathfrak{H}_l^+$  are constant. The SM contributions to the currents  $L^\mu$ ,  $R^\mu$  and  $T^{\mu\nu}$  depend on the photon field, and  $L^\mu$  additionally contains the weak leptonic charged current, cf. (2.27) and (2.30).

**Covariant derivatives** In contrast to the parameters defined in section 2, the external currents defined in this section are spacetime dependent, and the  $\chi$ PT Lagrangian derived in the next section contains contributions with derivatives acting on the external currents. To enforce invariance of  $\chi$ PT under the action of the *local*  $G_{LR}$  symmetry equations (2.45) and (2.46), these derivatives have to be promoted to covariant derivatives. The covariant derivative of a generic external current  $\mathfrak{J}$  is

$$i D_\mu \mathfrak{J}_{AC}^{B\dot{D}} \equiv i \partial_\mu \mathfrak{J}_{AC}^{B\dot{D}} + \sum_{i=1}^n L_{\mu a_i}^x \mathfrak{J}_{A_x \dot{C}}^{B\dot{D}} - \sum_{j=1}^m L_{\mu^x}^{b_j} \mathfrak{J}_{AC}^{B_x \dot{D}} + \sum_{k=1}^p R_{\mu \dot{c}_k}^{\dot{x}} \mathfrak{J}_{AC_x}^{B\dot{D}} - \sum_{l=1}^q R_{\mu \dot{x}}^{\dot{d}_l} \mathfrak{J}_{AC}^{B\dot{D}_x}, \quad (3.42)$$

where the capital indices denote multi-indices

$$\begin{aligned}
A &= a_1 \dots a_n , & A_x &= a_1 \dots a_{i-1} x a_{i+1} \dots a_n , \\
B &= b_1 \dots b_m , & B_x &= b_1 \dots b_{i-1} x b_{j+1} \dots b_m , \\
\dot{C} &= \dot{c}_1 \dots \dot{c}_p , & \dot{C}_x &= \dot{c}_1 \dots \dot{c}_{k-1} \dot{x} \dot{c}_{k+1} \dots \dot{c}_p , \\
\dot{D} &= \dot{d}_1 \dots \dot{d}_q , & \dot{D}_x &= \dot{d}_1 \dots \dot{d}_{l-1} \dot{x} \dot{d}_{l+1} \dots \dot{d}_q .
\end{aligned} \tag{3.43}$$

The current  $\Theta$  does not carry any flavour indices, but due to the axial anomaly it transforms like the trace of the logarithm of a unitary matrix  $\vartheta_a^b \equiv e^{i\Theta} \mathbf{1}_a^b$  with two flavour indices. Hence, its covariant derivative can be defined as

$$D_\mu \Theta \equiv \vartheta_\mu \equiv -i \langle \vartheta^\dagger D_\mu \vartheta \rangle_f = \partial_\mu \Theta - L_\mu + R_\mu . \tag{3.44}$$

This object is a chiral invariant and therefore not a covariant derivative in the proper sense. In analogy to gauge fields, the external currents  $\mathbf{L}^\mu$  and  $\mathbf{R}^\mu$  cannot appear by themselves. Instead  $\chi$ PT depends on the left- and right-handed field strength tensors

$$\mathbf{L}^{\mu\nu} = \partial^\mu \mathbf{L}^\nu - \partial^\nu \mathbf{L}^\mu - i [\mathbf{L}^\mu, \mathbf{L}^\nu] , \quad \mathbf{R}^{\mu\nu} = \partial^\mu \mathbf{R}^\nu - \partial^\nu \mathbf{R}^\mu - i [\mathbf{R}^\mu, \mathbf{R}^\nu] . \tag{3.45}$$

To prepare for the eventual decomposition of the  $\chi$ PT Lagrangian into SM and portal contributions, it is also convenient to define the left- and right-handed portal field strength tensors

$$\mathbf{V}_l^{\mu\nu} = \partial^\mu \mathbf{V}_l^\nu - \partial^\nu \mathbf{V}_l^\mu - i [\mathbf{V}_l^\mu, \mathbf{V}_l^\nu] , \quad \mathbf{V}_r^{\mu\nu} = \partial^\mu \mathbf{V}_r^\nu - \partial^\nu \mathbf{V}_r^\mu - i [\mathbf{V}_r^\mu, \mathbf{V}_r^\nu] . \tag{3.46}$$

## 4 Chiral perturbation theory

$\chi$ PT is an effective theory of the light unflavoured and strange pseudoscalar mesons with masses below roughly 1 GeV, which corresponds to the mass scale associated with the GD contribution to *e.g.* the proton mass. Experimentally, one observes nine such mesons  $\phi$ : three pions  $\pi^\pm$  and  $\pi^0$ , four kaons  $K^\pm$ ,  $K^0$ , and  $\bar{K}^0$ , and the two  $\eta$ - and  $\eta'$ -mesons. Neglecting their masses, the typical energy scale of interactions involving these mesons is determined by the meson decay constants, which are defined in terms of the hadronic matrix elements [144]

$$f_\phi = \frac{i}{2m_\phi^2} \langle 0 | \partial^\mu \langle (\mathbf{Q}_\mu - \bar{\mathbf{Q}}_\mu) \boldsymbol{\lambda}_\phi \rangle_f | \phi(p) \rangle e^{-ipx} , \tag{4.1}$$

where  $m_\phi$  is the mass of the meson in question,  $(\mathbf{Q}_\mu - \bar{\mathbf{Q}}_\mu)/2$  is axial-vector quark current, and the matrix  $\boldsymbol{\lambda}_\phi$  projects onto the relevant combination of quark flavours. In particular, the charged pion decay constant  $f_\pi = (65.1 \pm 0.4_{\text{exp}}) \text{ MeV}$ , for which  $\boldsymbol{\lambda}_\phi = \boldsymbol{\lambda}_u^d$ , determines the charged pion decay width [144]

$$\Gamma(\pi^\pm \rightarrow \ell^\pm \nu) = \frac{1}{16\pi m_\pi} \left( 1 - \frac{m_\ell^2}{m_\pi^2} \right) \frac{f_\pi^2 m_\ell^2}{v^4} |V_{ud}|^2 (m_\pi^2 - m_\ell^2) , \tag{4.2}$$

where  $m_\pi = (139.57018 \pm 0.00035_{\text{exp}}) \text{ MeV}$  is the mass of the charged pion and  $m_\ell$  is the mass of the charged lepton  $\ell^\pm = e^\pm, \mu^\pm$ .

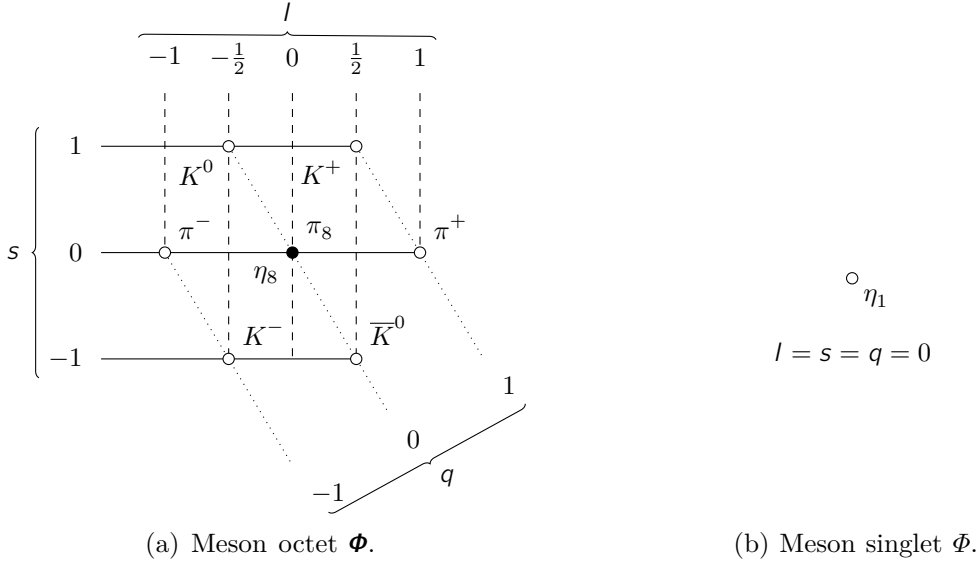


Figure 8: The light pseudoscalar mesons. Panel (a) shows the isospin  $I$ , strangeness  $s$  and electric charge  $q$  quantum numbers of the light pseudoscalar meson octet, and panel (b) shows the quantum numbers of the singlet. The three unflavoured mesons ( $\pi_8$ ,  $\eta_8$ , and  $\eta_1$ ) mix into the neutral mass eigenstates ( $\pi^0$ ,  $\eta$ , and  $\eta'$ ).

The light pseudoscalar mesons can be identified with the pseudo Nambu-Goldstone bosons (PNGBs) of the explicitly broken chiral  $G_{LR} = \text{U}(3)_L \times \text{U}(3)_R$  symmetry (2.5) of the kinetic QCD Lagrangian (2.4).  $\chi\text{PT}$  is defined via a perturbative expansion of QCD around the limit without explicit chiral symmetry breaking, which can be constructed by setting the external currents to zero while keeping only the zeroth order terms in the large  $n_c$  expansion. In this limit, the quark condensate (2.6) still spontaneously breaks the  $G_{LR}$  symmetry to a  $G_V = \text{U}(3)_V$  vector symmetry, so that the Goldstone theorem [180–182] implies the existence of nine massless Nambu-Goldstone bosons (NGBs), one for each spontaneously broken generator. Reintroducing the explicit symmetry breaking generated by the light quark masses (2.8), the other external currents (3.38) and (3.39), and the axial anomaly (2.10) as small perturbations, one obtains the  $\text{U}(3)$  version of  $\chi\text{PT}$ , which contains nine massive PNGBs. The PNGB masses scale as

$$m_\phi^2 \propto \mathcal{L}_{\text{broken}} , \quad (4.3)$$

where  $\mathcal{L}_{\text{broken}}$  is the part of the Lagrangian that contains the explicit symmetry breaking terms. In this version of  $\chi\text{PT}$ , it is necessary to expand QCD in powers of  $n_c^{-1}$  in order to control the impact of the axial anomaly. Without this expansion, the axial anomaly badly breaks the  $\text{U}(1)_A$  symmetry of QCD, and the perturbative expansion in the anomalous contribution to  $\mathcal{L}_{\text{broken}}$  becomes invalid. Following this approach, one obtains the  $\text{SU}(3)$  version of  $\chi\text{PT}$ , which contains only eight PNGBs, one for each broken generator of  $\text{SU}(3)_L \times \text{SU}(3)_R \subset G_{LR}$ . However, we work in the  $\text{U}(3)$  version, since it is better suited for understanding the coupling of the SM mesons to pseudoscalar hidden mediators such as ALPs.

In  $\text{U}(3)$   $\chi\text{PT}$ , the PNGBs parameterise the coset  $G_{LR}/G_V \cong \text{U}(3)_A$  in terms of a non-

linearly realised matrix valued field [105, 109, 149, 183]

$$\mathbf{g}(x) = \exp \frac{i\Phi(x)}{f_0} , \quad (4.4)$$

where the dimensionful parameter  $f_0$  determines the typical energy scale of  $\chi$ PT. At LO in the small momentum expansion of  $\chi$ PT, the meson decay constants in (4.1) are all identical and equal to  $f_0$ , that is,  $f_\phi = f_0$ , but higher order corrections cause the meson decay constants to acquire different values, *cf.* appendix D.1. Since the impact of higher order corrections is smallest for the pion, it is conventional to fix  $f_0$  by matching to the pion decay constant  $f_\pi$ . The PNGB matrix

$$\Phi(x) = \Phi(x) + \frac{1}{n_f} \Phi(x) , \quad \Phi(x) = \langle \Phi(x) \rangle_f , \quad (4.5)$$

transforms as a nonet under  $G_V$ . Its trace  $\Phi$  transforms as a singlet under  $G_V$ , while the traceless contribution  $\Phi$  transforms as an octet. Using the Gell-Mann (GM) matrices<sup>14</sup>  $\lambda_a$  and the rescaled identity matrix  $\lambda_0 = \sqrt{2/n_f} \mathbf{1}$ , which are normalised such that  $\langle \lambda_a \lambda_b \rangle_f = 2\delta_{ab}$ , to parameterise the PNGB octet and singlet according to

$$\Phi = \sum_{a \neq 0} \frac{\phi_a \lambda_a}{\sqrt{2}} = \begin{pmatrix} \frac{\eta_8}{\sqrt{6}} + \frac{\pi_8}{\sqrt{2}} & \pi^+ & K^+ \\ \pi^- & \frac{\eta_8}{\sqrt{6}} - \frac{\pi_8}{\sqrt{2}} & K^0 \\ K^- & \bar{K}^0 & -2\frac{\eta_8}{\sqrt{6}} \end{pmatrix} , \quad \Phi = \left\langle \frac{\phi_0 \lambda_0}{\sqrt{2}} \right\rangle_f = n_f \frac{\eta_1}{\sqrt{3}} , \quad (4.6)$$

their components can be identified with the light meson flavour eigenstates  $\phi_a = \{\pi^\pm, K^\pm, K^0, \bar{K}^0, \pi_8, \eta_8, \eta_1\}$ , whose quantum numbers are depicted in figure 8. There is a large mass-mixing between the  $\eta_8$ - and  $\eta_1$ -mesons. After diagonalisation, the two mass eigenstates are denoted as  $\eta$  and  $\eta'$ . Isospin violating contributions further induce a small mixing between the neutral pion and the two  $\eta$ -mesons, while EW corrections induce a feeble kinetic mixing between the charged kaons and pions.

#### 4.1 Flavour symmetry

In the absence of explicit symmetry breaking, the  $\chi$ PT action has to be invariant under the global  $G_{LR}$  flavour symmetry (2.5) of the kinetic QCD Lagrangian (2.4). The coset matrix  $\mathbf{g}$  and the trace of the pseudoscalar meson matrix  $\Phi/f_0 = -i\langle \ln \mathbf{g} \rangle_f$  transform under the action of  $G_{LR}$  as [105, 109, 149, 183]

$$\mathbf{g} \rightarrow \mathbf{V} \mathbf{g} \bar{\mathbf{V}} , \quad \frac{\Phi}{f_0} \rightarrow \frac{\Phi}{f_0} - i\langle \ln \mathbf{V} \bar{\mathbf{V}} \rangle_f . \quad (4.7)$$

The transformation behaviour of  $\Phi$  mirrors the behaviour of the pseudoscalar external current  $\Theta$  (2.45a), which is also a  $G_V$  singlet. When including the external currents  $J = \{\Omega, \Theta, \mathbf{M}, \mathbf{L}_\mu, \mathbf{R}_\mu, \mathbf{T}_{\mu\nu}, \mathbf{F}, \mathfrak{H}_s, \mathfrak{H}_r, \mathfrak{H}_l\}$ , the  $\chi$ PT action can be obtained by means of a spurion analysis,

---

<sup>14</sup> The GM matrices are  $\lambda_1 = \lambda_u^d + \lambda_d^u$ ,  $\lambda_4 = \lambda_u^s + \lambda_s^u$ ,  $\lambda_6 = \lambda_d^s + \lambda_s^d$ ,  $\lambda_3 = \lambda_u^u - \lambda_d^d$ ,  
 $i\lambda_2 = \lambda_u^d - \lambda_d^u$ ,  $i\lambda_5 = \lambda_u^s - \lambda_s^u$ ,  $i\lambda_7 = \lambda_d^s - \lambda_s^d$ ,  $\sqrt{n_f} \lambda_8 = \lambda_u^u + \lambda_d^d - 2\lambda_s^s$ .



	$\epsilon_{\text{UV}}$	$\epsilon_{\text{SM}}$	$\epsilon_{\text{EW}}$	$\delta$
Numerator	$v$	$\partial^2 \lesssim m_c^2$	$\Lambda_{\chi\text{PT}}^2$	$\partial^2 \lesssim m_K^2$
Denominator	$f_{\text{UV}}$	$\Lambda_{\text{SM}}^2$	$\Lambda_{\text{SM}}^2$	$\Lambda_{\chi\text{PT}}^2$

Table 7: Small parameters that are defined as ratios between the relevant UV, SM, and  $\chi\text{PT}$  scales. The small parameter  $\delta$  also captures the expansion in  $n_c^{-1}$  of U(3)  $\chi\text{PT}$ .  $\Lambda_{\text{SM}} = 4\pi v$  and  $\Lambda_{\chi\text{PT}} = 4\pi f_0$  are defined such that they include NDA loop factors. For momenta  $\partial^2 \lesssim m_K^2$ , one has  $\epsilon_{\text{SM}} = \delta \epsilon_{\text{EW}}$ .

which corresponds to enforcing the invariance of the  $\chi\text{PT}$  path integral under the *local* flavour symmetry (2.5) [105, 109, 149, 183–185]. This entails the promotion of the partial derivative  $\partial^\mu \mathbf{g}$  to a covariant derivative

$$D^\mu \mathbf{g} = \partial^\mu \mathbf{g} - i(\mathbf{L}^\mu \mathbf{g} - \mathbf{g} \mathbf{R}^\mu), \quad (4.8)$$

where the left- and right-handed external currents  $\mathbf{L}^\mu$  and  $\mathbf{R}^\mu$  effectively fulfil the role of gauge fields. Besides being parts of the covariant derivatives, these two external currents also contribute to the  $\chi\text{PT}$  action via operators involving the left- and right-handed field strength tensors  $\mathbf{L}_{\mu\nu}$  and  $\mathbf{R}_{\mu\nu}$ , *cf.* definition (3.45), while the remaining external currents appear as regular building blocks of the theory.  $G_{LR}$  invariant operators in  $\chi\text{PT}$  are then constructed by taking quark-flavour traces of either purely left- or right-handed products of the coset matrix  $\mathbf{g}$ , the external currents, and their covariant derivatives.

The spurion analysis is also a standard tool used to embed  $\chi\text{PT}$  into the remainder of the SM, by parameterising the coupling of QCD to the EW sector in terms of the external currents  $\Theta$ ,  $\mathbf{M}$ ,  $\mathbf{L}^\mu$ , and  $\mathbf{R}^\mu$ , which describe CP-violation, quark masses, and EM vector current interactions in the SM, respectively. For more details, see *e.g.* the general introductions to  $\chi\text{PT}$  in [184–187]. In the SM, the spurion approach neglects contributions to the  $\chi\text{PT}$  Lagrangian that are generated from diagrams with virtual photon exchanges. Starting at order  $\alpha_{\text{EM}} \propto e^2$ , one has to include an additional set of EM operators in order to complete  $\chi\text{PT}$ . For extensive listings of these operators, see *e.g.* [188–193]. In particular, they are necessary to obtain the correct SM estimates for *e.g.* the pion mass splitting and the  $\epsilon'/\epsilon$  ratio [194–196], which measures the correlation of CP-violation in decays of neutral kaons into pairs of charged pions,  $K^0 \rightarrow \pi^+ \pi^-$ , and neutral pions,  $K^0 \rightarrow \pi^0 \pi^0$ .

## 4.2 Power counting

When accounting only for the explicit symmetry breaking due to the axial anomaly, U(3)  $\chi\text{PT}$  is defined via a simultaneous expansion in small momenta  $\partial^2/\Lambda_{\chi\text{PT}}^2$  and  $n_c^{-1}$ , where  $\Lambda_{\chi\text{PT}} = 4\pi f_0 = (803 \pm 15_{\text{exp}} \pm \text{NNLO}) \text{ MeV}$  is the symmetry breaking scale of  $\chi\text{PT}$  [105, 109, 149, 175, 183]. Following [109], we combine both of these expansions by defining a single degree of smallness  $\delta \propto \partial^2/\Lambda_{\chi\text{PT}}^2 \propto n_c^{-1}$ . This is appropriate for kaon decays, since  $n_c^{-1} = 1/3 \simeq m_K^2/\Lambda_{\chi\text{PT}}^2$ . At lower energies, such as for  $\partial^2 \simeq m_\pi^2 \ll m_K^2$ , the suppression associated with the small momenta is a much better expansion parameter than  $n_c^{-1}$ . In this case, it is more appropriate to work with SU(2) or SU(3)  $\chi\text{PT}$ , so that the large  $n_c$  expansion, which is necessary in U(3)  $\chi\text{PT}$ , can be avoided. Besides the expansion in  $\delta$ , we also track the suppression due to  $\epsilon_{\text{SM}}$  and  $\epsilon_{\text{UV}}$ , as defined in (2.23) and (3.2), and we eliminate operators

that are doubly suppressed in either one of these two parameters. Table 7 summarises the relation between the four expansion parameters.

**Momentum expansion**  $\chi$ PT can be expanded in powers of  $\partial^2/\Lambda_{\chi\text{PT}}^2 = \partial^2/(4\pi f_0)^2$  by adopting the general power counting scheme for low energy EFTs [25], which is established by studying the behaviour of individual diagrams under a rescaling  $p_i \rightarrow xp_i$  of the external momenta  $p_i$ . Since  $f_0^2 \sim \partial^2$  defines the typical energy scale of  $\chi$ PT, the resulting power counting in  $\chi$ PT is equivalent to the  $(4\pi)^{-1}$  expansion of NDA [175]. Applying the NDA power counting rules, derivatives  $\partial_\mu$  are suppressed by factors of  $\sqrt{\delta}$ , while powers of the PNGB matrix  $\Phi$  are unsuppressed. Since the external currents  $L^\mu$  and  $R^\mu$  appear in the covariant derivative (4.8), they also count as  $\sqrt{\delta} \propto \partial_\mu/\Lambda_{\chi\text{PT}}$ . The external currents  $M$ ,  $\Gamma$ , and  $T^{\mu\nu}$  contribute to the PNGB masses, so relation (4.3) implies that all three of them count as  $M, \Gamma, T^{\mu\nu} \propto m_\phi^2 \propto \partial^2 \propto \delta$ . In summary, each of these building blocks counts as

$$g \propto 1, \quad \partial, L, R \propto \sqrt{\delta}, \quad M, \Gamma, T \propto \delta. \quad (4.9)$$

**Large  $n_c$  expansion** The standard formula for large  $n_c$  scaling behaviour for diagrams without four-quark operators (2.13) shows that the leading QCD diagrams with a given number of quark loops are suppressed by one factor of  $n_c^{-1}$  for each quark-loop. Since  $\chi$ PT operators with  $n_q$  quark flavour traces have to be generated by contributions in the QCD path-integral with at least  $n_q$  quark loops, each quark-flavour trace in  $\chi$ PT counts as  $n_c^{-1}$  [appendix A of 109]. The large  $n_c$  scaling behaviour of the leading QCD diagrams also directly implies that the external currents  $\Theta$  and  $\Omega$  count as  $\delta \propto n_c^{-1}$ .

Equation (2.40) establishes a modified large  $n_c$  scaling for QCD diagrams with four-quark vertices. It implies that  $\chi$ PT operators with one four-quark current insertion,  $\mathfrak{H}_x$  or  $H_x$ , are enhanced by a relative factor of  $n_c$  associated with the four-quark vertex. In addition, the leading contributions to the QCD path-integral with one four-quark insertion contain two quark loops but scale as if they contain only a single quark loop. Each additional quark loop that is not associated with the four-quark insertion still gives a suppression  $\propto n_c^{-1}$ . In total, this means that  $\chi$ PT operators with one four-quark current insertion and  $n_q = 1, 2$  quark flavour traces scale as  $n_c^2$ , while operators with one four-quark current insertion and  $n_q > 2$  quark flavour traces scale as  $n_c^{4-n_q}$ . In summary, each of the above building blocks counts as

$$S_\omega, \Theta \propto \delta, \quad \mathfrak{H}_x, H_x \propto \delta^{-1}, \quad \langle \circ \rangle_f^n \propto \delta^{\max(n-n_h, n_h)}, \quad n_h = 0, 1. \quad (4.10)$$

where  $n_h = 0, 1$  is the number of four-quark current insertions.

**Expansion in powers of  $\epsilon_{\text{SM}}$  and  $\epsilon_{\text{UV}}$**  The parameter  $\epsilon_{\text{SM}} = \partial^2/\Lambda_{\text{SM}}^2$  with  $\Lambda_{\text{SM}} = 4\pi v$  measures the degrees of smallness associated with higher-dimensional operators at low energies. However, it mixes the small momentum expansion of  $\chi$ PT with the suppression due to virtual  $W$ -boson exchanges. In order to separate these two expansions, we define  $\epsilon_{\text{SM}} = \delta\epsilon_{\text{EW}}$ , where  $\epsilon_{\text{EW}} = f_0^2/v^2 = \Lambda_{\chi\text{PT}}^2/\Lambda_{\text{SM}}^2$  is the ratio between the  $\chi$ PT and EW scales. With this definition, the external currents  $\Gamma$ ,  $T^{\mu\nu}$ ,  $\mathfrak{H}_x$ , and  $H_x$  are all suppressed by one factor of  $\epsilon_{\text{EW}}$  in  $\chi$ PT, independent of any additional momentum suppression. Additionally, the suppression due to

$n_t$	$n'_t$	$n_c^m$	$\delta^n$			
			0	1	2	3
	1, 2	2	$\partial^0 n_c^2$	$\partial^2 n_c^2$	$\partial^4 n_c^2$	$\partial^6 n_c^2$
1	3	1		$\partial^0 n_c^1$	$\partial^2 n_c^1$	$\partial^4 n_c^1$
2	4	0			$\partial^0 n_c^0$	$\partial^2 n_c^0$
3	5	-1				$\partial^0 n_c^{-1}$
			GD	$\chi$ PT		

Table 8: Impact of flavour traces on the  $\delta$ -counting of an operator.  $n_t$  counts the number of flavour traces in operators without four-quark current insertions, while  $n'_t$  counts the same number in operators with four-quark insertions. Note that  $m = 2 - n_t = \min(4 - n'_t, 2)$  and that  $\chi$ PT operators proportional to  $n_c^2$  are only possible in the modified four-quark counting scheme

factors of  $\epsilon_{UV}$  has to be taken into account when considering modifications due to the  $\Omega$  current, since the SM contribution  $\omega \propto g_s^{-2}$  is integrated out when constructing  $\chi$ PT, so that only the hidden sector contributions  $S_\omega$  remains. At LO in both  $\epsilon_{UV}$  and  $\epsilon_{EW}$ , the  $\chi$ PT action can be at most linear in each of the above currents.

### 4.3 Construction of the portal $\chi$ PT Lagrangian

We construct the complete  $\chi$ PT Lagrangian that couples the light pseudoscalar mesons to generic hidden sectors at LO. To this end, we first summarise the shape of the  $\chi$ PT Lagrangian when neglecting  $\epsilon_{EW}$  and  $\epsilon_{UV}$  suppressed hidden sector contributions. In this case, the only non-vanishing external currents are  $\mathbf{L}^\mu$ ,  $\mathbf{R}^\mu$ ,  $\mathbf{M}$ , and  $\Theta$ , and the resulting  $\chi$ PT Lagrangian is well established, see *e.g.* the discussions in [105, 109, 149, 183–187, 197]. Afterwards, we consider the  $\epsilon_{EW}$  and  $\epsilon_{UV}$  suppressed contributions and use the spurion approach to construct the novel contributions with general spacetime dependent currents  $S_\omega$ ,  $\mathbf{F}$ ,  $\mathfrak{H}_x$ , and  $\mathbf{H}_x$ .

The leading contributions to the connected part of the QCD path integral count as order  $n_c^2$ , and determine GD in the large  $n_c$  limit [151, 153–155]. Since meson dynamics are determined by connected QCD diagrams with at least one quark loop, which scale at most as order  $n_c$ ,  $\chi$ PT operators have to be suppressed by at least a factor of  $\delta$  compared to the leading QCD diagrams. The only chiral invariant that could contribute at this order is

$$\hat{\Theta} = i \left( \Theta - \frac{\Phi}{f_0} \right), \quad (4.11)$$

where the hat indicates a flavour invariant quantity. However, an operator proportional to  $\hat{\Theta}$  is forbidden by parity conservation [109, 149, 183]. Hence, the leading contributions to the  $\chi$ PT action are of order  $\delta^2$ . See table 8 for an overview of the possible orders of an operator.

**Order  $\delta^2$**  Operators that contribute at this order can count either as order  $\partial^2 n_c$  or order  $\partial^0 n_c^0$ . Operators that count as order  $\partial^2 n_c$  contain only a single quark-flavour trace. In the absence of explicit symmetry breaking due to the mass-like current  $\mathbf{M}$ , the only available

operator of this type is [105, 109, 149, 183–187, 197]

$$\mathcal{L}_U^{D^2} = \frac{f_0^2}{2} \langle U_\mu U^\mu \rangle_f, \quad (4.12)$$

where the *left-handed* Maurer-Cartan (MC) field associated with  $\mathbf{g}$  is

$$U_\mu = \mathbf{u}_\mu - \mathbf{L}_\mu + \widehat{\mathbf{R}}_\mu, \quad \mathbf{u}_\mu = i \mathbf{g} \partial_\mu \mathbf{g}^\dagger = -i (\partial_\mu \mathbf{g}) \mathbf{g}^\dagger, \quad \widehat{\mathbf{R}}_\mu = \mathbf{g} \mathbf{R}_\mu \mathbf{g}^\dagger \quad (4.13)$$

and  $\mathbf{u}_\mu$  is the MC field obtained when neglecting the external currents  $\mathbf{L}_\mu$  and  $\mathbf{R}_\mu$ . Bold hatted operators such as  $\widehat{\mathbf{R}}_\mu$  are composite operators constructed from an external current and the coset matrix  $\mathbf{g}$  such that they transform under  $G_{LR}$  in the same way as  $U_\mu$ .<sup>15</sup> The MC field transforms as

$$U_\mu \rightarrow \mathbf{V} U_\mu \mathbf{V}^\dagger \quad (4.14)$$

and corresponds to the low energy realisation (LER) of the conserved current associated with *left-handed* chiral quark flavour rotations, *cf.* section 2.2. It obeys the relation

$$D_\mu U_\nu - D_\nu U_\mu = i [U_\mu, U_\nu] - \mathbf{L}_{\mu\nu} + \widehat{\mathbf{R}}_{\mu\nu}, \quad \widehat{\mathbf{R}}_{\mu\nu} = \mathbf{g} \mathbf{R}_{\mu\nu} \mathbf{g}^\dagger, \quad (4.15a)$$

$$\partial_\mu \mathbf{u}_\nu - \partial_\nu \mathbf{u}_\mu = i [\mathbf{u}_\mu, \mathbf{u}_\nu], \quad (4.15b)$$

and its flavour trace

$$U^\mu = \langle U^\mu \rangle_f = \frac{D^\mu \Phi}{f_0} = \frac{\partial^\mu \Phi}{f_0} - L^\mu + R^\mu \quad (4.16)$$

encodes the covariant derivative of the trace of the coset matrix. Note that the above object  $D_\mu \Phi$  is not a covariant derivative in the strict sense, since it remains invariant under chiral rotations rather than following the transformation law for  $\Phi$  in equation (4.7). When accounting for the quark mass-like current  $\mathbf{M}$ , it is possible to construct a second operator that also contributes at order  $\partial^2 n_c$  [109, 183–187, 197]

$$\mathcal{L}_U^M = \frac{f_0^2 b_0}{2} \widehat{\mathbf{M}} + \text{h.c.}, \quad (4.17)$$

where

$$\widehat{\mathbf{M}} = \langle \widehat{\mathbf{M}} \rangle_f, \quad \widehat{\mathbf{M}} = \mathbf{g} \mathbf{M}, \quad \widehat{\mathbf{M}} \rightarrow \mathbf{V} \widehat{\mathbf{M}} \mathbf{V}^\dagger. \quad (4.18)$$

This nonet mass term gives rise to the dominant contribution to the physical masses of the pions, kaons, and the  $\eta$ -meson. The mass of the heavy  $\eta'$ -meson is dominated by the contribution of the third and final term in the LO  $\chi$ PT Lagrangian, the PNGB singlet mass term [109, 149, 152, 183]

$$\mathcal{L}_U^{\Theta^2} = \frac{f_0^2 m_0^2}{2n_f} \widehat{\Theta}^2. \quad (4.19)$$

---

<sup>15</sup>  $\mathbf{g}$  is defined such that it is adjointed in the mass term (4.17) whenever the canonical quark mass matrix  $\mathbf{M}$  is adjoint. Furthermore, we define the MC field to be left-handed (rather than right-handed) in order to simplify the description of  $W$ -boson induced processes. However, note that relations that involve only  $U_\mu$ ,  $\vartheta_\mu$ , and hatted quantities are invariant under a change of either definition, provided that the hat-operation is first redefined such that it transform external currents into purely right-handed (rather than left-handed) objects and then reapplied appropriately.

This term contains two flavour traces and no derivatives, so that it enters at order  $\partial^0 n_c^0$  rather than  $\partial^2 n_c$ . It is associated with the explicit chiral symmetry breaking due to the axial anomaly (2.10). Putting all three contributions together, the complete LO Lagrangian

$$\mathcal{L}_U^{\delta^2} = \mathcal{L}_U^{D^2} + \mathcal{L}_U^M + \mathcal{L}_U^{\Theta^2} \quad (4.20)$$

yields the LO EOM

$$\frac{1}{2}(gD^2 g^\dagger - D^2 g g^\dagger) = \frac{b_0}{2}(\widehat{M} - \widehat{M}^\dagger) + \frac{m_0^2}{n_f} \widehat{\Theta} \mathbf{1} . \quad (4.21)$$

Together with the general identity (4.13), this EOM implies that, without loss of generality, terms containing  $gD^2 g^\dagger$  and its Hermitian conjugate can always be eliminated from higher order Lagrangians.

**Order  $\delta^3$**  Starting at this order, the  $\chi$ PT action can, in principle, contain operators with covariant derivatives acting on  $\mathbf{L}^{\mu\nu}$ ,  $\mathbf{R}^{\mu\nu}$ ,  $\mathbf{M}$ , and  $\Theta$ . However, up to corrections of order  $\delta^4$  or higher, partial integration (PI) can always be used to eliminate operators with derivatives acting on  $\mathbf{L}^{\mu\nu}$ ,  $\mathbf{R}^{\mu\nu}$ ,  $\mathbf{M}$  in favour of operators with derivatives acting only on  $\mathbf{g}$  or  $\Theta$ .

Operators that contribute at order  $\delta^3$  can count either as order  $\partial^4 n_c$ , order  $\partial^2 n_c^0$ , or order  $\partial^0 n_c^{-1}$ . Operators that count as order  $\partial^4 n_c$  can contain only a single quark-flavour trace. In the absence of external currents, the only available operators of this type are [109, 183]

$$\mathcal{L}_U^{D^4} = (2L_2 + L_3)\langle U^\mu U_\mu U^\nu U_\nu \rangle_f + L_2\langle U_\mu U_\nu U^\mu U^\nu \rangle_f , \quad (4.22)$$

where contributions with more than one derivative acting on a single coset matrix  $\mathbf{g}$  can be eliminated using PI, the EOM (4.21), or identity (4.13). The quark mass-like current  $\mathbf{M}$  generates the additional contributions [109, 183]

$$\mathcal{L}_U^{D^2 M} = L_5 b_0 \langle \widehat{M} U_\mu U^\mu \rangle_f + \text{h.c.} , \quad \mathcal{L}_U^{M^2} = L_8 b_0^2 \left( \langle \widehat{M}^2 \rangle_f + \text{h.c.} \right) + H_2 b_0^2 \langle \widehat{M}^\dagger \widehat{M} \rangle_f . \quad (4.23)$$

In the operator proportional to  $H_2$ , the dependence on the coset field  $\mathbf{g}$  drops out, so that the term does not contribute to perturbatively computed  $S$ -matrix elements, but it has to be added to the Lagrangian as a counter term in order to renormalise the theory [105, 109, 183–185, 197]. The field strength tensors  $\mathbf{L}_{\mu\nu}$  and  $\mathbf{R}_{\mu\nu}$  generate the contributions [105, 109, 183]

$$\mathcal{L}_U^{D^2 V} = -i L_9 \langle U^\mu U^\nu (\mathbf{L}_{\mu\nu} + \widehat{\mathbf{R}}_{\mu\nu}) \rangle_f , \quad (4.24a)$$

$$\mathcal{L}_U^{V^2} = L_{10} \langle \mathbf{L}^{\mu\nu} \widehat{\mathbf{R}}_{\mu\nu} \rangle_f + H_1 \langle \mathbf{L}_{\mu\nu} \mathbf{L}^{\mu\nu} + \widehat{\mathbf{R}}_{\mu\nu} \widehat{\mathbf{R}}^{\mu\nu} \rangle_f , \quad (4.24b)$$

where the operator proportional to  $H_1$  is another counter term. The operators that count as order  $\partial^2 n_c^0$  contain two flavour traces. In the absence of external currents, the only available operator of this type is the kinetic term [109, 183]

$$\mathcal{L}_U^{DD} = \frac{f_0^2}{2n_f} \Lambda_1 U_\mu U^\mu . \quad (4.25)$$

The external currents  $\mathbf{M}$  and  $\Theta$  induce the further mass-like term [109, 183]

$$\mathcal{L}_U^{M\Theta} = \frac{f_0^2 b_0}{2n_f} \Lambda_2 \widehat{M} \widehat{\Theta} + \text{h.c.} , \quad (4.26)$$

and a final counter term that depends on the covariant derivative of  $\Theta$  defined in (3.44) [109, 183]

$$\mathcal{L}_U^{\vartheta^2} = \frac{f_0^2}{2n_f} H_0 \vartheta_\mu \vartheta^\mu . \quad (4.27)$$

There is no kinetic mixing term proportional to  $U_\mu \vartheta^\mu$ , since this operator can always be eliminated via a shift of  $\Phi$ . There are also no operators of order  $\partial^0 n_c^{-1}$ , since the only candidate operator is proportional to  $\widehat{\Theta}^3$ , and it is forbidden due to parity conservation in QCD.

**Wess-Zumino-Witten action** Since the NGBs are pseudoscalar fields, a parity transformation corresponds to the combined transformation of spatial inversion  $x \leftrightarrow -x$  and meson conjugation  $\mathbf{g} \leftrightarrow \mathbf{g}^\dagger$ . The contributions derived so far are invariant under both transformations separately, so that the resulting  $\chi$ PT Lagrangian is more symmetric than QCD. In the absence of external currents, there is no four dimensional Lagrangian that breaks this additional symmetry [198], but starting at order  $\delta^3$  it is possible to construct a so-called Wess-Zumino-Witten (WZW) contribution to the  $\chi$ PT action that takes the form of a five dimensional integral over a sub-manifold of the nine dimensional space of field values that can be assumed by the coset matrix  $\mathbf{g}(x)$  [199]. This integral can be connected to an action written in terms of a Lagrangian density by identifying Minkowski space with the four dimensional boundary of this sub-manifold. Hence, the WZW term can be written as [199]

$$\Gamma_u^{n_c} = -\frac{n_c}{(2\pi)^2} \int dx^5 \epsilon_{ijklm} \omega_0^{ijklm}(\mathbf{u}^i) , \quad \omega_0^{ijklm}(\mathbf{u}^i) = \frac{2}{5!} \langle \mathbf{u}^i \mathbf{u}^j \mathbf{u}^k \mathbf{u}^l \mathbf{u}^m \rangle_f , \quad (4.28)$$

where  $\omega_0^{ijklm}(\mathbf{u}^i)$  is the pure-gauge CS term and the  $i, j, k, \dots$  denote coordinate indices of the five-dimensional sub-manifold. The left- and right-handed external currents  $\mathbf{L}^\mu$  and  $\mathbf{R}^\mu$  generate additional WZW contributions that can be written in the form of a conventional four dimensional Lagrangian [199–202]

$$\mathcal{L}_U^{n_c} = \frac{n_c}{(2\pi)^2} \epsilon_{\mu\nu\rho\sigma} (\rho^{\mu\nu\rho\sigma}(\mathbf{u}^\mu + \widehat{\mathbf{R}}^\mu, \mathbf{L}^\mu) + \rho^{\mu\nu\rho\sigma}(\widehat{\mathbf{R}}^\mu, -\mathbf{u}^\mu)) , \quad (4.29)$$

where the Bardeen counter-term of two vector currents  $\mathbf{V}_i^\mu$  is

$$\rho^{\mu\nu\rho\sigma}(\mathbf{V}_0^\mu, \mathbf{V}_1^\mu) = \frac{2}{4!} \left\langle \mathbf{V}_0^\mu \sigma_1^{\nu\rho\sigma} + \sigma_0^{\mu\nu\rho} \mathbf{V}_1^\sigma + \frac{i}{2} \mathbf{V}_0^\mu \mathbf{V}_1^\nu \mathbf{V}_0^\rho \mathbf{V}_1^\sigma \right\rangle_f . \quad (4.30)$$

This term shares a common contribution with the four dimensional gauge transformation of the five dimensional CS term

$$\omega_1^{\mu\nu\rho\sigma} = \frac{1}{3!} \langle \mathbf{v}_\epsilon \partial^\mu \sigma_i^{\nu\rho\sigma} \rangle_f , \quad \sigma_i^{\mu\nu\rho} = \frac{1}{2} \mathbf{F}_i^{\mu\nu} \mathbf{V}_i^\rho + \frac{1}{2} \mathbf{V}_i^\mu \mathbf{F}_i^{\nu\rho} + i \mathbf{V}_i^\mu \mathbf{V}_i^\nu \mathbf{V}_i^\rho , \quad (4.31)$$

where  $\mathbf{v}_\epsilon$  is a gauge parameter. The WZW action (4.28) and the gauged WZW Lagrangian (4.29) constitute the LO contributions to interactions with an odd number of mesons such as  $K^+ K^- \rightarrow \pi^+ \pi^- \pi^0$  and  $\pi^0 \rightarrow \gamma\gamma$ .

$\delta^2$				$\delta^3$			
$\Lambda_{\chi\text{PT}}$	$f_0$	$b_0$	$m_0$	$4L_5$	$4L_8$	$2H_2$	$\Lambda_2$
$4\pi f_0$	$\sqrt{n_c}$	$n_c^{-1/2} \Lambda_{\chi\text{PT}}$	$n_c^{-3/2} \Lambda_{\chi\text{PT}}$	$n_c(4\pi)^{-2}$	$n_c(4\pi)^{-2}$	$n_c(4\pi)^{-2}$	$n_c^{-1}$

Table 9: NDA and large  $n_c$  scaling of selected coefficients that appear in the order  $\delta^2$  and  $\delta^3$  Lagrangians. Additionally, we have made the omitted symmetry factors explicit.

**Low energy coefficients and loops** The prefactors of operators that contribute at order  $\partial^{2n} n_c^m$  scale as

$$\text{coefficient} \propto \Lambda_{\chi\text{PT}}^{2-2n} f_0^2 n_c^{m+n-2}, \quad \Lambda_{\chi\text{PT}}, f_0 \propto \sqrt{n_c}, \quad (4.32)$$

where  $f_0$  scales as  $\sqrt{n_c}$  in order to reflect the large  $n_c$  counting of the kinetic Lagrangian (4.12) in the LO  $\chi\text{PT}$  Lagrangian. The standard notation, which we also follow, does not make this scaling explicit. However, we have summarised the omitted NDA scaling and symmetry prefactors in table 9 and will quote numerical values of the dimensionless next-to-leading order (NLO) coefficient with symmetry factors and factors of  $4\pi$  made explicit.

Diagrams with  $n_l$  loops are suppressed by factors  $(4\pi f_0)^{-2n_l} \propto (4\pi)^{-2n_l} n_c^{-n_l} \propto \delta^{2n_l}$  compared to tree-level diagrams. This implies that diagrams with one loop start to contribute at next-to-next-to-leading order (NNLO). Since we restrict ourselves to NLO contributions, we do not consider these loop corrections. In particular, we fix the values of the low energy coefficients (LECs) by using tree-level predictions for the light meson observables. However, it is necessary to emphasise that one-loop contributions are expected to be numerically sizeable due to enhancement from large chiral logarithms that scale as  $\propto \ln \partial^2 / \mu^2$ . In addition, one has to account for these corrections in order to capture the scale dependence of the  $L_i$  and  $H_i$  parameters. As a result, the tree-level estimates for the LO and NLO LECs can only be expected to be order-of-magnitude accurate. Since the dominant corrections at NNLO are generated by chiral loops, we expect that our estimates are the most well aligned with the NNLO estimates that one obtains when working with a relatively small renormalisation scale, such as  $\mu^2 = m_{K^\pm}^2$ .

In total, the LO and NLO U(3)  $\chi\text{PT}$  Lagrangians contain 13 LECs: Three LO coefficients  $f_0$ ,  $b_0$ ,  $m_0$ , and ten NLO coefficients  $L_i$ ,  $H_i$ , and  $\Lambda_i$ . The coefficients  $f_0$ ,  $m_0$ , and  $\Lambda_i$  remain finite even when accounting for loop corrections, but in general the coefficient  $b_0$ , the  $L_i$ , and the  $H_i$  have to be renormalised. We use the NLO tree-level estimates derived in appendix D.1, which gives

$$f_0 = (63.9 \pm 1.2_{\text{exp}}) \text{ MeV} \pm \text{NNLO}, \quad m_0 = 4\pi(76.3 \pm 1.4_{\text{exp}}) \text{ MeV} \pm \text{NNLO}, \quad (4.33)$$

and

$$\sqrt{b_0 m_{\text{ud}}} = 4\pi(10.68 \pm 0.08_{\text{exp}}) \text{ MeV} \pm \text{NNLO}, \quad (4.34a)$$

$$\sqrt{b_0 m_{\text{s}}} = 4\pi(50.95 \pm 0.28_{\text{exp}}) \text{ MeV} \pm \text{NNLO}. \quad (4.34b)$$

See figure 9 for a comparison of the energy scales involved in this work. For the subsequent discussion in section 4.4, we also require the values of the NLO parameters  $L_5$  and  $L_8$ . Using

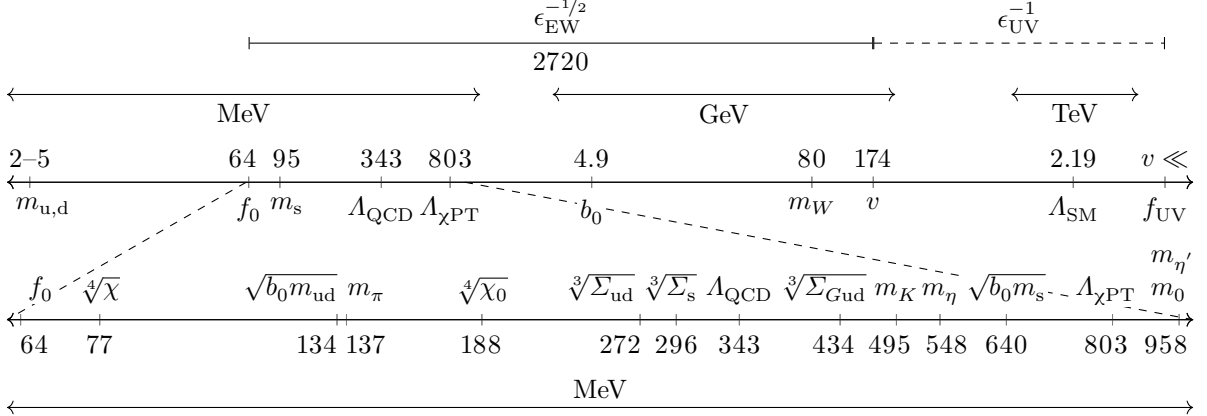


Figure 9: Illustration of the energy scales appearing in portal  $\chi$ PT. The numeric values correspond to the central values, for simplicity we omit all uncertainties.

the tree-level results from appendix D.1, one obtains the estimates

$$4(4\pi)^2 L_5 = 0.66 \pm 0.04_{\text{exp}} \pm \text{NNLO} , \quad A_2 = 0.814 \pm 0.023_{\text{exp}} \pm \text{NNLO} , \quad (4.35a)$$

$$4(4\pi)^2 L_8 = 0.215 \pm 0.033_{\text{exp}} \pm \text{NNLO} , \quad (4.35b)$$

which are renormalisation scale independent at this level of accuracy.

#### 4.3.1 Weak current contributions

The weak currents  $\boldsymbol{\Gamma}$ ,  $\boldsymbol{T}^{\mu\nu}$ ,  $\mathfrak{H}_l$ ,  $\mathfrak{H}_s$ , and  $\mathfrak{H}_r$  are suppressed by powers of  $\epsilon_{\text{EW}}$ , so that they are only relevant in quark-flavour violating transitions. As we have already discarded the quark-flavour conserving contributions to these currents in sections 2 and 3, the  $\chi$ PT operators that involve them will automatically violate quark flavour. We only include the leading contributions for each current. These contributions can be either of order  $\epsilon_{\text{EW}}\delta$ ,  $\epsilon_{\text{EW}}\delta^2$ , or  $\epsilon_{\text{EW}}\delta^3$ .

**Dipole contributions** The dipole current  $\boldsymbol{\Gamma}$  transforms under chiral flavour rotations like the mass-like current  $\boldsymbol{M}$ , so it couples to  $\chi$ PT in the same way. Hence, there is only one operator with  $\boldsymbol{\Gamma}$  at order  $\epsilon_{\text{EW}}\delta^2$ ,

$$\mathcal{L}_U^\Gamma = \frac{\epsilon_{\text{EW}} f_0^2 b_0}{2} \kappa_\Gamma \hat{\Gamma} + \text{h.c.} , \quad \hat{\Gamma} = \langle \hat{\Gamma} \rangle_f , \quad \hat{\Gamma} = g \boldsymbol{\Gamma} . \quad (4.36)$$

where  $\kappa_\Gamma$  is a free parameter. For the sake of completeness, we also note that there are three additional contributions with  $\boldsymbol{\Gamma}$  that enter at order  $\epsilon_{\text{EW}}\delta^3$ . These are

$$\mathcal{L}_U^{\Gamma D^2} = \frac{\epsilon_{\text{EW}} b_0}{4} \kappa_\Gamma^{D^2} \langle \hat{\Gamma} \boldsymbol{U}_\mu \boldsymbol{U}^\mu \rangle_f + \text{h.c.} , \quad \mathcal{L}_U^{\Gamma \Theta} = \frac{\epsilon_{\text{EW}} f_0^2 b_0}{2 n_f} \kappa_\Gamma^\Theta \hat{\Gamma} \hat{\Theta} + \text{h.c.} , \quad (4.37a)$$

$$\mathcal{L}_U^{\Gamma M} = \frac{\epsilon_{\text{EW}} b_0^2}{2} \left( \kappa_\Gamma^M \langle \hat{\Gamma} \hat{\boldsymbol{M}} \rangle_f + \kappa_\Gamma^{M'} \langle \hat{\Gamma} \hat{\boldsymbol{M}}^\dagger \rangle_f \right) + \text{h.c.} , \quad (4.37b)$$



	QCD					$\chi$ PT			
current	$\mathbf{H}_s$	$\mathbf{H}_r$	$\mathbf{H}_l^-$	$\mathbf{H}_l^+$	$\mathfrak{H}_l^+$	$H_1$	$H_8$	$H_b$	$H_{27}$
SM	$\mathbf{h}_s$	$\mathbf{h}_r$	$\mathbf{h}_l^-$	$\mathbf{h}_l^+$	$\mathfrak{h}_l^+$	$h_1$	$h_8$	$h_b$	$h_{27}$
BSM	$\mathbf{S}_s$	$\mathbf{S}_r$	$\mathbf{S}_l^-$	$\mathbf{S}_l^+$	$\mathfrak{S}_l^+$	$S_1$	$S_8$	$S_b$	$S_{27}$
representation	8				27	1			

Table 10: Currents that couple to the QCD four-quark operators introduced in section 2.3 and the derived parameters we use in  $\chi$ PT, *cf.* equations (4.41), (4.44), and (4.46). The table indicates the names for the SM and BSM contributions, as well as their representations under  $G_{LR}$ .

The  $\kappa_F^x$  with  $x = D^2, \Theta, M$ , and  $M'$  are four more free parameters, and the second operator in (4.37b) is another counter term. The impact of the term  $\mathcal{L}_U^{\Gamma D^2}$  in the SM, where  $\Gamma \rightarrow \gamma$  is a constant, has been discussed in [117]. The authors also estimate the parameter  $\kappa_F^{D^2}$ . Further operators with covariant derivatives acting on  $\widehat{\mathbf{H}}$  can be eliminated using PI.

**Tensor contributions** Without loss of generality, the tensorial current is traceless in Lorentz space,  $\mathbf{T}_\mu^\mu = 0$ , so that its two Lorentz indices have to be contracted by either two covariant derivatives or a field strength tensor. Hence, the leading contributions with  $\mathbf{T}^{\mu\nu}$  count as  $\mathcal{O}(\epsilon_{\text{EW}} \partial^4 n_c) \sim \mathcal{O}(\epsilon_{\text{EW}} \delta^3)$ . The two available operators of this type are

$$\mathcal{L}_U^{TD^2} = \frac{\epsilon_{\text{EW}}}{4f_0} \kappa_T^{D^2} \langle \widehat{\mathbf{T}}_{\mu\nu} \mathbf{U}^\mu \mathbf{U}^\nu \rangle_f + \text{h.c.}, \quad \mathcal{L}_U^{TV} = \frac{\epsilon_{\text{EW}}}{2f_0} \kappa_T^{LR} \langle \widehat{\mathbf{T}}_{\mu\nu} (\mathbf{L}^{\mu\nu} + \widehat{\mathbf{R}}^{\mu\nu}) \rangle_f + \text{h.c.}, \quad (4.38)$$

where  $\widehat{\mathbf{T}}_{\mu\nu} = \mathbf{g} \mathbf{T}_{\mu\nu}$  and the  $\kappa_T$  are free parameters. This result is consistent with the list of operators obtained in [203], which also includes terms that are quadratic in  $\mathbf{T}^{\mu\nu}$ .

**Four-quark contributions** The leading operators with one four-quark insertion contain either two covariant derivatives or one quark-mass insertion. According to the modified large  $n_c$  power counting (2.40), the contributions to the QCD path-integral that generate these operators contain two quark loops but scale as  $n_c^2$ . Therefore, the leading operators count as  $\mathcal{O}(\epsilon_{\text{EW}} \delta) = \mathcal{O}(\epsilon_{\text{EW}} n_c^2 \partial^2)$  and they can contain either one or two quark-flavour traces, where, in stark contrast to operators that are not induced by the four-quark currents, the second flavour trace is *not* associated with a large  $n_c$  suppression factor. Furthermore, operators with covariant derivatives acting on the four-quark currents can be eliminated using PI, while operators with two covariant derivatives acting on the same coset-matrix  $\mathbf{g}$  can be eliminated using either the identity (4.13) or the EOM (4.21).

We first consider the operators that contain the octet contributions to the four-quark currents  $\mathbf{H}_x$  (3.39) with  $x = l, r, s$  (*cf.* table 10), and then proceed to the operators that contain the 27-plet current (3.39)  $\mathfrak{H}_l^+$ . The only leading octet operators are

$$\langle \mathbf{H}_x \mathbf{U}_\mu \mathbf{U}^\mu \rangle_f, \quad \langle \mathbf{H}_x \mathbf{U}_\mu \rangle_f \mathbf{U}^\mu, \quad \langle \mathbf{H}_x (\widehat{\mathbf{M}} + \text{h.c.}) \rangle_f, \quad (4.39)$$

where  $\mathbf{U}_\mu$  and  $\widehat{\mathbf{M}}$  denote the octet contributions to  $\mathbf{U}_\mu$  and  $\widehat{\mathbf{M}}$ . In order to make contact with the standard form of the four-quark  $\chi$ PT operators in the SM, we explicitly extract the

quark-flavour violating contributions by replacing  $\mathbf{H}_x \rightarrow \langle \mathbf{H}_x \rangle_s^d \boldsymbol{\lambda}_s^d + \text{h.c.}$ . The resulting order  $\epsilon_{\text{EW}}\delta$  octet contributions are

$$\mathcal{L}_U^{HD^2} = -\frac{\epsilon_{\text{EW}}f_0^2}{2} \left( H_8 \langle \mathbf{U}_\mu \mathbf{U}^\mu \rangle_d^s + H_1 \langle \mathbf{U}^\mu \rangle_s^d U_\mu \right) + \text{h.c.} , \quad (4.40a)$$

$$\mathcal{L}_U^{HM} = -\frac{\epsilon_{\text{EW}}f_0^2 b_0}{2} H_b \langle \widehat{\mathbf{M}} + \widehat{\mathbf{M}}^\dagger \rangle_d^s + \text{h.c.} , \quad (4.40b)$$

where the three parameters  $H_8$ ,  $H_1$ , and  $H_b$  are strangeness violating matrix elements of linear combinations of the QCD four-quark currents (*cf.* table 10)

$$H_y = \langle \kappa_y^+ \mathbf{H}_l^+ + \kappa_y^- \mathbf{H}_l^- + \kappa_y^r \mathbf{H}_r + \kappa_y^s \mathbf{H}_s \rangle_s^d , \quad (4.41)$$

with  $y = b, 1, 8$  and twelve free parameters  $\kappa_y^x$  with  $x = +, -, r, s$ . The only leading 27-plet operator is

$$\langle \langle \mathbf{U}_\mu \mathfrak{H}_l^+ \mathbf{U}^\mu \rangle \rangle_f = \frac{1}{2} (\mathbf{U}_{\mu b}^a \mathbf{U}_d^{\mu c} + \mathbf{U}_{\mu d}^a \mathbf{U}_b^{\mu c}) \mathfrak{H}_l^{+bd}{}_{ac} . \quad (4.42)$$

Using the first identity of (2.60) to explicitly isolate the quark-flavour violating contributions, one has

$$\langle \langle \mathbf{U}_\mu \mathfrak{H}_l^+ \mathbf{U}^\mu \rangle \rangle_f|_{\Delta s=\pm 1} = \frac{2}{n_f - 1} (n_f \mathbf{U}_{\mu d}^s \mathbf{U}_u^{\mu u} + (n_f - 1) \mathbf{U}_{\mu d}^u \mathbf{U}_u^{\mu s}) \mathfrak{H}_l^{+su}{}_{du} + \text{h.c.} \quad (4.43)$$

The resulting order  $\epsilon_{\text{EW}}\delta$  27-plet contribution is

$$\mathcal{L}_U^{\mathfrak{H}D^2} = -\frac{\epsilon_{\text{EW}}f_0^2}{2} H_{27} (n_f \mathbf{U}_{\mu d}^s \mathbf{U}_u^{\mu u} + (n_f - 1) \mathbf{U}_{\mu d}^u \mathbf{U}_u^{\mu s}) + \text{h.c.} , \quad H_{27} = \kappa_{27} \mathfrak{H}_l^{+du}{}_{su} . \quad (4.44)$$

Hence, the complete  $\chi$ PT four-quark Lagrangian is

$$\mathcal{L}_U^H = \mathcal{L}_U^{HD^2} + \mathcal{L}_U^{HM} + \mathcal{L}_U^{\mathfrak{H}D^2} , \quad (4.45)$$

where the SM contribution is consistent with the standard expressions found *e.g.* in [114, 115, 186]. Using (3.39), we split the scalar currents  $H_y$  (4.41) and (4.44) into SM and portal contributions

$$H_y = h_y + S_y , \quad S_y = h_{yi} \frac{\epsilon_{\text{UV}}}{v} s_i , \quad i = 1, 2 , \quad (4.46)$$

where  $y = b, 1, 8$ , and 27. While the SM parameters  $h_8$ ,  $h_1$ , and  $h_{27}$  are fixed by SM observations, the SM parameter  $h_b$  and the BSM parameters  $h_{yi}$  with  $i = 1, 2$  have to be estimated using non-perturbative methods such as the large  $n_c$  expansion.

#### 4.3.2 Flavour-singlet current contributions

The  $G_{LR}$  singlet current  $\Omega = \omega + S_\omega$  contains a SM contribution  $\omega = 2\pi/\alpha_s$  and a hidden contribution  $S_\omega$ , but the SM contribution is implicitly integrated out when constructing  $\chi$ PT, so that it cannot appear in the Lagrangian directly. Accounting for the hidden current  $S_\omega$ ,

it is possible to construct additional chiral invariants by multiplying it by each of the chiral invariants that contribute to the previously derived Lagrangians. Since  $S_\omega$  insertions are suppressed by a factor of  $\delta \sim n_c^{-1}$ , the leading strangeness conserving contributions to the resulting sum of invariants count as  $\delta^3$ , while the leading strangeness violating contributions count as  $\epsilon_{\text{EW}}\delta^2$  and  $\epsilon_{\text{EW}}\delta^3$ . The full singlet current Lagrangian is

$$\mathcal{L}_U^{S_\omega} = \mathcal{L}_U^{S_\omega}_{\delta^3} + \mathcal{L}_U^{S_\omega \text{EW}}_{\delta^2} + \mathcal{L}_U^{S_\omega \text{EW}}_{\delta^3} , \quad \mathcal{L}_U^{S_\omega}_{\delta^n} = S_\omega \Upsilon_U \delta^{n-1} , \quad (4.47)$$

where the strong terms are

$$\Upsilon_U \delta^2 = \kappa_\omega^{D^2} \mathcal{L}_U^{D^2} + \kappa_\omega^M \mathcal{L}_U^M + \kappa_\omega^{\Theta^2} \mathcal{L}_U^{\Theta^2} , \quad (4.48)$$

and the EW suppressed terms are

$$\Upsilon_U^{\text{EW}}_{\delta^2} = \kappa_\omega^{HD^2} \mathcal{L}_U^{HD^2} + \kappa_\omega^{HM} \mathcal{L}_U^{HM} + \kappa_\omega^{\delta D^2} \mathcal{L}_U^{\delta D^2} , \quad \Upsilon_U^{\text{EW}}_{\delta^2} = \kappa_\omega^\Gamma \mathcal{L}_U^\Gamma . \quad (4.49)$$

The  $\kappa_\omega$  are seven free parameters. In the following, we abbreviate

$$\Upsilon_U = \Upsilon_U \delta^2 + \Upsilon_U^{\epsilon_{\text{EW}}} + \Upsilon_U^{\epsilon_{\text{EW}}} \delta^2 . \quad (4.50)$$

The above result is consistent with the interaction Lagrangian used in [204] to capture the coupling of the SU(3)  $\chi$ PT to a light Higgs boson. The treatment in [204] neglects the chromo- and electromagnetic interactions captured by  $\mathcal{L}_U^\Gamma$  as well as the 27-plet interactions captured by  $\mathcal{L}_U^{\delta D^2}$ . Furthermore, the SU(3)  $\chi$ PT Lagrangian in [204] does not contain the contribution  $\mathcal{L}_U^{\Theta^2}$ , which only appears in the U(3)  $\chi$ PT.

### 4.3.3 Stress-energy tensor

The complete LO  $\chi$ PT action contains the Lagrangian contributions

$$\mathcal{L}_U \delta^2 = \mathcal{L}_U^{D^2} + \mathcal{L}_U^M + \mathcal{L}_U^{\Theta^2} , \quad \mathcal{L}_U^{\text{EW}}_{\delta^2} = \mathcal{L}_U^H , \quad \mathcal{L}_U^{\text{EW}}_{\delta^2} = \mathcal{L}_U^\Gamma + \mathcal{L}_U^{S_\omega \text{EW}}_{\delta^2} , \quad (4.51)$$

while the NLO  $\chi$ PT action contains the Lagrangian contributions

$$\mathcal{L}_U \delta^3 = \mathcal{L}_U^{D^4} + \mathcal{L}_U^{D^2 M} + \mathcal{L}_U^{M^2} + \mathcal{L}_U^{DD} + \mathcal{L}_U^{M\Theta} + \mathcal{L}_U^{\vartheta^2} + \mathcal{L}_U^{D^2 V} + \mathcal{L}_U^{V^2} + \mathcal{L}_U^{S_\omega}_{\delta^3} + \mathcal{L}_U^{n_c} , \quad (4.52a)$$

$$\mathcal{L}_U^{\text{EW}}_{\delta^3} = \mathcal{L}_U^{D^2 H} + \mathcal{L}_U^{MH} + \mathcal{L}_U^{\Theta H} + \mathcal{L}_U^{D^2 T} + \mathcal{L}_U^{VT} + \mathcal{L}_U^{S_\omega \text{EW}}_{\delta^3} \quad (4.52b)$$

as well as the ungauged WZW term  $\Gamma_u^{n_c}$  (4.28). In the next section, we use the trace of the SM Hilbert stress-energy tensor to estimate the novel parameters  $\kappa_\omega$  that appear in the singlet current Lagrangian (4.47). Neglecting the contributions due to the  $S_\omega$  current, which does not appear in the SM, the trace of the Hilbert stress-energy tensor at order  $\delta^2$  is

$$\mathcal{T}_U = 2g^{\mu\nu} \frac{\delta \mathcal{L}_U}{\delta g^{\mu\nu}} - 4\mathcal{L}_U = -2\mathcal{L}_U^{D^2} - 4\mathcal{L}_U^M - 4\mathcal{L}_U^{\Theta^2} + \mathcal{T}_U^{\text{EW}} , \quad (4.53)$$

where

$$\mathcal{T}_U^{\text{EW}} = -\mathcal{L}_u^{\partial W} - 4\mathcal{L}_U^\Gamma - 2\mathcal{L}_U^{HD^2} - 4\mathcal{L}_U^{HM} - 2\mathcal{L}_U^{\delta D^2} \quad (4.54)$$

collects the contributions due to the EW currents. The charged-current contribution

$$\mathcal{L}_u^{\partial W} = -f_0^2 \langle I_{W\mu} \mathbf{u}^\mu \rangle_f \quad (4.55)$$

is also a part of the kinetic  $\chi$ PT Lagrangian (4.12). This term appears separately because it contains a vierbein  $e_a^\mu$  when the theory is embedded into a generic spacetime with background metric tensor  $g^{\mu\nu}$ . Due to this vierbein, the derivative contribution for the kinetic Lagrangian

$$g^{\mu\nu} \frac{\delta \mathcal{L}_U^{D^2}}{\delta g^{\mu\nu}} = \mathcal{L}_U^{D^2} - \frac{1}{2} \mathcal{L}_u^{\partial W} \quad (4.56)$$

picks up a leftover term with a relative prefactor of  $-1/2$ .

#### 4.4 Matching of $\chi$ PT to QCD

So far, we derived the shape of the modified  $\chi$ PT Lagrangian in the presence of generic external currents  $J = \{S_\omega, \Theta, \mathbf{M}, \mathbf{L}^\mu, \mathbf{R}^\mu, \mathbf{T}^{\mu\nu}, \mathbf{F}, \mathfrak{H}_s, \mathfrak{H}_r, \mathfrak{H}_l\}$ . We now aim to provide part of the means necessary to constrain the QCD portal sector Wilson coefficients at energies above the mass of the charm quark using bounds on hidden sector induced low energy meson transition amplitudes obtained from  $\chi$ PT.

A key element is that one has to estimate the 27 free parameters  $\kappa \in \{\kappa_\Gamma^x, \kappa_T^x, \kappa_y^x, \kappa_\omega^x\}$ , which appear in the  $\epsilon_{UV}$  and  $\epsilon_{EW}$  suppressed sectors. This then makes it possible to translate bounds from hidden sector induced meson transitions into constraints on the external currents as they appear in the  $\chi$ PT Lagrangian. These currents are defined such that they are identical to the external currents that appear in the low energy QCD Lagrangian with three light u, d, and s quark flavours. To fully connect  $\chi$ PT to QCD in the perturbative regime, it is also necessary to match this version of QCD to its counterpart that includes dynamical charm and bottom quarks. We leave the work of matching these two versions of QCD to future investigations, and instead consider only how to estimate the  $\kappa$  parameters in  $\chi$ PT. The six parameters  $\kappa_\Gamma^{D^2}$ ,  $\kappa_\Gamma^\Theta$ ,  $\kappa_\Gamma^M$ ,  $\kappa_\Gamma^{M'}$ ,  $\kappa_T^{D^2}$ , and  $\kappa_T^{LR}$  can be fixed using SM observations, and we focus on those parameters for which this is not possible:

1. We estimate the seven parameters  $\kappa_\omega^x$  that couple  $\chi$ PT to the external current  $S_\omega$ , which vanishes in the SM. These parameters can be quantified using the anomalous trace-relation for the stress-energy tensor (2.65). In the past, this technique has already been used to estimate four out of the seven parameters [106]. Here, we follow the same strategy to determine the remaining three parameters.
2. We estimate the free parameter  $\kappa_\Gamma$ , which couples  $\chi$ PT to the chromomagnetic dipole current  $\mathbf{F}$  at order  $\delta^2$ , and the combination of parameters  $\kappa_\Gamma^M + \kappa_\Gamma^{M'}$ , which couple  $\chi$ PT to the same current at order  $\delta^3$ . In principle, SM interactions do contribute to both dipole currents  $\mathbf{F}$  and  $\mathbf{T}^{\mu\nu}$ , and we expect that SM observations can be used to constrain the order  $\delta^3$  parameters  $\kappa_\Gamma^x$  and  $\kappa_T^x$  that couple  $\chi$ PT to the dipole currents. However, the order  $\delta^2$  SM contribution to the operator associated with the parameter  $\kappa_\Gamma$  can be reabsorbed into the quark mass matrix, so that this parameter is not fixed by SM observations. Instead, we estimate its value, and the values of  $\kappa_\Gamma^M$  and  $\kappa_\Gamma^{M'}$ , by matching it to the lattice QCD prediction for the vacuum condensate of the chromomagnetic operator, which is reasonably well known [162, 165, 166].

3. We estimate the thirteen parameters  $\kappa_y^x$ , which appear in the  $\chi$ PT four-quark Lagrangian. These parameters enter into SM predictions only via the linear combinations that constitute the octet and 27-plet coefficients  $h_8$ ,  $h_1$ , and  $h_{27}$ , so that SM observations do not yield enough information to completely fix their values. At LO in the large  $n_c$  expansion, the factorization rule (2.14) can be used to estimate the  $\kappa_y^x$  parameters [107, 108, 110–112, 205, 206]. However, this approximation fails to accurately reproduce *e.g.* the  $\Delta I = 1/2$  rule in the SM, which is an approximate selection rule for kaon decays that results from the fact that the octet coefficients  $h_{8,1}$ , which mediate only  $\Delta I = 1/2$  transitions, are an order of magnitude larger than the 27-plet coefficient  $h_{27}$ , which mediates both  $\Delta I = 1/2$  and  $\Delta I = 3/2$  transitions. For this reason, we expect that one has to include corrections beyond the large  $n_c$  limit to extract order-of-magnitude accurate estimates of the portal sector Wilson coefficients  $c_{ii}$  from bounds on hidden sector induced meson transitions. To obtain improved estimates for the  $\kappa$  parameters, we adapt the strategies used in [106–108, 112, 205], and neglect the contributions generated by the penguin operators  $O_{3i}$ ,  $O_{4i}$ , and  $O_{5i}$ . Since these operators are generated at 1-loop they are suppressed by factors of  $(4\pi)^{-2}$  compared to the tree-level operators  $O_{1i}$  and  $O_{2i}$ . The penguin operator  $O_{6i}$  is also generated at 1-loop, but it is expected to generate the dominant penguin contribution to kaon decay amplitudes [106, 112, 205–207].

#### 4.4.1 Scale dependence of the external currents

Many of the external currents are scale-dependent, and therefore the estimates that one obtains for the LECs and  $\kappa$  parameters in the  $\chi$ PT Lagrangian depend on the scale at which the external currents are evaluated. In general, the scale-dependence of the external currents has to cancel with the one of the LECs and  $\kappa$  parameters. If  $\chi$ PT is matched to the version of QCD without the charm quark, so that there are no threshold effects, this implies that the hidden currents can always be evaluated at some arbitrary higher scale, say,  $\mu_{\text{QCD}} = 1\text{--}2\text{ GeV}$ , provided that one adjusts the values of the LECs and  $\kappa$  parameters accordingly.

This approach has been used to deal with the scale dependence of the mass-like current  $\mathbf{M}$  and the anomalous axial singlet current  $R^\mu - L^\mu = \vartheta^\mu - \partial^\mu \Theta$ ,<sup>16</sup> which renormalise according to [109]

$$\mathbf{M} = Z_M^{-1} \mathbf{M}^{\text{bare}}, \quad \vartheta_\mu = Z_\vartheta^{-1} \vartheta_\mu^{\text{bare}}. \quad (4.57)$$

The factors  $Z_\vartheta$  and  $Z_M$  relate the renormalised quark current corresponding associated with  $\mathbf{M}$  and  $\vartheta^\mu$  to their bare counterparts

$$\mathbf{Q} = Z_M \mathbf{Q}^{\text{bare}}, \quad Q^\mu - \bar{Q}^\mu = Z_\vartheta (Q^\mu - \bar{Q}^\mu)^{\text{bare}}. \quad (4.58)$$

Extracting the renormalisation of the scalar axial current from (4.57) gives

$$(L^\mu - R^\mu) = Z_\vartheta^{-1} (L^\mu - R^\mu)^{\text{bare}} - (1 - Z_\vartheta^{-1}) \partial^\mu \Theta^{\text{bare}}, \quad (4.59)$$

where  $\partial^\mu \Theta = \partial^\mu \Theta^{\text{bare}}$ .<sup>16</sup> This equation reflects the fact that the axial anomaly mixes the scalar axial vector current with the derivative of the pseudoscalar current  $\partial_\mu \Theta$ . We can see

---

<sup>16</sup> The currents  $J_{\text{inv}} = \{\Theta, L^\mu + R^\mu, \mathbf{L}^\mu \pm \mathbf{R}^\mu\}$  do not renormalise and are therefore scale-independent in QCD [109, section 6.6 in 208].

explicitly that the  $\chi$ PT Lagrangian is invariant under a change of the QCD renormalisation scale, provided that it is written in terms of the renormalised singlet meson field [109]

$$\hat{\Theta} = i \left( \Theta - \frac{\Phi}{f_0} \right) = i Z_\vartheta^{-1} \left( \Theta - \frac{\Phi^{\text{bare}}}{f_0} \right) \quad (4.60)$$

as well as the renormalised LECs

$$b_0 = Z_M b_0^{\text{bare}}, \quad m_0 = Z_\vartheta m_0^{\text{bare}}, \quad 1 + \Lambda_2 = Z_\vartheta (1 + \Lambda_2^{\text{bare}}), \quad (4.61a)$$

$$H_0 = Z_\vartheta^2 H_0^{\text{bare}}, \quad 1 + \Lambda_1 = Z_\vartheta^2 (1 + \Lambda_1^{\text{bare}}). \quad (4.61b)$$

The scale-dependent values of the renormalised LECs  $b_0$ ,  $m_0$ , and  $\Lambda_{1,2}$  can now be fixed by computing  $\chi$ PT observables in terms of the renormalised currents  $\mathbf{M} = \mathbf{M}(\mu_{\text{QCD}})$  and  $L^\mu - R^\mu = (L^\mu - R^\mu)(\mu_{\text{QCD}})$ . Of course, this renormalisation procedure only eliminates divergences associated with the strong interaction. We emphasise that the  $\chi$ PT action written in terms of the above fields and LECs still has to be renormalised as usual when accounting for loop corrections starting at NNLO. As a result, one has to distinguish between the renormalisation scale of  $\chi$ PT  $\mu_{\chi\text{PT}}$  and the renormalisation scale of QCD  $\mu_{\text{QCD}}$ , which are not necessarily the same. In general, the renormalised LECs and parameters depend on *both* scales. Here and in the remainder of section 4.4, we only consider the dependence on  $\mu_{\text{QCD}}$ , and so we suppress the dependence on  $\mu_{\chi\text{PT}}$  in the notation.

In the following, we apply the above renormalisation procedure to the  $\epsilon_{\text{EW}}$  or  $\epsilon_{\text{UV}}$  suppressed currents  $J = \{S_\omega, \mathbf{F}, \mathbf{T}^{\mu\nu}, \mathbf{H}_l^+, \mathbf{H}_l^\pm, \mathbf{H}_{r,s}\}$ , and absorb their scale dependence into the values of the free parameters  $\kappa$ . The upshot of this prescription is that, when matching  $\chi$ PT to QCD without the charm quark, we can freely choose the renormalisation scale  $\mu_{\text{QCD}}$ , even choosing a value well above the charm quark mass. Of course, this would not work if we were to attempt to match  $\chi$ PT to perturbatively computed low-energy observables in QCD, since choosing a large renormalisation scale  $\mu_{\text{QCD}} \gg m_c$  would mean that we neglect precisely the non-perturbative contributions on the QCD side that dominate the physics of the strong interaction at low energies. However, this is not an issue when matching  $\chi$ PT to the results of *non*-perturbative computations, such as those done in lattice QCD, where no expansion in  $\omega^{-1}$  is made. In fact, the scale  $\mu_{\text{QCD}} = 2 \text{ GeV}$  is a standard choice when computing low-energy observables such as the quark masses and condensates in lattice QCD with and without the charm quark [128, 148, 165].

#### 4.4.2 $\chi$ PT realizations of QCD operators

To establish a point of contact between  $\chi$ PT and QCD that does not rely on a perturbative expansion in  $\omega^{-1}$ , we use a standard technique employed *e.g.* in [105–107, 109–112], and construct a set of well-defined LERs for QCD gauge-singlets as functional derivatives of the path integral with respect to the external currents. For the sake of completeness, we outline the general procedure and then summarise the resulting  $\chi$ PT LERs that are relevant to the subsequent discussion.

$\delta^n$	1		2			3			
$J$	$H_x$	$\mathfrak{H}_x$	$\Theta$	$L_\mu$	$R_\mu$	$\Omega$	$M$	$\Gamma$	$T_{\mu\nu}$
$\delta^k$	0		0	$1/2$		0	1		
$O$	$O_x$	$\mathfrak{O}_x$	$w$	$Q_\mu$	$\overline{Q}_\mu$	$\Upsilon$	$Q$	$\tilde{Q}$	$Q_{\mu\nu}$
$\delta^{n-k}$	1		2	$3/2$		3	2		

Table 11: Order in  $\delta$  at which we evaluate the LERs. The first row shows the order in  $\delta$  at which we evaluate the  $\chi$ PT generating functional, the second row shows the  $\delta$  scaling of the external current, and the final row shows the resulting order in  $\delta$  for the LER. While a momentum suppression  $\propto \partial^2$  counts towards the scaling of the external currents, a large  $n_c$  suppression does not, because it is associated with the structure of the QCD diagrams that couple to the external current rather than with the current itself. The order in  $\delta$  at which we evaluate the  $\chi$ PT generating functional is chosen such that we include the leading nonvanishing contribution for each operator. For  $Q$ , we also include NLO contributions, since these enter at LO into the approximate factorised expressions for the four-quark operators. Note also that the product of operators does not scale as the sum of their individual suppressions. For instance,  $Q_\mu Q^\mu \propto n_c^2 \partial^2 \propto \delta$ , rather than  $\delta^{3/2} \times \delta^{3/2} = \delta^3$ , as one might naively expect.

**Constructing low energy realisations** In general, the expectation value of any local, gauge invariant QCD operator  $O_i$  that couples to an external current  $J_i$  is

$$\text{tr } O_i(x) \rho = \frac{\delta \ln \mathcal{Z}_Q[J_j]}{\delta J_i(x)} , \quad (4.62)$$

where the von Neumann density matrix  $\rho$  encodes the state of the system,

$$\mathcal{Z}_Q[J_j] = \int \mathcal{D}\varphi \rho \exp\left(i S_Q[\varphi] + i \int d^4x J_j(x) O_j(x)\right) \quad (4.63)$$

is the generating functional in the presence of external currents  $J_i$ , and  $\varphi$  symbolically denotes the quark and gluon fields. The  $\chi$ PT generating functional approximates the QCD generating functional for small  $\delta$ ,

$$\ln \mathcal{Z}_Q[J_j] = \ln \mathcal{Z}_U[J_j] + \mathcal{O}(\delta^n) . \quad (4.64)$$

If an external current scales as  $J_i(x) \propto \delta^k$ , then inserting this relation into the expectation value (4.62) gives

$$\text{tr } O_i(x) \rho = \frac{\delta \ln \mathcal{Z}_U[J_j]}{\delta J_i(x)} + \mathcal{O}(\delta^{n-k}) = \text{tr } \frac{\delta S_U}{\delta J_i} \rho + \mathcal{O}(\delta^{n-k}) . \quad (4.65)$$

Since this has to hold for any physical choice of  $\rho$ , one finds the LERs

$$O_i(x) = \frac{\delta S_U}{\delta J_i} + \mathcal{O}(\delta^{n-k}) . \quad (4.66)$$

**Operators** The LERs of the colour singlet (2.10) and the quark bilinears (2.21) associated with the  $L_\mu$ ,  $R_\mu$ ,  $M$ , and  $\Theta$  currents are well established. At leading order in  $\delta$ , they are [105, 107, 109, 184, 209]

$$Q_\mu = -f_0^2 U_\mu , \quad \overline{Q}_\mu = -f_0^2 g^\dagger U_\mu g , \quad Q = -\frac{1}{2} f_0^2 b_0 g , \quad w = -i f_0^2 \frac{m_0^2}{n_f} \hat{\Theta} . \quad (4.67)$$

The LO contributions to  $\mathbf{Q}_\mu$  and  $\overline{\mathbf{Q}}_\mu$  count as order  $\partial n_c$ , while the LO contribution to  $\mathbf{Q}$  counts as order  $n_c$ . In order to estimate the four-quark coefficients  $\kappa_x^s$  at order  $\partial^2 n_c^2$ , which is the first non-vanishing order, it is necessary to also track NLO corrections to the LER of  $\mathbf{Q}$  that count as  $\partial^2 n_c$ . This gives the expression

$$\mathbf{Q} = -\frac{1}{2}f_0^2 b_0 \left(1 + \Delta\mathbf{Q}^{\text{NLO}}\right) \mathbf{g} , \quad (4.68)$$

where

$$\Delta\mathbf{Q}^{\text{NLO}} = \frac{1}{2f_0^2} \left( 4L_5 \mathbf{U}_\mu \mathbf{U}^\mu + 2b_0 \left( 4L_8 \widehat{\mathbf{M}} + 2H_2 \widehat{\mathbf{M}}^\dagger \right) \right) + \frac{\Lambda_2}{n_f} \widehat{\Theta} - \epsilon_{\text{EW}} (H_b \boldsymbol{\lambda}_s^{\text{d}} + \text{h.c.}) . \quad (4.69)$$

Note that this expression differs from its SU(3) counterpart by the appearance of the term proportional to  $\Lambda_2$ , which does not exist in SU(3)  $\chi$ PT [105–107].

We apply the same technique to obtain LERs for operators associated with the  $\epsilon_{\text{EW}}$  and  $\epsilon_{\text{UV}}$  suppressed currents. We find that the LERs of the colour singlet (2.4) and the quark bilinears (2.29) associated with the  $\mathbf{T}_{\mu\nu}$ ,  $\boldsymbol{\Gamma}$ , and  $S_\omega$  currents are

$$\mathbf{Q}^{\mu\nu} = -f_0 \left( \kappa_T^{D^2} \mathbf{U}^\mu \mathbf{U}^\nu + \kappa_T^{LR} (\mathbf{L}^{\mu\nu} + \widehat{\mathbf{R}}^{\mu\nu}) \right) \mathbf{g} , \quad \widetilde{\mathbf{Q}} = -\frac{1}{2}f_0^4 b_0 \kappa_\Gamma \mathbf{g} , \quad \mathcal{R} = -\mathcal{R}_U . \quad (4.70)$$

At NLO, the LER of the scalar quark bilinear  $\widetilde{\mathbf{Q}}$  is

$$\widetilde{\mathbf{Q}} = -\frac{1}{2}f_0^4 b_0 \left( \kappa_\Gamma + \Delta\widetilde{\mathbf{Q}}^{\text{NLO}} \right) \mathbf{g} , \quad (4.71)$$

where

$$\Delta\widetilde{\mathbf{Q}}^{\text{NLO}} = \frac{1}{2f_0^2} \left( \kappa_\Gamma^{D^2} \mathbf{U}_\mu \mathbf{U}^\mu + 2b_0 \left( \kappa_\Gamma^M \widehat{\mathbf{M}} + \kappa_\Gamma^{M'} \widehat{\mathbf{M}}^\dagger \right) \right) + \frac{\kappa_\Gamma^\Theta}{n_f} \widehat{\Theta} . \quad (4.72)$$

Finally, the LERs of the octet quark quadrilinear (2.52) and (2.57) associated with the  $\mathbf{H}_x$  currents are

$$\mathbf{O}_{x\text{d}}^s = \frac{1}{2}f_0^4 \left( \kappa_8^x \langle \mathbf{U}_\mu \mathbf{U}^\mu \rangle_{\text{d}}^s + \kappa_1^x \langle \mathbf{U}^\mu \rangle_{\text{s}}^{\text{d}} U_\mu + \kappa_b^x b_0 \left\langle \widehat{\mathbf{M}} + \widehat{\mathbf{M}}^\dagger \right\rangle_{\text{d}}^s \right) , \quad (4.73)$$

where  $x = +, -, r, s$ , and the LER of the 27-plet quark quadrilinear (2.58) associated with the  $\mathfrak{H}_l^+$  current is

$$2n_{27} \mathfrak{D}_l^{+\text{su}} = \frac{1}{2}f_0^4 \kappa_{27} (n_f \mathbf{U}^{\mu s}_{\text{d}} \mathbf{U}_{\mu \text{u}}^{\text{u}} + (n_f - 1) \mathbf{U}^{\mu \text{u}}_{\text{d}} \mathbf{U}_{\mu \text{u}}^s) . \quad (4.74)$$

**Lagrangians** Using the above LERs, one obtains approximate  $\chi$ PT expressions for various individual contributions to the QCD Lagrangian

$$\mathcal{L}_Q^M = \mathcal{L}_U^M + \mathcal{L}_U^{HM} , \quad \mathcal{L}_Q^\Gamma = \mathcal{L}_U^\Gamma , \quad \mathcal{L}_Q^W = \mathcal{L}_U^{DW} , \quad \mathcal{L}_Q^H = \mathcal{L}_U^H . \quad (4.75)$$

Note that the mass-like four-quark octet term contributes not only to the LER of the four-quark Lagrangian, but also to the LER of the mass Lagrangian.



#### 4.4.3 Determination of selected parameters

We now estimate the 22  $\kappa$  parameters  $\kappa_\omega^x$ ,  $\kappa_\Gamma$ ,  $\kappa_\Gamma^M + \kappa_\Gamma^{M'}$ , and  $\kappa_y^x$ . As mentioned in the introduction to this section, we do not estimate the five parameters  $\kappa_\Gamma^{D^2}$ ,  $\kappa_\Gamma^M - \kappa_\Gamma^{M'}$ ,  $\kappa_\Gamma^\Theta$  and  $\kappa_T^x$ , which couple  $\chi$ PT to the  $\boldsymbol{\Gamma}$  and  $\boldsymbol{T}^{\mu\nu}$  currents at order  $\epsilon_{\text{EW}}\delta^3$ , and leave this work to future investigations. To illustrate the use of the LERs and to prepare for the estimation of the four-quark parameters  $\kappa_x^y$ , we first discuss two well-known computations that match  $\chi$ PT to the lattice QCD predictions for the quark condensates and the topological susceptibility of QCD.

**Quark condensates** The LER for the quark bilinear  $\boldsymbol{Q}$  (4.68) relates the parameters  $b_0$  and  $4L_8 - 2H_2$  to the values of the chiral quark condensates (2.6). In the isospin conserving limit  $m_u, m_d \rightarrow m_{\text{ud}} = (m_u + m_d)/2$ , one obtains the  $\chi$ PT predictions [105, 106]

$$\Sigma_{\text{ud}} = f_0^2 b_0 + b_0^2 m_{\text{ud}} (4L_8 + 2H_2), \quad \Sigma_s = f_0^2 b_0 + b_0^2 m_s (4L_8 + 2H_2). \quad (4.76)$$

The quark condensates are proportional to  $b_0$  and degenerate at LO. Their splitting is captured at NLO by the parameter  $4L_8 + 2H_2$ . Using the lattice values of condensates in equation (2.6) yields the estimates

$$b_0 = \frac{m_s \Sigma_{\text{ud}} - m_{\text{ud}} \Sigma_s}{f_0^2 (m_s - m_{\text{ud}})} = 4\pi(387 \pm 13_{\text{exp}} \pm 23_{\text{lat}}) \text{ MeV} \pm \text{NNLO}, \quad (4.77a)$$

$$4L_8 + 2H_2 = \frac{\Sigma_s - \Sigma_{\text{ud}}}{b_0^2 (m_s - m_{\text{ud}})} = (4\pi)^{-2} (0.48 \pm 0.022_{\text{exp}} \pm 0.26_{\text{lat}}) \pm \text{NNLO}. \quad (4.77b)$$

While  $b_0$  depends on the QCD renormalisation scale in the same way as  $\Sigma_{\text{ud}}$  and  $\Sigma_s$ , the dependence cancels in the expression for  $4L_8 + 2H_2$ , which depends only on the renormalisation scale independent ratio of the quark condensates (2.7). Since  $L_8$  can be estimated from the  $\eta$ -meson mass splitting and mixing angle, *cf.* equations (4.35) and (D.22), the above expression can be used to estimate the value of the counter-term parameter

$$2(4\pi)^2 H_2 = 0.27 \pm 0.033_{\text{exp}} \pm 0.26_{\text{lat}} \pm \text{NNLO}. \quad (4.78)$$

This parameter does not enter directly into perturbatively computed  $S$ -matrix elements, but it is needed for the large  $n_c$  estimate of the four-quark parameters  $\kappa_x^s$ .

**Topological susceptibility** The LER of the quark condensate can be combined with the LER of  $w$  (4.67) and relation (2.12) to express the topological susceptibility (2.11) as a combination of  $\chi$ PT parameters. Since diagrams with internal quark loops do not contribute to the QCD path integral at zeroth order in the large  $n_c$  expansion, QCD behaves similar to a pure YM theory with no quark fields in this limit. Hence, a direct estimate of the topological susceptibility using the LO LER (4.67) for  $w$  yields an estimate for the *quenched* susceptibility [109, 148, 149, 152]

$$\chi_0 = f_0^2 \frac{m_0^2}{n_f} = (188.1 \pm 2.4_{\text{exp}})^4 \text{ MeV}^4 \pm \text{NNLO}. \quad (4.79)$$

Combining this result with the LO estimate of the quark condensate (4.76) and relation (2.12), one obtains the estimate

$$\frac{f_0^2}{\chi} = \frac{n_f}{m_0^2} + \frac{\langle \mathbf{m}^{-1} \rangle_f}{b_0} = \frac{3}{m_0^2} + \frac{2}{m_\pi^2} + \frac{1}{2m_K^2 - m_\pi^2} = \frac{f_0^2}{(76.9 \pm 1.3_{\text{exp}})^4 \text{ MeV}^4 \pm \text{NNLO}} , \quad (4.80)$$

for the topological susceptibility of QCD, which lies within the error bars of the lattice result (2.11). See appendix D.1 for the definition of the pion and kaon mass parameters  $m_\pi$  and  $m_K$ .

**Flavour singlet contribution** We estimate the three new  $\kappa_\omega$  coefficients that appear in the  $S_\omega$  contribution to  $\chi$ PT by following the strategy used in [106, 210, 211], where the trace of the QCD stress-energy tensor (2.65)

$$\beta_s \mathcal{T} = -\mathcal{T}_Q - \mathcal{L}_Q^M + \mathcal{L}_Q^\Gamma + \mathcal{L}_Q^T - \mathcal{L}_Q^W + 2\mathcal{L}_Q^H \quad (4.81)$$

has been used to express the gluon-kinetic term  $\mathcal{T}$  as a linear combination of the trace of the stress-energy tensor and the other terms in the QCD Lagrangian. Using the  $\chi$ PT expression for the trace of the stress-energy tensor (4.53) as well as the LERs for the other terms in the Lagrangian (4.75), this gives the LO LER of the gluon-kinetic term

$$\begin{aligned} \beta_s \mathcal{T}_U &= \mathcal{L}_U^\Gamma - \mathcal{L}_U^M - \mathcal{L}_U^{DW} + 2\mathcal{L}_U^H - \mathcal{T}_U \\ &= 2\mathcal{L}_U^{D^2} + 3\mathcal{L}_U^M + 4\left(\mathcal{L}_U^{\Theta^2} + \mathcal{L}_U^{HD^2} + \mathcal{L}_U^{\mathfrak{H}D^2}\right) + 5(\mathcal{L}_U^\Gamma + \mathcal{L}_U^{HM}) . \end{aligned} \quad (4.82)$$

In principle, the contribution to the trace of the stress-energy due to the quark masses receives a further correction associated with their anomalous dimension [157, 158, 160], and we expect the same to hold for the contributions due to the other external currents. However, since the term  $\mathcal{L}_U^{S_\omega}$  has to be independent of  $\mu_{\text{QCD}}$ , we can choose to evaluate the above relation at a sufficiently large renormalisation scale  $\mu_{\text{QCD}} \gg 1 \text{ GeV}$ , where the impact of quantum corrections to the external current contributions to the stress-energy tensor is small due to asymptotic freedom. With this choice, and provided that we also evaluate  $S_\omega(\mu_{\text{QCD}})$  at the same scale, the above relation becomes a valid approximation. In addition, the  $\beta$ -function at this scale is well-approximated by its leading term  $\beta_s = \beta_0 + \mathcal{O}(\omega^{-1}(\mu_{\text{QCD}}))$ . Hence, choosing to evaluate relation (4.82) at  $\mu_{\text{QCD}} \gg 1$ , the seven coefficients that appear in Lagrangian (4.47) are given as

$$\kappa_\omega^{D^2} = \frac{2}{\beta_0} , \quad \kappa_\omega^M = \frac{3}{\beta_0} , \quad \kappa_\omega^{\Theta^2} = \kappa_\omega^{HD^2} = \kappa_\omega^{\mathfrak{H}D^2} = \frac{4}{\beta_0} , \quad \kappa_\omega^\Gamma = \kappa_\omega^{HM} = \frac{5}{\beta_0} . \quad (4.83)$$

While the coefficients  $\kappa_\omega^{D^2}$ ,  $\kappa_\omega^M$ ,  $\kappa_\omega^{HD^2}$ , and  $\kappa_\omega^{HM}$  are known [106], the coefficients  $\kappa_\omega^{\mathfrak{H}D^2}$ ,  $\kappa_\omega^{\Theta^2}$ , and  $\kappa_\omega^\Gamma$  are a new result.

**Chromomagnetic contribution and quark gluon condensates** We estimate the parameter  $\kappa_\Gamma$  and the linear combination  $\kappa_\Gamma^M + \kappa_\Gamma^{M'}$  by matching the  $\chi$ PT prediction for the

condensate of the chromomagnetic quark bilinear  $\tilde{Q}$  to the quark-gluon condensates (2.32). Using the LERs (4.70), the condensates are given as

$$\frac{\Sigma_{G\text{ud}}}{(4\pi)^2} = f_0^4 b_0 \kappa_\Gamma + b_0^2 m_{\text{ud}} (\kappa_\Gamma^M + \kappa_\Gamma^{M'}) , \quad \frac{\Sigma_{G\text{s}}}{(4\pi)^2} = f_0^4 b_0 \kappa_\Gamma + b_0^2 m_{\text{s}} (\kappa_\Gamma^M + \kappa_\Gamma^{M'}) . \quad (4.84)$$

The  $4\pi$  enhancement of the condensates is a consequence of definition (2.28), in which we have not included the loop factor into the operator, but written it as an explicit contribution to the Lagrangian. Matching this prediction to the lattice and QCD sum rule values of the condensate from equation (2.33), one obtains the estimates

$$\kappa_\Gamma = \frac{m_{\text{s}} \Sigma_{G\text{ud}} - m_{\text{ud}} \Sigma_{G\text{s}}}{\Lambda_{\chi\text{PT}}^2 f_0^2 b_0 (m_{\text{s}} - m_{\text{ud}})} = 1.21 \pm 0.06_{\text{exp}} \pm 0.06_{\text{lat}} \pm \text{NNLO} . \quad (4.85\text{a})$$

$$\kappa_\Gamma^M + \kappa_\Gamma^{M'} = \frac{\Sigma_{G\text{s}} - \Sigma_{G\text{ud}}}{\Lambda_{\chi\text{PT}}^2 b_0^2 (m_{\text{s}} - m_{\text{ud}})} = -(4\pi)^{-2} (0.20 \pm 0.004_{\text{exp}} \pm 0.31_{\text{lat}} \pm \text{NNLO}) . \quad (4.85\text{b})$$

The negative prefactor of  $\kappa_\Gamma^M + \kappa_\Gamma^{M'}$  and the fact that its value is consistent with being zero reflects that  $\Sigma_{G\text{s}}$  has been estimated to be slightly smaller than  $\Sigma_{G\text{ud}}$ , while its value is consistent with both condensates being equal to each other within their error bars.

**Four-quark contributions** Written in terms of the parameters  $\kappa_y^x$  and the Wilson coefficients  $c_{\iota i}$ , the octet and 27-plet coefficients in the four-quark Lagrangian are given as

$$h_{yi} = \frac{1}{4} V_{\text{su}}^\dagger V_{\text{ud}} [\kappa_y^+ (c_{12i}^+ + (n_f + 2)c_{34i}^+) - \kappa_y^- (c_{12i}^- + c_{34i}^+) + 4\kappa_y^r c_{5i} + 4\kappa_y^s c_{6i}] , \quad (4.86\text{a})$$

$$h_{27i} = \frac{1}{4} V_{\text{su}}^\dagger V_{\text{ud}} \kappa_{27} \frac{n_f + 1}{n_f + 2} c_{12i}^+ , \quad c_{\iota\kappa i}^\pm = c_{\iota i} \pm c_{\kappa i} , \quad (4.86\text{b})$$

where  $i = 0, 1$ , and  $2$ . Following the convention introduced in section 3.3.2, we denote the SM Wilson coefficients as  $h_x = h_{x0}$  and  $c_\iota = c_{\iota 0}$ . See also sections 2.1 and 4.3.1, where we define these coefficients. Since the coefficients  $h_{yi}$  have to be independent of the QCD renormalisation scale, the scale dependence of the Wilson coefficients cancels with the scale dependence of the thirteen  $\kappa_y^x$  parameters.

The large  $n_c$  factorisation rule (2.14) can be used to estimate the parameters at LO in  $\delta$  [110, 111]. The main idea is to combine the vacuum saturation hypothesis (2.14) with the LERs of the quark bilinears (4.67) and (4.68) to obtain approximate large  $n_c$  realisations for the octet and 27-plet operators. These can then be compared with the exact LERs for the four-quark operators (4.73) and (4.74) that have been obtained by varying the  $\chi\text{PT}$  with respect to the  $\mathfrak{H}_l^+$  and  $\mathbf{H}_x$  currents. The resulting approximate large  $n_c$  realisations for the octet operators are

$$\mathcal{O}_{\text{s d}}^{\text{s}} = \frac{1}{4} f_0^2 b_0^2 \left( 4L_5 \langle \mathbf{U}^\mu \mathbf{U}_\mu \rangle_{\text{d}}^{\text{s}} + (4L_8 + 2H_2) b_0 \langle \widehat{\mathbf{M}} + \widehat{\mathbf{M}}^\dagger \rangle_{\text{d}}^{\text{s}} \right) , \quad \mathcal{O}_{\text{r d}}^{\text{s}} = f_0^4 \mathbf{U}^{\mu\text{s}}_{\text{d}} U_\mu , \quad (4.87\text{a})$$

$$\mathcal{O}_{\text{l d}}^{-\text{s}} = f_0^4 \left( \frac{2}{n_f} \mathbf{U}^{\mu\text{s}}_{\text{d}} U_\mu - \frac{1}{2n_8} \langle \mathbf{U}^\mu \mathbf{U}_\mu \rangle_{\text{d}}^{\text{s}} \right) , \quad \mathcal{O}_{\text{l d}}^{+\text{s}} = f_0^4 \left( \frac{2}{n_f} \mathbf{U}^{\mu\text{s}}_{\text{d}} U_\mu + \frac{1}{2n_8} \langle \mathbf{U}^\mu \mathbf{U}_\mu \rangle_{\text{d}}^{\text{s}} \right) , \quad (4.87\text{b})$$

and the approximate large  $n_c$  realizations for the 27-plet operator is

$$\mathfrak{D}_l^{\text{su}} = \frac{1}{2} f_0^4 \left( 1 + \frac{1}{4n_8^+} \right) \mathbf{U}^{\mu s}_{\text{d}} \mathbf{U}^{\text{u}}_{\mu \text{u}} + \frac{1}{2} f_0^4 \left( 1 - \frac{1}{4n_8^+} \right) \mathbf{U}^{\mu \text{u}}_{\text{d}} \mathbf{U}^s_{\mu \text{u}} . \quad (4.87\text{c})$$

where  $\langle \circ \rangle_i^j = \langle \circ \lambda_j^i \rangle_f$ . Matching these expression to the exact LERs (4.73) and (4.74), one obtains the LO estimates  $\bar{\kappa}$  [110, 111]

$$\bar{\kappa}_1^r = 2 , \quad \bar{\kappa}_8^+ = \frac{1}{n_8^+} = \frac{4}{5} , \quad \bar{\kappa}_{27} = \frac{n_{27}}{n_8^+} = 2 , \quad (4.88\text{a})$$

$$\bar{\kappa}_1^- = \bar{\kappa}_1^+ = \frac{4}{n_f} = \frac{4}{3} , \quad -\bar{\kappa}_8^- = \frac{1}{n_8^-} = 4 , \quad (4.88\text{b})$$

and

$$\bar{\kappa}_8^s = \frac{n_f}{2} \bar{\kappa}_1^s = \frac{1}{2} \frac{b_0^2}{f_0^2} 4L_5 = 2.00 \pm 0.16_{\text{exp}} \pm 0.13_{\text{lat}} , \quad (4.89\text{a})$$

$$\bar{\kappa}_b^s = \frac{1}{2} \frac{b_0^2}{f_0^2} (4L_8 + 2H_2) = 1.45 \pm 0.10_{\text{exp}} \pm 0.8_{\text{lat}} . \quad (4.89\text{b})$$

The remaining parameters  $\kappa_y^x$  vanish in the large  $n_c$  limit,  $\bar{\kappa} = 0$ . In this approximation, the parameters  $\kappa_y^{\pm, r}$  and  $\kappa_{27}$  are renormalisation scale independent, while the  $\kappa_y^s$  run as  $b_0^2 \sim \Sigma_{\text{ud}}^2/f_0^4$ . This is consistent with the scale dependence of the SM four-quark Wilson coefficients: In the large  $n_c$  limit, the  $c_i$  coefficients with  $i \neq 6$  are in fact renormalisation scale independent, while  $c_6$  remains scale-dependent and runs as  $b_0^{-2}$  [107, 212, 213]. This running of  $c_6$ , which we have absorbed into the values of the  $\kappa_y^s$ , is the physical cause behind the enhancement factors  $b_0^2/f_0^2$  of the singlet operators and cancels the suppression associated with the factors  $L_5$  and  $2L_8 + H_2$ .

Moving beyond the large  $n_c$  limit, we expect that the resulting corrections to the  $\kappa_y^x$  coefficients should depend only on the operator that is being factorised,

$$\kappa_y^x = k^x \bar{\kappa}_y^x , \quad \kappa_{27} = k_{27} \bar{\kappa}_{27} . \quad (4.90)$$

Since the 27-plet contribution proportional to  $\kappa_{27}$  is obtained by factorising the same combination of QCD operators as the symmetric octet contribution proportional to  $\kappa_y^+$ , we also expect  $k_{27} = k^+$ . Keeping only contributions from  $c_{1i}$ ,  $c_{2i}$ , and  $c_{6i}$ , the resulting predictions for the octet and 27-plet coefficients can be written as

$$h_{8i} = \frac{1}{2} V_{\text{su}}^\dagger V_{\text{ud}} \left( \frac{k^+ c_{12i}^+}{2n_8^+} + \frac{k^- c_{12i}^-}{2n_8^-} + 4L_5 \frac{b_0^2}{f_0^2} k^s c_{6i} \right) , \quad (4.91\text{a})$$

$$h_{1i} = \frac{1}{n_f} V_{\text{su}}^\dagger V_{\text{ud}} \left( k^+ c_{12i}^+ - k^- c_{12i}^- + 4L_5 \frac{b_0^2}{f_0^2} k^s c_{6i} \right) , \quad (4.91\text{b})$$

$$h_{bi} = \frac{1}{2} V_{\text{su}}^\dagger V_{\text{ud}} (4L_8 + 2H_2) \frac{b_0^2}{f_0^2} k^s c_{6i} , \quad (4.91\text{c})$$

$$h_{27i} = \frac{1}{4} V_{\text{su}}^\dagger V_{\text{ud}} \frac{n_{27}}{n_8^+} \frac{n_f + 1}{n_f + 2} k^+ c_{12i}^+ . \quad (4.91\text{d})$$

The correction factors  $k^x$  can be fixed by matching them to kaon decay amplitudes. Neglecting electromagnetic contributions, the experimentally determined amplitudes for  $K \rightarrow \pi\pi$  decays [144]

$$\mathcal{A}(K^0 \rightarrow \pi^+\pi^-) = (277.22 \pm 0.12_{\text{exp}}) \text{ eV} , \quad \mathcal{A}(K^+ \rightarrow \pi^+\pi^0) = (18.18 \pm 0.04_{\text{exp}}) \text{ eV} , \quad (4.92a)$$

$$\mathcal{A}(K^0 \rightarrow \pi^0\pi^0) = (259.18 \pm 0.22_{\text{exp}}) \text{ eV} . \quad (4.92b)$$

They can be parameterised as [111]

$$\mathcal{A}(K^0 \rightarrow \pi^+\pi^-) = \mathcal{A}_{1/2} + \mathcal{A}_{3/2} , \quad \mathcal{A}(K^+ \rightarrow \pi^+\pi^0) = \frac{3}{\sqrt{2}} \mathcal{A}_{3/2} , \quad (4.93a)$$

$$\mathcal{A}(K^0 \rightarrow \pi^0\pi^0) = \mathcal{A}_{1/2} - 2\mathcal{A}_{3/2} . \quad (4.93b)$$

The amplitudes  $\mathcal{A}_{1/2}$  and  $\mathcal{A}_{3/2}$  are associated with  $\Delta I = 1/2$  and  $\Delta I = 3/2$  transitions, respectively. In the limit  $m_u, m_d \rightarrow m_{\text{ud}}$ , they are [171]

$$\mathcal{A}_{1/2} = \epsilon_{\text{EW}} \frac{m_K^2 - m_\pi^2}{4f_0} \left( h_8 + \frac{1}{3} h_{27} \right) , \quad \mathcal{A}_{3/2} = \epsilon_{\text{EW}} \frac{m_K^2 - m_\pi^2}{4f_0} \frac{5}{3} h_{27} . \quad (4.94)$$

Hence, the absolute values and relative phase of the complex currents are

$$|h_8| = 2.23 \pm 0.09_{\text{exp}} \pm \text{NLO} , \quad \arg h_8 - \arg h_{27} = (45.03 \pm 0.77_{\text{exp}})^\circ \pm \text{NLO} , \quad (4.95a)$$

$$|h_{27}| = 0.0425 \pm 0.0018_{\text{exp}} \pm \text{NLO} . \quad (4.95b)$$

The final parameter  $h_1$  can be fixed by matching it to  $K_L \rightarrow \gamma\gamma$  decays [112], which results in

$$h_1 = (0.37 \pm 0.05_{\text{exp}}) h_8 , \quad |h_1| = 0.82 \pm 0.12_{\text{exp}} \pm \text{NLO} . \quad (4.96)$$

Finally, inverting equations (4.91), one obtains

$$V_{\text{su}}^\dagger V_{\text{ud}} k^- c_{12}^- = \frac{2}{3} h_8 + \frac{1}{2} h_{27} - h_1 , \quad V_{\text{su}}^\dagger V_{\text{ud}} k^s c_6 = \frac{f_0^2}{4L_5 b_0^2} \left( \frac{2}{3} h_8 - 2h_{27} + 2h_1 \right) , \quad (4.97a)$$

$$V_{\text{su}}^\dagger V_{\text{ud}} k^+ c_{12}^+ = \frac{5}{2} h_{27} . \quad (4.97b)$$

Therefore the absolute values are

$$|V_{\text{su}}^\dagger V_{\text{ud}} k^- c_{12}^-| = 0.69 \pm 0.13_{\text{exp}} \pm \text{NLO} , \quad (4.98a)$$

$$|V_{\text{su}}^\dagger V_{\text{ud}} k^+ c_{12}^+| = 0.106 \pm 0.005_{\text{exp}} \pm \text{NLO} , \quad (4.98b)$$

$$|V_{\text{su}}^\dagger V_{\text{ud}} k^s c_6| = 0.125 \pm 0.013_{\text{exp}} \pm 0.015_{\text{lat}} \pm \text{NLO} . \quad (4.98c)$$

Since the values of the SM Wilson coefficients are well known even at relatively low scales, such as  $\mu_{\text{QCD}} = 1 \text{ GeV}$  [179], this relation makes it possible to extract estimates for the correction coefficients  $k^x$ . In turn, these can be used to constrain the shape of the portal Wilson coefficients  $c_{1i}$ ,  $c_{2i}$ , and  $c_{6i}$  with  $i = 1, 2$  using bounds on the corresponding  $h_{yi}$  obtained from searches for hidden sector induced meson transitions. Keep in mind that we have considered only the leading contributions have for example neglected the impact of the penguin operators associated with  $c_{3i}$ ,  $c_{4i}$ , and  $c_{5i}$ .

## 4.5 Transition to the physical vacuum

The two SM mass like terms (4.37b) and (4.40b) contain the tadpole contribution

$$\mathcal{L}_U^{hm} + \mathcal{L}_U^{hm} \supset \frac{i \epsilon_{EW} f_0 b_0}{2} h'_b \langle [\mathbf{m}, \Phi] \rangle_{\text{d}}^s + \text{h.c.} , \quad h'_b = h_b - \kappa_\Gamma \langle \mathbf{m}_q^{-1} \boldsymbol{\gamma}_G \rangle_{\text{s}}^{\text{d}} , \quad (4.99)$$

which generates a finite VEV for the PNGB matrix  $\Phi$ . When computing purely hadronic kaon decay rates in the SM such as  $K \rightarrow \pi\pi$  and  $K \rightarrow \pi\pi\pi$ , diagrams that contain tadpole vertices exactly cancel with the other contributions from the mass-like terms (4.37b) and (4.40b), so that the final transition amplitudes do not depend on  $h'_b$  [42, 114, 115]. This reflects the fact that the mass-like terms can be eliminated entirely defining a rotated meson field [114]

$$\mathbf{g}' = \mathbf{W}^\dagger \mathbf{g} \overline{\mathbf{W}}^\dagger , \quad \langle 0 | \mathbf{g}' | 0 \rangle = \mathbf{1} . \quad (4.100)$$

Accounting for the impact of the chromomagnetic dipole Lagrangian (4.37b), which is often neglected [114], the appropriate rotation matrices are

$$\mathbf{W} = e^{-i(\alpha_L \boldsymbol{\lambda}_7 + \beta_L \boldsymbol{\lambda}_6)} = \mathbf{1} + \mathcal{O}(\epsilon_{EW}) , \quad \overline{\mathbf{W}} = e^{i(\alpha_R \boldsymbol{\lambda}_7 + \beta_R \boldsymbol{\lambda}_6)} = \mathbf{1} + \mathcal{O}(\epsilon_{EW}) , \quad (4.101)$$

where the angles  $\alpha_{L/R}$  and  $\beta_{L/R}$  defined by

$$\frac{\beta_L}{\alpha_L} = \frac{\beta_R}{\alpha_R} = -\tan(\arg h'_b) , \quad (4.102a)$$

$$|\alpha_L + i\beta_L| \pm |\alpha_R + i\beta_R| = \arctan\left(\epsilon_{EW} |h'_b| \frac{m_s \pm m_d}{m_s \mp m_d}\right) \simeq \epsilon_{EW} |h'_b| \left(1 \pm 2 \frac{m_d}{m_s}\right) , \quad (4.102b)$$

measure the size of EW contributions to the light quark masses. After this field redefinition, the entries of the diagonalised quark mass matrix

$$\mathbf{m}' = \overline{\mathbf{W}} \mathbf{m} \mathcal{O}(h'_b) \mathbf{W} , \quad \mathcal{O}(x) = \mathbf{1} - \epsilon_{EW} (x \boldsymbol{\lambda}_s^{\text{d}} + \text{h.c.}) \quad (4.103)$$

correspond to the experimentally determined quark masses. In general, using the redefined external currents

$$\mathbf{M}' = \mathbf{m}' + \mathbf{S}'_m = \overline{\mathbf{W}} (\mathbf{M} \mathcal{O}(h'_b + S_b) + \epsilon_{EW} \kappa_\Gamma \mathbf{S}_\gamma) \mathbf{W} . \quad (4.104)$$

and

$$\mathbf{L}'_\mu = \mathbf{W}^\dagger \mathbf{L}_\mu \mathbf{W} , \quad \mathbf{R}'_\mu = \overline{\mathbf{W}} \mathbf{R}_\mu \overline{\mathbf{W}}^\dagger , \quad \Theta' = \Theta + i \langle \ln \mathbf{W} \overline{\mathbf{W}} \rangle_f , \quad (4.105)$$

in place of the original ones, the net effect of the field redefinition is two-fold: i) both mass-like terms  $\mathcal{L}_U^{HM}$  and  $\mathcal{L}_U^\Gamma$  are eliminated from the  $\chi$ PT Lagrangian, being reabsorbed into  $\mathbf{M}'$ , and ii) while these mass-like term still contribute to  $\Upsilon_U$ , in contrast to (4.83), they now contribute with new relative prefactors of

$$\kappa_\omega^{HM} - \kappa_\omega^M = \kappa_\omega^H - \kappa_\omega^M = \frac{2}{\beta_0} . \quad (4.106)$$

The rotated mass and octet Lagrangians are

$$\mathcal{L}'^H_U = \mathcal{L}^{HD^2}_U + \mathcal{L}^{SD^2}_U , \quad (4.107a)$$

$$\mathcal{L}'^M_U = \frac{f_0^2 b_0}{2} \widehat{M}' + \text{h.c.} , \quad \mathcal{L}'^{HM}_U = -\frac{\epsilon_{\text{EW}} f_0^2 b_0}{2} H_b \left\langle \widehat{M}' + \widehat{M}'^\dagger \right\rangle_{\text{d}}^s + \text{h.c.} , \quad (4.107b)$$

while the rotated  $G_{LR}$  singlet contributions to the  $\chi$ PT Lagrangian are

$$\mathcal{L}^{S_\omega}_{U\delta^n} = S_\omega \Upsilon_{U\delta^{n-1}} , \quad \mathcal{L}^{S_\omega \text{EW}}_{U\delta^n} = S_\omega \Upsilon_{U\delta^{n-1}}^{\text{EW}} , \quad (4.108)$$

where

$$\beta_0 \Upsilon'_{U\delta^2} = 2\mathcal{L}^{D^2}_U + 3\mathcal{L}'^M_U + 4\mathcal{L}^{\Theta^2}_U , \quad \beta_0 \Upsilon'_{U\delta}^{\text{EW}} = 2(\mathcal{L}'^H_U + \mathcal{L}'^{HM}_U) , \quad \beta_0 \Upsilon'_{U\delta^2}^{\text{EW}} = 2\mathcal{L}^F_U . \quad (4.109)$$

## 4.6 Expanded Lagrangian

The final Lagrangian that captures the LO interactions between the light mesons and each of the external currents is

$$\mathcal{L}^{\text{LO}}_U = \mathcal{L}'_{U\delta^2} + \mathcal{L}'_{U\delta^3} + \mathcal{L}'_{U\delta}^{\text{EW}} + \mathcal{L}'_{\delta^2}^{\text{EW}} + \mathcal{L}'_{\delta^3}^{\text{EW}} \quad (4.110)$$

where the strong contributions are

$$\mathcal{L}'_{U\delta^2} = \mathcal{L}^{D^2}_U + \mathcal{L}'^M_U + \mathcal{L}^{\Theta^2}_U , \quad \mathcal{L}'_{U\delta^3} = \mathcal{L}'^{S_\omega}_{U\delta^3} + \mathcal{L}^{n_c}_U , \quad (4.111)$$

and the  $\epsilon_{\text{EW}}$  suppressed contributions are

$$\mathcal{L}'_{U\delta}^{\text{EW}} = \mathcal{L}'^H_U , \quad \mathcal{L}'_{U\delta^2}^{\text{EW}} = \mathcal{L}'^{S_\omega}_{U\delta^2} , \quad \mathcal{L}'_{U\delta^3}^{\text{EW}} = \mathcal{L}^{TD^2}_U + \mathcal{L}^{TV}_U + \mathcal{L}'_{U\delta^3}^{S_\omega \text{EW}} . \quad (4.112)$$

The individual terms are given in Lagrangians (4.12), (4.19), (4.29), (4.38), (4.107), and (4.108).

To ease the application of this result to phenomenological computations, we decompose the Lagrangian into individual contributions that mediate either purely hadronic meson interactions or the coupling of  $\chi$ PT to specific combinations of the SM and portal currents. Although the final  $\chi$ PT Lagrangian contains interactions with both one and two photons, we restrict ourselves to explicitly listing interactions with at most a single photon field. This is sufficient for capturing a large number of interesting hidden sector induces transitions, such as *e.g.*  $\pi^0 \rightarrow \gamma\gamma_{\text{dark}}$ .

**Order  $\delta^2$**  The gauged kinetic Lagrangian (4.12)  $\mathcal{L}^{D^2}_U$  contains the ungauged kinetic Lagrangian

$$\mathcal{L}^{\partial^2}_u = \frac{f_0^2}{2} \langle \mathbf{u}_\mu \mathbf{u}^\mu \rangle_f , \quad (4.113)$$

and couples the mesons to the photon current via the interaction

$$\mathcal{L}^{\partial A}_u = f_0^2 \langle \mathbf{u}_\mu (\widehat{\mathbf{r}}^\mu_A - \mathbf{l}^\mu_A) \rangle_f . \quad (4.114)$$

It also couples the mesons to the hidden currents  $\mathbf{V}_l^\mu$  and  $\widehat{\mathbf{V}}_r^\mu$  via the interactions

$$\mathcal{L}_u^{\partial V_l} = -f_0^2 \langle \mathbf{V}_l'^\mu \mathbf{u}_\mu \rangle_f, \quad \mathcal{L}_u^{AV_l} = -f_0^2 \langle \mathbf{V}_l'^\mu \widehat{\mathbf{r}}_{A\mu} \rangle_f, \quad (4.115a)$$

$$\mathcal{L}_u^{\partial V_r} = f_0^2 \langle \widehat{\mathbf{V}}_r'^\mu \mathbf{u}_\mu \rangle_f, \quad \mathcal{L}_u^{AV_r} = -f_0^2 \langle \widehat{\mathbf{V}}_r'^\mu l_{A\mu} \rangle_f. \quad (4.115b)$$

The rotated mass Lagrangian (4.107b) and the anomaly Lagrangian (4.19) contain the purely hadronic mass-terms

$$\mathcal{L}_u'^m = \frac{f_0^2 b_0}{2} \widehat{m}' + \text{h.c.}, \quad \mathcal{L}_u^\theta = -\frac{f_0^2 m_0^2}{2n_f} \widehat{\theta}^2 \quad (4.116)$$

and couple the mesons to the complex scalar  $\mathbf{S}_m'$  current and the pseudoscalar  $S_\theta$  current via the interactions

$$\mathcal{L}_u'^{S_m} = \frac{f_0^2 b_0}{2} \widehat{S}_m' + \text{h.c.}, \quad \mathcal{L}_u^{S_\theta} = -\frac{f_0^2 m_0^2}{n_f} \widehat{\theta} \widehat{S}_\theta. \quad (4.117)$$

**Order  $\delta^3$**  The order  $\delta^3$  contribution to the rotated singlet Lagrangian (4.108) couples mesons to the  $S_\omega$  current via the interactions

$$\mathcal{L}_u'^{S_\omega}{}_{\delta^3} = \frac{S_\omega}{\beta_0} \left( 2 \left( \mathcal{L}_u^{\partial^2} + \mathcal{L}_u^{\partial A} \right) + 3 \mathcal{L}_u'^m + 4 \mathcal{L}_u^\theta \right) \quad (4.118)$$

and the WZW Lagrangian (4.29) couples mesons to the hidden currents  $\mathbf{V}_l^\mu$  and  $\mathbf{V}_r^\mu$ . The coupling to  $\mathbf{V}_l^\mu$  is mediated by the Lagrangians

$$\mathcal{L}_u^{n_c V_l} = \frac{2n_c}{4!(2\pi)^2} \epsilon_{\mu\nu\rho\sigma} \langle -i \mathbf{V}_l'^\mu \mathbf{u}^\nu \mathbf{u}^\rho \mathbf{u}^\sigma \rangle_f, \quad (4.119a)$$

$$\mathcal{L}_u^{n_c V_l A} = \frac{2n_c}{4!(2\pi)^2} \epsilon_{\mu\nu\rho\sigma} \left\langle \mathbf{V}_l'^\mu \left( \left\{ l_A^{\nu\rho} + \frac{1}{2} \widehat{\mathbf{r}}_A^{\nu\rho}, \mathbf{u}^\sigma \right\} - i \mathbf{u}^\nu (l_A^\rho - \widehat{\mathbf{r}}_A^\rho) \mathbf{u}^\sigma - i \{ l_A^\nu - \widehat{\mathbf{r}}_A^\nu, \mathbf{u}^\rho \mathbf{u}^\sigma \} \right) \right\rangle_f, \quad (4.119b)$$

and the coupling to  $\mathbf{V}_r^\mu$  is mediated by the Lagrangians

$$\mathcal{L}_u^{n_c V_r} = \frac{2n_c}{4!(2\pi)^2} \epsilon_{\mu\nu\rho\sigma} \langle -i \widehat{\mathbf{V}}_r'^\mu \mathbf{u}^\nu \mathbf{u}^\rho \mathbf{u}^\sigma \rangle_f, \quad (4.120a)$$

$$\mathcal{L}_u^{n_c V_r A} = \frac{2n_c}{4!(2\pi)^2} \epsilon_{\mu\nu\rho\sigma} \left\langle \widehat{\mathbf{V}}_r'^\mu \left( \left\{ \frac{1}{2} l_A^{\nu\rho} + \widehat{\mathbf{r}}_A^{\nu\rho}, \mathbf{u}^\sigma \right\} - i \mathbf{u}^\nu (l_A^\rho - \widehat{\mathbf{r}}_A^\rho) \mathbf{u}^\sigma - i \{ l_A^\nu - \widehat{\mathbf{r}}_A^\nu, \mathbf{u}^\rho \mathbf{u}^\sigma \} \right) \right\rangle_f. \quad (4.120b)$$

**Order  $\epsilon_{\text{EW}}\delta$**  At this order, the kinetic-like Lagrangians (4.40) and (4.44) that appear in the rotated four-quark Lagrangian (4.107a) generate additional contributions to the kinetic-like term

$$\mathcal{L}_u^{h\partial^2} = -\frac{\epsilon_{\text{EW}} f_0^2}{2} (h_8 \langle \mathbf{u}_\mu \mathbf{u}^\mu \rangle_d^s + h_1 \mathbf{u}^{\mu s} u_\mu) + \text{h.c.}, \quad (4.121a)$$

$$\mathcal{L}_u^{\bar{h}\partial^2} = -\frac{\epsilon_{\text{EW}} f_0^2}{2} h_{27} (n_f \mathbf{u}_{\mu d}^s \mathbf{u}^{\mu u} + (n_f - 1) \mathbf{u}_{\mu d}^u \mathbf{u}^{\mu s}) + \text{h.c.}, \quad (4.121b)$$



and couple the mesons to the photon current via the interactions

$$\mathcal{L}_u^{h\partial A} = -\frac{\epsilon_{\text{EW}} f_0^2}{2} (h_8 \langle \{ \mathbf{u}_\mu, \hat{\mathbf{r}}_A^\mu - \mathbf{l}_A^\mu \} \rangle_{\text{d}}^{\text{s}} + h_1 \hat{\mathbf{r}}_{\text{Ad}}^{\mu \text{s}} u_\mu) + \text{h.c.} , \quad (4.122\text{a})$$

$$\mathcal{L}_u^{\mathfrak{h}\partial A} = -\frac{\epsilon_{\text{EW}} f_0^2}{2} h_{27} (n_f (\mathbf{u}_{\mu \text{d}}^{\text{s}} (\hat{\mathbf{r}}_A^\mu - \mathbf{l}_A^\mu)_{\text{u}}^{\text{u}} + \hat{\mathbf{r}}_{\text{A}\mu \text{d}}^{\text{s}} \mathbf{u}_{\text{u}}^{\mu \text{u}}) + (n_f - 1) (\hat{\mathbf{r}}_{\text{A}\mu \text{d}}^{\text{u}} \mathbf{u}_{\text{u}}^{\mu \text{s}} + \mathbf{u}_{\mu \text{d}}^{\text{u}} \hat{\mathbf{r}}_{\text{Au}}^{\mu \text{s}})) + \text{h.c.} . \quad (4.122\text{b})$$

They also couple mesons to the hidden vector currents  $\mathbf{V}_l^\mu$  and  $\mathbf{V}_r^\mu$  and the hidden scalar currents  $S_8$ ,  $S_1$ ,  $S_b$ , and  $S_{27}$ . Neglecting strangeness conserving contributions generated by interactions involving  $\mathbf{V}_l^{\mu \text{s}}$ , the coupling to  $\mathbf{V}_l^\mu$  is mediated by the octet terms

$$\mathcal{L}_u^{h\partial V_l} = \frac{\epsilon_{\text{EW}} f_0^2}{2} (h_8 \langle \{ \mathbf{V}_l^\mu, \mathbf{u}_\mu \} \rangle_{\text{d}}^{\text{s}} + h_1 \mathbf{u}_{\mu \text{d}}^{\text{s}} V_l^\mu) + \text{h.c.} , \quad (4.123\text{a})$$

$$\mathcal{L}_u^{hAV_l} = \frac{\epsilon_{\text{EW}} f_0^2}{2} (h_8 \langle \{ \mathbf{V}_l^\mu, \hat{\mathbf{r}}_{\text{A}\mu} \} \rangle_{\text{d}}^{\text{s}} + h_1 \hat{\mathbf{r}}_{\text{A}\mu \text{d}}^{\text{s}} V_l^\mu) + \text{h.c.} , \quad (4.123\text{b})$$

and the 27-plet terms

$$\mathcal{L}_u^{\mathfrak{h}\partial V_l} = \frac{\epsilon_{\text{EW}} f_0^2}{2} h_{27} n_f \mathbf{u}_{\mu \text{d}}^{\text{s}} \mathbf{V}_l^{\mu \text{u}} + \text{h.c.} , \quad \mathcal{L}_u^{\mathfrak{h}AV_l} = \frac{\epsilon_{\text{EW}} f_0^2}{2} h_{27} n_f \hat{\mathbf{r}}_{\text{A}\mu \text{d}}^{\text{s}} \mathbf{V}_l^{\mu \text{u}} + \text{h.c.} . \quad (4.124)$$

The coupling to  $\mathbf{V}_r^\mu$  is mediated by the octet terms

$$\mathcal{L}_u^{h\partial V_r} = -\frac{\epsilon_{\text{EW}} f_0^2}{2} \left( h_8 \langle \{ \hat{\mathbf{V}}_r^\mu, \mathbf{u}_\mu \} \rangle_{\text{d}}^{\text{s}} + h_1 (\hat{\mathbf{V}}_{r \text{d}}^{\mu \text{s}} u_\mu + \mathbf{u}_{\mu \text{d}}^{\text{s}} \hat{\mathbf{V}}_r^\mu) \right) + \text{h.c.} , \quad (4.125\text{a})$$

$$\mathcal{L}_u^{hAV_r} = -\frac{\epsilon_{\text{EW}} f_0^2}{2} \left( h_8 \langle \{ \hat{\mathbf{V}}_r^\mu, \hat{\mathbf{r}}_{\text{A}\mu} - \mathbf{l}_{\text{A}\mu} \} \rangle_{\text{d}}^{\text{s}} + h_1 \hat{\mathbf{r}}_{\text{A}\mu \text{d}}^{\text{s}} \hat{\mathbf{V}}_r^\mu \right) + \text{h.c.} , \quad (4.125\text{b})$$

and the 27-plet terms

$$\begin{aligned} \mathcal{L}_u^{\mathfrak{h}\partial V_r} = & -\frac{\epsilon_{\text{EW}} f_0^2}{2} h_{27} \left( n_f (\mathbf{u}_{\mu \text{d}}^{\text{s}} \hat{\mathbf{V}}_{r \text{u}}^{\mu \text{u}} + \hat{\mathbf{V}}_{r \text{d}}^{\mu \text{s}} \mathbf{u}_{\mu \text{u}}^{\text{u}}) \right. \\ & \left. + (n_f - 1) (\hat{\mathbf{V}}_{r \text{d}}^{\mu \text{u}} \mathbf{u}_{\mu \text{u}}^{\text{s}} + \mathbf{u}_{\mu \text{d}}^{\text{u}} \hat{\mathbf{V}}_{r \text{u}}^{\mu \text{s}}) \right) + \text{h.c.} , \end{aligned} \quad (4.126\text{a})$$

$$\begin{aligned} \mathcal{L}_u^{\mathfrak{h}AV_r} = & -\frac{\epsilon_{\text{EW}} f_0^2}{2} h_{27} \left( n_f (\hat{\mathbf{V}}_{r \text{d}}^{\mu \text{s}} (\hat{\mathbf{r}}_{\text{A}\mu} - \mathbf{l}_{\text{A}\mu})_{\text{u}}^{\text{u}} + \hat{\mathbf{r}}_{\text{A}\mu \text{d}}^{\text{s}} \hat{\mathbf{V}}_{r \text{u}}^{\mu \text{u}}) \right. \\ & \left. + (n_f - 1) (\hat{\mathbf{V}}_{r \text{d}}^{\mu \text{u}} \hat{\mathbf{r}}_{\text{A}\mu \text{u}}^{\text{s}} + \hat{\mathbf{r}}_{\text{A}\mu \text{d}}^{\text{u}} \hat{\mathbf{V}}_{r \text{u}}^{\mu \text{s}}) \right) + \text{h.c.} . \end{aligned} \quad (4.126\text{b})$$

Finally, the coupling to the  $S_y$  currents with  $y = b, 1, 8, 27$  is mediated by the octet terms

$$\mathcal{L}_u^{\partial^2 S} = -\frac{\epsilon_{\text{EW}} f_0^2}{2} (S_8 \langle \mathbf{u}_\mu \mathbf{u}^\mu \rangle_{\text{d}}^{\text{s}} + S_1 \mathbf{u}_{\mu \text{d}}^{\mu \text{s}} u_\mu) + \text{h.c.} , \quad (4.127\text{a})$$

$$\mathcal{L}_u^{\text{AS}} = -\frac{\epsilon_{\text{EW}} f_0^2}{2} (S_8 \langle \{ \mathbf{u}_\mu, \hat{\mathbf{r}}_A^\mu \} - \mathbf{l}_A^\mu \rangle_{\text{d}}^{\text{s}} + S_1 \hat{\mathbf{r}}_{\text{Ad}}^{\mu \text{s}} u_\mu) + \text{h.c.} , \quad (4.127\text{b})$$

and the 27-plet terms

$$\mathcal{L}_u^{\partial^2 \mathfrak{S}} = -\frac{\epsilon_{\text{EW}} f_0^2}{2} S_{27} (\mathbf{u}_{\mu d}^s \mathbf{u}_{\mu u}^{\mu u} + (n_f - 1) \mathbf{u}_{\mu d}^u \mathbf{u}_{\mu u}^{\mu s}) + \text{h.c.} , \quad (4.128a)$$

$$\mathcal{L}_u^{\text{A}\mathfrak{S}} = -\frac{\epsilon_{\text{EW}} f_0^2}{2} S_{27} (n_f (\mathbf{u}_{\mu d}^s (\hat{\mathbf{r}}_A^\mu - \mathbf{I}_A^\mu)_u^u + \hat{\mathbf{r}}_{A\mu d}^s \mathbf{u}_{\mu u}^{\mu u}) + (n_f - 1) (\hat{\mathbf{r}}_{A\mu d}^u \mathbf{u}_{\mu u}^{\mu s} + \mathbf{u}_{\mu d}^u \hat{\mathbf{r}}_{A u}^{\mu s})) + \text{h.c.} . \quad (4.128b)$$

**Order  $\epsilon_{\text{EW}} \delta^2$**  At this order, the gauged kinetic Lagrangian (4.12) couples the mesons to the photon the weak-leptonic charged currents via the interactions

$$\mathcal{L}_u^{\text{AW}} = -f_0^2 \langle \mathbf{I}_W^\mu \hat{\mathbf{r}}_{A\mu} \rangle_f , \quad \mathcal{L}_u^{\partial W} = -f_0^2 \langle \mathbf{u}_\mu \mathbf{I}_W^\mu \rangle_f . \quad (4.129)$$

It also couples the mesons to the hidden current  $\hat{\mathbf{V}}_r^\mu$  via the interaction

$$\mathcal{L}_u^{WV_r} = -f_0^2 \langle \hat{\mathbf{V}}_r^\mu \mathbf{I}_{W\mu} \rangle_f . \quad (4.130)$$

The rotated singlet Lagrangian (4.108) couples mesons to the  $S_\omega$  current via the interactions

$$\mathcal{L}_u^{S_\omega \text{EW}} = \frac{2S_\omega}{\beta_0} \left( \mathcal{L}_u^{h\partial^2} + \mathcal{L}_u^{\mathfrak{h}\partial^2} + \mathcal{L}_u^{h\partial A} + \mathcal{L}_u^{\mathfrak{h}\partial A} + \mathcal{L}_u^{hm} \right) , \quad (4.131)$$

where

$$\mathcal{L}_u^{hm} = -\frac{\epsilon_{\text{EW}} f_0^2 b_0}{2} h_b \langle \hat{\mathbf{m}}' + \hat{\mathbf{m}}'^{\dagger} \rangle_d^s + \text{h.c.} \quad (4.132)$$

**Order  $\epsilon_{\text{EW}} \delta^3$**  At this order, the rotated singlet Lagrangian (4.108) couples mesons to the  $S_\omega$  current via the interactions

$$\mathcal{L}_u^{S_\omega \text{EW}} = \frac{2S_\omega}{\beta_0} \left( \mathcal{L}_u^{\partial W} + \mathcal{L}_u^{\text{AW}} + \mathcal{L}_u^\gamma \right) , \quad (4.133)$$

where

$$\mathcal{L}_u^\gamma = \frac{\epsilon_{\text{EW}} f_0^2 b_0}{2} \kappa_I \hat{\gamma} + \text{h.c.} \quad (4.134)$$

The dipole Lagrangian (4.38) couples mesons to the hidden currents  $\mathbf{V}_l^\mu$ ,  $\mathbf{V}_r^\mu$ , and  $\mathbf{T}_\tau^{\mu\nu}$  via the interactions

$$\mathcal{L}_u^{T\partial^2} = \frac{\epsilon_{\text{EW}} \kappa_T^{D^2}}{f_0} \langle \hat{\mathbf{T}}_\tau^{\mu\nu} \mathbf{u}_\mu \mathbf{u}_\nu \rangle_f + \text{h.c.} , \quad \mathcal{L}_u^{TV} = \frac{\epsilon_{\text{EW}} \kappa_T^{LR}}{f_0} \langle \hat{\mathbf{T}}_\tau^{\mu\nu} \mathbf{I}_{A\mu\nu} \rangle_f + \text{h.c.} , \quad (4.135a)$$

$$\mathcal{L}_u^{T\partial V} = \frac{\epsilon_{\text{EW}} \kappa_T^{D^2}}{f_0} \langle \hat{\mathbf{T}}_\tau^{\mu\nu} (\mathbf{u}_\mu (\mathbf{I}_{A\nu} - \hat{\mathbf{r}}_{A\nu}) + (\mathbf{I}_{A\mu} - \hat{\mathbf{r}}_{A\mu}) \mathbf{u}_\nu) \rangle_f + \text{h.c.} \quad (4.135b)$$

Finally, the WZW Lagrangian (4.29) couples mesons to the hidden currents  $\mathbf{V}_l^\mu$  and  $\mathbf{V}_r^\mu$ . The coupling to  $\mathbf{V}_l^\mu$  is mediated by the term

$$\mathcal{L}_u^{n_c V_l W} = \frac{2n_c}{4!(2\pi)^2} \epsilon_{\mu\nu\rho\sigma} \langle \mathbf{V}_l^\mu (\{ \mathbf{I}_W^{\nu\rho}, \mathbf{u}^\sigma \} - i \mathbf{u}^\nu \mathbf{I}_W^\rho \mathbf{u}^\sigma - i \{ \mathbf{I}_W^\nu, \mathbf{u}^\rho \mathbf{u}^\sigma \}) \rangle_f , \quad (4.136)$$

and the coupling to  $\mathbf{V}_r^\mu$  is mediated by the term

$$\mathcal{L}_u^{n_c V_r W} = \frac{2n_c}{4!(2\pi)^2} \epsilon_{\mu\nu\rho\sigma} \langle \hat{\mathbf{V}}_r^\mu \left( \frac{1}{2} \{ \mathbf{I}_W^{\nu\rho}, \mathbf{u}^\sigma \} - i \mathbf{u}^\nu \mathbf{I}_W^\rho \mathbf{u}^\sigma - i \{ \mathbf{I}_W^\nu, \mathbf{u}^\rho \mathbf{u}^\sigma \} \right) \rangle_f . \quad (4.137)$$

## 5 Portal interactions of the light pseudoscalar mesons

In this section, we illustrate the information encoded inside the  $\chi$ PT action derived in the previous section by extracting a set of concrete interactions. In particular, we expand the  $\chi$ PT action in terms of the meson matrix  $\Phi$  in order to extract the bilinear and trilinear terms that are induced by the hidden messengers and that contribute to meson decays with at most one SM meson in the final state. These decays are among the primary channels for production of hidden particles at fixed target experiments, such as  $K^\pm \rightarrow \pi^\pm s_i$ ,  $K^\pm \rightarrow l^\pm \xi_a$ , and  $\pi^0 \rightarrow \gamma v_\mu$ . They also include invisible decays of neutral mesons into light hidden fields, which can be constrained with collider or fixed target observations, such as [85, 214].

In section 5.1, we list the portal interactions that result from expanding the portal  $\chi$ PT Lagrangian up to quadratic order in the meson matrix  $\Phi$ . Whenever relevant, we additionally show the contributions that originate from the SM  $\chi$ PT action. We refer to appendix D for a more detailed discussion of the expansion procedure. In section 5.2, we then evaluate the flavour traces extracted in section 5.1, and provide the interactions that couple the individual singlet and octet mesons to flavour blind hidden sectors.

The SM  $\chi$ PT Lagrangian mixes the neutral singlet and octet mesons with each other, so that they do not coincide with mass eigenstates of the theory. The diagonalisation procedure used to construct the mass eigenstates and the corresponding mixing angles is well established and reported in appendix D.1 for sake of completeness. In addition, certain one-meson portal interactions mix the SM mesons with the hidden spin 0 messenger. At LO in  $\epsilon_{UV}$ , it is not necessary to diagonalise these interactions, which can be treated perturbatively when computing microscopic scattering and decay rates. To facilitate computations in which it is necessary to re-sum the mixing, we present an explicit computation of the mixing angles between SM gauge eigenstates and messengers in appendix D.2.

### 5.1 One- and two-meson interactions

Here we list the one- and two-meson interactions, as described above. In general, the one-meson interactions mix the SM mesons with hidden sector particles or mediate non-hadronic decays into some combination of leptons, photons, and hidden particles. The two-meson interactions mediate semi-hadronic decays with a single meson in the final state. Due to the mixing between mesons and messenger particles, pure SM interactions with two or three mesons can also contribute to processes with messenger fields in the final state. Therefore, whenever relevant, we list the pure SM terms contributing to such processes.

**Order  $\delta^2$**  At this order, the photon Lagrangian (4.114) encodes the *SM two-meson interaction*

$$\mathcal{L}_{\Phi^2}^{\partial A} = -i \langle \mathbf{v}_A^\mu [\Phi, \partial_\mu \Phi] \rangle_f, \quad (5.1)$$

which mediates radiation of virtual photons. This interaction also contributes to decays with associated photon production, such as  $\phi_i \rightarrow \phi_j \gamma s_k$  and  $\phi_i \rightarrow \phi_j \gamma v_\mu$ .

The kinetic-like Lagrangians in (4.115) couple  $\chi$ PT to the portal currents  $\mathbf{V}_l^\mu$  and  $\mathbf{V}_r^\mu$  via the one-meson interactions

$$\mathcal{L}_\Phi^{\partial V_l} = -f_0 \langle \mathbf{V}_l'^\mu \partial_\mu \Phi \rangle_f, \quad \mathcal{L}_\Phi^{\partial V_r} = f_0 \langle \mathbf{V}_r'^\mu \partial_\mu \Phi \rangle_f, \quad (5.2)$$

and the two-meson interactions

$$\mathcal{L}_{\Phi^2}^{\partial V_l} = -\frac{i}{2} \langle \mathbf{V}_l'^\mu [\boldsymbol{\Phi}, \partial_\mu \boldsymbol{\Phi}] \rangle_f, \quad \mathcal{L}_{\Phi^2}^{\partial V_r} = -\frac{i}{2} \langle \mathbf{V}_r'^\mu [\boldsymbol{\Phi}, \partial_\mu \boldsymbol{\Phi}] \rangle_f, \quad (5.3a)$$

$$\mathcal{L}_{\Phi^2}^{\text{AV}_l} = \frac{1}{2} \langle \mathbf{V}_l'^\mu [\boldsymbol{\Phi}, [\boldsymbol{\Phi}, \mathbf{v}_{A\mu}]] \rangle_f, \quad \mathcal{L}_{\Phi^2}^{\text{AV}_r} = \frac{1}{2} \langle \mathbf{V}_r'^\mu [\boldsymbol{\Phi}, [\boldsymbol{\Phi}, \mathbf{v}_{A\mu}]] \rangle_f. \quad (5.3b)$$

The one-meson interactions mediate decays such as  $\phi_i \rightarrow \ell_a \xi_b$  and  $\phi_i \rightarrow \ell_a \nu_b s_j$ . They are also responsible for invisible neutral meson decays into hidden particles. Even though these channels are not directly measurable experimentally, their relative weights compared to decays with invisible SM final states constrain the coupling of mesons to NP, complementing the constraints obtained from decays that feature observable SM final states and hidden fields. The two-meson interactions mediate decays such as  $\phi_i \rightarrow \phi_j s_k s_l$ ,  $\phi_i \rightarrow \phi_j \ell_a \xi_b$ , and  $\phi_i \rightarrow \phi_j \gamma v_\mu$ . The decay  $\phi_i \rightarrow \phi_j \gamma v_\mu$  producing a photon receives contributions from both (5.3a) and (5.3b). However, diagrams that contain the interaction (5.3a), which does not involve photons directly, also have to contain a SM interaction (5.1), which radiates the required photon. If the hidden sector contains secluded neutral particles  $X$ , which can act *e.g.* as DM and interact with the SM only via the hidden field, the two-meson interactions can also give rise to decays mediated by an off-shell messenger exchange, such as  $\phi_i \rightarrow \phi_j v_\mu^* \rightarrow \phi_j \bar{X} X$ .

The quark-mass Lagrangian in (4.116) couples  $\chi$ PT to the imaginary and real parts of the portal current  $S'_m$  via the one- and two-meson interactions

$$\mathcal{L}_{\Phi}^{S'_m} = -f_0 b_0 \langle \boldsymbol{\Phi} \text{Im } S'_m \rangle_f, \quad \mathcal{L}_{\Phi^2}^{S'_m} = -\frac{b_0}{2} \langle \boldsymbol{\Phi}^2 \text{Re } S'_m \rangle_f. \quad (5.4)$$

These one-meson interactions are similar to the one in (5.2), which couple  $\chi$ PT to  $\mathbf{V}_l$  and  $\mathbf{V}_r$ , and mix the SM mesons with the hidden spin 0 messenger and mediate neutral meson decays into hidden spin 0 particles. The two-meson interactions mediate decays such as  $\phi_i \rightarrow \phi_j s_k$  and  $\phi_i \rightarrow \phi_j s_k s_l$ . Like the interactions (5.3), they can also give rise to decays with photons in the final state, such as  $\phi_i \rightarrow \phi_j s_k \gamma$ , as well as decays into secluded particles  $X$  that are mediated by an off-shell messenger exchange, such as  $\phi_i \rightarrow \phi_j s_k^* \rightarrow \phi_j \bar{X} X$ .

Finally, the anomaly Lagrangian in (4.116) couples  $\chi$ PT to the portal current  $S_\theta$  via the one-meson interaction

$$\mathcal{L}_{\Phi}^{S_\theta} = f_0 \frac{m_0^2}{n_f} S_\theta \boldsymbol{\Phi}, \quad (5.5)$$

which mixes the singlet  $\eta_1$ -meson with the spin 0 messenger.

**Order  $\delta^3$**  At this order, the singlet Lagrangian (4.118) couples  $\chi$ PT to the portal current  $S_\omega$  via the one-meson interactions

$$\mathcal{L}_{\Phi}^{S_\omega} = \frac{S_\omega}{\beta_0} 4\mathcal{L}_{\Phi}^{\theta}, \quad \mathcal{L}_{\Phi}^{\theta} = \frac{f_0 m_0^2}{n_f} \theta \boldsymbol{\Phi}, \quad (5.6)$$

and the two-meson interactions

$$\mathcal{L}_{\Phi^2}^{S_\omega} = \frac{S_\omega}{\beta_0} \left( 2 \left( \mathcal{L}_{\Phi^2}^{\partial^2} + \mathcal{L}_{\Phi^2}^{\partial A} \right) + 3\mathcal{L}_{\Phi^2}^m + 4\mathcal{L}_{\Phi^2}^{\theta} \right), \quad (5.7)$$

where

$$\mathcal{L}_{\Phi^2}^{\partial^2} = \frac{1}{2} \langle \partial_\mu \Phi \partial^\mu \Phi \rangle_f, \quad \mathcal{L}_{\Phi^2}^\theta = -\frac{m_0^2}{2n_f} \Phi^2, \quad \mathcal{L}_{\Phi^2}^{m_0} = -\frac{b_0}{2} \langle \Phi^2 m \rangle_f. \quad (5.8)$$

The one-meson interactions (5.6) mix the singlet  $\eta_1$  with spin 0 messenger particles, but this mixing is negligible because it is strongly suppressed by the QCD theta angle. The two-meson interactions (5.7) are similar to the one in (5.4). They mediate decays into spin 0 messengers, such as  $\phi_i \rightarrow \phi_j s_k$  and  $\phi_i \rightarrow \phi_j \gamma s_k$ , as well as decays into secluded particles  $X$ , such as  $\phi_i \rightarrow \phi_j \bar{X} X$ .

The WZW Lagrangians (4.119a) and (4.119b) couple  $\chi$ PT to the portal current  $V_l^\mu$  via the one-meson interaction

$$\mathcal{L}_{\Phi}^{n_c V_l A} = \frac{\epsilon_{\mu\nu\rho\sigma}}{(4\pi)^2 f_0} \frac{3}{4} \langle \Phi \{ \mathbf{v}_A^{\rho\sigma}, \mathbf{V}_l^{\mu\nu} \} \rangle_f, \quad (5.9)$$

and the two-meson interactions

$$\mathcal{L}_{\Phi^2}^{n_c V_l A} = \frac{\epsilon_{\mu\nu\rho\sigma}}{(4\pi)^2 f_0^2} \frac{i}{4} \langle \mathbf{V}_l^{\mu\nu} (3 \{ \mathbf{v}_A^{\rho\sigma}, [\Phi, \partial^\nu \Phi] \} + 2 \{ [\Phi, \mathbf{v}_A^{\rho\sigma}], \partial^\nu \Phi \}) \rangle_f. \quad (5.10)$$

Finally, the WZW Lagrangians (4.120a) and (4.120b) couple  $\chi$ PT to the portal current  $V_r^\mu$  via the one-meson interaction

$$\mathcal{L}_{\Phi}^{n_c V_r A} = \frac{\epsilon_{\mu\nu\rho\sigma}}{(4\pi)^2 f_0} \frac{3}{4} \langle \Phi \{ \mathbf{v}_A^{\rho\sigma}, \mathbf{V}_r^{\mu\nu} \} \rangle_f, \quad (5.11)$$

and the two-meson interactions

$$\mathcal{L}_{\Phi^2}^{n_c V_r A} = \frac{\epsilon_{\mu\nu\rho\sigma}}{(4\pi)^2 f_0^2} \frac{i}{4} \langle \mathbf{V}_r^{\mu\nu} (3 \{ \mathbf{v}_A^{\rho\sigma}, [\Phi, \partial^\nu \Phi] \} + 4 \{ [\Phi, \mathbf{v}_A^{\rho\sigma}], \partial^\nu \Phi \} - 6 [\Phi, \{ \mathbf{v}_A^{\rho\sigma}, \partial^\nu \Phi \}]) \rangle_f. \quad (5.12)$$

The one-meson interactions (5.9) and (5.11) mediate decays such as  $\phi_i \rightarrow \gamma v_\mu$  and  $\phi_i \rightarrow \gamma \ell_a \xi_b$ , while the two-meson interactions (5.10) and (5.12) mediate decays such as  $\phi_i \rightarrow \phi_j \gamma v_\mu$ . Notice that the WZW action is the only contribution that mediates non-hadronic meson decays with a spin 1 messenger particles in the final state. In particular, the order  $\delta^3$  Lagrangians (4.22) to (4.27), which one may expect to do so, do not mediate such transitions.

**Order  $\epsilon_{\text{EW}} \delta$**  At this order, the octet Lagrangians (4.121a) and (4.122a) encode the strangeness-violating *SM two-meson interactions*

$$\mathcal{L}_{\Phi^2}^{h\partial^2} = -\frac{\epsilon_{\text{EW}}}{2} (h_8 \langle \partial_\mu \Phi \partial^\mu \Phi \rangle_d^s + h_1 \partial^\mu \Phi_d^s \partial_\mu \Phi) + \text{h.c.}, \quad (5.13a)$$

$$\mathcal{L}_{\Phi^2}^{h\partial A} = -i \frac{\epsilon_{\text{EW}}}{2} h_8 \langle \{ \partial_\mu \Phi, [\Phi, \mathbf{v}_A^\mu] \} \rangle_d^s + \text{h.c.} \quad (5.13b)$$

The 27-plet Lagrangians (4.121b) and (4.122b) encode the additional strangeness-violating *SM two-meson interactions*

$$\mathcal{L}_{\Phi^2}^{h\partial^2} = -\frac{\epsilon_{\text{EW}}}{2} h_{27} (n_f \partial^\mu \Phi_u^u \partial_\mu \Phi_d^s + (n_f - 1) \partial_\mu \Phi_d^u \partial^\mu \Phi_u^s) + \text{h.c.}, \quad (5.14a)$$

$$\mathcal{L}_{\Phi^2}^{h\partial A} = -i \frac{\epsilon_{\text{EW}}}{2} h_{27} (n_f - 1) (\langle [\Phi, \mathbf{v}_A^\mu] \rangle_d^u \partial^\mu \Phi_u^s + \partial_\mu \Phi_d^u \langle [\Phi, \mathbf{v}_A^\mu] \rangle_u^s) + \text{h.c.} \quad (5.14b)$$

These interactions mix kaons with pions and  $\eta$ -mesons, and also mediate decays such as  $\phi_i \rightarrow \phi_j \ell_a \ell_a$ , where both charged leptons are of the same flavour. Similarly to (5.1), the latter interactions also contribute to decays with associated photon production, such as  $\phi_i \rightarrow \phi_j \gamma s_j$  and  $\phi_j \rightarrow \phi_j \gamma v_\mu$ . The octet Lagrangian (4.123) couples  $\chi$ PT to the portal current  $V_l^\mu$  via the strangeness-violating one-meson interactions

$$\mathcal{L}_\Phi^{h\partial V_l} = \frac{\epsilon_{\text{EW}} f_0}{2} (h_8 (\mathbf{V}_l^{\mu d} + \mathbf{V}_l^{\mu s}) + h_1 V_l^\mu) \partial_\mu \boldsymbol{\Phi}_d^s + \text{h.c.}, \quad (5.15)$$

and the strangeness-violating two-meson interactions

$$\mathcal{L}_{\Phi^2}^{h\partial V_l} = i \frac{\epsilon_{\text{EW}}}{4} (h_8 (\mathbf{V}_l^{\mu d} + \mathbf{V}_l^{\mu s}) + h_1 V_l^\mu) \langle [\boldsymbol{\Phi}, \partial_\mu \boldsymbol{\Phi}] \rangle_d^s + \text{h.c.}, \quad (5.16a)$$

$$\mathcal{L}_{\Phi^2}^{hAV_l} = -\frac{\epsilon_{\text{EW}}}{4} (h_8 (\mathbf{V}_l^{\mu d} + \mathbf{V}_l^{\mu s}) + h_1 V_l^\mu) \langle [\boldsymbol{\Phi}, [\boldsymbol{\Phi}, \mathbf{v}_{A\mu}]] \rangle_d^s + \text{h.c.}. \quad (5.16b)$$

The 27-plet Lagrangian (4.124) couples  $\chi$ PT to the portal current  $V_l^\mu$  via the strangeness-violating one-meson interaction

$$\mathcal{L}_\Phi^{h\partial V_l} = \frac{\epsilon_{\text{EW}} f_0}{2} h_{27} n_f \mathbf{V}_l^{\mu u} \partial_\mu \boldsymbol{\Phi}_{\mu d}^s + \text{h.c.}, \quad (5.17)$$

and the strangeness-violating two-meson interactions

$$\mathcal{L}_{\Phi^2}^{h\partial V_l} = i \frac{\epsilon_{\text{EW}}}{4} h_{27} n_f \mathbf{V}_l^{\mu u} \langle [\boldsymbol{\Phi}, \partial_\mu \boldsymbol{\Phi}] \rangle_d^s + \text{h.c.}, \quad (5.18a)$$

$$\mathcal{L}_{\Phi^2}^{hAV_l} = -\frac{\epsilon_{\text{EW}}}{4} h_{27} n_f \mathbf{V}_l^{\mu u} \langle [\boldsymbol{\Phi}, [\boldsymbol{\Phi}, \mathbf{v}_{A\mu}]] \rangle_d^s + \text{h.c.}. \quad (5.18b)$$

The octet Lagrangian (4.125) couples  $\chi$ PT to the portal current  $V_r^\mu$  via the strangeness-violating one-meson interaction

$$\mathcal{L}_\Phi^{h\partial V_r} = -\frac{\epsilon_{\text{EW}} f_0}{2} (h_8 (\mathbf{V}_r^{\mu d} + \mathbf{V}_r^{\mu s}) + h_1 V_r^\mu) \partial_\mu \boldsymbol{\Phi}_d^s + \text{h.c.}, \quad (5.19)$$

and the strangeness-violating two-meson interactions

$$\begin{aligned} \mathcal{L}_{\Phi^2}^{h\partial V_r} = & -i \frac{\epsilon_{\text{EW}}}{4} (2h_8 \langle [\boldsymbol{\Phi}, \mathbf{V}_r^\mu], \partial_\mu \boldsymbol{\Phi} \rangle_d^s \\ & + (h_8 (\mathbf{V}_r^{\mu d} + \mathbf{V}_r^{\mu s}) + h_1 V_r^\mu) \langle [\boldsymbol{\Phi}, \partial_\mu \boldsymbol{\Phi}] \rangle_d^s) + \text{h.c.}, \end{aligned} \quad (5.20a)$$

$$\begin{aligned} \mathcal{L}_{\Phi^2}^{hAV_r} = & \frac{\epsilon_{\text{EW}}}{4} (2h_8 \langle [\boldsymbol{\Phi}, \mathbf{V}_r^\mu], [\boldsymbol{\Phi}, \mathbf{v}_{A\mu}] \rangle_d^s \\ & + (h_8 (\mathbf{V}_r^{\mu d} + \mathbf{V}_r^{\mu s}) + h_1 V_r^\mu) \langle [\boldsymbol{\Phi}, [\boldsymbol{\Phi}, \mathbf{v}_{A\mu}]] \rangle_d^s) + \text{h.c.}. \end{aligned} \quad (5.20b)$$

The 27-plet Lagrangian (4.126) couples  $\chi$ PT to the portal current  $V_r^\mu$  via the strangeness-violating one-meson interaction

$$\mathcal{L}_\Phi^{h\partial V_r} = -\frac{\epsilon_{\text{EW}} f_0}{2} n_f h_{27} \mathbf{V}_r^{\mu u} \partial_\mu \boldsymbol{\Phi}_d^s + \text{h.c.}, \quad (5.21)$$

and the strangeness-violating two-meson interactions

$$\mathcal{L}_{\Phi^2}^{\mathfrak{h}\partial V_r} = -i \frac{\epsilon_{\text{EW}}}{4} h_{27} (n_f \langle [\Phi, \partial_\mu \Phi] \rangle_{\text{d}}^{\text{s}} \mathbf{V}_{r\text{u}}^{\mu\text{u}} + 2(n_f - 1) (\langle [\Phi, \mathbf{V}_r^\mu] \rangle_{\text{d}}^{\text{u}} \partial_\mu \Phi_{\text{u}}^{\text{s}} + \partial_\mu \Phi_{\text{d}}^{\text{u}} \langle [\Phi, \mathbf{V}_r^\mu] \rangle_{\text{u}}^{\text{s}})) + \text{h.c.} , \quad (5.22\text{a})$$

$$\mathcal{L}_{\Phi^2}^{\mathfrak{h}AV_r} = \frac{\epsilon_{\text{EW}}}{4} h_{27} (n_f \langle [\Phi, [\Phi, \mathbf{v}_{A\mu}]] \rangle_{\text{d}}^{\text{s}} \mathbf{V}_{r\text{u}}^{\mu\text{u}} + 2(n_f - 1) (\langle [\Phi, \mathbf{V}_{r\mu}] \rangle_{\text{d}}^{\text{u}} \langle [\Phi, \mathbf{v}_A^\mu] \rangle_{\text{u}}^{\text{s}} + \langle [\Phi, \mathbf{v}_{A\mu}] \rangle_{\text{d}}^{\text{u}} \langle [\Phi, \mathbf{V}_r^\mu] \rangle_{\text{u}}^{\text{s}})) + \text{h.c.} . \quad (5.22\text{b})$$

The one-meson interactions (5.15), (5.17), (5.19), and (5.21) are similar to the one-meson interactions in (5.2) and (5.4) and mediate only invisible decays. The two-meson interactions (5.16), (5.18), (5.20), and (5.22) are similar to the interactions (5.3), (5.10), and (5.12). They mediate decays with photons in the final state, such as  $\phi_i \rightarrow \phi_j \gamma v_\mu$ , as well as decays into secluded particles  $X$ , such as  $\phi_i \rightarrow \phi_j v_\mu^* \rightarrow \phi_j \bar{X} X$ .

Finally, the octet Lagrangian (4.127) couples  $\chi\text{PT}$  to the portal currents  $S_y$  via the strangeness-violating two-meson interactions

$$\mathcal{L}_{\Phi^2}^{\partial^2 S} = -\frac{\epsilon_{\text{EW}}}{2} (S_8 \langle \partial_\mu \Phi \partial^\mu \Phi \rangle_{\text{d}}^{\text{s}} + S_1 \partial^\mu \Phi_{\text{d}}^{\text{s}} \partial_\mu \Phi) + \text{h.c.} , \quad (5.23\text{a})$$

$$\mathcal{L}_{\Phi^2}^{\text{AS}} = -i \frac{\epsilon_{\text{EW}}}{2} S_8 \langle \{ \partial_\mu \Phi, [\Phi, \mathbf{v}_A^\mu] \} \rangle_{\text{d}}^{\text{s}} + \text{h.c.} , \quad (5.23\text{b})$$

while the 27-plet Lagrangian (4.128) also couples  $\chi\text{PT}$  to the portal currents  $S_y$  via the strangeness-violating two-meson interactions

$$\mathcal{L}_{\Phi^2}^{\partial^2 \mathfrak{S}} = -\frac{\epsilon_{\text{EW}}}{2} n_f S_{27} \left( \partial_\mu \Phi_{\text{d}}^{\text{s}} \partial^\mu \Phi_{\text{u}}^{\text{u}} + \frac{n_f - 1}{n_f} \partial_\mu \Phi_{\mu\text{d}}^{\text{u}} \partial^\mu \Phi_{\text{u}}^{\text{s}} \right) + \text{h.c.} , \quad (5.24\text{a})$$

$$\mathcal{L}_{\Phi^2}^{\text{AS}} = -i \frac{\epsilon_{\text{EW}}}{2} (n_f - 1) S_{27} ([\Phi, \mathbf{v}_A^\mu]_{\text{d}}^{\text{u}} \partial^\mu \Phi_{\text{u}}^{\text{s}} + \partial_\mu \Phi_{\text{d}}^{\text{u}} [\Phi, \mathbf{v}_A^\mu]_{\text{u}}^{\text{s}}) + \text{h.c.} . \quad (5.24\text{b})$$

These interactions are similar to the two-meson interactions in (5.4). They mediate decays such as  $\phi_i \rightarrow \phi_j s_k$ ,  $\phi_i \rightarrow \phi_j s_k \gamma$ , and  $\phi_i \rightarrow \phi_j \bar{X} X$ , with secluded particles  $X$  in the final state.

**Order  $\epsilon_{\text{EW}} \delta^2$**  At this order, the kinetic Lagrangian (4.129) encodes the *SM one-meson interactions*

$$\mathcal{L}_{\Phi}^{\partial W} = -f_0 \langle I_W^\mu \partial_\mu \Phi \rangle_f , \quad \mathcal{L}_{\Phi}^{\text{AW}} = -i f_0 \langle I_W^\mu [\Phi, \mathbf{v}_{A\mu}] \rangle_f , \quad (5.25)$$

and the *SM two-meson interactions*

$$\mathcal{L}_{\Phi^2}^{\partial W} = -\frac{i}{2} \langle I_W^\mu [\Phi, \partial_\mu \Phi] \rangle_f , \quad \mathcal{L}_{\Phi^2}^{\text{AW}} = \frac{1}{2} \langle I_W^\mu [\Phi, [\Phi, \mathbf{v}_{A\mu}]] \rangle_f . \quad (5.26)$$

The one-meson interactions mediate non-hadronic charged meson decays such as  $\phi_i \rightarrow \ell_a \nu_a$ , while the two-meson interactions mediate semi-hadronic three-body decays such as  $\phi_i \rightarrow \phi_j \ell_a \nu_a$ . The kinetic Lagrangian (4.130) couples  $\chi\text{PT}$  to the portal current  $\mathbf{V}_r^\mu$  via the one-meson interaction

$$\mathcal{L}_{\Phi}^{WV_r} = i f_0 \langle \mathbf{V}_r^\mu [\Phi, I_{W\mu}] \rangle_f , \quad (5.27)$$

and the two-meson interaction

$$\mathcal{L}_{\Phi^2}^{WV_r} = \frac{1}{2} \langle \mathbf{V}_r^\mu [\boldsymbol{\Phi}, [\boldsymbol{\Phi}, \mathbf{I}_{W\mu}]] \rangle_f . \quad (5.28)$$

The one-meson interactions mediate decays such as  $\phi_i \rightarrow \ell_a \nu_b v_\mu$ , while the two-meson interactions mediate decays such as  $\phi_i \rightarrow \phi_j \ell_a \nu_b v_\mu$ . The singlet Lagrangian (4.131) couples  $\chi$ PT to the portal current  $S_\omega$  via the one-meson interaction

$$\mathcal{L}_\Phi'^{S_\omega} = \frac{S_\omega}{\beta_0} 2\mathcal{L}_\Phi'^{hm} , \quad \mathcal{L}_\Phi'^{hm} = -i \frac{\epsilon_{\text{EW}} f_0 b_0}{2} h_b \langle [\boldsymbol{\Phi}, \mathbf{m}'] \rangle_d^s + \text{h.c.} , \quad (5.29)$$

and the two-meson interactions

$$\mathcal{L}_{\Phi^2}^{S_\omega} = \frac{S_\omega}{\beta_0} 2 \left( \mathcal{L}_{\Phi^2}^{hm} + 2 \left( \mathcal{L}_{\Phi^2}^{h\partial^2} + \mathcal{L}_{\Phi^2}^{h\partial A} + \mathcal{L}_{\Phi^2}^{h\partial^2} + \mathcal{L}_{\Phi^2}^{h\partial A} \right) \right) , \quad \mathcal{L}_{\Phi^2}^{hm} = \frac{\epsilon_{\text{EW}} b_0}{4} h_b \langle \{\boldsymbol{\Phi}^2, \mathbf{m}\} \rangle_d^s + \text{h.c.} . \quad (5.30)$$

The one-meson interaction (5.29) is similar to the one meson interaction (5.6) and mixes neutral kaons with the hidden spin 0 messenger. However, in contrast to interaction (5.6), the mixing here is not suppressed by the QCD theta angle, and therefore not in general negligible. The two-meson interactions (5.30) are similar to the two-meson interactions in (5.4) and (5.24) and mediate decays such as  $\phi_i \rightarrow \phi_j s_k$ ,  $\phi_i \rightarrow \phi_j s_k \gamma$ , and  $\phi_i \rightarrow \phi_j \bar{X} X$ .

**Order  $\epsilon_{\text{EW}} \delta^3$**  At this order, the singlet Lagrangian (4.133) couples  $\chi$ PT to the portal current  $S_\omega$  via the one-meson interactions

$$\mathcal{L}_\Phi'^{S_\omega} = \frac{S_\omega}{\beta_0} 2 \left( \mathcal{L}_\Phi^{\partial W} + \mathcal{L}_\Phi^{AW} + \mathcal{L}_\Phi^\gamma \right) , \quad \mathcal{L}_\Phi^\gamma = -\epsilon_{\text{EW}} f_0 b_0 \kappa_\Gamma \langle \boldsymbol{\Phi} \text{Im} \boldsymbol{\gamma} \rangle_f , \quad (5.31)$$

and the two-meson interactions

$$\mathcal{L}_{\Phi^2}^{S_\omega} = \frac{S_\omega}{\beta_0} 2 \left( \mathcal{L}_{\Phi^2}^{\partial W} + \mathcal{L}_{\Phi^2}^{AW} + \mathcal{L}_{\Phi^2}^\gamma \right) , \quad \mathcal{L}_{\Phi^2}^\gamma = -\frac{\epsilon_{\text{EW}} b_0}{2} \kappa_\Gamma \langle \boldsymbol{\Phi}^2 \text{Re} \boldsymbol{\gamma} \rangle_f . \quad (5.32)$$

The one-meson interactions that involve the dipole current  $\boldsymbol{\gamma}$  are similar to the interactions (5.4), (5.6), and (5.29) and mix neutral kaons with the hidden spin 0 messenger. The one-meson interactions that involve the weak leptonic charged current  $l_W^\mu$  mediate decays such as  $\phi_i \rightarrow \ell_a \nu_b s_j$ . The two-meson interactions (5.32) mediate decays such as  $\phi_i \rightarrow \phi_j s_k$ ,  $\phi_i \rightarrow \phi_j s_k \gamma$ ,  $\phi_i \rightarrow \phi_j \bar{X} X$ , and  $\phi_i \rightarrow \phi_j \ell_a \nu_b s_k$ . The tensor Lagrangian (4.135) couples  $\chi$ PT to the portal current  $\mathbf{T}_\tau^{\mu\nu}$  via the two-meson interactions

$$\mathcal{L}_{\Phi^2}^{T\partial^2} = \frac{\epsilon_{\text{EW}}}{f_0^3} \kappa_T^{D^2} \langle \mathbf{T}_\tau^{\mu\nu} \partial_\mu \boldsymbol{\Phi} \partial_\nu \boldsymbol{\Phi} \rangle_f + \text{h.c.} , \quad \mathcal{L}_{\Phi^2}^{TV} = -\frac{\epsilon_{\text{EW}}}{2f_0^3} \kappa_T^{LR} \langle \mathbf{T}_\tau^{\mu\nu} [\boldsymbol{\Phi}, [\boldsymbol{\Phi}, \mathbf{v}_{A\mu\nu}]] \rangle_f + \text{h.c.} , \quad (5.33a)$$

$$\mathcal{L}_{\Phi^2}^{T\partial V} = i \frac{\epsilon_{\text{EW}}}{f_0^3} \kappa_T^{D^2} \langle \mathbf{T}_\tau^{\mu\nu} (\partial^\mu \boldsymbol{\Phi} [\boldsymbol{\Phi}, \mathbf{v}_{A\nu}] + [\boldsymbol{\Phi}, \mathbf{v}_{A\mu}] \partial^\nu \boldsymbol{\Phi}) \rangle_f + \text{h.c.} . \quad (5.33b)$$



These interactions mediate decays such as  $\phi_i \rightarrow \phi_j \gamma s_k$  and  $\phi_i \rightarrow \phi_j \gamma \gamma s_k$ . The WZW Lagrangian (4.136) couple  $\chi$ PT to the portal current  $V_l^\mu$  via the one-meson interactions

$$\mathcal{L}_\Phi^{NV_l W} = \frac{\epsilon_{\mu\nu\rho\sigma}}{(4\pi)^2 f_0} \frac{1}{2} \langle \Phi \{ I_W^{\rho\sigma}, V_l^{\mu\nu} \} \rangle_f, \quad (5.34)$$

and the two-meson interactions

$$\mathcal{L}_\Phi^{NV_l W} = \frac{\epsilon_{\mu\nu\rho\sigma}}{(4\pi)^2 f_0^2} \frac{i}{2} \langle V_l^\mu (\{ I_W^{\rho\sigma}, [\Phi, \partial^\nu \Phi] \} + 2\partial^\rho \Phi I_W^\nu \partial^\sigma \Phi - 2\{\partial^\rho \Phi \partial^\sigma \Phi, I_W^\nu\}) \rangle_f. \quad (5.35)$$

Finally, the WZW Lagrangian (4.137) couple  $\chi$ PT to the portal current  $V_r^\mu$  via the one-meson interactions

$$\mathcal{L}_\Phi^{NV_r W} = \frac{\epsilon_{\mu\nu\rho\sigma}}{(4\pi)^2 f_0} \frac{1}{4} \langle \Phi \{ I_W^{\rho\sigma}, V_r^{\mu\nu} \} \rangle_f, \quad (5.36)$$

and the two-meson interactions

$$\mathcal{L}_\Phi^{NV_r W} = \frac{\epsilon_{\mu\nu\rho\sigma}}{(4\pi)^2 f_0^2} \frac{i}{4} \langle V_r^\mu (\{ I_W^{\rho\sigma}, [\Phi, \partial^\nu \Phi] \} + 4\partial^\rho \Phi I_W^\nu \partial^\sigma \Phi - 4\{\partial^\rho \Phi \partial^\sigma \Phi, I_W^\nu\}) \rangle_f. \quad (5.37)$$

The one-meson interactions (5.34) and (5.36) mediate decays such as  $\phi_i \rightarrow v_\mu \ell_a \nu_b$ , while the two-meson interactions (5.35) and (5.37) mediate decays such as  $\phi_i \rightarrow \phi_j \ell_a \nu_b v_\mu$ .

## 5.2 Flavour-blind hidden sectors

In this section, we focus on the coupling of  $\chi$ PT to flavour-blind hidden sectors and evaluate the  $\chi$ PT flavour traces to provide the one- and two-meson interactions in terms of the singlet and octet meson eigenstates  $\pi_8, \eta_8, \eta_1, \pi^\pm, K^\pm, K^0, \bar{K}^0$ . Mixing between the  $\pi_8, \eta_8$ , and  $\eta_1$  gives rise to the physical mass eigenstates  $\pi^0, \eta$ , and  $\eta'$ , while  $K^0$  and  $\bar{K}^0$  are diagonalised into the two physical mass eigenstates  $K_S^0$  and  $K_L^0$ .

The hidden sector is flavour blind only if the EW scale PETs are flavour blind. After integrating out the heavy SM particles, the resulting strong scale PETs can still violate quark-flavour due to virtual  $W$ -boson exchanges. Hence, the octet contributions to corresponding strong-scale portal currents are given as

$$S'_m = \lambda_d^s S'_{md} + \lambda_s^d S'_{ms}, \quad V_l'^\mu = \lambda_d^s V_l'^{\mu s} + \text{h.c.}, \quad V_r'^\mu = 0, \quad T_\tau^{\mu\nu} = T_\tau^{[\mu\nu]}, \quad (5.38)$$

where  $S'_{md}, S'_{ms}, V_l'^{\mu s}$ , and  $T_\tau^{\mu\nu}$  capture the contributions due to  $W$ -boson exchanges, so that they are suppressed by a factor of  $\epsilon_{\text{SM}}$ . This also implies that we can replace the primed currents in (4.105) with their unprimed counterparts. At order  $\epsilon_{\text{SM}}$ , the right-handed current  $V_r^\mu$  in (3.32) does not receive any contributions from higher dimensional operators. Hence, it has to be flavour blind even at the strong scale, and its octet contribution vanishes.

**Order  $\delta^2$**  After evaluating the flavour traces, the SM two-meson photon interactions (5.1) are

$$\mathcal{L}_{\phi^2}^{\partial A} = -i e A^\mu (\pi^+ \overleftrightarrow{\partial}_\mu \pi^- + K^+ \overleftrightarrow{\partial}_\mu K^-) . \quad (5.39)$$

The corresponding kinetic-like interactions (5.2) and (5.3) that couple  $\chi$ PT to the portal currents  $\mathbf{V}_l^\mu$  and  $\mathbf{V}_r^\mu$  become

$$\mathcal{L}_{\phi}^{\partial V_l} = -f_0 V_l^\mu \partial_\mu \frac{\eta_1}{\sqrt{3}} - f_0 (\mathbf{V}_{ls}^{\mu d} \partial_\mu K^0 + \text{h.c.}) , \quad \mathcal{L}_{\phi}^{\partial V_r} = f_0 V_r^\mu \partial_\mu \frac{\eta_1}{\sqrt{3}} , \quad (5.40a)$$

and

$$\mathcal{L}_{\phi^2}^{\partial V_l} = -\frac{i}{2} \left( \mathbf{V}_{ls}^{\mu d} \left( \pi^- \overleftrightarrow{\partial}_\mu K^+ + K^0 \overleftrightarrow{\partial}_\mu \left( \frac{\pi_8}{\sqrt{2}} - 3 \frac{\eta_8}{\sqrt{6}} \right) \right) - \text{h.c.} \right) , \quad (5.41a)$$

$$\mathcal{L}_{\phi^2}^{AV_l} = -e A_\mu (\mathbf{V}_{ls}^{\mu d} K^+ \pi^- + \text{h.c.}) . \quad (5.41b)$$

The mass-like interactions (5.4) that couple  $\chi$ PT to the portal current  $\mathbf{S}'_m$  become

$$\mathcal{L}_{\phi}^{\prime S_m} = -f_0 b_0 \text{Im } S'_m \frac{\eta_1}{\sqrt{3}} - f_0 b_0 ((\text{Im } \mathbf{S}'_m)_s^d K^0 + \text{h.c.}) , \quad (5.42)$$

and

$$\begin{aligned} \mathcal{L}_{\phi^2}^{\prime S_m} = & -\frac{b_0}{n_f} \text{Re } S'_m \left( \frac{1}{2} (\pi_8^2 + \eta_8^2 + \eta_1^2) + \pi^+ \pi^- + K^+ K^- + K^0 \bar{K}^0 \right) \\ & - \frac{b_0}{2} \left( (\text{Re } \mathbf{S}'_m)_s^d \left( K^+ \pi^- + K^0 \left( 2 \frac{\eta_1}{\sqrt{3}} - \frac{\pi_8}{\sqrt{2}} - \frac{\eta_8}{\sqrt{6}} \right) \right) + \text{h.c.} \right) . \end{aligned} \quad (5.43)$$

Finally, the anomalous interaction (5.5) that couples  $\chi$ PT to the portal current  $S_\theta$  becomes

$$\mathcal{L}_{\phi}^{S_\theta} = f_0 m_0^2 S_\theta \frac{\eta_1}{\sqrt{3}} . \quad (5.44)$$

**Order  $\delta^3$**  After evaluating the flavour traces, the singlet interactions (5.6) and (5.7) that couple  $\chi$ PT to  $S_\omega$  become

$$\mathcal{L}_{\phi}^{\prime S_\omega} = \frac{S_\omega}{\beta_0} 4 \mathcal{L}_{\phi}^{\theta} , \quad \mathcal{L}_{\phi^2}^{\prime S_\omega} = \frac{S_\omega}{\beta_0} \left( 2 (\mathcal{L}_{\phi^2}^{\partial^2} + \mathcal{L}_{\phi^2}^{\partial A}) + 3 \mathcal{L}_{\phi^2}^{\prime m} + 4 \mathcal{L}_{\phi^2}^{\theta} \right) , \quad (5.45)$$

where the SM Lagrangians

$$\mathcal{L}_{\phi}^{\theta} = f_0 m_0^2 \theta \frac{\eta_1}{\sqrt{3}} , \quad \mathcal{L}_{\phi^2}^{\theta} = -\frac{m_0^2}{2} n_f \left( \frac{\eta_1}{\sqrt{3}} \right)^2 , \quad (5.46)$$

and

$$\begin{aligned} \mathcal{L}_{\phi^2}^{\partial^2} = & \frac{1}{2} (\partial_\mu \pi_8 \partial^\mu \pi_8 + \partial_\mu \eta_8 \partial^\mu \eta_8 + \partial_\mu \eta_1 \partial^\mu \eta_1) \\ & + \partial_\mu \pi^+ \partial^\mu \pi^- + \partial_\mu K^+ \partial^\mu K^- + \partial_\mu K^0 \partial^\mu \bar{K}^0 , \end{aligned} \quad (5.47a)$$

$$\begin{aligned} \mathcal{L}_{\phi^2}^{\prime m} = & -\frac{b_0}{2} \left( (m'_u + m'_d) \pi^+ \pi^- + (m'_u + m'_s) K^+ K^- + (m'_d + m'_s) K^0 \bar{K}^0 \right. \\ & \left. + m'_u \left( \frac{\eta_1}{\sqrt{3}} + \frac{\eta_8}{\sqrt{6}} + \frac{\pi_8}{\sqrt{2}} \right)^2 + m'_d \left( \frac{\eta_1}{\sqrt{3}} + \frac{\eta_8}{\sqrt{6}} - \frac{\pi_8}{\sqrt{2}} \right)^2 + m'_s \left( \frac{\eta_1}{\sqrt{3}} - 2 \frac{\eta_8}{\sqrt{6}} \right)^2 \right) , \end{aligned} \quad (5.47b)$$

are identical to the SM Lagrangians in (5.6) and (5.8). The WZW interactions (5.9) and (5.10) that couple  $\chi$ PT to the portal current  $\mathbf{V}_l^\mu$  become

$$\mathcal{L}_\Phi^{NV_l A} = \frac{2n_c e \tilde{F}_{\mu\nu}}{3(4\pi)^2 f_0} \left( \partial^\mu V_l^\nu \left( \frac{\pi_8}{\sqrt{2}} + \frac{\eta_8}{\sqrt{6}} \right) - (\partial^\mu \mathbf{V}_{l s}^{\nu d} K^0 + \text{h.c.}) \right), \quad (5.48)$$

and

$$\mathcal{L}_{\Phi^2}^{NV_l A} = \frac{i n_c e \tilde{F}_{\mu\nu}}{3(4\pi)^2 n_f f_0^2} \left( V_l^\mu (\pi^+ \overleftrightarrow{\partial}^\nu \pi^- + K^+ \overleftrightarrow{\partial}^\nu K^-) - n_f \mathbf{V}_{l s}^{\mu d} \left( K^0 \overleftrightarrow{\partial}^\nu \left( \frac{\pi_8}{\sqrt{2}} - 3 \frac{\eta_8}{\sqrt{6}} \right) \right) \right). \quad (5.49)$$

Finally, the WZW interactions (5.11) and (5.12) that couple  $\chi$ PT to the portal current  $\mathbf{V}_r^\mu$  become

$$\mathcal{L}_\Phi^{NV_r A} = \frac{2n_c e \tilde{F}_{\mu\nu}}{3(4\pi)^2 f_0} \partial^\mu V_r^\nu \left( \frac{\pi_8}{\sqrt{2}} + \frac{\eta_8}{\sqrt{6}} \right), \quad (5.50)$$

and

$$\mathcal{L}_{\Phi^2}^{NV_r A} = \frac{-i n_c e \tilde{F}_{\mu\nu}}{3(4\pi)^2 n_f f_0^2} V_r^\mu (\pi^+ \overleftrightarrow{\partial}^\nu \pi^- + K^+ \overleftrightarrow{\partial}^\nu K^-). \quad (5.51)$$

**Order  $\epsilon_{\text{EW}} \delta$**  After evaluating the flavour-traces, the SM octet interactions (5.13) are

$$\mathcal{L}_{\phi^2}^{h\partial^2} = -\frac{\epsilon_{\text{EW}}}{2} \left( h_8 \partial^\mu K^+ \partial_\mu \pi^- + \partial^\mu K^0 \left( h_8 \partial_\mu \left( \frac{\pi_8}{\sqrt{2}} + \frac{\eta_8}{\sqrt{6}} \right) + n_f h_1 \partial_\mu \frac{\eta_1}{\sqrt{3}} \right) \right) + \text{h.c.}, \quad (5.52a)$$

$$\mathcal{L}_{\phi^2}^{h\partial A} = -i \frac{e \epsilon_{\text{EW}}}{2} h_8 A^\mu (\pi^- \overleftrightarrow{\partial}_\mu K^+) + \text{h.c.} \quad (5.52b)$$

The SM 27-plet interactions (5.14) are

$$\mathcal{L}_{\phi^2}^{h\partial^2} = -\frac{\epsilon_{\text{EW}}}{2} h_{27} \left( n_f \partial^\mu \left( \frac{\pi_8}{\sqrt{2}} + \frac{\eta_8}{\sqrt{6}} \right) \partial_\mu K^0 + (n_f - 1) \partial_\mu \pi^- \partial^\mu K^+ \right) + \text{h.c.}, \quad (5.53a)$$

$$\mathcal{L}_{\phi^2}^{h\partial A} = -i \frac{e \epsilon_{\text{EW}}}{2} h_{27} (n_f - 1) A_\mu (\pi^- \overleftrightarrow{\partial}^\mu K^+) + \text{h.c.} \quad (5.53b)$$

Since the octet contribution to the left-handed portal current  $\mathbf{V}_l^\mu$  is generated by diagrams that involve virtual  $W$ -boson exchanges, it counts as  $\mathbf{V}_l^\mu \propto \epsilon_{\text{EW}}$ . At order  $\epsilon_{\text{EW}}$ , the latter and the octet contribution  $\mathbf{V}_r^\mu$  to the right-handed portal current  $\mathbf{V}_r^\mu$  can be both neglected in the 27-plet interactions (5.17), (5.18), (5.21), and (5.22), which then vanish. The octet interactions (5.15) and (5.16) that couple  $\chi$ PT to the singlet portal current  $V_l^\mu$  become

$$\mathcal{L}_\phi^{h\partial V_l} = \frac{\epsilon_{\text{EW}} f_0}{2} h_1 V_l^\mu \partial_\mu K^0 + \text{h.c.}, \quad (5.54)$$

and

$$\mathcal{L}_{\phi^2}^{h\partial V_l} = i \frac{\epsilon_{\text{EW}}}{4} h_1 V_l^\mu \left( \pi^- \overleftrightarrow{\partial}_\mu K^+ + \left( 3 \frac{\eta_8}{\sqrt{6}} - \frac{\pi_8}{\sqrt{2}} \right) \overleftrightarrow{\partial}_\mu K^0 \right) + \text{h.c.}, \quad (5.55a)$$

$$\mathcal{L}_{\phi^2}^{hAV_l} = \frac{e \epsilon_{\text{EW}}}{2} h_1 V_l^\mu A_\mu K^+ \pi^- + \text{h.c.} \quad (5.55b)$$

The octet interactions (5.19) and (5.20) that couple  $\chi$ PT to the portal current  $V_r^\mu$  become

$$\mathcal{L}_\phi^{h\partial V_r} = -\frac{\epsilon_{\text{EW}} f_0}{2} h_1 V_r^\mu \partial_\mu K^0 + \text{h.c.} , \quad (5.56)$$

and

$$\mathcal{L}_\phi^{h\partial V_r} = -i \frac{\epsilon_{\text{EW}}}{4} h_1 V_r^\mu \left( \pi^- \overleftrightarrow{\partial}_\mu K^+ + \left( 3 \frac{\eta_8}{\sqrt{6}} - \frac{\pi_8}{\sqrt{2}} \right) \overleftrightarrow{\partial}_\mu K^0 \right) + \text{h.c.} , \quad (5.57a)$$

$$\mathcal{L}_\phi^{hAV_r} = -\frac{e\epsilon_{\text{EW}}}{2} h_1 V_r^\mu A_\mu K^+ \pi^- + \text{h.c.} . \quad (5.57b)$$

The octet interactions (5.23) that couple  $\chi$ PT to the portal currents  $S_y$  become

$$\mathcal{L}_\phi^{\partial^2 S} = -\frac{\epsilon_{\text{EW}}}{2} \left( S_8 \partial^\mu K^+ \partial_\mu \pi^- \right. \quad (5.58a)$$

$$\left. + \partial^\mu K^0 \left( -S_8 \partial_\mu \left( \frac{\pi_8}{\sqrt{2}} + \frac{\eta_8}{\sqrt{6}} \right) + n_f S_1 \partial_\mu \frac{\eta_1}{\sqrt{3}} \right) \right) + \text{h.c.} ,$$

$$\mathcal{L}_\phi^{AS} = -i \frac{e\epsilon_{\text{EW}}}{2} S_8 A_\mu (\pi^- \overleftrightarrow{\partial}_\mu K^+) + \text{h.c.} . \quad (5.58b)$$

Finally, the 27-plet interactions (5.24) that couple  $\chi$ PT to the portal currents  $S_y$  become

$$\mathcal{L}_\phi^{\partial^2 \mathfrak{S}} = -\frac{\epsilon_{\text{EW}}}{2} n_f S_{27} \left( \partial_\mu K^0 \partial^\mu \left( \frac{\pi_8}{\sqrt{2}} + \frac{\eta_8}{\sqrt{6}} \right) + \frac{n_f - 1}{n_f} \partial_\mu \pi^- \partial^\mu K^+ \right) + \text{h.c.} , \quad (5.59a)$$

$$\mathcal{L}_\phi^{A\mathfrak{S}} = -i \frac{e\epsilon_{\text{EW}}}{2} (n_f - 1) S_{27} A_\mu \pi^- \overleftrightarrow{\partial}^\mu K^+ + \text{h.c.} . \quad (5.59b)$$

**Order  $\epsilon_{\text{EW}} \delta^2$**  After evaluating the flavour traces, the SM one- and two-meson charged-current interactions (5.25) and (5.26) are

$$\mathcal{L}_\phi^{\partial W} = -f_0 (I_{Wd}^\mu \partial_\mu \pi^+ + I_{Ws}^\mu \partial_\mu K^+ + \text{h.c.}) , \quad (5.60a)$$

$$\mathcal{L}_\phi^{AW} = i f_0 e A_\mu (I_{Wd}^\mu \pi^+ + I_{Ws}^\mu K^+ - \text{h.c.}) , \quad (5.60b)$$

and

$$\mathcal{L}_\phi^{\partial W} = -\frac{i}{2} \left( I_{Wd}^\mu \left( 2\pi^+ \overleftrightarrow{\partial}_\mu \frac{\pi_8}{\sqrt{2}} + K^+ \overleftrightarrow{\partial}_\mu \overline{K}^0 \right) \right. \quad (5.61a)$$

$$\left. + I_{Ws}^\mu \left( \pi^+ \overleftrightarrow{\partial}_\mu K^0 - K^+ \overleftrightarrow{\partial}_\mu \left( \frac{\pi_8}{\sqrt{2}} + 3 \frac{\eta_8}{\sqrt{6}} \right) \right) - \text{h.c.} \right) ,$$

$$\mathcal{L}_\phi^{AW} = \frac{1}{2} e A_\mu \left( I_{Wd}^\mu \left( 2\pi^+ \frac{\pi_8}{\sqrt{2}} + K^+ \overline{K}^0 \right) \right. \quad (5.61b)$$

$$\left. + I_{Ws}^\mu \left( K^+ \left( \frac{\pi_8}{\sqrt{2}} + 3 \frac{\eta_8}{\sqrt{6}} \right) + \pi^+ K^0 \right) + \text{h.c.} \right) .$$

The singlet interactions (5.29) and (5.30) that couple  $\chi$ PT to the portal current  $S_\omega$  become

$$\mathcal{L}_\phi^{S_\omega} = \frac{S_\omega}{\beta_0} 2\mathcal{L}_\phi^{hm} , \quad \mathcal{L}_\phi^{S_\omega} = \frac{S_\omega}{\beta_0} 2 \left( \mathcal{L}_\phi^{hm} + 2 \left( +\mathcal{L}_\phi^{h\partial^2} + \mathcal{L}_\phi^{h\partial A} + \mathcal{L}_\phi^{\mathfrak{h}\partial^2} + \mathcal{L}_\phi^{\mathfrak{h}\partial A} \right) \right) , \quad (5.62)$$

where the SM Lagrangians

$$\mathcal{L}_\phi^{hm} = -i \frac{\epsilon_{EW} f_0 b_0}{2} h_b (m'_s - m'_d) K^0 + \text{h.c.} , \quad (5.63a)$$

$$\mathcal{L}_{\phi^2}^{hm} = \frac{\epsilon_{EW} b_0}{4} h_b (m'_d + m'_s) \left( K^+ \pi^- - K^0 \left( \frac{\pi_8}{\sqrt{2}} + \frac{\eta_8}{\sqrt{6}} \right) \right) + \text{h.c.} \quad (5.63b)$$

are identical to the SM Lagrangians in (5.29) and (5.30).

**Order  $\epsilon_{EW} \delta^3$**  After evaluating the flavour traces, the singlet interactions (5.31) and (5.32) that couple  $\chi$ PT to the portal current  $S_\omega$  become

$$\mathcal{L}_\phi^{S_\omega} = \frac{S_\omega}{\beta_0} 2 \left( \mathcal{L}_\phi^{\partial W} + \mathcal{L}_\phi^{AW} + \mathcal{L}_\phi^\gamma \right) , \quad \mathcal{L}_{\phi^2}^{S_\omega} = \frac{S_\omega}{\beta_0} 2 \left( \mathcal{L}_{\phi^2}^{\partial W} + \mathcal{L}_{\phi^2}^{AW} + \mathcal{L}_{\phi^2}^\gamma \right) , \quad (5.64)$$

where the SM Lagrangians

$$\mathcal{L}_\phi^\gamma = -\epsilon_{EW} f_0 b_0 \kappa_\Gamma (\text{Im } \boldsymbol{\gamma})_s^d K^0 + \text{h.c.} , \quad (5.65)$$

$$\mathcal{L}_{\phi^2}^\gamma = -\frac{\epsilon_{EW} b_0}{2} \kappa_\Gamma (\text{Re } \boldsymbol{\gamma})_s^d \left( K^+ \pi^- - K^0 \left( \frac{\pi_8}{\sqrt{2}} + \frac{\eta_8}{\sqrt{6}} \right) \right) + \text{h.c.} , \quad (5.66)$$

are identical to the SM Lagrangians in (5.31) and (5.32). The tensor interactions (5.33) that couple  $\chi$ PT to the portal current  $\boldsymbol{T}_\tau^{\mu\nu}$  become

$$\mathcal{L}_{\phi^2}^{T\partial^2} = 2 \frac{\epsilon_{EW}}{f_0^3} \kappa_T^{D^2} (\text{Re } \boldsymbol{T}_\tau^{\mu\nu})_s^d \left( \partial_\mu K^+ \partial_\nu \pi^- - \partial_\mu K^0 \partial_\nu \left( \frac{\pi_8}{\sqrt{2}} + \frac{\eta_8}{\sqrt{6}} \right) \right) + \text{h.c.} , \quad (5.67a)$$

$$\mathcal{L}_{\phi^2}^{TV} = -\frac{e\epsilon_{EW}}{f_0^3} \kappa_T^{LR} F_{\mu\nu} (\text{Re } \boldsymbol{T}_\tau^{\mu\nu})_s^d 2K^+ \pi^- + \text{h.c.} , \quad (5.67b)$$

$$\mathcal{L}_{\phi^2}^{T\partial V} = \frac{e\epsilon_{EW}}{f_0^3} \kappa_T^{D^2} A_\nu (\text{Im } \boldsymbol{T}_\tau^{[\mu\nu]})_s^d \partial_\mu (2K^+ \pi^-) + \text{h.c.} . \quad (5.67c)$$

The WZW interactions (5.34) and (5.35) that couple  $\chi$ PT to  $\mathbf{V}_l^\mu$  become

$$\mathcal{L}_\Phi^{NV_l W} = \frac{2n_c \epsilon_{\mu\nu\rho\sigma}}{3(4\pi)^2 n_f f_0} \partial^\mu V_l^\nu (I_{W^s}^{\rho\sigma u} K^+ + I_{W^d}^{\rho\sigma u} \pi^+ + \text{h.c.}) , \quad (5.68)$$

and

$$\begin{aligned} \mathcal{L}_{\Phi^2}^{NV_l W} = & \frac{i n_c \epsilon_{\mu\nu\rho\sigma}}{3(4\pi f_0)^2 n_f} V_l^\mu \left( I_{W^s}^{\rho\sigma u} \left( \pi^+ \overleftrightarrow{\partial}^\nu K^0 - K^+ \overleftrightarrow{\partial}^\nu \left( \frac{\pi_8}{\sqrt{2}} + 3 \frac{\eta_8}{\sqrt{6}} \right) \right) \right. \\ & + I_{W^d}^{\rho\sigma u} \left( 2\pi^+ \overleftrightarrow{\partial}^\nu \frac{\pi_8}{\sqrt{2}} + K^+ \overleftrightarrow{\partial}^\nu \overline{K}^0 \right) - 3I_{W^d}^{\nu u} \left( 2\partial^\rho \frac{\pi_8}{\sqrt{2}} \partial^\sigma \pi^+ + \partial^\rho K^+ \partial^\sigma \overline{K}^0 \right) \\ & \left. - 3I_{W^s}^{\nu u} \left( \partial^\rho \left( \frac{\pi_8}{\sqrt{2}} + 3 \frac{\eta_8}{\sqrt{6}} \right) \partial^\sigma K^+ + \partial^\rho \pi^+ \partial^\sigma K^0 \right) + \text{h.c.} \right) . \quad (5.69) \end{aligned}$$

Finally, the WZW interactions (5.36) and (5.37) that couple  $\chi$ PT to  $\mathbf{V}_r^\mu$  become

$$\mathcal{L}_\Phi^{NV_r W} = \frac{n_c \epsilon_{\mu\nu\rho\sigma}}{3(4\pi)^2 n_f f_0} \partial^\mu V_r^\nu (I_{W^s}^{\rho\sigma u} K^+ + I_{W^d}^{\rho\sigma u} \pi^+ + \text{h.c.}) , \quad (5.70)$$

and

$$\begin{aligned} \mathcal{L}_{\Phi^2}^{NV_r W} = & \frac{i n_c \epsilon_{\mu\nu\rho\sigma}}{3(4\pi f_0)^2} \frac{1}{n_f} V_r^\mu \left( \frac{1}{2} I_{Ws}^{\rho\sigma u} \left( \pi^+ \overleftrightarrow{\partial}^\nu K^0 - K^+ \overleftrightarrow{\partial}^\nu \left( \frac{\pi_8}{\sqrt{2}} + 3 \frac{\eta_8}{\sqrt{6}} \right) \right) \right. \\ & + \frac{1}{2} I_{Wd}^{\rho\sigma u} \left( 2\pi^+ \overleftrightarrow{\partial}^\nu \frac{\pi_8}{\sqrt{2}} + K^+ \overleftrightarrow{\partial}^\nu \overline{K}^0 \right) - 3 I_{Wd}^{\nu u} \left( 2\partial^\rho \frac{\pi_8}{\sqrt{2}} \partial^\sigma \pi^+ + \partial^\rho K^+ \partial^\sigma \overline{K}^0 \right) \\ & \left. - 3 I_{Ws}^{\nu u} \left( \partial^\rho \left( \frac{\pi_8}{\sqrt{2}} + 3 \frac{\eta_8}{\sqrt{6}} \right) \partial^\sigma K^+ + \partial^\rho \pi^+ \partial^\sigma K^0 \right) + \text{h.c.} \right). \quad (5.71) \end{aligned}$$

## 6 Meson interactions of hidden sector models

In this section, we apply the results of sections 4 and 5 to compute generic transition amplitudes for golden channels used to search for NP in meson experiments. This step serves first to validate our results with preexisting computations and second to exemplify their use to compute meson decays involving a hidden particle. We consider one example for each messenger type that is captured by the PET framework:

**Spin 0 messengers** The decay  $K^\pm \rightarrow \pi^\pm s_i$  is a smoking gun process for ALP searches at kaon factories, see *e.g.* [81, 84]. It can be especially relevant within the context of interpreting the recent KOTO excess [215]. Scalar, pseudoscalar and complex scalar messengers couple to the  $\chi$ PT Lagrangian via a large variety of external currents. As a result, this type of process clearly demonstrates the power of the PET framework to perform global parameter scans instead of considering only one specific SM extension at a time.

**Spin 1/2 messengers** The decay  $K^\pm \rightarrow \ell^\pm \xi_a$  is a key signature for light HNL searches [79, 83]. If  $\xi_a$  is a HNL, the computation of the transition amplitude is straightforward, as the HNL couples to the SM only via its mixing with neutrinos [8–13]. After diagonalising this mixing, the HNL couples to QCD via a single operator that mirrors the leptonic charged current interaction in the SM. Up to leading order in  $\alpha_{\text{EM}}$  and the  $4\pi$  counting of NDA, this operator is also the only one that couples QCD directly to a completely generic spin 1/2 messenger. Since we do not diagonalise the portal interactions, we keep track of both the mixing and the charged current operator. As discussed in section 3.1.2, this means that the final decay amplitude also captures hidden sectors that contain a non-trivial secluded sector in addition to the messenger field. The net-effect is that the mixing angles  $\theta_{bi}$  in equation (6.60), which measure the size of the HNL amplitude, are replaced with effective mixing angles  $\theta_{ba}$  in equation (6.56) that measure both the impact of the mixing of  $\xi_a$  with neutrinos and the direct production via the four-fermion operator.

**Spin 1 messengers** The decay  $\pi^0 \rightarrow \gamma v_\mu$  is a smoking gun process for dark photon searches, see *e.g.* [82]. If  $v_\mu$  couples to  $\chi$ PT like a vector particle in a parity conserving theory, such as in common models of dark photons, the parity-odd WZW action generates the only contribution to the decay amplitude. *A priori*, one might expect that the parity-even order  $\delta^3$  contributions to the  $\chi$ PT action in Lagrangians (4.22) to (4.27) can mediate neutral pion decays  $\pi^0 \rightarrow \gamma a_\mu$  into messengers  $a_\mu$  that couple to  $\chi$ PT like axial-vectors in a parity conserving theory. However, as mentioned below equation (5.12),

this does not occur. For this reason, the dark photon decay amplitude actually encompasses the production of generic spin 1 messengers.

To summarise, our decay amplitudes for hidden (pseudo-)scalar messengers, HNLs and dark photons capture the production of generic hidden spin 0,  $1/2$  and 1 messengers to LO in  $\alpha_{\text{EM}}$ ,  $\epsilon_{\text{EW}}$ , and the NDA  $4\pi$  counting.

## 6.1 Charged kaon decay to charged pions and hidden scalars

We compute the transition amplitude for charged kaon decays  $K^\pm \rightarrow \pi^\pm s_i$  into spin 0 messengers  $s_i$ . These decays can be induced via *seven out of the ten* portal currents that contained in the portal  $\chi\text{PT}$  Lagrangian. To compute the complete generic decay amplitude, we first consider decays mediated by each of these currents individually, and compute the leading contributions to the corresponding partial decay amplitudes. We then sum these contributions to obtain a universal expression.

In general, the  $\delta$  and  $\epsilon_{\text{EW}}$  scaling behaviour of each partial amplitude can be different for each of the seven portal currents, and the final result for the decay amplitude will mix contributions of different order in  $\delta$  and  $\epsilon_{\text{EW}}$ . For instance, a quark-flavour violating contribution to the current  $\text{Re } \mathbf{S}_m \propto \epsilon_{\text{UV}} s_i$  induces an amplitude in (6.15a) that formally scales as  $\epsilon_{\text{UV}} \delta^2$ , with no suppression due to  $\epsilon_{\text{EW}}$ , while the currents  $\mathbf{S}_x \propto \epsilon_{\text{UV}} s_i/v$  induce an amplitude in (6.15a) that scales as  $\epsilon_{\text{UV}} \epsilon_{\text{EW}}^{3/2} \delta$ , and the current  $S_\omega \propto \epsilon_{\text{UV}} s_i/v$  induces an amplitude (6.15b) that scales as  $\epsilon_{\text{UV}} \epsilon_{\text{EW}}^{3/2} \delta^2$ . In the case of the  $S_\omega$  and  $\mathbf{S}_x$  currents, the additional  $\epsilon_{\text{EW}}^{1/2}$  suppression results from the fact that the underlying EW scale portal operators are of dimension five rather than dimension four. When considering a specific SM extension, it may be possible to neglect the higher order contributions if they appear in conjunction with lower order contributions. However, to capture the coupling of  $\chi\text{PT}$  to fully generic hidden sectors, it is necessary to keep track of all contributions, since *a priori* a hidden sector can couple to  $\chi\text{PT}$  via any one of the portal currents.

### 6.1.1 Single scalar portal current contributions

In section 3.3.2, we have given the complete list of portal interactions that contribute to each external current at LO. The relevant contributions that mediate  $K^\pm \rightarrow \pi^\pm s_i$  decays are those with exactly one hidden spin 0 messenger and no other SM or hidden fields,

$$S_\omega = \frac{\epsilon_{\text{UV}}}{v} c_i^{S_\omega} s_i, \quad \mathbf{S}_m \supset \epsilon_{\text{UV}} \left( c_i^{S_m} + c_{\partial^2 i}^{S_m} \frac{1}{v^2} \partial^2 \right) s_i, \quad \mathbf{S}_s = \mathbf{h}_{si} \frac{\epsilon_{\text{UV}}}{v} s_i, \quad (6.1a)$$

$$S_\theta = \frac{\epsilon_{\text{UV}}}{v} c_i^{S_\theta} s_i, \quad \mathbf{S}_\gamma = \epsilon_{\text{UV}} \left( \lambda_d^s c_{i\bar{s}d}^\gamma + \lambda_s^d c_{i\bar{d}s}^\gamma \right) s_i, \quad \mathbf{S}_r = \mathbf{h}_{ri} \frac{\epsilon_{\text{UV}}}{v} s_i, \quad (6.1b)$$

$$\mathbf{S}_l = \mathbf{h}_{li} \frac{\epsilon_{\text{UV}}}{v} s_i. \quad (6.1c)$$

Since  $\partial^2/v^2 \propto \epsilon_{\text{EW}} \delta$ , the second term in  $\mathbf{S}_m$  induces amplitudes that are suppressed by an additional factor  $\epsilon_{\text{EW}} \delta$  compared to the contributions generated by the first term. In the following, we simplify the expressions by approximating  $m_u, m_d \rightarrow m_{\text{ud}}$  and  $\epsilon_s \equiv m_{\text{ud}}/m_s \rightarrow 0$ .

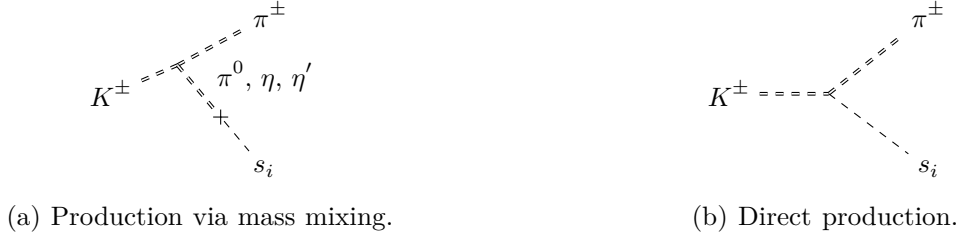


Figure 10: Feynman diagrams for the  $K^\pm \rightarrow \pi^\pm s_i$  process.

Matching to  $\chi$ PT and transitioning to the physical vacuum, this gives the modified currents

$$\mathbf{S}'_m = \epsilon_{\text{UV}} \left( \mathbf{c}_i'^{S_m} + \mathbf{c}_i^{S_m} \frac{1}{\partial^2} \partial^2 \right) s_i + \mathcal{O}(\epsilon_{\text{EW}}^2, \epsilon_s^2), \quad S_y = h_{yi} \frac{\epsilon_{\text{UV}}}{v} s_i, \quad (6.2)$$

where the parameters  $h_{yi}$  are given in equation (4.91), and

$$\begin{aligned} \mathbf{c}_i'^{S_m} = & \mathbf{c}_i^{S_m} + 2\epsilon_{\text{EW}} \left[ \epsilon_s (h_b'^\dagger \boldsymbol{\lambda}_d^s - h_b' \boldsymbol{\lambda}_s^d) \mathbf{c}_i^{S_m} - h_b'^\dagger \mathbf{c}_i^{S_m} \boldsymbol{\lambda}_d^s \right] \\ & - \frac{\epsilon_{\text{EW}} \mathbf{m}}{v} (h_{bi} \boldsymbol{\lambda}_s^d + \text{h.c.}) + \epsilon_{\text{EW}} \kappa_\Gamma (c_{i\bar{s}d}^\gamma \boldsymbol{\lambda}_d^s + c_{i\bar{d}s}^\gamma \boldsymbol{\lambda}_s^d) + \mathcal{O}(\epsilon_{\text{EW}}^{3/2}, \epsilon_s^2). \end{aligned} \quad (6.3)$$

The strength of strangeness-violating contributions to  $\mathbf{S}'_m$  is measured by the Wilson coefficients

$$\mathbf{c}_i'^{S_m d} = \mathbf{c}_i^{S_m d} - \epsilon_{\text{EW}} \left( 2h_b' \epsilon_s \mathbf{c}_i^{S_m d} + \frac{m_s}{v} h_{bi} - \kappa_\Gamma c_{i\bar{d}s}^\gamma \right), \quad (6.4a)$$

$$\mathbf{c}_i'^{S_m s} = \mathbf{c}_i^{S_m s} + \epsilon_{\text{EW}} \left( 2h_b'^\dagger \left( \epsilon_s \mathbf{c}_i^{S_m s} - \mathbf{c}_i^{S_m d} \right) - \epsilon_s \frac{m_s}{v} h_{bi}^\dagger + \kappa_\Gamma c_{i\bar{s}d}^\gamma \right). \quad (6.4b)$$

### 6.1.2 Relevant interactions

At tree-level,  $K^\pm \rightarrow \pi^\pm s_i$  decays are mediated by portal interactions with either one or two mesons. The former give rise to indirect production via mixing of the messenger with the SM mesons, while the latter give rise to direct production. Both types of interaction are listed in section 5.1.

We first consider the case of indirect production via the process depicted in the diagram in figure 10a. The one-meson interactions mix the hidden scalar with the neutral SM mesons, and contribute to  $K^\pm \rightarrow \pi^\pm s_i$  decays via off-shell  $K^\pm \rightarrow \pi^\pm \pi^{0*}$ ,  $K^\pm \rightarrow \pi^\pm \eta^*$ , and  $K^\pm \rightarrow \pi^\pm \eta'^*$  transitions, in which the neutral meson subsequently oscillates into the hidden scalar. Hence, the diagram in figure 10a contains two vertices: i) a trilinear SM vertex with one  $K^\pm$ -leg, one  $\pi^\mp$ -leg, and one neutral meson leg, and ii) a one-meson portal interaction that captures the meson to hidden scalar mixing. The expressions for the trilinear SM interactions are known, and can be extracted from the SM  $\chi$ PT Lagrangian by following the procedure that we summarise in appendix D.3. The resulting Lagrangian is

$$\mathcal{L}_{K\pi\Phi} = -\frac{i\epsilon_{\text{EW}}}{2f_0} \left( 2V_{K\pi\pi} \frac{\pi^0}{\sqrt{2}} + 3V_{K\pi\eta} \frac{\eta}{\sqrt{3}} + 3V_{K\pi\eta'} \frac{\eta'}{\sqrt{3}} \right) K^+ \pi^- \quad (6.5)$$



where we have defined the functions

$$V_{K\pi\pi} = \frac{1}{4}[(h_8 + 7h_{27})\partial_{\pi^0}\partial_K - 5h_{27}\partial_{\pi^0}\partial_{\pi^-} - (h_8 + 2h_{27})\partial_{\pi^-}\partial_K] , \quad (6.6a)$$

$$V_{K\pi\eta} = \frac{1}{6\sqrt{2}}c_\eta[(3h_8 + 6h_{27})\partial_\pi\partial_K - (h_8 + 3\sqrt{2}t_\eta h_1 - 3h_{27})\partial_\eta\partial_K - (2h_8 - 3\sqrt{2}t_\eta h_1 + 9h_{27})\partial_\eta\partial_\pi] , \quad (6.6b)$$

$$V_{K\pi\eta'} = \frac{1}{6\sqrt{2}}s_\eta[(3h_8 + 6h_{27})\partial_\pi\partial_K - (h_8 - 3\sqrt{2}t_\eta^{-1}h_1 - 3h_{27})\partial_\eta\partial_K - (2h_8 + 3\sqrt{2}t_\eta^{-1}h_1 + 9h_{27})\partial_\eta\partial_\pi] . \quad (6.6c)$$

Notice that there is no  $K^\pm\pi^\mp K^0$  SM vertex. Therefore, we do not have to keep track of the mixing between the neutral kaons and the messenger. This also means that we can neglect EW contributions to type ii) interactions. The hidden currents  $\text{Im } \mathbf{S}'_m$  and  $S_\theta$  induce the only relevant type ii) vertices, given within the interactions (5.4) and (5.5). Extracting the vertices, one obtains

$$\mathcal{L}_\Phi^{S_\theta} = \frac{\epsilon_{\text{UV}}m_0^2 f_0 c_i^{S_\theta}}{v} \left( c_\eta \frac{\eta'}{\sqrt{3}} - s_\eta \frac{\eta}{\sqrt{3}} \right) s_i , \quad (6.7a)$$

$$\mathcal{L}_\Phi^{S'_m} \supset -\epsilon_{\text{UV}}f_0 b_0 \left( c_{s_i\pi} \frac{\pi^0}{\sqrt{2}} + c_{s_i\eta} \frac{\eta}{\sqrt{3}} + c_{s_i\eta'} \frac{\eta'}{\sqrt{3}} \right) s_i + \mathcal{O}(\epsilon_{\text{EW}}) , \quad (6.7b)$$

where the Wilson coefficients are

$$c_{s_i\pi} = \text{Im } \mathbf{c}_i^{S'_m \text{u}} - \text{Im } \mathbf{c}_i^{S'_m \text{d}} , \quad (6.8a)$$

$$c_{s_i\eta} = -s_\eta \text{Im } c_i^{S'_m} + \frac{c_\eta}{\sqrt{2}} \left( \text{Im } \mathbf{c}_i^{S'_m \text{u}} + \text{Im } \mathbf{c}_i^{S'_m \text{d}} - 2 \text{Im } \mathbf{c}_i^{S'_m \text{s}} \right) , \quad (6.8b)$$

$$c_{s_i\eta'} = c_\eta \text{Im } c_i^{S'_m} + \frac{s_\eta}{\sqrt{2}} \left( \text{Im } \mathbf{c}_i^{S'_m \text{u}} + \text{Im } \mathbf{c}_i^{S'_m \text{d}} - 2 \text{Im } \mathbf{c}_i^{S'_m \text{s}} \right) . \quad (6.8c)$$

We now move on to the case of direct production via the process depicted in the diagram in figure 10b. This diagram consists of a single trilinear portal vertex with one  $K^\pm$ -leg, one  $\pi^\mp$ -leg, and one hidden spin 0 messenger leg. The hidden current  $\text{Re } \mathbf{S}'_m$  induces the vertices

$$\mathcal{L}_\Phi^{S'_m} \supset -\frac{b_0}{2}\epsilon_{\text{UV}}K^+\pi^-\left(c_{K\pi s_i} + \text{Re } \mathbf{c}_{\partial^2 i s}^{S'_m \text{d}} \frac{\partial^2}{v^2}\right)s_i + \mathcal{O}(\epsilon_{\text{EW}}^2) , \quad (6.9)$$

which are part of the interactions (5.4), where

$$c_{K\pi s_i} = \text{Re } \mathbf{c}_i^{S'_m \text{d}} + \frac{\epsilon_{\text{EW}}}{2} \left( (m_K^2 - m_\pi^2) \text{Re } \mathbf{c}_i^{S'_m \text{u}} + m_K^2 \text{Re } \mathbf{c}_i^{S'_m \text{d}} - m_\pi^2 \text{Re } \mathbf{c}_i^{S'_m \text{s}} \right) \theta_{K^\pm\pi^\mp} \\ - \frac{\epsilon_{\text{EW}}}{2} \left( 2h'_b \left( \epsilon_s \mathbf{c}_i^{S'_m \text{d}} - \epsilon_s \mathbf{c}_i^{S'_m \text{s}\dagger} + \mathbf{c}_i^{S'_m \text{d}\dagger} \right) + \frac{m_{\text{ud}} + m_s}{v} h_{bi} - \kappa_I (c_{i\text{ds}}^\gamma + c_{i\text{sd}}^\gamma) \right) . \quad (6.10)$$

The hidden currents  $S_y$  induce the vertices

$$\mathcal{L}_\Phi^{\partial^2 S} + \mathcal{L}_\Phi^{\partial^2 \mathfrak{S}} \supset -\frac{\epsilon_{\text{UV}}\epsilon_{\text{EW}}}{2v} (h_{8i} + (n_f - 1)h_{27i}) s_i \partial_\mu \pi^- \partial^\mu K^+ , \quad (6.11)$$

which are encompassed by the interactions (5.23) and (5.24). Finally, the  $S_\omega$  current induces the vertices

$$\mathcal{L}'_{\phi^2 S_\omega} \supset \frac{\epsilon_{UV} \epsilon_{EW} c_i^{S_\omega}}{v \beta_0} (h'_b m_K^2 K^+ \pi^- - (h_8 + (n_f - 1) h_{27}) \partial^\mu K^+ \partial_\mu \pi^-) s_i, \quad (6.12)$$

which are given within the interactions (5.30). These vertices contribute at order  $\delta^3$  rather than order  $\delta^2$  due to the large  $n_c$  dependence of the  $\beta$  function, which scales as  $\beta_0 \sim n_c$ . As mentioned below equation (5.6),  $S_\omega$  induces also a one-meson vertex that mixes the  $\eta_1$  singlet with the messenger. However, this interaction is suppressed by the QCD  $\theta$  angle and is always negligible with respect to the above trilinear portal vertices.

### 6.1.3 Partial decay width

In summary, the hidden currents  $\text{Im } S'_m$  and  $S_\theta$  couple to  $\chi$ PT via bilinear one-meson portal interactions, while the hidden currents  $\text{Re } S'_m$ ,  $S_\omega$ , and the  $S_y$  couple to  $\chi$ PT via trilinear two-meson portal interactions. Putting everything together, the complete transition amplitude can be decomposed as

$$\mathcal{A}(K^+ \rightarrow \pi^+ s_i) = \mathcal{A}_{\text{direct}} + \mathcal{A}_{\text{mixing}}. \quad (6.13)$$

The amplitude for direct production via the trilinear interactions is

$$\mathcal{A}_{\text{direct}} = \mathcal{A}_m^{\text{Re}} + \mathcal{A}_h + \mathcal{A}_\omega, \quad (6.14)$$

where

$$\mathcal{A}_m^{\text{Re}} = -\frac{\epsilon_{UV} b_0}{2} \left( c_{K\pi s_i} - \text{Re } c_{\partial^2 i s}^{S_m} \frac{m_s^2}{v^2} \right), \quad \mathcal{A}_h = -\frac{\epsilon_{UV} \epsilon_{EW}}{2v} X_i, \quad (6.15a)$$

$$\mathcal{A}_\omega = \frac{\epsilon_{UV} \epsilon_{EW} c_i^{S_\omega}}{\beta_0 v} (h'_b m_K^2 - X_0). \quad (6.15b)$$

The quantities

$$X_i = \frac{1}{2} (h_{8i} + (n_f - 1) h_{27i}) (m_K^2 + m_\pi^2 - m_s^2) \quad (6.16)$$

measure the dependence on the octet and 27-plet coefficients  $h_{8i}$  and  $h_{27i}$ . Following the discussion in appendix D.2, the amplitude for indirect production  $\mathcal{A}_{\text{mixing}}$  can be written in terms of the generic meson-to-messenger mixing angles

$$\theta_{\pi s_i} = \epsilon_{UV} f_0 \frac{b_0 c_{s_i \pi}}{m_s^2 - m_\pi^2}, \quad \theta_{\eta s_i} = \epsilon_{UV} f_0 \frac{b_0 c_{s_i \eta} + c_i^{S_\theta} s_\eta \frac{m_0^2}{v}}{m_s^2 - m_\eta^2}, \quad (6.17a)$$

$$\theta_{\eta' s_i} = \epsilon_{UV} f_0 \frac{b_0 c_{s_i \eta'} - c_i^{S_\theta} c_\eta \frac{m_0^2}{v}}{m_s^2 - m_{\eta'}^2}. \quad (6.17b)$$

This results in

$$\mathcal{A}_{\text{mixing}} = \mathcal{A}_m^{\text{Im}} + \mathcal{A}_\theta = -i \frac{\epsilon_{EW}}{2f_0} \left( \theta_{\pi s_i} V_{K\pi\pi} + \theta_{\eta s_i} V_{K\pi\eta} + \theta_{\eta' s_i} V_{K\pi\eta'} \right). \quad (6.18)$$

In momentum space, and evaluated on-shell, the functions (6.6) become

$$V_{K\pi\pi} = \frac{1}{8} [5h_{27}(2m_K^2 - m_s^2 - m_\pi^2) + (2h_8 + 9h_{27})(m_s^2 - m_\pi^2)] , \quad (6.19a)$$

$$V_{K\pi\eta} = \frac{c_\eta}{12\sqrt{2}} [(2h_8 - 3\sqrt{2}t_\eta h_1 + 9h_{27})(2m_K^2 - m_s^2 - m_\pi^2) - (4h_8 + 3\sqrt{2}t_\eta h_1 + 3h_{27})(m_s^2 - m_\pi^2)] , \quad (6.19b)$$

$$V_{K\pi\eta'} = \frac{s_\eta}{12\sqrt{2}} [(2h_8 + 3\sqrt{2}t_\eta^{-1} h_1 + 9h_{27})(2m_K^2 - m_s^2 - m_\pi^2) - (4h_8 - 3\sqrt{2}t_\eta^{-1} h_1 + 3h_{27})(m_s^2 - m_\pi^2)] . \quad (6.19c)$$

All of the above amplitudes are determined entirely by  $m_K^2$ ,  $m_\pi^2$ , and  $m_s^2$ , with no remaining angular dependence. The resulting partial decay width is

$$\Gamma(K^+ \rightarrow \pi^+ s_i) = \frac{1}{8\pi m_K} \rho(x_\pi, x_s) |\mathcal{A}(K^+ \rightarrow \pi^+ s_i)|^2 , \quad (6.20)$$

where the phase-space factor is

$$\rho(x_\pi, x_s) = \sqrt{\left(\frac{1 - x_\pi - x_s}{2}\right)^2 - x_\pi x_s} , \quad x_i = \frac{m_i^2}{m_K^2} , \quad (6.21)$$

and the squared amplitude is

$$|\mathcal{A}(K^+ \rightarrow \pi^+ s_i)|^2 = |\text{Re } \mathcal{A}|^2 + |\text{Im } \mathcal{A}|^2 , \quad (6.22)$$

where

$$|\text{Re } \mathcal{A}|^2 = \frac{\epsilon_{\text{UV}}^2 b_0^2}{4} \left| \text{Re} \left( c_{K\pi s_i} - \mathbf{c}_{\partial^2 i s}^{S_m d} \frac{m_s^2}{v^2} \right) + \frac{\epsilon_{\text{EW}}}{b_0 v} \left( X_i + 2 \frac{c_i^{S_\omega}}{\beta_0} (X_0 - h'_b m_K^2) \right) \right|^2 , \quad (6.23a)$$

$$|\text{Im } \mathcal{A}|^2 = \frac{1}{4} \left| \epsilon_{\text{UV}} b_0 \text{Im } c_{K\pi s_i} + \frac{\epsilon_{\text{EW}}}{f_0} \left( \theta_{\pi s_i} V_{K\pi\pi} + \theta_{\eta s_i} V_{K\pi\eta} + \theta_{\eta' s_i} V_{K\pi\eta'} \right) \right|^2 . \quad (6.23b)$$

Hence, the decay width reads

$$\begin{aligned} \Gamma(K^+ \rightarrow \pi^+ s_i) &= 2\pi m_K \left( \frac{\epsilon_{\text{UV}}}{2} \frac{b_0}{4\pi m_K} \right)^2 \rho(x_\pi, x_s) \\ &\quad \left( \left| \text{Re} \left( c_{K\pi s_i} - \mathbf{c}_{\partial^2 i s}^{S_m d} \frac{m_s^2}{v^2} \right) + \frac{\epsilon_{\text{EW}}}{b_0 v} \left( X_i + 2 \frac{c_i^{S_\omega}}{\beta_0} (X_0 - h'_b m_K^2) \right) \right|^2 \right. \\ &\quad \left. + \left| \text{Im } c_{K\pi s_i} + \frac{\epsilon_{\text{EW}}}{\epsilon_{\text{UV}} f_0 b_0} \left( \theta_{\pi s_i} V_{K\pi\pi} + \theta_{\eta s_i} V_{K\pi\eta} + \theta_{\eta' s_i} V_{K\pi\eta'} \right) \right|^2 \right) . \end{aligned} \quad (6.24)$$

#### 6.1.4 Flavour-blind hidden sectors

Starting from the results given in the previous section, we derive the full amplitude squared for  $K^\pm \rightarrow \pi^\pm s_i$  decays in the case of flavour-blind portal interactions. For such portal interactions, the Wilson coefficients (6.8) and (6.10) simplify to

$$c_{s_i \pi} = 0 , \quad c_{s_i \eta} = -s_\eta \text{Im } c_i^{S_m} , \quad c_{s_i \eta'} = c_\eta \text{Im } c_i^{S_m} , \quad (6.25)$$

and

$$\text{Re } c_{K\pi s_i} = \frac{\epsilon_{\text{EW}}}{n_f} (h_8 + (n_f - 1)h_{27} - h'_b) \text{Re } c_i^{S_m} \quad (6.26a)$$

$$+ \text{Re } \mathbf{c}_i^{S_m d} - \epsilon_{\text{EW}} \left( \frac{m_K^2}{b_0 v} \text{Re } h_{bi} - \frac{\kappa_\Gamma}{2} \text{Re}(c_{i\text{ds}}^\gamma + c_{i\text{sd}}^\gamma) \right),$$

$$\text{Im } c_{K\pi s_i} = \epsilon_{\text{EW}} \left( \frac{h'_b}{n_f} (1 - 2\epsilon_s) \text{Im } c_i^{S_m} + \frac{m_K^2}{b_0 v} \text{Im } h_{bi} - \frac{\kappa_\Gamma}{2} \text{Im}(c_{i\text{ds}}^\gamma - c_{i\text{sd}}^\gamma) \right), \quad (6.26b)$$

while the mixing angles become

$$\theta_{\eta s_i} = -\frac{s_\eta \epsilon_{\eta_1 s_i}}{m_s^2 - m_\eta^2}, \quad \theta_{\eta' s_i} = \frac{c_\eta \epsilon_{\eta_1 s_i}}{m_s^2 - m_{\eta'}^2}, \quad \epsilon_{\eta_1 s_i} = \epsilon_{\text{UV}} f_0 \left( b_0 \text{Im } c_i^{S_m} - c_i^{S_\theta} \frac{m_0^2}{v} \right). \quad (6.27)$$

### 6.1.5 Explicit portal currents for specific hidden sector models

PETs including hidden spin 0 fields can be motivated from a broad range of BSM models and are realised for instance in models of DM (see *e.g.* [216–221]), inflation (see *e.g.* [222, 223]), naturalness (see *e.g.* [224–229]) and baryogenesis (see *e.g.* [88] for references). Spin 0 particles can be grouped into several categories, depending on their portal interactions with the SM at the EW scale. We briefly summarise these categories and describe how the PET procedure can be applied to each of them. Additionally, we provide the relevant PET operators at the GeV scale, and their connection to the hidden currents, for ALPs and real scalar models, which are among the most studied realisations of light spin 0 messengers.

**ALPs** ALPs are PGBs associated with the spontaneous breaking of an approximate global symmetry. Hence, they arise in a multitude of theoretically well motivated models, ranging from string theory (see *e.g.* [230–232]) to QCD. The original axion field is the PGB of the Peccei-Quinn symmetry [16–19], which has been introduced in order to solve the strong CP problem and is broken by the axial anomaly of QCD.<sup>17</sup>

Depending on the underlying theoretical model, ALPs can have theoretically unconstrained couplings with the SM gauge bosons and derivative couplings with the SM fermions. The latter couplings can be traded for non-flavour blind Yukawa couplings, as described in appendix A.2. Up to dimension five, the most general Lagrangian before EWSB is given by [93, 233–236]

$$\mathcal{L}_a = \mathcal{L}_a^{\text{hidden}} + \mathcal{L}_a^{\text{portal}}, \quad \mathcal{L}_a^{\text{hidden}} = \frac{1}{2} \partial_\mu a \partial^\mu a + \frac{1}{2} m_a^2 a^2. \quad (6.28)$$

Here  $a$  is the ALP field and the portal interactions are

$$\mathcal{L}_a^{\text{portal}} = \frac{a}{f_a} \left( c_W W_{\mu\nu} \widetilde{W}^{\mu\nu} + c_B B_{\mu\nu} \widetilde{B}^{\mu\nu} + c_G G_{\mu\nu} \widetilde{G}^{\mu\nu} \right. \\ \left. + (i \mathbf{c}_u q \bar{u} \widetilde{H}^\dagger + \mathbf{c}_d q \bar{d} H^\dagger + \mathbf{c}_e \ell \bar{e} H^\dagger + \text{h.c.}) \right), \quad (6.29)$$

<sup>17</sup> It has been long thought that axions in the MeV range were excluded, however this might not be the case. We refer to [20] for a critical overview of bounds on MeV axions.

where  $f_a$  is the energy scale associated with the ALP and the  $c_i$  (with  $i = G, W, B$ ) and  $\mathbf{c}_i$  (with  $i = u, d, e$ ) are scalar and matrix valued Wilson coefficient in flavour space, respectively. For models that comply with minimal flavour violation, the coefficient matrices in the Yukawa interactions are aligned with and of comparable strength as the SM Yukawa matrices  $\mathbf{y}_i$ . All coefficients have been defined after using the EOM for the Higgs and fermion fields in order to eliminate the derivative interactions of the ALP, for details see [93, 235, 236]. For QCD axions, the mass term is generated by the QCD quark condensate, so that  $f_a m_a \propto m_\pi^2$ , while for generic ALP models, both the scale  $f_a$  and the mass term  $m_a$  are free parameters of the theory. The mass term is part of the Lagrangian describing the internal structure of the hidden sector, which we do not need in our procedure, and it is listed here only for completeness. Considering the portal Lagrangian (6.29), we recognise that all terms can be matched to the spin 0 portal operators defined in table 2. Hence, the relevant currents that drive the phenomenology of ALPs at the EW scale are given by

$$\mathbf{S}_m^X = \mathbf{c}_X \frac{a}{f_a}, \quad S_\theta = c_G \frac{a}{f_a}, \quad S_\theta^X = c_X \frac{a}{f_a}, \quad (6.30)$$

where we have used  $\epsilon_{UV} = v/f_a$ , after confronting eq. (6.29) with the pertinent PETs in table 2. Comparing with equation (6.1), the resulting portal current that couple QCD to ALPs at the strong scale are

$$\mathbf{S}_m \supset \mathbf{c}_{S_m} \frac{v}{f_a} a, \quad \mathfrak{S}_x = \mathfrak{h}_x \frac{a}{f_a}, \quad S_\theta = c_{S_\theta} \frac{a}{f_a}, \quad \mathbf{S}_\gamma = (\boldsymbol{\lambda}_d^s c_{sd}^\gamma + \boldsymbol{\lambda}_s^d c_{ds}^\gamma) \frac{v}{f_a} a, \quad (6.31a)$$

where we have used the EOMs for the ALP to resorb the  $\partial^2/v^2$  contribution from the general expression in (6.1) into  $\mathbf{c}_{S_m}$ . In addition, the term in Lagrangian (6.29) that contains the photon field strength tensor gives rise to the Primakoff effect [237], which our work does not modify.

The axial current  $S_\theta$  and the imaginary part of the Yukawa current  $\mathbf{S}_m$  mix the ALP with pions and  $\eta$ -mesons, and give rise to ‘indirect’ production via diagram 10a. The remaining currents give rise to ‘direct’ production via diagram 10b. For models that comply with minimal flavour violation, the coefficients  $\mathbf{c}_{S_m}$ ,  $c_{sd}^\gamma$ , and  $c_{ds}^\gamma$  are aligned with and of comparable size as their SM counterparts,

$$v \mathbf{c}_{S_m} \sim \mathbf{m}, \quad v c_{sd}^\gamma \sim m_d, \quad v c_{ds}^\gamma \sim m_s. \quad (6.32)$$

In  $\chi$ PT, one finally obtains the currents

$$\mathbf{S}_m' = \mathbf{c}'^{S_m} \frac{v}{f_a} a + \mathcal{O}(\epsilon_{EW}^2, \epsilon_s^2), \quad S_y = h_y \frac{a}{f_a}, \quad (6.33)$$

where the coefficient  $\mathbf{c}'^{S_m}$  is defined like its generic counterpart  $\mathbf{c}_i'^{S_m}$  in equation (6.3), except with the generic Wilson coefficients replaced according to

$$\left( \mathbf{c}_i^{S_m} + \mathbf{c}_{\partial^2 i}^{S_m} \frac{1}{v^2} \partial^2 \right) \rightarrow \mathbf{c}^{S_m}, \quad c_i^{S_\theta} \rightarrow c^{S_\theta}, \quad c_{isd}^\gamma \rightarrow c_{sd}^\gamma, \quad c_{ids}^\gamma \rightarrow c_{ds}^\gamma, \quad h_{yi} \rightarrow h_y. \quad (6.34)$$

Hence, the complete amplitude for  $K^\pm \rightarrow \pi^\pm a$  decays is

$$\mathcal{A}(K^+ \rightarrow \pi^+ a) = \mathcal{A}_{\text{direct}} + \mathcal{A}_{\text{mixing}}, \quad (6.35)$$

where the direct contribution is

$$\mathcal{A}_{\text{direct}} = \mathcal{A}_m^{\text{Re}} + \mathcal{A}_h = -\frac{b_0 v}{2f_a} c_{K\pi a} - \frac{\epsilon_{\text{EW}}}{2f_a} X_0, \quad (6.36)$$

while the indirect contribution for production via meson-to-axion mixing is

$$\mathcal{A}_{\text{mixing}} = \mathcal{A}_m^{\text{Im}} + \mathcal{A}_\theta = -i \frac{\epsilon_{\text{EW}}}{2f_0} (\theta_{\pi a} V_{K\pi\pi} + \theta_{\eta a} V_{K\pi\eta} + \theta_{\eta' a} V_{K\pi\eta'}) , \quad (6.37)$$

where the mixing angles are now

$$\theta_{\pi a} = \frac{f_0}{f_a} \frac{b_0 v c_{a\pi}}{m_a^2 - m_\pi^2}, \quad \theta_{\eta a} = \frac{f_0}{f_a} \frac{b_0 v c_{a\eta} + c_{S_\theta} m_0^2 s_\eta}{m_a^2 - m_\eta^2}, \quad \theta_{\eta' a} = \frac{f_0}{f_a} \frac{b_0 v c_{a\eta'} - c_{S_\theta} m_0^2 c_\eta}{m_a^2 - m_{\eta'}^2}. \quad (6.38)$$

The coefficients  $c_{K\pi a}$  and  $c_{aX}$  are defined like their generic counterparts  $c_{K\pi i}$  and  $c_{s_i X}$  in equations (6.8) and (6.10), except that the Wilson coefficients are replaced according to (6.34). If the Wilson coefficients in Lagrangian (6.29) are aligned with the SM Yukawa couplings, as it is usually the case, all amplitudes above are of the same order and equally contribute to the decay rate. However, for flavour-blind ALPs with  $c_X \sim 1$  in (6.30), the amplitudes  $\mathcal{A}_m^{\text{Re}}$  and  $\mathcal{A}_m^{\text{Im}}$  are much bigger than the other two and dominate the decay rate.

We note that the indirect amplitude encompasses *e.g.* the production amplitude of proper QCD axions given in [20], where the authors have neglected the 27-plet contributions  $\propto h_{27}$  as well as the finite pion and axion masses  $m_\pi^2, m_a^2 \rightarrow 0$ . In this approximation, the function  $V_{K\pi\pi}$  vanishes, and the resulting expression becomes independent of the axion-to-pion mixing angle  $\theta_{\pi a}$ .

**Light real scalar fields** This type of field can appear in a huge variety of BSM models, ranging from DM models, where the scalar is protected by a  $\mathbb{Z}_2$  symmetry (see *e.g.* [238, 239]), to models for baryogenesis (see *e.g.* [88]), and two Higgs-doublet models (2HDMs) (see *e.g.* [240, 241]), such as the inert doublet model, see *e.g.* [242]. Additionally, there are interesting candidates in SUSY with R-parity conservation, such as the saxino, which is the scalar R-odd component of the axion superfield. The saxino mass is typically of the same order of the gravitino mass, however there are models in which it can be naturally at a low scale, see *i.e.* [243]. The most common hidden Lagrangian can be cast as

$$\mathcal{L}_s = \mathcal{L}_s^{\text{hidden}} + \mathcal{L}_s^{\text{portal}}, \quad \mathcal{L}_s^{\text{hidden}} = \frac{1}{2} \partial_\mu s \partial^\mu s + \lambda s^2 + \lambda' s^3 + \lambda'' s^4, \quad (6.39)$$

where the  $\lambda$  denote the self-couplings, however, being part of the hidden Lagrangian they are not relevant for the PET approach. The portal interactions are

$$\begin{aligned} \mathcal{L}_s^{\text{portal}} = & \frac{\alpha_0}{\Lambda} s D^\mu H^\dagger D_\mu H + \left( \alpha_1 s + \alpha_2 s^2 + \frac{\alpha_3}{\Lambda} s^3 \right) H^\dagger H + \frac{\alpha_4}{\Lambda} s (H^\dagger H)^2 \\ & + \frac{s}{\Lambda} (i c_u q \bar{u} \tilde{H}^\dagger + c_d q \bar{d} H^\dagger + c_e \bar{\ell} e H^\dagger + \text{h.c.}) + \frac{c_W}{\Lambda} s W_{\mu\nu} W^{\mu\nu} + \frac{c_B}{\Lambda} s B_{\mu\nu} B^{\mu\nu} + \frac{c_G}{\Lambda} s G_{\mu\nu} G^{\mu\nu}, \end{aligned} \quad (6.40)$$

where the  $\alpha_i$ , the  $c_X$  with  $X = W, B, G$ , and the  $\mathbf{c}_x$  with  $x = u, d, e$  are dimensionless Wilson coefficients and coefficient matrices, respectively. The self- and portal-couplings involving an odd number of scalar fields are only present if the scalar field does not obey a  $\mathbb{Z}_2$  symmetry. The PET framework is suitable for  $n$  equal spin hidden messengers, hence it can describe several cases, such as: i) a single hidden scalar messenger, which is even under the symmetry of the secluded sector and arises for instance in simplified DM models [244], ii) a DM candidate which is odd under the  $\mathbb{Z}_2$  symmetry, the typical example being the singlet scalar Higgs portal model [245, 246], and iii) models with  $\mathbb{Z}_n$  symmetries (see *e.g.* [247] for DM models). Depending on the symmetries of the model, the real scalar  $s$  can mix with the SM Higgs boson or assume a non-zero VEV, however we will not discuss these possibilities here. Typically, the scalar portal Lagrangian (6.40) only includes terms up to dimension four, while we include here also EW scale terms of dimension five using the PET approach. A term which is especially relevant for light scalar fields is the coupling with the gluon field strength tensor, which is present for instance in theories with a dilaton field, see *e.g.* [248].

In order to demonstrate that the generic decay amplitude (6.13) encompasses and is consistent with standard computations, we apply this general result to the case of light Higgs production in charged kaon decays  $K^\pm \rightarrow \pi^\pm h$ . We compare our results with those obtained in [106], where  $h$  is considered to be the SM Higgs boson, and [249], where it is taken to be the lightest Higgs particle of a 2HDM model. The computation in [106] was performed before the discovery of the top-quark and the Higgs boson, so that the Higgs was still allowed to be lighter than the charged kaons. In general, a light Higgs boson, with a mass  $m_h < m_K$ , couples to QCD at the strong scale directly via quark Yukawa interactions, and additionally via effective  $hGG$  and  $h\bar{q}q\bar{q}q$  vertices, which arise after integrating out the heavy SM DOFs. Translating these interactions into the hidden current picture, the only non-vanishing Wilson coefficients in equations (6.2) and (6.3) are [106, 249]

$$\epsilon_{UV}\mathbf{c}_i^{S_m} = \frac{1}{v}(\boldsymbol{\kappa}\mathbf{m} - m_s\kappa_{ds}\boldsymbol{\lambda}_s^d - m_{ud}\kappa_{ds}^\dagger\boldsymbol{\lambda}_d^s), \quad \epsilon_{UV}c_i^{S_\omega} = 2\kappa_G, \quad \epsilon_{UV}h_{yi} = -2\kappa_W h_y, \quad (6.41)$$

where  $\boldsymbol{\kappa} = \text{diag}(\kappa_u, \kappa_d, \kappa_d)$ . The coefficients  $\kappa_u$  and  $\kappa_d$  measure the coupling of the Higgs-particle to the up-type and down-type quarks in the SM, respectively. In the case of a light 2HDM Higgs-particle, one has  $\kappa_G = (2\kappa_u + \kappa_d)/3$ , while the remaining  $\kappa_x$  are free parameters. In case of the SM Higgs boson, one has [106]

$$\kappa_u = \kappa_d = \kappa_G = \kappa_W = 1. \quad (6.42)$$

The constant  $\kappa_{ds} \sim \epsilon_{EW}$  is determined by matching the low energy theory to the EW scale description. In general, it can be parameterised as [249, 250]

$$\kappa_{ds} = 2 \sum_{u=u,c,t} V_{du}^\dagger V_{us} x_u f(x_u), \quad x_u = \frac{m_u^2}{\Lambda_{SM}^2}, \quad (6.43)$$

and  $f(x_u)$  is a model dependent function. For the SM Higgs-particle, assuming  $x_u \ll (4\pi)^{-2}$ , and neglecting the running of the Wilson coefficients between the EW and strong scales, one has  $f(x_u) = 3/4$  [106]. In the case of the 2HDM, the corresponding expression is known, but quite

complicated. It can be found *e.g.* in [250–252]. Using equation (6.41), the coefficient (6.10) becomes

$$\epsilon_{\text{UV}} c_{K\pi s_i} = \frac{m_\pi^2}{2vb_0}(\kappa_u - \kappa_d)\epsilon_{\text{EW}}(h_8 + (n_f - 1)h_{27}) + \frac{m_K^2}{vb_0}(2\epsilon_{\text{EW}}\kappa_W h_b - \kappa_{\text{ds}}) + \mathcal{O}(\epsilon_s^2) . \quad (6.44)$$

The overall  $K^\pm \rightarrow \pi^\pm h$  decay amplitude receives contributions from the partial amplitudes  $\mathcal{A}_m^{\text{Re}}$ ,  $\mathcal{A}_\omega$ , and  $\mathcal{A}_h$ , all of which mediate direct production. There is no meson-to-Higgs mixing because the Higgs is scalar, rather than a pseudoscalar, particle. One obtains

$$\mathcal{A}_m^{\text{Re}} = \frac{m_K^2}{2v}(\kappa_{\text{ds}} - 2\kappa_W\epsilon_{\text{EW}}h_b) - \frac{m_\pi^2}{4v}(\kappa_u - \kappa_d)\epsilon_{\text{EW}}(h_8 + (n_f - 1)h_{27}) , \quad (6.45a)$$

$$\mathcal{A}_h = \frac{\epsilon_{\text{EW}}m_K^2}{2v}\kappa_W(h_8 + (n_f - 1)h_{27})\left(1 + \frac{m_\pi^2 - m_s^2}{m_K^2}\right) , \quad (6.45b)$$

$$\mathcal{A}_\omega = \frac{\epsilon_{\text{EW}}m_K^2}{2v}\frac{2\kappa_G}{\beta_0}\left(2h'_b - (h_8 + (n_f - 1)h_{27})\left(1 + \frac{m_\pi^2 - m_s^2}{m_K^2}\right)\right) . \quad (6.45c)$$

Thus, the full amplitude is

$$\begin{aligned} \mathcal{A}(K^+ \rightarrow \pi^+ h) = & \frac{m_K^2}{v}\left[\left(\frac{\kappa_W}{2} - \frac{\kappa_G}{\beta_0}\right)\epsilon_{\text{EW}}(h_8 + (n_f - 1)h_{27})\left(1 + \frac{m_\pi^2 - m_s^2}{m_K^2}\right)\right. \\ & \left. + \frac{\kappa_d - \kappa_u}{4}\epsilon_{\text{EW}}(h_8 + (n_f - 1)h_{27})\frac{m_\pi^2}{m_K^2} - 2\epsilon_{\text{EW}}\left(\frac{\kappa_W}{2}h_b - \frac{\kappa_G}{\beta_0}h'_b\right) + \kappa_{\text{ds}}\right] . \end{aligned} \quad (6.46)$$

This result encompasses the one given in [249], where the contributions from the 27-plet and chromomagnetic operators have been neglected, which amounts to replacing  $h_{27} \rightarrow 0$  and  $h'_b \rightarrow h_b$ .<sup>18</sup> Using the values (6.42), one also obtains the result given in [106].<sup>19</sup>

**Pseudoscalars** Pseudoscalar particles are predicted in many extensions to the Higgs sector, see *e.g.* [253, 254] and the recently proposed relaxion field (see *e.g.* [228, 255]), and have more general characteristics as compared to ALPs. The latter are restricted by being PGBs, while generic pseudoscalar particles can couple to the SM via additional portal operators at the EW scale, most notably a direct coupling with the Higgs boson. In this sense, these particle combine features that arise in both ALPs and light scalar models.

**Complex Scalars** As explained in section 3, PETs can describe complex scalars as a combination of two distinct real spin 0 fields that can be either scalar or pseudoscalar. There are several interesting models with light complex scalar fields, see *e.g.* [256]. Additionally, complex scalars commonly arise in SUSY models, such as the sgoldstino [257–264], which can naturally be in the MeV mass range, the sneutrino [265–269], which appears in the minimal supersymmetric Standard Model, and the additional complex scalar field introduced in the next-to-minimal supersymmetric Standard Model, see *e.g.* [270] for a review.

<sup>18</sup> In [249] the amplitude is expressed in terms of  $2g_{\mathcal{H}} = \kappa_{\text{ds}}$ ,  $k_G = 2\kappa_G/\beta_0$ ,  $\gamma_8 = \epsilon_{\text{EW}}h_8/4$ , and  $\tilde{\gamma}_8 = \epsilon_{\text{EW}}h_1/4$ .

<sup>19</sup> In [106] the amplitude is written in terms of the quantities  $\xi = \kappa_{\text{ds}}^\dagger$ ,  $\kappa \equiv 2/\beta_0$ ,  $\gamma_1 = \epsilon_{\text{EW}}h_8$ , and  $\gamma_2 = \epsilon_{\text{EW}}h_b$ .



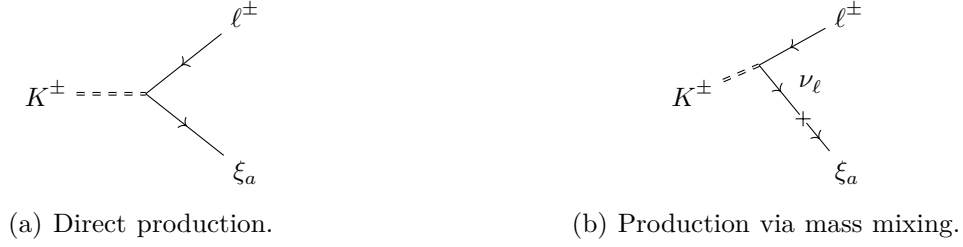


Figure 11: Feynman diagrams for the  $K^\pm \rightarrow \ell^\pm \xi_a$  process.

## 6.2 Charged kaon decay to charged leptons and hidden fermions

In this section, we compute the transition amplitude for production of a generic fermionic messenger  $\xi_a$  in charged kaon decays  $K^\pm \rightarrow \ell^\pm \xi_a$  at LO in  $\delta$ .

### 6.2.1 Relevant interactions

At tree-level,  $K^\pm \rightarrow \ell^\pm \xi_a$  decays are described by the two types of diagrams, depicted in figure 11: i) diagrams with a single trilinear one-meson  $K^\pm \rightarrow \ell^\pm \xi_a$  portal vertex that directly couples  $\chi$ PT to hidden sectors, and ii) diagrams with one trilinear  $K^\pm \rightarrow \ell^\pm \nu_\ell$  SM vertex and a second  $\nu_\ell \rightarrow \xi_a$  portal vertex that indirectly couples  $\chi$ PT to hidden sectors by mixing the SM neutrinos with the fermionic messenger. The relevant portal current contributions to type i) diagrams are those with exactly one hidden spin 1/2 messenger and one charged lepton. Using the list of portal currents in section 3.3.2, the only such contribution is

$$V_l^\mu \supset \frac{\epsilon_{UV}}{2} c_{\bar{u}s a}^{L\dagger} \lambda_s^u \xi_a^\dagger \bar{\sigma}_\mu e_b + \text{h.c.} , \quad (6.47)$$

where  $e$  and  $c_{\bar{u}s}^{L\dagger}$  are doublets in flavour space that capture the coupling to both  $e^\pm$  and  $\mu^\pm$ . The corresponding vertex mediating charged kaon decays is encoded inside the kinetic-like one meson portal interactions (5.2), leading to

$$\mathcal{L}_K^{\partial V_l} = -\frac{\epsilon_{UV} f_0}{v^2} c_{\bar{u}s, ba}^{L\dagger} \xi_a^\dagger \bar{\sigma}_\mu e_b \partial^\mu K^+ . \quad (6.48)$$

To compute diagrams of type ii), we have to specify both the neutrino to hidden fermion mixing vertex and the trilinear SM vertex. The mixing vertex is given as

$$\mathcal{L}_{\nu_b \xi_a} = -\epsilon_{UV} v (c_{ba}^\nu \nu_b \xi_a + \text{h.c.}) , \quad (6.49)$$

where  $\nu$  and  $c_a^\nu$  are doublets in flavour space that capture the mixing of both  $\nu_e$  and  $\nu_\mu$ . The trilinear SM vertex is encoded inside the kinetic-like one meson interactions (5.25), leading to

$$\mathcal{L}_K^{\partial W} = \frac{f_0 V_{us}}{v^2} \partial_\mu K^+ \sum_{b=e, \mu} \nu_b^\dagger \bar{\sigma}^\mu \ell_b . \quad (6.50)$$

### 6.2.2 Partial decay width

The vertices (6.47) to (6.49) are written in the two-component notation of [129]. Applying the Feynman rules for the two-component spinor notation [129, 271] to compute the two types of diagrams illustrated in figure 11, one obtains the full decay amplitude

$$\mathcal{A}(K^+ \rightarrow \ell_b^+ \xi_a) = \mathcal{A}_{\text{direct}} + \mathcal{A}_{\text{mixing}} , \quad (6.51)$$

where the partial amplitudes are

$$\mathcal{A}_{\text{direct}} = -i \frac{\epsilon_{\text{UV}} f_0}{v^2} c_{\bar{u}s,ba}^{L\dagger} x^\dagger(p_\xi, s_\xi) \bar{\sigma}_\mu y(p_\ell, s_\ell) p_K^\mu , \quad (6.52a)$$

$$\mathcal{A}_{\text{mixing}} = i \frac{\epsilon_{\text{UV}} f_0}{v m_\xi^2} c_{ba}^\nu V_{\text{us}} y(p_\xi, s_\xi) \sigma_\nu \bar{\sigma}_\mu y(p_\ell, s_\ell) p_\xi^\nu p_K^\mu , \quad (6.52b)$$

and the functions  $x(p, s)$  and  $y(p, s)$  are the polarisation spinors for two-component fermion fields. The resulting helicity-summed partial decay width is

$$\Gamma(K^+ \rightarrow \ell_b^+ \xi_a) = 2\pi m_K \left( \epsilon_{\text{UV}} \epsilon_{\text{EW}} \frac{m_K}{4\pi f_0} \right)^2 \rho(x_\ell, x_\xi) \left| c_{\bar{u}s,ba}^L + \frac{c_{ba}^\nu V_{\text{us}} v}{m_\xi} \right|^2 , \quad x_i = \frac{m_i^2}{m_K^2} , \quad (6.53)$$

where the phase-space factor is

$$\rho(x_\ell, x_\xi) = (x_\ell + x_\xi - (x_\ell - x_\xi)^2) \sqrt{\left( \frac{1 - x_\ell - x_\xi}{2} \right)^2 - x_\ell x_\xi} . \quad (6.54)$$

In terms of the partial decay width for the process  $K^+ \rightarrow \ell_b^+ \nu_b$ , this is

$$\Gamma(K^+ \rightarrow \ell_b^+ \xi_a) = \Gamma(K^+ \rightarrow \ell_b^+ \nu_b) \frac{\rho(x_\ell, x_\xi)}{\rho(x_\ell, 0)} |\theta_{ba}|^2 , \quad (6.55)$$

where the SM partial decay width and the effective mixing angle are

$$\Gamma(K^+ \rightarrow \ell_b^+ \nu_b) = 2\pi m_K \left( \epsilon_{\text{EW}} \frac{m_K}{4\pi f_0} \right)^2 |V_{\text{us}}|^2 \rho(x_\ell, 0) , \quad \theta_{ba} = \epsilon_{\text{UV}} \left( \frac{c_{ba}^\nu v}{m_\xi} + \frac{c_{\bar{u}s,ba}^L}{V_{\text{us}}} \right) . \quad (6.56)$$

### 6.2.3 Explicit portal currents for specific hidden sector models

Gauge singlet fermionic hidden fields are common in BSM models. In the SM, left-handed neutrinos are the only fields without a right-handed partner. Therefore, it is natural to consider that such fields exist, but have so far not been observed due to their feeble interactions with SM fields. One or more right-handed neutrinos can be added to the SM and can play an important role in several mechanisms of BSM physics, via their mixing with ordinary neutrinos. They can be used to generate neutrino masses (via one of the seesaw mechanisms), are required in leptogenesis models, and can act as DM. Since the nature of (right-handed) neutrinos is not known, the hidden messengers can be either Majorana or Dirac particles. The latter case is described in our framework by two hidden Weyl fermions. For reviews on the plethora of BSM models with right-handed neutrinos we refer to *e.g.* [63, 65, 272]. Many BSM models with

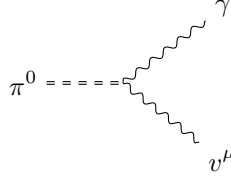


Figure 12: Feynman diagram for the  $\pi^0 \rightarrow \gamma v^\mu$  process.

right-handed neutrinos are commonly embedded into SUSY theories, see various realisation of type-I and inverse seesaw, *e.g.* [273–277].

As an example for a model with HNLs, we consider the type-I seesaw model. The minimal type-I seesaw Lagrangian couples the SM to a pair of two sterile Majorana neutrinos [8–13],

$$\mathcal{L}_\nu = \mathcal{L}_\nu^{\text{portal}} + \mathcal{L}_\nu^{\text{hidden}} , \quad \mathcal{L}_\nu^{\text{hidden}} = \frac{1}{2} (\bar{\nu}_i^\dagger i \not{\partial} \bar{\nu}_i - M_{ij} \bar{\nu}_i \bar{\nu}_j) + \text{h.c.} , \quad (6.57)$$

where

$$\mathcal{L}_\nu^{\text{portal}} = -y_{ia} \bar{\nu}_i \ell_a \tilde{H}^\dagger + \text{h.c.} \quad (6.58)$$

Here,  $M_{ij} = M_{ji}$  denotes the sterile neutrino Majorana mass matrix, and  $y_{ai}$  is the coupling strength of the sterile neutrino Yukawa interactions. Without loss of generality,  $M_{ij} = \text{diag}(M_1, M_2)$ . The sterile neutrinos do not couple directly to QCD, and the only contribution to the EW scale portal currents is

$$\Xi_a = -\bar{\nu}_i y_{ia} . \quad (6.59)$$

At the strong scale, this interaction generates the mass-mixing

$$\mathcal{L}_\nu^{\text{portal}} \rightarrow -y_{ia} \bar{\nu}_i \nu_a v + \text{h.c.} , \quad (6.60)$$

so that  $\epsilon_{UV} v c_{bi}^\nu = v y_{ib}$ . Hence, the effective mixing angle is just the physical mixing angle between the SM neutrino and the sterile neutrino,  $\theta_{bi} = v y_{ib} / M_i$ .

Another category of hidden fermionic fields is given by the axinos, which are SUSY partners of the axions, see *e.g.* [278, 279]. They are unrelated to the neutrino sector, unless R-parity violation is allowed. Axinos can be produced for instance by gluon fusion or in neutralino decays, which are useful mechanisms for searches in beam dump experiments or at colliders, and can be naturally in the MeV mass range, see *e.g.* [280].

### 6.3 Neutral pion decay to photons and hidden vectors

In this section, we consider anomalous neutral pion decays into hidden spin 1 messengers,  $\pi^0 \rightarrow \gamma v_\mu$ , at order  $\delta^3$ . Unlike in the previous sections, we now include EM contributions up to order  $\alpha_{\text{EM}}$ . However, we neglect all EW contributions that are suppressed by factors of  $\epsilon_{\text{EW}}$ , as this process is flavour conserving.

#### 6.3.1 Relevant portal current contributions

The relevant portal current contributions are those with a single hidden vector field. Using the list of portal currents in section 3.3.2, the only contributions of this type are

$$V_l^\mu \supset \epsilon_{UV} c_v^L v^\mu , \quad V_r^\mu = \epsilon_{UV} c_v^R v^\mu . \quad (6.61)$$

Figure 12 depicts the only relevant Feynman diagram. In principle the process can be mediated by two types of diagrams: i) diagrams with a trilinear  $\pi^0 \rightarrow \gamma\gamma$  SM vertex and a mixing vertex that makes the SM photon oscillate into a hidden spin 1 particle, and ii) diagrams with a direct trilinear  $\pi^0 \rightarrow \gamma v_\mu$  portal vertex. Choosing an appropriate operator basis, there is no type i) diagram, since the kinetic mixing term can always be eliminated from the theory using the SM EOM, in favour of a coupling to the SM fermion fields. As a result, only the diagram of type ii) contributes to the decay amplitude  $\pi^0 \rightarrow \gamma v_\mu$ . This interaction vertex arises from the anomalous WZW contribution, which enters at order  $\delta^3$ .

### 6.3.2 Partial decay width

The interaction corresponding to the diagram in figure 12 is contained in Lagrangian (5.9). By extracting from it the contribution with a singlet pion, one obtains

$$\mathcal{L}_{\pi \rightarrow \gamma v} \equiv \frac{n_c}{3} \frac{1}{(4\pi)^2 f_0} (2\mathbf{V}_v^{\mu\nu u} + \mathbf{V}_v^{\mu\nu d}) \frac{\pi_8}{\sqrt{2}} e \tilde{F}_{\mu\nu} , \quad (6.62)$$

where  $\mathbf{V}_v^\mu \equiv \mathbf{V}_l^\mu + \mathbf{V}_r^\mu$  and the photon field is canonically normalised. Using expressions (6.61), one has

$$\mathbf{V}_v^\mu = \epsilon_{UV} (\mathbf{c}_v^R + \mathbf{c}_v^L) v^\mu . \quad (6.63)$$

The above expression implies that the WZW does not couple neutral pions to the axial-vector current  $\mathbf{V}_a^\mu \equiv \mathbf{V}_l^\mu - \mathbf{V}_r^\mu$ . This is to be expected, since the WZW mediates parity violating transitions, while neutral pion decays into a photon and a hidden axial-vector would conserve parity. The partial decay width for  $\pi^0 \rightarrow \gamma v_\mu$  decays is

$$\Gamma(\pi^0 \rightarrow \gamma v) = \frac{1}{16\pi m_\pi} \left(1 - \frac{m_v^2}{m_\pi^2}\right) \overline{|\mathcal{A}(\pi^0 \rightarrow \gamma v)|^2} , \quad (6.64)$$

where the square amplitude is

$$\overline{|\mathcal{A}(\pi^0 \rightarrow \gamma v)|^2} = \left(\frac{n_c}{3} \frac{\epsilon_{UV}}{4\pi f_0}\right)^2 \frac{\alpha_{EM}}{4\pi} [2(\mathbf{c}_v^R + \mathbf{c}_v^L)_u + (\mathbf{c}_v^R + \mathbf{c}_v^L)_d]^2 (m_\pi^2 - m_v^2)^2 . \quad (6.65)$$

In terms of the partial decay width for the process  $\pi^0 \rightarrow \gamma\gamma$  it reads

$$\Gamma(\pi^0 \rightarrow \gamma v) = 2\epsilon_{eff}^2 \Gamma(\pi^0 \rightarrow \gamma\gamma) \left(1 - \frac{m_v^2}{m_\pi^2}\right)^3 , \quad (6.66)$$

where

$$\Gamma(\pi^0 \rightarrow \gamma\gamma) = 2\pi m_\pi \left(\frac{n_c}{3} \frac{\alpha_{EM}}{4\pi} \frac{m_\pi}{4\pi f_0}\right)^2 , \quad \epsilon_{eff} = \epsilon_{UV} \frac{2(\mathbf{c}_v^R + \mathbf{c}_v^L)_u + (\mathbf{c}_v^R + \mathbf{c}_v^L)_d}{2e(2\mathbf{q}_u^u + \mathbf{q}_d^d)} , \quad (6.67)$$

are the SM partial decay width and the effective mixing parameter.

### 6.3.3 Explicit portal currents for specific hidden sector models

Relatively light vectors states (*i.e.* below the GeV scale) that are very weakly coupled to the SM fields represent attractive physics targets for experimental searches at the cross-over of the intensity and high-energy frontiers. In the literature there are several proposals, with different motivations, for vector portal models. The simplest realisations do not charge the SM fields under the new gauge group related to the hidden vectors, giving rise to kinetic mixing portals. An attractive alternative is given by gauging certain combinations of SM fields under the new U(1), in order to achieve for instance anomaly free or UV complete models. Examples of the latter models are the  $B - L$  or the  $L_\mu - L_\tau$  anomaly free models, see *e.g.* [281–286]. For a broad overview of the different models, physics motivations and experimental constraints, we refer to the reviews [63, 256, 287].

Here, we consider the simplest dark photon model, which is QED-like, from [288, 289], with a single hidden vector  $v_\mu$ . The hidden Lagrangian is given by

$$\mathcal{L}_v = \mathcal{L}_v^{\text{hidden}} + \mathcal{L}_v^{\text{portal}} , \quad \mathcal{L}_v^{\text{hidden}} = -\frac{1}{4}F'^{\mu\nu}F'_{\mu\nu} + \frac{1}{2}m_v^2 v_\mu v^\mu , \quad (6.68)$$

and the portal interaction is

$$\mathcal{L}_v^{\text{portal}} = -\frac{\epsilon}{2}F^{\mu\nu}F'_{\mu\nu} . \quad (6.69)$$

In this equation,  $\epsilon$  is the kinetic mixing parameter between the hidden vector and the photon and  $F'_{\mu\nu}$  is the field strength tensor of the hidden vector. We show part of the hidden Lagrangian, however, this is not needed for our purposes. First, it is not actually relevant how the dark photon acquires a mass. This can be achieved by the spontaneous symmetry breaking of the symmetry to which the dark photon is associated, requiring a dark Higgs, or could be achieved via the Stückelberg mechanism [290, 291], if the symmetry is a U(1). As long as the dark Higgs is heavier than the  $\chi$ PT scale and is integrated out, equation (6.65) is not modified by the mass generation mechanism. Second, we remain agnostic about the remaining particle content of the hidden sector, which might include fermionic states  $X$ , charged under the new U(1), that couple only to the dark photon (we already mentioned this possibility in section 5.1). A model similar to (6.69) that couples to the hypercharge instead of the EM charge is obtained by substituting the quantum electrodynamics (QED) U(1) with the hypercharge U(1) field in the SM.

The expected branching ratio for the process  $\pi^0 \rightarrow \gamma v_\mu$  is known, see *e.g.* [82], and is equivalent to equation (6.65), which can be seen by rewriting the kinetic mixing Lagrangian (6.69) in terms of the portal operators using the SM EOM. Afterwards, the dark photon field couples to QCD via the neutral current interaction

$$\mathcal{L}_v^{\text{portal}} \rightarrow -\langle \mathbf{v}'_\mu (\mathbf{Q}^\mu + \overline{\mathbf{Q}}^\mu) \rangle_f , \quad \mathbf{v}'_\mu = \epsilon e \mathbf{q} v_\mu . \quad (6.70)$$

Hence,  $\epsilon_{\text{UV}}(\mathbf{c}_v^L + \mathbf{c}_v^R) = \epsilon e \mathbf{q}$ , and therefore  $\epsilon_{\text{eff}} = \epsilon$ .

## 7 Conclusion

In this paper, we have developed a framework of PETs, which extend EFTs associated with the SM by coupling them to generic hidden messenger fields with masses at or below the

characteristic energy scale of the relevant EFT. This framework enables the coupling of SM fields to light hidden sectors while remaining largely agnostic about the internal structure of the hidden sector, which can include secluded particles that do not couple directly to the SM but interact with each other and the messenger fields. It also accounts for the coupling to heavier hidden sectors via the inclusion of higher dimensional operators in PET Lagrangians. Throughout the paper, we have focused primarily on hidden fields with masses at or below the strong scale, for which there are extensive searches at intensity frontier experiments. However, we emphasise that the PET framework, and in particular the portal SMEFTs we derived in section 3, also capture messengers that are much heavier, as long as their mass is within the regime of applicability of the corresponding EFT.

Using the PET framework, we have first constructed EW scale and strong scale PETs that couple SMEFT and LEFT to a messenger of spin 0,  $1/2$ , or 1. The resulting portal SMEFTs encompass all available portal operators up to dimension five, while the portal LEFTs additionally encompass all dimension six and seven operators that contribute to quark-flavour violating transitions at LO in  $\epsilon_{\text{EW}}$ ,  $\alpha_{\text{EM}}$ , and the NDA  $4\pi$  counting scheme. We have found that all portal SMEFTs conserve baryon number, and that the spin 0 and 1 messenger portal SMEFTs conserve lepton number. In the case of spin  $1/2$  messenger, the portal operators can violate lepton number by one unit,  $|\Delta L| \leq 1$ . Additionally, this messenger does not couple to any of the quark fields or the right-chiral charged lepton fields, while the spin 1 messenger only couples to pairs of quarks and leptons with identical chirality, so that it cannot act as a separate source of chiral symmetry breaking. We used all these properties to constrain the portal LEFTs, so that the resulting LEFTs should be understood as a low energy approximation of the corresponding portal SMEFTs, where the heavy SM DOFs have been integrated out.

We have parameterised the coupling of QCD to hidden sectors at the strong scale in terms of ten external currents  $J \in \{\Omega, \Theta, \mathbf{M}, \mathbf{L}^\mu, \mathbf{R}^\mu, \mathbf{T}^{\mu\nu}, \mathbf{\Gamma}, \mathfrak{H}_l, \mathfrak{H}_r, \mathfrak{H}_s\}$ , and used a spurion analysis to derive the corresponding PETs that couple the hidden messengers to the U(3) version of  $\chi\text{PT}$ , which contains an  $\eta_1$  singlet meson in addition to the light pseudoscalar meson octet of SU(3)  $\chi\text{PT}$ . The spurion analysis is the standard technique used to embed  $\chi\text{PT}$  in the remainder of the SM at LO in  $\alpha_{\text{EM}}$ . Hence, the coupling of  $\chi\text{PT}$  to the currents  $\Theta, \mathbf{M}, \mathbf{L}^\mu$ , and  $\mathbf{R}^\mu$ , which capture the impact of photons, the light SM leptons, and the QCD theta angle in the SM, is well understood [105, 109, 149, 183–187, 197]. Similarly, the coupling of  $\chi\text{PT}$  to  $\mathbf{T}^{\mu\nu}$  has been studied in [203].

Here, we have extended the spurion technique to also account for the space-time dependent external currents  $\mathbf{\Gamma}, \mathfrak{H}_l, \mathfrak{H}_r, \mathfrak{H}_s$ , and  $\Omega$ . The SM contributions to all these currents are constant, and the SM contribution to the current  $\Omega = \omega + S_\omega$  is the inverse fine-structure constant of QCD  $\omega \propto g_s^{-2}$ . Since strong interactions are integrated out when constructing  $\chi\text{PT}$ , only the portal contribution  $S_\omega$  can appear in the  $\chi\text{PT}$  action.  $S_\omega$  encompasses *e.g.* the coupling of  $\chi\text{PT}$  to a light Higgs boson  $h$  via the interaction  $hG_{\mu\nu}G^{\mu\nu}$ , previously studied *e.g.* in [106]. We generalise that description to account for the coupling of  $\chi\text{PT}$  to a fully generic current  $S_\omega$ . The constant SM contributions to the dipole current  $\mathbf{\Gamma}$  and the four-quark currents  $\mathfrak{H}_x$  are usually included into  $\chi\text{PT}$  by appealing directly to the transformation behaviour of the QCD dipole and four-quark operators under global quark-flavour rotations [42, 114–117]. Since it is difficult to generalise this transformation behaviour approach to space-time dependent external currents, we have used the more powerful spurion approach. In order to include the four-quark currents

$\mathfrak{H}_x$  into the power counting for U(3)  $\chi$ PT, which is defined via a simultaneous expansion in momenta  $\partial^2$  and large  $n_c$ , we have generalised the standard QCD large  $n_c$  counting formula..

The final  $\chi$ PT Lagrangian contains 27 free coefficients  $\kappa \in \{\kappa_\Gamma^x, \kappa_T^x, \kappa_y^x, \kappa_\omega^x\}$ . In order to make it possible to constrain interactions in the portal LEFTs using bounds on hidden sector induced meson transitions, we have estimated 22 of these coefficients using a number of well-established techniques for the non-perturbative matching of  $\chi$ PT to QCD. Four of the seven coefficients  $\kappa_\omega$ , which measure the coupling of  $\chi$ PT to the  $S_\omega$  current, have already been estimated by using the anomalous trace relation of the QCD stress-energy tensor (2.65) [106]. Using this strategy, we have fixed the remaining three coefficients. The thirteen  $\kappa_x^y$  coefficients, which measure the coupling of  $\chi$ PT to the octet and 27-plet currents  $\mathfrak{H}_l$ ,  $\mathfrak{H}_r$ , and  $\mathfrak{H}_s$ , are well known in the large  $n_c$  limit [107, 108, 110–112, 205, 206]. However, corrections that appear for finite  $n_c^{-1}$  are known to be important when estimating the strength of the four-quark operators in the SM, and we expect the same to be true for the four-quark operators in the portal sector. Hence, we have adapted the strategies used in [106–108, 112, 205], and obtained improved estimates for the  $\kappa_x^y$  coefficients by matching them to experimental values of the octet and 27-plet coefficients  $h_{8,1,27}$ . Finally, we have estimated the coefficients  $\kappa_\Gamma$  and  $\kappa_\Gamma^M + \kappa_\Gamma^{M'}$ , which measure the coupling of  $\chi$ PT to the dipole current  $\Gamma$ , by matching the  $\chi$ PT prediction for the vacuum condensates of the QCD dipole quark bilinear (2.29) to the corresponding lattice values in (2.32).

To facilitate the application of our results, we have listed all one- and two-meson interactions that arise from the LO portal  $\chi$ PT action. We have then computed the most general transition amplitudes for three golden channels, which are used to constrain the coupling to hidden sectors in fixed-target experiments: i)  $K^\pm \rightarrow \pi^\pm s_i$ , ii)  $K^\pm \rightarrow \ell^\pm \xi_a$ , and iii)  $\pi^0 \rightarrow \gamma v_\mu$ .<sup>20</sup> For the spin 0 messenger, we have computed a universal decay amplitude and connected it to simple realisations of ALPs and scalar portal models. For spin  $1/2$  fields, we have mapped our generic decay amplitude to the case of HNL by rewriting it in terms of a generalised effective mixing angle. We have also connected our comprehensive expression for the spin 1 messengers to the case of QED-like dark photon model by using the photon EOM to express the kinetic mixing operator in terms of our portal operators.

## Outlook

The work we have presented in this paper opens up several potentially interesting avenues for further investigation, which range from formal improvements of the PET framework to theoretical work to expand its regime of applicability and further to a number of relevant phenomenological applications.

In this paper, we have focused primarily on completing a minimal version of portal  $\chi$ PT that can be used to make concrete predictions for meson decays at intensity experiments, and have left open some questions that need to be addressed in order to complete the PET framework. For instance, one has to connect the EW and strong scale PETs in order to constrain the shape of portal Lagrangians at the EW scale by means of low-energy experiments. This connection can be established *e.g.* via an explicit procedure of successive matching and running, where the Wilson coefficients for each portal interaction are run down from the EW scale ( $\mu \sim v$ ) to

<sup>20</sup> Recall that the fields  $s_i$ ,  $\xi_a$  and  $v_\mu$  denote generic spin 0, spin  $1/2$  and spin 1 messengers, respectively.

the strong scale ( $\mu \lesssim m_c$ ), while integrating out each heavy SM DOF as it becomes inactive. Further, it is necessary to complete the matching between the strong scale PETs and  $\chi$ PT by determining the remaining  $\kappa$  coefficients related to the external currents  $\boldsymbol{\Gamma}$  and  $\boldsymbol{T}^{\mu\nu}$ . This is an unavoidable procedure to relate meson scattering and decay amplitudes induced by these two currents to the corresponding dipole operators in QCD.

In addition, there are several avenues that can be pursued to extend the PET framework by expanding the range of models that it is able to capture. First, it is possible to include *e.g.* portal operators up to dimension six at the EW scale, which would allow for describing a larger class of DM models. Second, one can construct PETs for hidden sector models with higher spin messengers or with multiple messengers. In appendix B.2, we have already constructed portal SMEFTs for spin  $3/2$  and  $2$  messengers, but it remains to construct the corresponding portal LEFTs at the strong scale, as well as the resulting portal  $\chi$ PT Lagrangian at LO. Finally, while the PETs we have constructed already account for the possibility of multiple messengers with *identical* spin, for a fully general description of models with multiple portals, it might be interesting to add portal operators that encompass hidden fields with *different* spin.

Finally, one can apply the PET framework to make predictions for various experimental setups besides the low-energy fixed target experiments that have been the focus of this work. For instance, EW scale PETs can be used to constrain hidden sectors at collider experiments, *e.g.* at the LHC, similarly to how SMEFT is being used to constrain the coupling to heavy new sectors, and to make predictions for flavour physics experiments, such as LHCb [292], or for beam dump experiments, such as SHiP, which produce an enormous amount of heavy  $D$ - and  $B$ -mesons. In order to apply the PET approach to heavy meson physics and a wide range of other experimental setups, it will be useful to construct PETs that extend a large class of EFTs in the SM, such as HEFT, HQET, NRQCD, and SCET.

In the long term, this program of building and linking various PETs at many different energy scales will make it possible to perform a truly global parameter scan, which could be used to constrain light hidden sectors in a very general way, as it will combine different observations at the EW scale, from flavour physics experiments, and from intensity experiments. This goal will require the ability to compute a large variety of amplitudes for a wide range of distinct hidden-sector induced transitions. In order to simplify this task, it is thus sensible to implement the various PETs into tools that automatise Feynman rules, such as FEYNRULES [293], and to produce model files for software packages, such as MADGRAPH [294], MADDM [295, 296] and MADDUMP [297], which are able to compute the matrix elements and the necessary theoretical predictions.

## Acknowledgement

We are very grateful to Marco Drewes and Jean-Marc Gérard for fruitful discussions and the feedback they have provided all along the preparation of this work. We thank Eduardo Cortina Gil, Anthony Francis, Martin Hoferichter, Ken Mimasu, Urs Wenger and Uwe-Jens Wiese for useful discussions. Chiara Arina has been supported by the Innoviris ATTRACT 2018 104 BECAP 2 agreement. Jan Hajer has been supported by the Fonds Spéciaux de Recherche (FSR) incoming postdoc fellowship of Université catholique de Louvain (UCLouvain) and is now supported by the Schweizerischer Nationalfonds zur Förderung der wissenschaftlichen Forschung (SNF) under the project № 200020/175502. Philipp Klose has been partially



supported by the UCLouvain FSR funding scheme and the Innoviris ATTRACT 2018 104 BECAP 2 agreement, and is now supported by the SNF under grant № 200020B-188712.

## A Construction of portal effective theories

In this appendix we describe the techniques we use to construct EW and strong scale PETs that extend an EFT of the SM by coupling the SM DOFs to a hidden messenger that is lighter than the characteristic energy scale of the relevant EFT. We summarise the NDA power counting scheme, and give a number of well-known reduction techniques used to obtain a minimal basis of independent portal operators for each PET.

### A.1 Naive dimensional analysis

After integrating out the heavy SM DOFs, the strong scale PETs may contain portal operators with dimension larger than five. The higher dimensional operators are suppressed by powers of  $\epsilon_{\text{SM}} \equiv \partial^2/\Lambda_{\text{SM}}^2$ . In addition, operators that receive contributions from tree-level diagrams at the EW scale theory will be suppressed by loop factors of  $(4\pi)^{-1}$ . These loop factors can be integrated into the power counting using NDA [175–178]. The NDA counting scheme assumes that the EFT Lagrangian can be written as [176]

$$\mathcal{L} = \mathcal{L}^{d \leq 4} + \sum_i c_i O_i, \quad (\text{A.1})$$

where the  $c_i$  are Wilson coefficients and the  $O_i$  denote effective operators of dimension  $d_i > 4$ . The renormalisable Lagrangian  $\mathcal{L}^{d \leq 4}$  contains gauge interactions with couplings  $g_i$ , Yukawa interactions with couplings  $y_i$ ,  $\phi^3$  interactions with couplings  $\kappa_i$ , and  $\phi^4$  interactions with couplings  $\lambda_i$ . Assuming that the kinetic part of the Lagrangian is canonically normalised, NDA stipulates that the Wilson coefficients  $c_i$  are expected to be of order one, or smaller, if the  $O_i$  are normalised as

$$O_i \propto \frac{\Lambda^4}{(4\pi)^2} \left(\frac{g}{4\pi}\right)^{n_g} \left(\frac{y}{4\pi}\right)^{n_y} \left(\frac{\kappa}{4\pi\Lambda}\right)^{n_\kappa} \left(\frac{\lambda}{(4\pi)^2}\right)^{n_\lambda} \left(\frac{p^2}{\Lambda^2}\right)^{n_p} \left(\frac{4\pi\phi}{\Lambda}\right)^{n_\phi} \left(\frac{(4\pi)^2\psi\psi}{\Lambda^3}\right)^{2n_\psi}, \quad (\text{A.2})$$

where  $\Lambda$  is a high-energy scale associated with a small momentum expansion in powers of  $\epsilon \propto \sqrt{s}/\Lambda$ ,  $\phi$  and  $\psi$  denote bosonic and fermionic fields present in the effective theory, and  $p^2$  stands for any light mass scale (*i.e.* it includes both derivatives  $\partial \propto p$  and light masses  $m \propto p$ ).

The NDA power counting is self-consistent in the sense that an arbitrary diagram with insertions of higher dimensional operators normalised according to (A.2) is renormalised by operators with the same  $4\pi$  normalization. That is, the Wilson coefficients mix as [176]

$$\delta c_i \propto \prod_j c_j, \quad (\text{A.3})$$

which implies that the Wilson coefficients should satisfy  $c_i \lesssim 1$ , even if the underlying UV theory is strongly coupled [178]. If the UV theory is weakly coupled, the Wilson coefficients may be much smaller than one,  $c_i \ll 1$ , so that the  $4\pi$  power counting of NDA can be broken by

strongly hierarchical values of the Wilson coefficients, which could potentially satisfy  $4\pi c_i \ll c_j$  for certain  $i \neq j$ .

When using the NDA counting scheme to discriminate between portal operators at the strong scale, we specifically count  $(4\pi)^{-1}$  suppression factors associated with loops in the EW scale diagrams that generate each strong scale operator. Since the renormalisable  $d = 3, 4$  operators in the strong scale theory are generated by tree-level diagrams at zeroth order in  $\epsilon_{\text{EW}}$ , their normalization should not contain any explicit factors of  $(4\pi)$ . This requirement implies that the small portal coupling  $\epsilon_{\text{UV}}$  has to be associated with a factor  $(4\pi)^{-1}$ , so that *e.g.* an operator  $\epsilon_{\text{UV}} \bar{q} q s_i$  scales as  $(4\pi)^0$  rather than  $(4\pi)^1$ . This is completely analogous to the  $(4\pi)^{-1}$  suppression that has to accompany each SM Yukawa coupling. In view of our choice gauge field normalization, which ensures that the covariant derivatives  $D_\mu = \partial_\mu - i A_\mu$  are independent of the gauge couplings, the SM photon field strength tensor needs also to be associated with a factor of  $(4\pi)^{-1}$ . In principle, this reasoning also applies to gluon field strength tensors, but the corresponding factor of  $(4\pi)^{-1}$  does not result in any relative suppression, since  $g_s/4\pi$  is not a small parameter in the non-perturbative regime of QCD. Therefore, we do not keep track of the factors of  $4\pi$  associated with the gluon field strength tensor. Summarising, we normalise each portal operator at the strong scale as follows,

$$O_i \propto \left( \frac{\Lambda_{\text{SM}}^2}{4\pi} \right)^2 \left( \frac{e}{4\pi} \right)^{n_e} \left( \frac{p^2}{\Lambda_{\text{SM}}^2} \right)^{n_p} \left( \frac{F^{\mu\nu}}{\Lambda_{\text{SM}}^2} \right)^{n_F} \left( \frac{4\pi \psi_{\text{SM}}}{\Lambda_{\text{SM}}^{3/2}} \right)^{n_\psi} \\ \times \left( \frac{1}{4\pi} \right)^{\vartheta(n_s + n_v + n_\xi/2)} \frac{\epsilon_{\text{UV}}}{4\pi} \left( \frac{4\pi s_i}{\Lambda_{\text{SM}}} \right)^{n_s} \left( \frac{4\pi v_i^\mu}{\Lambda_{\text{SM}}} \right)^{n_v} \left( \frac{4\pi \xi_a}{\Lambda_{\text{SM}}^{3/2}} \right)^{n_\xi}, \quad (\text{A.4})$$

where  $\psi_{\text{SM}}$  stands for SM fermions, and  $p \sim D_\mu, m$  now denotes either a covariant derivative or a light mass scale. The function

$$\vartheta(x) = \begin{cases} 1 & x > 1 \\ 0 & x \leq 1 \end{cases} \quad (\text{A.5})$$

measures how many hidden fields the operator contains. If it contains more than one hidden boson or more than two hidden fermions, the operator has to have been generated by EW scale diagrams that contain at least one hidden sector interaction, and according to the general NDA counting scheme this interactions has to be associated with suppression by at least one factor  $(4\pi)^{-1}$ .

## A.2 Reduction techniques

In general, a naive listing of all available operators at each order in the power counting contains a number of redundant operators that can be expressed as a linear combination of other operators at the same or higher order in the power counting. In the following, we list a number of standard reduction techniques that we use to identify minimal bases of portal operators without redundancies: Further details on these reduction techniques can be found in [29, 298–300] and references therein.

**Algebraic identities** directly associate operators with each other. In our analysis, we use

- **Bianchi identities** that relate the covariant derivatives of field strength tensors  $V^{\mu\nu}$ . One has

$$D^\mu V^{\nu\rho} + D^\nu V^{\rho\mu} + D^\rho V^{\mu\nu} = 0 . \quad (\text{A.6})$$

In particular, these identities imply that

$$\sigma_{\mu\nu}(D^\rho V^{\mu\nu} + 2D^\mu V^{\nu\rho}) = 0 , \quad D_\mu \tilde{V}^{\mu\nu} = 0 . \quad (\text{A.7})$$

- **Fierz completeness relations** that relate products of fermion bilinears [298, 299]. These are often given in terms of four component fermions, see for instance [299]. In the two-component notation of [129], the Fierz identities we use take the form

$$\psi_a \psi_b \psi_c \psi_d = \frac{1}{2} \psi_a \psi_d \psi_c \psi_b + \frac{1}{4} \psi_a \bar{\sigma}_{\mu\nu} \psi_d \psi_c \bar{\sigma}^{\mu\nu} \psi_b , \quad (\text{A.8a})$$

$$\psi_a^\dagger \psi_b^\dagger \psi_c^\dagger \psi_d^\dagger = \frac{1}{2} \psi_a^\dagger \psi_d^\dagger \psi_c^\dagger \psi_b^\dagger + \frac{1}{4} \psi_a^\dagger \sigma_{\mu\nu} \psi_d^\dagger \psi_c^\dagger \sigma^{\mu\nu} \psi_b^\dagger , \quad (\text{A.8b})$$

and

$$\psi_a^\dagger \bar{\sigma}_\mu \psi_b \psi_c \sigma^\mu \psi_d^\dagger = 2 \psi_a^\dagger \psi_d^\dagger \psi_c \psi_b , \quad (\text{A.9a})$$

$$\psi_a^\dagger \bar{\sigma}_\mu \psi_b \psi_c^\dagger \bar{\sigma}^\mu \psi_d = - \psi_a^\dagger \bar{\sigma}_\mu \psi_d \psi_c^\dagger \bar{\sigma}^\mu \psi_b , \quad (\text{A.9b})$$

$$\psi_a \sigma_\mu \psi_b^\dagger \psi_c \sigma^\mu \psi_d^\dagger = - \psi_a \sigma_\mu \psi_d^\dagger \psi_c \sigma^\mu \psi_b^\dagger , \quad (\text{A.9c})$$

as well as

$$\psi_a \bar{\sigma}_{\mu\nu} \psi_d \psi_c^\dagger \sigma^{\mu\nu} \psi_b^\dagger = 0 , \quad (\text{A.10})$$

and finally

$$\psi_a \psi_b \psi_c^\dagger \bar{\sigma}^\mu \psi_d = \frac{1}{2} \psi_a \psi_d \psi_c^\dagger \bar{\sigma}^\mu \psi_b - i \frac{3}{8} \psi_a \bar{\sigma}^{\mu\nu} \psi_d \psi_c^\dagger \bar{\sigma}_\nu \psi_b , \quad (\text{A.11a})$$

$$\psi_a^\dagger \psi_b^\dagger \psi_c^\dagger \bar{\sigma}^\mu \psi_d = \frac{1}{2} \psi_a^\dagger \bar{\sigma}^\mu \psi_d \psi_c^\dagger \psi_b^\dagger - i \frac{3}{8} \psi_a^\dagger \bar{\sigma}_\nu \psi_d \psi_c^\dagger \sigma^{\mu\nu} \psi_b^\dagger . \quad (\text{A.11b})$$

**Partial integration** can be used to rearrange (covariant) derivatives within the operators, assuming that the fields vanish at infinity.

**Field redefinitions** of the shape

$$\phi(x) \rightarrow \phi(x) - \epsilon^n f[\phi](x) , \quad (\text{A.12})$$

where  $\epsilon$  is a small parameter of the theory and  $f[\phi](x)$  is a polynomial that depends only on powers of  $\phi$  and its derivatives evaluated at  $x$ , can be used to eliminate operators proportional to the zeroth order EOM for the effective DOFs that appear at order  $\epsilon^n$  [29, 178, 301, 302]. The repetition of this procedure at each order in  $\epsilon$  makes it possible to eliminate operators proportional to the zeroth order EOM at all orders in  $\epsilon$ .

### A.3 Standard Model equations of motions

In this section, we collect the EOMs for the SM fields we use throughout this work.

#### A.3.1 EOMs at the electroweak scale

At the EW scale, the SM EOMs for fermions are

$$i \not{D} \ell = y_e e H , \quad i \not{D} e = y_e^\dagger H^\dagger \ell \quad (\text{A.13a})$$

$$i \not{D} q = y_u u \tilde{H} + y_d d H , \quad i \not{D} u = y_u^\dagger \tilde{H}^\dagger q , \quad i \not{D} d = y_d^\dagger H^\dagger q , \quad (\text{A.13b})$$

where the  $y_i$  ( $i = e, u, d$ ) denote the SM Yukawa coupling matrices. The EOMs for SM bosons are given by

$$D^2 H = (m^2 - \lambda |H|^2) H - e^\dagger y_e^\dagger \ell - d^\dagger y_d^\dagger q - (\epsilon q)^\dagger y_u u , \quad (\text{A.14a})$$

$$\partial_\mu B^{\mu\nu} = \sum_{\text{all } f} y_f \bar{\psi}_f \gamma_\mu \psi_f + i y_h H^\dagger \vec{D}_\mu H , \quad (\text{A.14b})$$

$$(D_\mu W^{\mu\nu})^I = \phi^\dagger i \vec{D}^{\nu I} \phi + l_b^\dagger \vec{\sigma}^\nu T^I l_b + q_b^\dagger \vec{\sigma}^\nu T^I q_b , \quad (\text{A.14c})$$

$$2(D_\mu G^{\mu\nu})^x = u_a^\dagger \vec{\sigma}^\nu \lambda^x u_a + \bar{u}_a^\dagger \vec{\sigma}^\nu \lambda^x \bar{u}_a + \bar{d}_a^\dagger \vec{\sigma}^\nu \lambda^x \bar{d}_a + d_a^\dagger \vec{\sigma}^\nu \lambda^x d_a , \quad (\text{A.14d})$$

where  $\epsilon$  is the  $SU(2)_L$  totally anti-symmetric tensor, the index  $x$  denotes objects that transform as members of the adjoint representation of  $SU(3)_C$ , and the  $\lambda^x$  are GM matrices acting on triplets in *colour*-space.

#### A.3.2 EOMs at the strong scale

At the strong scale, the EOMs for SM fermions are given by

$$i \not{D} e_i = m_{ei} \bar{e}_i^\dagger , \quad i \not{D} d_i = m_{di} \bar{d}_i^\dagger , \quad i \not{D} u_i = m_{di} \bar{u}_i^\dagger , \quad i \not{D} \nu_i = 0 , \quad (\text{A.15a})$$

$$i \not{D} \bar{e}_i = m_{ei} e_i^\dagger , \quad i \not{D} \bar{d}_i = m_{di} d_i^\dagger , \quad i \not{D} \bar{u}_i = m_{di} u_i^\dagger . \quad (\text{A.15b})$$

At the same scale, the EOMs for SM bosons are

$$2(D_\mu G^{\mu\nu})^x = u_a^\dagger \vec{\sigma}^\nu \lambda^x u_a + \bar{u}_a^\dagger \vec{\sigma}^\nu \lambda^x \bar{u}_a + \bar{d}_a^\dagger \vec{\sigma}^\nu \lambda^x \bar{d}_a + d_a^\dagger \vec{\sigma}^\nu \lambda^x d_a , \quad (\text{A.16a})$$

$$\partial_\mu F^{\mu\nu} = \sum_{\text{light } f} q_f \psi_f^\dagger \vec{\sigma}^\nu \psi_f . \quad (\text{A.16b})$$

where  $q_f$  is the EM charge of the fermion in question.

For the PETs we construct, it is possible to combine the strong scale EOMs with the other reduction techniques to eliminate all operators with at least one covariant derivative acting on a SM fermion. Considering a generic Weyl fermion  $\psi_a$  with mass  $m_a$  and gauge charges  $q_a$ , and a field strength tensor  $V^{\mu\nu}$ , we get

$$D_\rho D^\rho \psi_a = \left( \not{D} - q_a \frac{1}{2} \vec{\sigma}_{\mu\nu} V^{\mu\nu} \right) \psi_a \xrightarrow{\text{EOM}} - \left( m_a^2 + q_a \frac{1}{2} \vec{\sigma}_{\mu\nu} V^{\mu\nu} \right) \psi_a , \quad (\text{A.17})$$

and further

$$\begin{aligned}
\mathcal{O}^\mu(\psi_a \overleftrightarrow{D}_\mu \psi_b) &= \frac{1}{2} \mathcal{O}^\mu \left( \psi_a \left[ \overleftrightarrow{D} \overleftrightarrow{\sigma}^\mu + \sigma^\mu \overleftrightarrow{D} \right] \psi_b \right) \\
&\xrightarrow{\text{PI}} -\mathcal{O}^\mu \left( \psi_a \left[ \overleftrightarrow{D} \overleftrightarrow{\sigma}^\mu - \sigma^\mu \overleftrightarrow{D} \right] \psi_b \right) + (i D^\nu \mathcal{O}^\mu)(\psi_a \overleftrightarrow{\sigma}_{\nu\mu} \psi_b) \\
&\xrightarrow{\text{EOM}} -i(m_b + m_a) \mathcal{O}^\mu \left( \overline{\psi}_a^\dagger \overleftrightarrow{\sigma}^\mu \psi_b + \psi_a \sigma^\mu \overline{\psi}_b^\dagger \right) + (i D^\nu \mathcal{O}^\mu)(\psi_a \overleftrightarrow{\sigma}_{\nu\mu} \psi_b) ,
\end{aligned} \tag{A.18}$$

and

$$\begin{aligned}
\mathcal{O}_\mu(\psi_a \overleftrightarrow{\sigma}^{\mu\nu} \overleftrightarrow{D}_\nu \psi_b) &= i \mathcal{O}_\mu \left( \psi_a \left[ \sigma^\mu \overleftrightarrow{D} + \overleftrightarrow{D} \overleftrightarrow{\sigma}^\mu - D^\mu - \overleftrightarrow{D}^\mu \right] \psi_b \right) \\
&\xrightarrow{\text{EOM}} (m_b + m_a) \mathcal{O}_\mu \left( \overline{\psi}_a^\dagger \overleftrightarrow{\sigma}^\mu \psi_b + \psi_a \sigma^\mu \overline{\psi}_b^\dagger \right) + (i D^\mu \mathcal{O}_\mu)(\psi_a \psi_b) ,
\end{aligned} \tag{A.19}$$

and

$$\begin{aligned}
\mathcal{O}(D_\rho \psi_a D^\rho \psi_b) &= \frac{1}{2} \mathcal{O}(D_\rho \psi_a) D^\rho \psi_b + \frac{1}{2} \mathcal{O}(D_\rho \psi_a) D^\rho \psi_b \\
&\xrightarrow{\text{PI}} -\frac{1}{2} \mathcal{O}(D^2 \psi_a) \psi_b - \frac{1}{2} \mathcal{O} \psi_a (D^2 \psi_b) - \frac{1}{2} (D_\rho \mathcal{O}) \partial_\rho (\psi_a \psi_b) \\
&\xrightarrow{\text{EOM}} \frac{1}{2} (D^2 \mathcal{O}) \psi_a \psi_b + \frac{1}{2} (m_a^2 + m_b^2) \mathcal{O} \psi_a \psi_b ,
\end{aligned} \tag{A.20}$$

and

$$\begin{aligned}
\mathcal{O}(D_\mu \psi_a \overleftrightarrow{\sigma}^{\mu\nu} D_\nu \psi_b) &= \frac{i}{2} \mathcal{O} \left( \psi_a \left[ \overleftrightarrow{D} \overleftrightarrow{\sigma}^\nu - \overleftrightarrow{D}_\mu \gamma^\nu \gamma^\mu \overleftrightarrow{D}_\nu \right] \psi_b \right) = i \mathcal{O} \left( \psi_a \left[ \overleftrightarrow{D} \overleftrightarrow{\sigma}^\nu - \overleftrightarrow{D}^\rho \overleftrightarrow{D}_\rho \right] \psi_b \right) \\
&\xrightarrow{\text{EOM}} i m_a m_b \mathcal{O} \overline{\psi}_a^\dagger \overline{\psi}_b^\dagger - i \mathcal{O}(D^\rho \psi_a D_\rho \psi_b) ,
\end{aligned} \tag{A.21}$$

as well as

$$\begin{aligned}
\mathcal{O}^{[\mu\nu]}(\psi_a^\dagger \overleftrightarrow{\sigma}_\nu \overleftrightarrow{D}_\mu \psi_b) &= \mathcal{O}^{[\mu\nu]} \frac{i}{2} \left( \psi_a^\dagger \left[ \sigma_{\mu\nu} \overleftrightarrow{D} - \overleftrightarrow{D} \overleftrightarrow{\sigma}_{\mu\nu} \right] \psi_b \right) \\
&\xrightarrow{\text{PI}} \mathcal{O}^{[\mu\nu]} i \left( \psi_a^\dagger \left[ \sigma_{\mu\nu} \overleftrightarrow{D} + \overleftrightarrow{D} \overleftrightarrow{\sigma}_{\mu\nu} \right] \psi_b \right) + D^\rho \mathcal{O}^{\mu\nu} \frac{i}{2} (\psi_a^\dagger [\overleftrightarrow{\sigma}_\rho \overleftrightarrow{\sigma}_{\mu\nu} + \sigma_{\mu\nu} \overleftrightarrow{\sigma}_\rho] \psi_b) \\
&\xrightarrow{\text{EOM}} \mathcal{O}^{[\mu\nu]} \left( m_b \psi_a^\dagger \sigma_{\mu\nu} \overline{\psi}_b^\dagger - m_a \overline{\psi}_a \overleftrightarrow{\sigma}_{\mu\nu} \psi_b \right) + \frac{i}{2} (\psi_a^\dagger \overleftrightarrow{\sigma}_\sigma \psi_b) D_\rho \tilde{\mathcal{O}}^{\rho\sigma} .
\end{aligned} \tag{A.22}$$

### A.3.3 Quark EOM including external currents

To compute the trace of the QCD Hilbert stress-energy tensor (2.65) in the presence of generic external currents, we include these currents into the quark EOMs. Therefore, they are

$$i \not{D} q^{\dagger b} = (\mathbf{M}^T \overline{q} + (\mathbf{T}_{\mu\nu}^T + \mathbf{\Gamma}^T G_{\mu\nu}) \overleftrightarrow{\sigma}^{\mu\nu} \overline{q} + \mathbf{L}_\mu^T \sigma^\mu q^\dagger)^b \tag{A.23a}$$

$$- \frac{|V|_{\text{sd}}^2}{v^2} \left( 2 \mathfrak{H}_{lac}^{bd} \sigma^\mu q^{\dagger a} q^{\dagger c} \overline{\sigma}_\mu q_d + \mathfrak{H}_{rac}^{bd} \sigma^\mu q^{\dagger a} \overline{q}^{\dagger c} \sigma_\mu \overline{q}_d^\dagger - \mathfrak{H}_{sac}^{db} \overline{q}^{\dagger c} q^{\dagger a} \overline{q}_d^\dagger \right) ,$$

$$i \not{D} \overline{q}_a^\dagger = (\mathbf{M} q - (\mathbf{T}_{\mu\nu} + \mathbf{\Gamma} G_{\mu\nu}) \sigma^{\mu\nu} q + \mathbf{R}_\mu \sigma^\mu \overline{q}^\dagger)_a \tag{A.23b}$$

$$+ \frac{|V|_{\text{sd}}^2}{v^2} \left( \mathfrak{H}_{rc\dot{a}}^{bd} \sigma^\mu \overline{q}_d^\dagger q^{\dagger c} \overline{\sigma}_\mu q_b + \mathfrak{H}_{sc\dot{a}}^{bd} q_d q^{\dagger c} \overline{q}_b^\dagger \right) .$$

## B Electroweak scale portal operators

In this appendix, we first collect the redundant EW scale portal operators for messengers with spin 0,  $1/2$ , and 1, and then present the portal operators for messengers with spin  $3/2$  and 2.

### B.1 Redundant portal operators with messenger field up to spin one

The operators listed in table 2 form a complete basis in the sense that it is impossible to further reduce the number of independent portal operators by using the standard reduction techniques discussed in appendix A.2. In particular, we have used the SM EOM to minimise the number of derivatives appearing within each operator, but for certain applications, it may be more convenient to work with alternative bases of portal operators. To facilitate this, we list below the redundant EW portal operators that can be constructed in PETs based on SMEFT, and show which techniques were used to trade them.

The redundant **spin 0** portal operators are

$$\partial_\mu \partial_\nu s_i B^{\mu\nu} \xleftrightarrow{\text{PI}} \partial_\mu s_i \partial_\nu B^{\mu\nu} \xleftrightarrow{\text{PI}} s_i \partial_\mu \partial_\nu B^{\mu\nu} = 0 , \quad (\text{B.1})$$

as well as

$$\partial^\mu s_i (H^\dagger \overleftrightarrow{D}_\mu H) \xleftrightarrow{\text{PI}} s_i (H^\dagger D^2 H - \text{h.c.}) , \quad (\text{B.2a})$$

$$\partial^2 s_i |H|^2 \xleftrightarrow{\text{PI}} \partial_\mu s_i \partial^\mu |H|^2 \xleftrightarrow{\text{PI}} s_i (H^\dagger D^2 H + \text{h.c.}) + \text{non-redundant} \quad (\text{B.2b})$$

and

$$\partial_\mu s_i q_a^\dagger \overleftrightarrow{\sigma}^\mu q_b \xleftrightarrow{\text{PI}} s_i q_a^\dagger \not{D} q_b , \quad \partial_\mu s_i u_a^\dagger \sigma^\mu u_b \xleftrightarrow{\text{PI}} s_i u_a^\dagger \not{D} u_b , \quad \partial_\mu s_i d_a^\dagger \sigma^\mu d_b \xleftrightarrow{\text{PI}} s_i d_a^\dagger \not{D} d_b , \quad (\text{B.2c})$$

$$\partial_\mu s_i \ell_a^\dagger \overleftrightarrow{\sigma}^\mu \ell_b \xleftrightarrow{\text{PI}} s_i \ell_a^\dagger \not{D} \ell_b , \quad \partial_\mu s_i e_a^\dagger \sigma^\mu e_b \xleftrightarrow{\text{PI}} s_i e_a^\dagger \not{D} e_b . \quad (\text{B.2d})$$

Notice that the remaining operators  $(H^\dagger D^2 H \pm \text{h.c.})$  and  $\psi_a^\dagger \not{D} \psi_b$  on the right-hand side of these expressions can be replaced with Yukawa type portal operators using the SM EOMs.

The only redundant **spin  $1/2$**  portal operators are

$$D_\mu \xi_a^\dagger \overleftrightarrow{\sigma}^\mu \ell_a \tilde{H}^\dagger + \text{h.c.} \xleftrightarrow{\text{PI}} \xi_a^\dagger \not{D} \ell_a \tilde{H}^\dagger + \text{non-redundant} , \quad (\text{B.3})$$

where the remaining operator on the right-hand side can also be replaced with Yukawa type portal operators using the SM EOMs.

Finally, the redundant **spin 1** portal operators are

$$\partial_\nu v_\mu \tilde{B}^{\mu\nu} \xleftrightarrow{\text{PI}} v_\mu \partial_\nu \tilde{B}^{\mu\nu} = 0 , \quad \partial_\nu v_\mu B^{\mu\nu} \xleftrightarrow{\text{PI}} v_\mu \partial_\nu B^{\mu\nu} , \quad (\text{B.4})$$

where the only remaining operator  $v_\mu \partial_\nu B^{\mu\nu}$  can also be replaced with Yukawa type portal operators using the SM EOMs.

Finally, we already argued in section 3.2 that the number of independent portal operators given in table 2 can be further reduced by using the EOMs proper to the hidden sector. However, these EOMs depend strongly on the internal structure of the latter, the modelling of which is beyond the scope of this paper.

	$d$	Higgs	Yukawa + h.c.	Fermions	Gauge bosons
	4		$\xi_{a\mu}^\dagger \bar{\sigma}^\mu \ell_b \tilde{H}^\dagger$		
$\xi_\mu^a$ + h.c.	5	$\xi_{a\mu} \xi_b^\mu  H ^2$ $\xi_{a\mu} \sigma^{\mu\nu} \xi_{b\nu}  H ^2$	$(\partial^\mu \xi_{a\mu}) \ell_b \tilde{H}^\dagger$ $(\partial_\nu \xi_{a\mu}) \bar{\sigma}^{\mu\nu} \ell_b \tilde{H}^\dagger$ $\xi_{a\mu} \ell_b D^\mu \tilde{H}^\dagger$ $\xi_{a\mu} \bar{\sigma}^{\mu\nu} \ell_b D_\nu \tilde{H}^\dagger$		$\xi_{a\mu} \xi_{b\nu} B^{\mu\nu}$ $\xi_{a\rho} \sigma^{\mu\nu} \xi_b^\rho B_{\mu\nu}$ $\xi_{a\mu} \sigma^{\mu\rho} \xi_b^\nu B_{\nu\rho}$ $\xi_{a\mu} \sigma^{\mu\rho} \xi_b^\nu \tilde{B}_{\nu\rho}$ $\xi_{a\alpha} \sigma_\mu^\rho \xi_{b\beta} B_{\nu\rho} \epsilon^{\alpha\beta\mu\nu}$
	3				$t_{\mu\nu} B^{\mu\nu}$ $\tilde{t}_{\mu\nu} B^{\mu\nu}$
$t_{\mu\nu}$	5	$t^{\mu\nu} D_\mu H^\dagger D_\nu H$ $\tilde{t}^{\mu\nu} D_\mu H^\dagger D_\nu H$ $(\partial_\mu t^{\mu\nu})(H^\dagger \vec{D}_\nu H)$	$t^{\mu\nu} q_a \sigma_{\mu\nu} u_b \tilde{H}$ $t^{\mu\nu} q_a \sigma_{\mu\nu} d_b H$ $t^{\mu\nu} \ell_a \sigma_{\mu\nu} e_b H$	$(\partial^\mu t_{\mu\nu}) q_a^\dagger \bar{\sigma}^\nu q_b$ $(\partial^\mu t_{\mu\nu}) u_a^\dagger \sigma^\nu u_b$ $(\partial^\mu t_{\mu\nu}) d_a^\dagger \sigma^\nu d_b$ $(\partial^\mu t_{\mu\nu}) \ell_a^\dagger \bar{\sigma}^\nu \ell_b$ $(\partial^\mu t_{\mu\nu}) e_a^\dagger \sigma^\nu e_b$ $(\partial^\mu \tilde{t}_{\mu\nu}) q_a^\dagger \bar{\sigma}^\nu q_b$ $(\partial^\mu \tilde{t}_{\mu\nu}) u_a^\dagger \sigma^\nu u_b$ $(\partial^\mu \tilde{t}_{\mu\nu}) d_a^\dagger \sigma^\nu d_b$ $(\partial^\mu \tilde{t}_{\mu\nu}) \ell_a^\dagger \bar{\sigma}^\nu \ell_b$ $(\partial^\mu \tilde{t}_{\mu\nu}) e_a^\dagger \sigma^\nu e_b$	$t_{\mu\nu} G^{\mu\rho} G_\rho^\nu$ $\tilde{t}_{\mu\nu} G^{\mu\rho} G_\rho^\nu$ $t_{\mu\nu} \tilde{G}^{\mu\rho} \tilde{G}_\rho^\nu$ $t_{\mu\nu} G^{\mu\rho} \tilde{G}_\rho^\nu$ $\tilde{t}_{\mu\nu} W^{\mu\rho} W_\rho^\nu$ $t_{\mu\nu} \tilde{W}^{\mu\rho} \tilde{W}_\rho^\nu$ $\tilde{t}_{\mu\nu} W^{\mu\rho} \tilde{W}_\rho^\nu$ $\tilde{t}_{\mu\nu} B^{\mu\rho} B_\rho^\nu$ $t_{\mu\nu} \tilde{B}^{\mu\rho} \tilde{B}_\rho^\nu$ $t_{\mu\nu} B^{\mu\rho} \tilde{B}_\rho^\nu$ $t_{\mu\nu} B^{\mu\nu}  H ^2$ $\tilde{t}_{\mu\nu} B^{\mu\nu}  H ^2$

Table 12: List of all portal operators up to dimension five that couple SMEFT to hidden spin  $3/2$  fermionic fields  $\xi_a^\mu$  and tensor fields  $t^{\mu\nu}$ . The first column specifies the type of portal, the second column denotes the dimension  $d$  of the portal operator and the remaining columns label the SM sectors to which the hidden field couples. In the case of the vector-fermion PETs, each operator is supplemented by its Hermitian conjugate. The bold operators couple to the strong sector of the SM.

## B.2 Rarita-Schwinger and Fierz-Pauli fields

Here we briefly discuss the case in which the SM couples to hidden  $3/2$  Weyl fields  $\xi_i^\mu(x)$  with  $i = 1, 2$  or to a spin 2 field  $t^{\mu\nu}$ . Without loss of generality, we take  $t \equiv t_\mu^\mu = 0$ , since the scalar DOF  $t$  couples to the SM via the operators collected in table 2. Table 12 collects the complete list of portal operators up to dimension five for both spin  $3/2$  fermion and tensorial messenger fields.

A standard example of hidden spin  $3/2$  fields coupling to the SM model are the gravitinos appearing in supergravity models. Although their precise mass depends on the details of the model, they can easily be much lighter than the other supersymmetric particles [303, 304], leading to interesting phenomenology [305–307], and placing it into the regime of PETs.

Broadly speaking, there are two separate energy ranges in which spin 2 messengers constitute viable extensions of the SM. On the one hand, in extra-dimension models, see *e.g.* [308–311], besides the massless zero mode, higher order graviton excitations are interesting portals for NP, and their allowed mass range lies in the TeV scale [312–314]. They can be described by portal SMEFTs at high-energy colliders [315, 316] or for models of TeV scale DM [317]. On

the other hand, bimetric theories of gravity [318, 319], called bigravity, feature an new massive interacting spin 2 state. This new boson can be a DM candidate. However, either its mass range is beyond the sensitivity of intensity experiments, lying below the eV range, see [320], or it lies in the MeV range but its interaction strength with ordinary matter is so negligible to make a detection hopeless, see [312, 321, 322]. Finally, models with hidden spin 2 glueballs have been proposed [323, 324], but in this case the prospects for detection in the mass range of interest would also be low. However, we do not preclude the possibility of a viable theory involving those fields which can be detected by light meson factories.

## C Portal operators at the strong scale

In this appendix, we give a complete basis of both strangeness conserving and violating portal operators at the strong scale that are suppressed by at most a factor of  $\epsilon_{UV}/v^3$  while respecting the general restrictions outlined in section 3.3. In particular, we assume that the strong scale PETs are a low energy limit of a corresponding portal SMEFT, and also include operators that are sub-leading in the  $(4\pi)$  counting of NDA. The relevant leading strangeness violating QCD operators are listed in table 4, and the sub-leading strangeness violating operators are given in table 5. For spin 0 and  $1/2$  mediators, the relevant portal operators may be of dimension  $d \leq 7$ , while for spin 1 mediators, the portal operators are of dimension  $d \leq 6$ . This basis is constructed using the reduction techniques summarised in appendix A, see also [300] for additional details.

We follow the two component notation in [129] for fermionic fields, and distinguish between portal operators with either zero, two or four fermionic fields. To list the operators, it is convenient to define stand-ins for various SM  $SU(3)_c$  colour gauge singlets. For SM fermions, we define the following neutral pairs

$$(qq)_0 \in \{\bar{u}_a u_b, \bar{d}_a d_b\}, \quad (\psi\psi)'_0 \in \{(qq)_0, \bar{e}_a e_b\}, \quad (\psi\psi)_0 \in \{(\psi\psi)'_0, \nu_a \nu_b\}, \quad (\text{C.1a})$$

$$(q^\dagger q^\dagger)_0 \in \{\bar{u}_a^\dagger u_b^\dagger, \bar{d}_a^\dagger d_b^\dagger\}, \quad (\psi^\dagger \psi)'_0 \in \{u_a^\dagger u_b, d_a^\dagger d_b, e_a^\dagger e_b\}, \quad (\psi^\dagger \psi)_0 \in \{(\psi^\dagger \psi)'_0, \nu_a^\dagger \nu_b\}, \quad (\text{C.1b})$$

$$\bar{u}_a^\dagger \bar{u}_b, \bar{d}_a^\dagger \bar{d}_b, \bar{e}_a^\dagger \bar{e}_b\},$$

and the following charged pairs

$$(qq)_+ \in \{\bar{u}_a d_b, \bar{d}_a u_b\}, \quad (\psi^\dagger \psi)_+ \in \{d_a^\dagger u_b, \bar{d}_a^\dagger \bar{u}_b, e_a^\dagger \nu_b\}, \quad (\text{C.2a})$$

$$(q^\dagger q^\dagger)_- \in \{\bar{u}_a^\dagger d_b^\dagger, \bar{d}_a^\dagger u_b^\dagger\}, \quad (\psi^\dagger \psi)_- \in \{u_a^\dagger d_b, \bar{u}_a^\dagger \bar{d}_b, \nu_a^\dagger e_b\}, \quad (\text{C.2b})$$

where the indices run over all available flavours at the strong scale ( $a, b = u, d, s$  for quarks,  $a, b = e, \mu$  for charged leptons and  $a, b = \nu_e, \nu_\mu, \nu_\tau$  for neutrinos) and the subscript specifies the total electric charge of each fermionic pair. For the gauge bosons, we indicate their field strength tensors with

$$V^{\mu\nu} \in \{F^{\mu\nu}, G^{\mu\nu}\}. \quad (\text{C.3})$$

For operators with more than one occurrence of  $V^{\mu\nu}$ , we adopt the convention that all of these instances denote the same field strength tensor within each operator. For instance, the object  $V^{\mu\nu} V_{\mu\nu}$  may denote  $F^{\mu\nu} F_{\mu\nu}$  or  $G^{\mu\nu} G_{\mu\nu}$  but *not*  $F^{\mu\nu} G_{\mu\nu}$ . The Fierz completeness



relations (A.8), (A.9), and (A.11) reduce the number of independent four-fermion operators. We can then restrict ourselves to products of the colour singlets (C.1) and (C.2) without loss of generality. For operators without quarks, we can further restrict ourselves to products involving only the neutral singlets (C.1).

### C.1 Scalar portal

At order  $\epsilon_{UV}/v^3$ , the scalar portal operators can be of dimension seven or less. We list all portal operators that include at most two hidden real scalar fields ( $s_i$  with  $i = 1, 2$ ).

**Zero-fermion operators** can contain either one, two, or three field strength tensors. The operators with one field strength tensor are

$$s_i \partial_\nu s_j \partial_\mu s_k F^{\mu\nu}, \quad s_i \partial_\nu s_j \partial_\mu s_k \tilde{F}^{\mu\nu}. \quad (\text{C.4})$$

The operators with two field strength tensors are

$$s_i \langle V_{\mu\nu} V^{\mu\nu} \rangle_c, \quad s_i s_j \langle V_{\mu\nu} V^{\mu\nu} \rangle_c, \quad s_i s_j s_k \langle V_{\mu\nu} V^{\mu\nu} \rangle_c, \quad s_i \langle D_\rho V_{\mu\nu} D^\rho V^{\mu\nu} \rangle_c, \quad (\text{C.5a})$$

$$s_i \langle V_{\mu\nu} \tilde{V}^{\mu\nu} \rangle_c, \quad s_i s_j \langle V_{\mu\nu} \tilde{V}^{\mu\nu} \rangle_c, \quad s_i s_j s_k \langle V_{\mu\nu} \tilde{V}^{\mu\nu} \rangle_c, \quad s_i \langle D_\rho V_{\mu\nu} D^\rho \tilde{V}^{\mu\nu} \rangle_c. \quad (\text{C.5b})$$

The operators with three field strength tensors are

$$s_i \langle G_\mu^\nu G_\rho^\mu G_\nu^\rho \rangle_c, \quad s_i \langle \tilde{G}_\mu^\nu G_\rho^\mu G_\nu^\rho \rangle_c. \quad (\text{C.6})$$

**Two-fermion operators** can contain at most a single SM field strength tensor. The operators without field strength tensor may contain no more than two derivatives. The operators with zero derivatives are

$$s_i (\psi\psi)_0, \quad s_i s_j (\psi\psi)_0, \quad s_i s_j s_k (\psi\psi)_0, \quad s_i s_j s_k s_l (\psi\psi)_0. \quad (\text{C.7})$$

The operators with one derivative are

$$s_i \overleftrightarrow{\partial}_\mu s_j (\psi^\dagger \bar{\sigma}^\mu \psi)_0, \quad s_i s_j \overleftrightarrow{\partial}_\mu s_k (\psi^\dagger \bar{\sigma}^\mu \psi)_0. \quad (\text{C.8})$$

The operators with two derivatives are

$$\partial^2 s_i (\psi\psi)_0, \quad s_i \partial^2 s_j (\psi\psi)_0, \quad \partial_\mu s_i \partial^\mu s_j (\psi\psi)_0. \quad (\text{C.9})$$

The operators with a single SM field strength tensor and no derivatives are

$$s_i (\psi \bar{\sigma}_{\mu\nu} V^{\mu\nu} \psi)_0, \quad s_i s_j (\psi \bar{\sigma}_{\mu\nu} V^{\mu\nu} \psi)_0. \quad (\text{C.10})$$

The operators with a single SM field strength tensor and one derivative are

$$\partial_\nu s_i (\psi^\dagger \bar{\sigma}_\mu V^{\mu\nu} \psi)_0, \quad \partial_\nu s_i (\psi^\dagger \bar{\sigma}_\mu \tilde{V}^{\mu\nu} \psi)_0. \quad (\text{C.11a})$$

All the operators above are accompanied by their Hermitian conjugate.

**Four-fermion operators** cannot contain any derivatives or field strength tensors. They are

$$s_i(\psi^\dagger \bar{\sigma}^\mu \psi)_0(\psi^\dagger \bar{\sigma}_\mu \psi)_0, \quad s_i(\psi^\dagger \bar{\sigma}^\mu \psi)_+(\psi^\dagger \bar{\sigma}_\mu \psi)_-, \quad s_i(qq)_0(q^\dagger q^\dagger)_0, \quad s_i(qq)_+(q^\dagger q^\dagger)_-, \quad (\text{C.12})$$

plus Hermitian conjugates. The operator  $s_i(\psi^\dagger \bar{\sigma}^\mu \psi)_+(\psi^\dagger \bar{\sigma}_\mu \psi)_-$  contains only combinations with either two or four quarks. Using the Fierz identity (A.9), combinations with four leptons can be eliminated in favour of operators contained within  $s_i(\psi^\dagger \bar{\sigma}^\mu \psi)_0(\psi^\dagger \bar{\sigma}_\mu \psi)_0$ . At order  $\epsilon_{\text{EW}}$ , there are no operators  $s_i(\psi\psi)(\psi\psi)$  or  $s_i(\psi\bar{\sigma}^{\mu\nu}\psi)(\psi\bar{\sigma}_{\mu\nu}\psi)$ , since these involve at least two chirality flips for the SM fermions, suppressing them further by an additional factor of  $\sqrt{\epsilon_{\text{EW}}} \propto m_\psi/v$ .

## C.2 Fermionic portal

At order  $\epsilon_{\text{UV}}/v^3$ , a fermionic portal particle can couple to the SM via operators up to dimension  $d \leq 7$ . These operators can contain either two or four fermions. As before, it is sufficient to list portal operators with two hidden left-handed Weyl fermions  $\xi_i$  with  $i = 1, 2$  to account for both Majorana and Dirac fermionic fields in general.

**Two-fermion operators** can contain either zero, one, or two SM field strength tensors. The sole operator without field strength tensors is

$$\nu_a \xi_i. \quad (\text{C.13})$$

The operators with one field strength tensor are

$$\nu_a \bar{\sigma}_{\mu\nu} \xi_i F^{\mu\nu}, \quad \xi_i \bar{\sigma}_{\mu\nu} \xi_j F^{\mu\nu}, \quad \xi_i \bar{\sigma}_{\mu\nu} D^2 \xi_j F^{\mu\nu}, \quad \nu_a \bar{\sigma}_{\mu\nu} D^2 \xi_i F^{\mu\nu}, \quad (\text{C.14})$$

and

$$\nu_a^\dagger \bar{\sigma}_\mu D_\nu \xi_i F^{\mu\nu}, \quad \xi_i^\dagger \bar{\sigma}_\mu D_\nu \xi_j F^{\mu\nu}, \quad \xi_i \bar{\sigma}_{\mu\rho} D_\nu D^\mu \xi_j F^{\nu\rho}, \quad \nu_a \bar{\sigma}_{\mu\rho} D_\nu D^\mu \xi_i F^{\nu\rho}, \quad (\text{C.15a})$$

$$\nu_a^\dagger \bar{\sigma}_\mu D_\nu \xi_i \tilde{F}^{\mu\nu}, \quad \xi_i^\dagger \bar{\sigma}_\mu D_\nu \xi_j \tilde{F}^{\mu\nu}, \quad \xi_i \bar{\sigma}_{\mu\rho} D_\nu D^\mu \xi_j \tilde{F}^{\nu\rho}, \quad \nu_a \bar{\sigma}_{\mu\rho} D_\nu D^\mu \xi_i \tilde{F}^{\nu\rho}. \quad (\text{C.15b})$$

The operators with two field strength tensors are

$$\nu_a \xi_i \langle V^{\mu\nu} V_{\mu\nu} \rangle_c, \quad \xi_i \xi_j \langle V^{\mu\nu} V_{\mu\nu} \rangle_c, \quad \xi_i \sigma_{\mu\nu} \xi_j \langle V_\rho^\mu V^{\rho\nu} \rangle_c, \quad \nu_a \sigma_{\mu\nu} \xi_i \langle V_\rho^\mu V^{\rho\nu} \rangle_c, \quad (\text{C.16a})$$

$$\nu_a \xi_i \langle V^{\mu\nu} \tilde{V}_{\mu\nu} \rangle_c, \quad \xi_i \xi_j \langle V^{\mu\nu} \tilde{V}_{\mu\nu} \rangle_c, \quad \xi_i \sigma_{\mu\nu} \xi_j \langle V_\rho^\mu \tilde{V}^{\rho\nu} \rangle_c, \quad \nu_a \sigma_{\mu\nu} \xi_i \langle V_\rho^\mu \tilde{V}^{\rho\nu} \rangle_c, \quad (\text{C.16b})$$

All operators are accompanied by their Hermitian conjugate.

**Four-fermion operators** can contain at most one derivative. The operators without derivatives can be either of the scalar-scalar type or of the vector-vector type. The former are

$$\xi_i \xi_j \nu_a \xi, \quad \bar{d}_a u_b e_c \xi_i, \quad (\psi\psi)_0' \nu_a \xi_i, \quad (\psi\bar{\sigma}_{\mu\nu}\psi)_0' \nu_a \bar{\sigma}^{\mu\nu} \xi_i, \quad (\text{C.17a})$$

$$(\psi\psi)_0' \xi_i \xi_j, \quad (\psi\bar{\sigma}_{\mu\nu}\psi)_0' \xi_i \bar{\sigma}^{\mu\nu} \xi_j, \quad (\text{C.17b})$$

and

$$(\psi\psi)'_0 \nu_a^\dagger \xi_i^\dagger, \quad (\psi\psi)'_0 \xi_i^\dagger \xi_j^\dagger, \quad \bar{u}_a d_b e_a^\dagger \xi_i^\dagger, \quad (C.17c)$$

The vector-vector type operators are

$$\nu_a^\dagger \bar{\sigma}^\mu \xi_i \xi_j^\dagger \bar{\sigma}_\mu \xi_k, \quad d_a^\dagger \bar{\sigma}^\mu u_b \bar{e}_a^\dagger \bar{\sigma}_\mu \xi_i, \quad u_a^\dagger \bar{\sigma}^\mu d_b e_a^\dagger \bar{\sigma}_\mu \xi_i, \quad (\psi^\dagger \bar{\sigma}_\mu \psi)_0 \nu_a^\dagger \bar{\sigma}^\mu \xi_i, \quad (C.18a)$$

$$(\psi^\dagger \bar{\sigma}_\mu \psi)_0 \xi_i^\dagger \bar{\sigma}^\mu \xi_j. \quad (C.18b)$$

The operators with one derivative are

$$(\psi^\dagger \bar{\sigma}_\mu \psi)_0 \nu_a D^\mu \xi_i, \quad (\psi^\dagger \bar{\sigma}_\mu \psi)_0 \nu_a \bar{\sigma}^{\mu\nu} D_\nu \xi_i, \quad (\psi^\dagger \bar{\sigma}_\mu \psi)_0 \xi_i D^\mu \xi_j, \quad (\psi^\dagger \bar{\sigma}_\mu \psi)_0 \xi_i \bar{\sigma}^{\mu\nu} D_\nu \xi_j, \quad (C.19a)$$

$$d_a^\dagger \bar{\sigma}^\mu u_b e_c D^\mu \xi_i, \quad d_a^\dagger \bar{\sigma}^\mu u_b e_c \bar{\sigma}^{\mu\nu} D_\nu \xi_i, \quad \xi_i^\dagger \bar{\sigma}^\mu \nu_a \xi_j D_\mu \xi_k, \quad \xi_i^\dagger \bar{\sigma}_\mu \nu_a \xi_j \bar{\sigma}^{\mu\nu} D_\nu \xi_k, \quad (C.19b)$$

$$\nu_a^\dagger \bar{\sigma}^\mu \xi_i \xi_j D_\mu \xi_k, \quad \nu_a^\dagger \bar{\sigma}_\mu \xi_i \xi_j \bar{\sigma}^{\mu\nu} D_\nu \xi_k. \quad (C.19c)$$

All operators are accompanied by their Hermitian conjugate.

### C.3 Vector portal

At the EW scale, spin 1 messengers do not couple to SMEFT via operators of dimension five, hence the corresponding low energy portal Lagrangian can only contain interactions that are suppressed at most by a factor of  $\epsilon/v^2$  rather than  $\epsilon/v^3$ . At order  $\epsilon/v^2$ , hidden (axial-)vector mediators couple to the SM via operators of dimension  $d \leq 6$  only. Therefore, there are no portal operators with four SM fermions, since they would be at least of dimension seven.

It is convenient to define

$$\partial v \equiv \partial^\rho v_\rho, \quad v_{\mu\nu} \equiv \partial_{[\mu} v_{\nu]}, \quad \hat{v}_{\mu\nu} \equiv \partial_{\{\mu} v_{\nu\}}, \quad \tilde{v}_{\mu\nu} \equiv 2\epsilon_{\mu\nu\rho\sigma} \partial^\rho v^\sigma. \quad (C.20)$$

**Zero-fermion operators** can contain either one or two SM field strength tensors. The operators with one field strength tensor are

$$v^\rho v_\rho v_{\mu\nu} F^{\mu\nu}, \quad v_\nu v^\mu \hat{v}_{\mu\rho} F^{\nu\rho}, \quad v_\nu v^\mu v_{\mu\rho} \tilde{F}^{\nu\rho}, \quad \tilde{v}^{\mu\nu} \hat{v}_{\mu\rho} F_\nu^\rho, \quad (C.21a)$$

$$v^\rho v_\rho \tilde{v}_{\mu\nu} F^{\mu\nu}, \quad v_\nu v^\mu v_{\mu\rho} F^{\nu\rho}, \quad v_\nu v^\mu \tilde{v}_{\mu\rho} F^{\nu\rho}, \quad \tilde{v}^{\mu\nu} v_{\mu\rho} F_\nu^\rho, \quad (C.21b)$$

and

$$\partial v v_{\mu\nu} F^{\mu\nu}, \quad v_{\mu\nu} v_\rho \partial^\rho F^{\mu\nu}, \quad v_\mu \partial^2 v_\nu F^{\mu\nu}, \quad (C.22a)$$

$$\partial v v_{\mu\nu} \tilde{F}^{\mu\nu}, \quad v_{\mu\nu} v_\rho \partial^\rho \tilde{F}^{\mu\nu}, \quad v_\mu \partial^2 v_\nu \tilde{F}^{\mu\nu}. \quad (C.22b)$$

The operators with two field strength tensors are

$$v^\rho v_\rho \langle V^{\mu\nu} V_{\mu\nu} \rangle_c, \quad v_\mu v^\nu \langle V^{\mu\rho} V_{\nu\rho} \rangle_c, \quad \partial v \langle V^{\mu\nu} V_{\mu\nu} \rangle_c, \quad (C.23a)$$

$$v^\rho v_\rho \langle V^{\mu\nu} \tilde{V}_{\mu\nu} \rangle_c, \quad v_\mu v^\nu \langle V^{\mu\rho} \tilde{V}_{\rho\nu} \rangle_c, \quad \partial v \langle V^{\mu\nu} \tilde{V}_{\mu\nu} \rangle_c, \quad \partial_\mu v^\nu \langle V^{\mu\rho} \tilde{V}_{\rho\nu} \rangle_c. \quad (C.23b)$$

**Two-fermion operators** can contain a scalar-valued, vector-valued, or tensor-valued SM fermion bilinear. The operators with scalar- and tensor-valued fermion bilinears are

$$v^\rho v_\rho(\psi\psi)_0, \quad \partial v(\psi\psi)_0, \quad v_{\mu\nu}(\psi\bar{\sigma}^{\mu\nu}\psi)_0, \quad (\text{C.24})$$

plus Hermitian conjugates. The operators with vector-valued fermion bilinears are

$$v_\mu(\psi^\dagger\bar{\sigma}^\mu\psi)_0, \quad \widehat{v}_{\mu\nu}(\psi^\dagger\bar{\sigma}^\mu D^\nu\psi)_0, \quad v^\mu(\psi^\dagger\bar{\sigma}^\nu V_{\mu\nu}\psi)_0, \quad v_{\mu\nu}v^\nu(\psi^\dagger\bar{\sigma}^\mu\psi)_0, \quad (\text{C.25a})$$

$$v^\rho v_\rho v_\mu(\psi^\dagger\bar{\sigma}^\mu\psi)_0, \quad v_\mu v_\nu(\psi^\dagger\bar{\sigma}^\mu D^\nu\psi)_0, \quad v^\mu(\psi^\dagger\bar{\sigma}^\nu \widetilde{V}_{\mu\nu}\psi)_0, \quad \widehat{v}_{\mu\nu}v^\nu(\psi^\dagger\bar{\sigma}^\mu\psi)_0, \quad (\text{C.25b})$$

$$\widetilde{v}_{\mu\nu}v^\nu(\psi^\dagger\bar{\sigma}^\mu\psi)_0, \quad (\text{C.25c})$$

and

$$\partial v v_\mu(\psi^\dagger\bar{\sigma}^\mu\psi)_0, \quad \partial^2 v_\mu(\psi^\dagger\bar{\sigma}^\mu\psi)_0. \quad (\text{C.25d})$$

## D Expansion of the $\chi$ PT building blocks

In this appendix we provide details about the expansion of the chiral Lagrangians in terms of light mesons and hidden particle states. This material covers the necessary steps to derive the results of section 5 and provides the reader with the necessary tools to use the results obtained in section 4 and section 5 for their own calculations.

The matrix  $\mathbf{u}_\mu$  and the hatted external currents  $\widehat{\mathbf{X}} \in \{\widehat{\mathbf{M}}, \widehat{\mathbf{F}}, \widehat{\mathbf{T}}^{\mu\nu}\}$  and  $\widehat{\mathbf{Y}} \in \{\widehat{\mathbf{R}}_\mu, \widehat{\mathbf{R}}_{\mu\nu}\}$  can be expanded as

$$\widehat{\mathbf{X}} = g\mathbf{X} = \left(1 + \frac{i}{f_0}\boldsymbol{\Phi} - \frac{1}{2f_0^2}\boldsymbol{\Phi}^2 - \frac{i}{6f_0^3}\boldsymbol{\Phi}^3 + \dots\right)\mathbf{X}, \quad (\text{D.1a})$$

$$\widehat{\mathbf{Y}} = g\mathbf{Y}g^\dagger = \mathbf{Y} + \frac{i}{f_0}[\boldsymbol{\Phi}, \mathbf{Y}] - \frac{1}{2f_0^2}[\boldsymbol{\Phi}, [\boldsymbol{\Phi}, \mathbf{Y}]] - \frac{i}{6f_0^3}[\boldsymbol{\Phi}, [\boldsymbol{\Phi}, [\boldsymbol{\Phi}, \mathbf{Y}]]] + \dots, \quad (\text{D.1b})$$

$$\mathbf{u}_\mu = ig\partial_\mu g^\dagger = \frac{1}{f_0}\partial_\mu\boldsymbol{\Phi} + \frac{i}{2f_0^2}[\boldsymbol{\Phi}, \partial_\mu\boldsymbol{\Phi}] - \frac{1}{6f_0^3}[\boldsymbol{\Phi}, [\boldsymbol{\Phi}, \partial_\mu\boldsymbol{\Phi}]] + \dots. \quad (\text{D.1c})$$

Using the definition of the meson matrix  $\boldsymbol{\Phi}$

$$\boldsymbol{\Phi} = \boldsymbol{\phi} + \frac{1}{n_f}\bar{\boldsymbol{\phi}}, \quad \boldsymbol{\phi} = \begin{pmatrix} \frac{\eta_8}{\sqrt{6}} + \frac{\pi_8}{\sqrt{2}} & \pi^+ & K^+ \\ \pi^- & \frac{\eta_8}{\sqrt{6}} - \frac{\pi_8}{\sqrt{2}} & K^0 \\ K^- & \bar{K}^0 & -2\frac{\eta_8}{\sqrt{6}} \end{pmatrix}, \quad \bar{\boldsymbol{\phi}} = n_f \frac{\eta_1}{\sqrt{3}}, \quad (\text{D.2})$$

one obtains the individual contributions

$$\boldsymbol{\Phi}^2 = \begin{pmatrix} (\frac{\eta_8}{\sqrt{6}} + \frac{\pi_8}{\sqrt{2}})^2 + \pi^+\pi^- + K^+K^- & 2\pi^+\frac{\eta_8}{\sqrt{6}} + K^+\bar{K}^0 & \pi^+K^0 + K^+(\frac{\pi_8}{\sqrt{2}} - \frac{\eta_8}{\sqrt{6}}) \\ 2\pi^-\frac{\eta_8}{\sqrt{6}} + K^-K^0 & \pi^+\pi^- + (\frac{\eta_8}{\sqrt{6}} - \frac{\pi_8}{\sqrt{2}})^2 + K^0\bar{K}^0 & K^+\pi^- - K^0(\frac{\pi_8}{\sqrt{2}} + \frac{\eta_8}{\sqrt{6}}) \\ \pi^-\bar{K}^0 + K^-(\frac{\pi_8}{\sqrt{2}} - \frac{\eta_8}{\sqrt{6}}) & \pi^+K^- - \bar{K}^0(\frac{\pi_8}{\sqrt{2}} + \frac{\eta_8}{\sqrt{6}}) & K^+K^- + K^0\bar{K}^0 + 4(\frac{\eta_8}{\sqrt{6}})^2 \end{pmatrix}, \quad (\text{D.3a})$$

$$[\boldsymbol{\Phi}, \partial_\mu\boldsymbol{\Phi}] = \begin{pmatrix} \pi^+\overleftrightarrow{\partial}_\mu\pi^- + K^+\overleftrightarrow{\partial}_\mu K^- & 2\pi^+\overleftrightarrow{\partial}_\mu\frac{\pi_8}{\sqrt{2}} + K^+\overleftrightarrow{\partial}_\mu\bar{K}^0 & \pi^+\overleftrightarrow{\partial}_\mu K^0 - K^+\overleftrightarrow{\partial}_\mu(\frac{\pi_8}{\sqrt{2}} + 3\frac{\eta_8}{\sqrt{6}}) \\ 2\pi^-\overleftrightarrow{\partial}_\mu\frac{\pi_8}{\sqrt{2}} + K^0\overleftrightarrow{\partial}_\mu K^- & -\pi^+\overleftrightarrow{\partial}_\mu\pi^- + K^0\overleftrightarrow{\partial}_\mu\bar{K}^0 & -K^+\overleftrightarrow{\partial}_\mu\pi^- + K^0\overleftrightarrow{\partial}_\mu(\frac{\pi_8}{\sqrt{2}} - 3\frac{\eta_8}{\sqrt{6}}) \\ \bar{K}^0\overleftrightarrow{\partial}_\mu\pi^- + K^-\overleftrightarrow{\partial}_\mu(\frac{\pi_8}{\sqrt{2}} + 3\frac{\eta_8}{\sqrt{6}}) & -\pi^+\overleftrightarrow{\partial}_\mu K^- + \bar{K}^0\overleftrightarrow{\partial}_\mu(3\frac{\eta_8}{\sqrt{6}} - \frac{\pi_8}{\sqrt{2}}) & -K^+\overleftrightarrow{\partial}_\mu K^- - K^0\overleftrightarrow{\partial}_\mu\bar{K}^0 \end{pmatrix}. \quad (\text{D.3b})$$

The interactions involving the SM photon current are

$$[\boldsymbol{\Phi}, \mathbf{r}_A^\mu] = eA^\mu \begin{pmatrix} 0 & -\pi^+ & -K^+ \\ \pi^- & 0 & 0 \\ K^- & 0 & 0 \end{pmatrix}, \quad (\text{D.4a})$$

$$[\boldsymbol{\Phi}, [\boldsymbol{\Phi}, \mathbf{r}_A^\mu]] = -eA^\mu \begin{pmatrix} -2(\pi^+\pi^- + K^+K^-) & 2\pi^+\frac{\pi_8}{\sqrt{2}} + K^+\bar{K}^0 & K^+(3\frac{\eta_8}{\sqrt{6}} + \frac{\pi_8}{\sqrt{2}}) + \pi^+K^0 \\ 2\pi^-\frac{\pi_8}{\sqrt{2}} + K^-K^0 & 2\pi^+\pi^- & 2K^+\pi^- \\ K^-(3\frac{\eta_8}{\sqrt{6}} + \frac{\pi_8}{\sqrt{2}}) + \pi^-\bar{K}^0 & 2\pi^+K^- & 2K^+K^- \end{pmatrix}. \quad (\text{D.4b})$$

Finally, for interactions involving the hidden current  $\mathbf{V}_r$ , one has

$$[\mathbf{V}_r, \boldsymbol{\Phi}] = \begin{pmatrix} 0 & \pi^+(V_{ruu} - V_{rdd}) - K^+V_{rds} & K^+(V_{ruu} - V_{rss}) - \pi^+V_{rds} \\ \pi^-(V_{rdd} - V_{ruu}) + K^-V_{rds} & \bar{K}^0V_{rds} - K^0V_{rds} & K^0(V_{rdd} - V_{rss}) + V_{rds}(\frac{\pi_8}{\sqrt{2}} - 3\frac{\eta_8}{\sqrt{6}}) \\ K^-(V_{rss} - V_{ruu}) + \pi^-V_{rds} & \bar{K}^0(V_{rss} - V_{rdd}) + (3\frac{\eta_8}{\sqrt{6}} - \frac{\pi_8}{\sqrt{2}})V_{rds} & K^0V_{rds} - \bar{K}^0V_{rds} \end{pmatrix}. \quad (\text{D.5})$$

## D.1 Standard model meson phenomenology at NLO

We summarise the diagonalisation procedure for the U(3)  $\chi$ PT mesons and compute the resulting meson masses and decay constants at NLO. We use the approximation  $m'_u, m'_d \rightarrow m_{ud} \equiv (m'_u + m'_d)/2$ , which neglects the mixing between the neutral pion and the two  $\eta$ -mesons and we also neglect EM corrections for the charged meson masses, which are of order  $\alpha_{\text{EM}} \propto e^2$ . These EM contributions are given by

$$\Delta_\pi^{\text{EM}} = m_{\pi^\pm}^2 - m_{\pi^0}^2, \quad \Delta_K^{\text{EM}} = (1 + (0.84 \pm 0.25_{n_c})) \Delta_\pi^{\text{EM}} \quad (\text{D.6})$$

Where the correction factor captures the impact of NLO contributions [325, 326]. We use the EM contributions in combination with the measured values of the meson masses [144]

$$m_{\pi^\pm} = (139.57039 \pm 0.00017_{\text{exp}}) \text{ MeV}, \quad m_{K^\pm} = (493.677 \pm 0.013_{\text{exp}}) \text{ MeV}, \quad (\text{D.7a})$$

$$m_{\pi^0} = (134.9768 \pm 0.0005_{\text{exp}}) \text{ MeV}, \quad m_{K^0} = (497.611 \pm 0.013_{\text{exp}}) \text{ MeV}. \quad (\text{D.7b})$$

**Meson decay constants** The part of the NLO Lagrangian that mediates charged meson decays is

$$\mathcal{L}_\phi^{\partial W} + \mathcal{L}_\phi^{m\partial W} = -f_0 \langle l_W^\mu \partial_\mu \boldsymbol{\Phi} \rangle_f - \frac{2L_5 b_0}{f_0} \langle l_W^\mu \{ \mathbf{m}, \partial_\mu \boldsymbol{\Phi} \} \rangle_f. \quad (\text{D.8})$$

The resulting predictions for the meson decay constants are

$$\frac{f_\pi}{f_0} = 1 + 4L_5 \frac{m_\pi^2}{f_0^2} + \mathcal{O}(\delta^3), \quad \frac{f_K}{f_0} = 1 + 4L_5 \frac{m_K^2}{f_0^2} + \mathcal{O}(\delta^3), \quad (\text{D.9})$$

or equivalently

$$f_0 = \frac{m_K^2 f_\pi - m_\pi^2 f_K}{m_K^2 - m_\pi^2}, \quad 4L_5 = f_0 \frac{f_\pi - f_0}{m_\pi^2} = f_0 \frac{f_K - f_0}{m_K^2}, \quad (\text{D.10})$$

where

$$m_\pi^2 = m_{\pi^0}^2, \quad 2m_K^2 = m_{K^\pm}^2 + m_{K^0}^2 - \Delta_K^{\text{EM}}, \quad (\text{D.11})$$

are the charged meson masses without electromagnetic contributions. To fix the values of the parameters  $f_0$  and  $L_5$ , we use the measured values of the meson decay constants [144]

$$f_\pi = (65.1 \pm 0.6_{\text{exp}}) \text{ MeV}, \quad f_K = (77.85 \pm 0.15_{\text{exp}}) \text{ MeV}. \quad (\text{D.12})$$

Hence, one obtains the estimates

$$f_0 = (63.9 \pm 1.2_{\text{exp}} \pm \text{NNLO}) \text{ MeV}, \quad 4(4\pi)^2 L_5 = 0.66 \pm 0.04_{\text{exp}} \pm \text{NNLO}. \quad (\text{D.13})$$

**Masses and mixing angles** After diagonalising the neutral kaon sector via the field redefinition

$$\sqrt{2}K_L^0 = K^0 + \bar{K}^0, \quad -i\sqrt{2}K_S^0 = K^0 - \bar{K}^0, \quad (\text{D.14})$$

one obtains from the Lagrangians (4.116) the mass term

$$\mathcal{L}_{\phi^2}^m + \mathcal{L}_{\phi^2}^\theta = -m_\pi^2 \pi^+ \pi^- - m_K^2 K^+ K^- - \frac{1}{2} \left( m_\pi^2 \pi^{02} + m_K^2 (K_L^{02} + K_S^{02}) + \eta_2^T \mathbf{m}_{\eta_2}^2 \eta_2 \right). \quad (\text{D.15})$$

The NLO predictions for the pion and kaon mass parameters are

$$m_\pi^2 = b_0 m_{\text{ud}} \left( 1 + 8L_8 \frac{b_0 m_{\text{ud}}}{f_0^2} \right), \quad m_K^2 = \frac{b_0}{2} (m'_s + m_{\text{ud}}) \left( 1 + 4L_8 \frac{b_0 (m'_s + m_{\text{ud}})}{f_0^2} \right), \quad (\text{D.16})$$

while the prediction for the mass matrix of the the  $\eta$ -meson doublet  $\eta_2 = (\eta_8, \eta_1)^T$  is

$$\mathbf{m}_{\eta_2}^2 = \begin{pmatrix} m_{\eta_8}^2 & m_{\eta_8 \eta_1}^2 \\ m_{\eta_8 \eta_1}^2 & m_{\eta_1}^2 \end{pmatrix} = \left( M_K^2 - \frac{\Delta_{K\pi}}{2} \right) \mathbf{1}_{2 \times 2} + \begin{pmatrix} \Delta_{K\pi} & -\sqrt{2} \Delta_{K\pi} \\ -\sqrt{2} \Delta_{K\pi} & M_0^2 \end{pmatrix} + \mathcal{O}(\delta^3), \quad (\text{D.17})$$

where the quantities

$$M_K^2 = m_K^2 + \frac{2}{3} (m_K^2 - m_\pi^2) \left( \Lambda_2 + 3 \frac{4L_8}{f_0^2} (m_K^2 - m_\pi^2) \right), \quad M_0^2 = m_0^2 - 2\Lambda_2 m_K^2, \quad (\text{D.18a})$$

$$\Delta_{K\pi} = \frac{2}{3} (m_K^2 - m_\pi^2) \left( 1 - \Lambda_2 + 4 \frac{4L_8}{f_0^2} m_K^2 \right) \quad (\text{D.18b})$$

depend on the kaon and pion masses as well the three parameters  $m_0$ ,  $\Lambda_2$ , and  $L_8$ . The  $\eta_2$  mass eigenstates are

$$\eta = c_\eta \eta_8 - s_\eta \eta_1, \quad \eta' = c_\eta \eta_1 + s_\eta \eta_8, \quad m_\eta^2 + m_{\eta'}^2 = \text{tr } \mathbf{m}_{\eta_2}^2, \quad m_\eta^2 m_{\eta'}^2 = \det \mathbf{m}_{\eta_2}^2, \quad (\text{D.19})$$

and their mixing is determined by

$$m_{\eta_8}^2 = \frac{m_\eta^2 + m_{\eta'}^2 t_\eta^4}{1 + t_\eta^4}, \quad m_{\eta_1}^2 = \frac{m_{\eta'}^2 + m_\eta^2 t_\eta^4}{1 + t_\eta^4}, \quad m_{\eta_8 \eta_1}^2 = \frac{(m_{\eta'}^2 - m_\eta^2) t_\eta^2}{1 + t_\eta^4}. \quad (\text{D.20})$$

where the sine, cosine, and tangent functions of the  $\eta$  mixing angle is indicated by  $s_\eta$ ,  $c_\eta$ , and  $t_\eta$ , respectively. In order to fix the values of the free parameters we fit the above predictions to the experimentally obtained values for the  $\eta$ -meson masses and mixing angle [144, 327]

$$m_\eta = (547.862 \pm 0.018_{\text{exp}}) \text{ MeV} , \quad t_\eta = -0.29 \pm 0.09_{\text{exp}} , \quad (\text{D.21a})$$

$$m_{\eta'} = (957.78 \pm 0.06_{\text{exp}}) \text{ MeV} . \quad (\text{D.21b})$$

Hence, one obtains the estimates

$$m_0 = 4\pi(76.3 \pm 1.4_{\text{exp}} \pm \text{NNLO}) \text{ MeV} , \quad \Lambda_2 = 0.814 \pm 0.023_{\text{exp}} \pm \text{NNLO} , \quad (\text{D.22a})$$

$$4(4\pi)^2 L_8 = 0.215 \pm 0.033_{\text{exp}} \pm \text{NNLO} . \quad (\text{D.22b})$$

Finally, using equation (D.16) to fix the values of the parameters  $b_0 m_{\text{ud}}$  and  $b_0 m_s$ , results in

$$\sqrt{b_0 m_{\text{ud}}} = 4\pi(10.68 \pm 0.08_{\text{exp}} \pm \text{NNLO}) \text{ MeV} , \quad (\text{D.23a})$$

$$\sqrt{b_0 m_s} = 4\pi(50.95 \pm 0.28_{\text{exp}} \pm \text{NNLO}) \text{ MeV} . \quad (\text{D.23b})$$

**Weak interaction induced kinetic mixing** When computing matrix elements for quark-flavour violating transitions, one also has to account for kinetic mixing due to weak corrections, which is captured by the quadratic part of the octet and 27-plet Lagrangians

$$\begin{aligned} \mathcal{L}_{\phi^2}^{a\partial^2} + \mathcal{L}_{\phi^2}^{a\partial^2} = & -\frac{\epsilon_{\text{EW}}}{2} ((h_8 + (n_f - 1)h_{27})\partial_\mu K^+ \partial^\mu \pi^- + \text{h.c.}) \\ & - \epsilon_{\text{EW}}(-\text{Re } h_8 + n_f \text{Re } h_{27})\partial_\mu \frac{K_L^0}{\sqrt{2}} \partial^\mu \frac{\pi^0}{\sqrt{2}} \\ & - \epsilon_{\text{EW}}(-\text{Im } h_8 + n_f \text{Im } h_{27})\partial_\mu \frac{K_S^0}{\sqrt{2}} \partial^\mu \frac{\pi^0}{\sqrt{2}} \\ & - \epsilon_{\text{EW}}[n_f \text{Re } h_1 2\varepsilon_{\eta\eta'} + (-\text{Re } h_8 + n_f \text{Re } h_{27})]\partial_\mu \frac{K_L^0}{\sqrt{2}} \partial^\mu \frac{\eta}{\sqrt{6}} \\ & - \epsilon_{\text{EW}}[n_f \text{Im } h_1 2\varepsilon_{\eta\eta'} + (-\text{Im } h_8 + n_f \text{Im } h_{27})]\partial_\mu \frac{K_S^0}{\sqrt{2}} \partial^\mu \frac{\eta}{\sqrt{6}} \\ & + \epsilon_{\text{EW}}[n_f \text{Re } h_1 + (-\text{Re } h_8 + n_f \text{Re } h_{27})\varepsilon_{\eta\eta'}]\partial_\mu \frac{K_L^0}{\sqrt{2}} \partial^\mu \frac{\eta'}{\sqrt{3}} \\ & + \epsilon_{\text{EW}}[n_f \text{Im } h_1 + (-\text{Im } h_8 + n_f \text{Im } h_{27})\varepsilon_{\eta\eta'}]\partial_\mu \frac{K_S^0}{\sqrt{2}} \partial^\mu \frac{\eta'}{\sqrt{3}} , \quad (\text{D.24}) \end{aligned}$$

To LO in  $\epsilon_{\text{EW}}$ , these interactions can be diagonalised via the field redefinitions

$$\begin{pmatrix} \pi^+ \\ K^+ \end{pmatrix} \rightarrow \left[ \mathbf{1}_{2 \times 2} + \frac{\epsilon_{\text{EW}}}{2} \begin{pmatrix} 0 & m_{K^\pm \pi^\mp}^2 \theta_{\pi K} \\ -m_{\pi^\pm K^\mp}^2 \theta_{\pi K}^\dagger & 0 \end{pmatrix} \right] \begin{pmatrix} \pi^+ \\ K^+ \end{pmatrix} , \quad (\text{D.25a})$$

$$\begin{pmatrix} \pi^0 \\ K_L^0 \\ K_S^0 \\ \eta \\ \eta' \end{pmatrix} \rightarrow \left[ \mathbf{1}_{5 \times 5} + \frac{\epsilon_{\text{EW}}}{2} \begin{pmatrix} 0 & m_{K^0 \pi K}^2 \theta_{\pi K}^T & 0 & 0 \\ -m_{\pi^0 \pi K}^2 \theta_{\pi K} & \mathbf{0}_{2 \times 2} & -m_{\eta \eta K}^2 \theta_{\eta K} & -m_{\eta' \eta K}^2 \theta_{\eta' K} \\ 0 & m_{K^0 \eta K}^2 \theta_{\eta K}^T & 0 & 0 \\ 0 & m_{K^0 \eta' K}^2 \theta_{\eta' K}^T & 0 & 0 \end{pmatrix} \right] \begin{pmatrix} \pi^0 \\ K_L^0 \\ K_S^0 \\ \eta \\ \eta' \end{pmatrix} , \quad (\text{D.25b})$$

where the mixing angles are

$$\theta_{K^\pm \pi^\mp} \equiv \frac{1}{m_{K^\pm}^2 - m_{\pi^\pm}^2} (h_8 + (n_f - 1)h_{27}) , \quad (\text{D.26a})$$

$$\theta_{\pi K} \equiv \frac{1}{m_{K^0}^2 - m_{\pi^0}^2} \left( n_f \text{Re } h_1 2\varepsilon_{\pi\eta'} + (-\text{Re } h_8 + n_f \text{Re } h_{27})(1 + \varepsilon_{\pi\eta}) \right) , \quad (\text{D.26b})$$

$$\theta_{\eta K} \equiv \frac{1}{m_{K^0}^2 - m_{\eta}^2} \left( n_f \text{Re } h_1 2\varepsilon_{\eta\eta'} + (-\text{Re } h_8 + n_f \text{Re } h_{27})(1 - 3\varepsilon_{\pi\eta}) \right) , \quad (\text{D.26c})$$

$$\theta_{\eta' K} \equiv \frac{1}{m_{K^0}^2 - m_{\eta'}^2} \left( n_f \text{Re } h_1 + (-\text{Re } h_8 + n_f \text{Re } h_{27})(3\varepsilon_{\pi\eta'} + \varepsilon_{\eta\eta'}) \right) . \quad (\text{D.26d})$$

## D.2 Mixing between mesons and scalar messengers

In section 6, we compute a generic  $K^+ \rightarrow \pi^+ s_i$  decay amplitude by treating the bilinear portal interactions perturbatively. In some instances, it may be necessary to resum these bilinear interactions by diagonalising the portal Lagrangian. Following this strategy, one obtains additional portal interactions generated by both SM and internal hidden sector interactions, the size of which is measured by meson to hidden particle mixing angles.

In general, the bilinear interactions that couple  $\chi_{\text{PT}}$  to hidden sectors are

$$\mathcal{L}_{\Phi}^{S_m} + \mathcal{L}_{\Phi}^{S_\theta} = -f_0 b_0 \langle \Phi \text{Im } S'_m \rangle_f + \frac{f_0 m_0^2}{n_f} S_\theta \Phi = -\frac{1}{2} \phi_0^T \epsilon s + \text{h.c.} , \quad (\text{D.27})$$

where  $\phi_0^T = (\pi, K_L^0, K_S^0, \eta, \eta')$ ,  $s^T = (s_1, s_2, \dots)$ ,  $\epsilon = (\epsilon_1, \epsilon_2, \dots)$ , and

$$\epsilon_i = \epsilon_{\text{UV}} f_0 b_0 \begin{pmatrix} \frac{1}{\sqrt{2}} c_{s_i \pi} \\ \frac{1}{\sqrt{2}} \left( \text{Im } c_i^{S_m d} + \text{Im } c_i^{S_m s} \right) \\ \frac{1}{\sqrt{2}i} \left( \text{Im } c_i^{S_m d} - \text{Im } c_i^{S_m s} \right) \\ \frac{1}{\sqrt{3}} \left( c_{s_i \eta} + s_\eta \frac{m_0^2}{v b_0} c_i^{S_\theta} \right) \\ \frac{1}{\sqrt{3}} \left( c_{s_i \eta'} - c_\eta \frac{m_0^2}{v b_0} c_i^{S_\theta} \right) \end{pmatrix} . \quad (\text{D.28})$$

The coefficients  $c_{s_i X}$  and  $c_i^{S_m}$  are given in equations (6.1) and (6.8). For canonical quadratic hidden Lagrangians

$$\mathcal{L}^{\text{hidden}} \supset -\frac{1}{2} s^T (\partial^2 + m) s , \quad m = \text{diag}(m_1^2, m_2^2, \dots) \quad (\text{D.29})$$

the mass-mixing matrix is

$$\mathcal{L} \supset -\frac{1}{2} \begin{pmatrix} \phi_0^T & s^T \end{pmatrix} \begin{pmatrix} M & \epsilon \\ \epsilon^T & m \end{pmatrix} \begin{pmatrix} \phi_0 \\ s \end{pmatrix} , \quad M = \text{diag}(m_\pi^2, m_K^2, m_K^2, m_\eta^2, m_{\eta'}^2) . \quad (\text{D.30})$$

This matrix can be diagonalised using a unitary field redefinition

$$\begin{pmatrix} \phi_0 \\ s \end{pmatrix} \rightarrow \begin{pmatrix} \mathbf{1} & \theta \\ -\theta^T & \mathbf{1} \end{pmatrix} \begin{pmatrix} \phi_0 \\ s \end{pmatrix} + \mathcal{O}(\theta^2) , \quad \theta = (\theta_1, \theta_2, \dots) , \quad (\text{D.31})$$



where  $\theta$  is a solution of the matrix-valued equation

$$\epsilon = \theta m - M\theta . \quad (\text{D.32})$$

Assuming that all of the  $s_i$  share the same mass  $m_s = m_i$ , one obtains

$$\theta_i = (m_s^2 \mathbf{1} - M)^{-1} \epsilon_i . \quad (\text{D.33})$$

### D.3 Trilinear Standard Model vertices used in the $K^\pm \rightarrow \pi^\pm s_i$ decay

The hidden currents  $\text{Im } S_m$  and  $S_\theta$  contribute to the generic  $K^\pm \rightarrow \pi^\pm s_i$  amplitude via Feynman diagrams that contain a SM three-meson vertex with one charged kaon leg, one charged pion leg, and one neutral meson leg, with the neutral meson subsequently oscillating into a hidden scalar. The SM three-meson vertices are encoded by the kinetic Lagrangian (4.113), the octet Lagrangian (4.121a), and the 27-plet Lagrangian (4.121b),

$$\mathcal{L}_{\Phi^3} \equiv \mathcal{L}_{\Phi^3}^{\partial^2} + \mathcal{L}_{\Phi^3}^{a\partial^2} + \mathcal{L}_{\Phi^3}^{a\partial^2} , \quad (\text{D.34})$$

where

$$\mathcal{L}_{\Phi^3}^{\partial^2} = \frac{i}{2f_0} \langle \partial_\mu \Phi[\Phi, \partial^\mu \Phi] \rangle_f = 0 , \quad (\text{D.35a})$$

$$\mathcal{L}_{\Phi^3}^{a\partial^2} = -\frac{i\epsilon_{\text{EW}}}{4f_0} (h_8 \langle \{ \partial_\mu \Phi, [\Phi, \partial^\mu \Phi] \} \rangle_d^s + h_1 \langle [\Phi, \partial_\mu \Phi] \rangle_d^s \partial^\mu \Phi) + \text{h.c.} , \quad (\text{D.35b})$$

$$\begin{aligned} \mathcal{L}_{\Phi^3}^{a\partial^2} = & -\frac{i\epsilon_{\text{EW}}}{4f_0} h_{27} (3\partial_\mu \Phi_d^s [\Phi, \partial^\mu \Phi]_u^u + 2\partial_\mu \Phi_d^u [\Phi, \partial^\mu \Phi]_u^s \\ & + 3[\Phi, \partial_\mu \Phi]_d^s \partial^\mu \Phi_u^u + 2[\Phi, \partial_\mu \Phi]_d^u \partial^\mu \Phi_u^s) + \text{h.c.} \end{aligned} \quad (\text{D.35c})$$

Evaluating the flavour traces, the relevant terms with one  $K^+$ , one  $\pi^+$ , and one neutral meson are

$$\mathcal{L}_{\Phi^3} \supset \mathcal{L}_{K\pi\Phi} \equiv \mathcal{L}_{K\pi\Phi}^{a\partial^2} + \mathcal{L}_{K\pi\Phi}^{a\partial^2} , \quad (\text{D.36})$$

where

$$\begin{aligned} \mathcal{L}_{K\pi\Phi}^{a\partial^2} = & -\frac{i\epsilon_{\text{EW}}}{4f_0} \left[ h_8 (3\partial_{\pi^-} \partial_{K^+} - \partial_{\eta_8} \partial_{K^+} - 2\partial_{\eta_8} \partial_{\pi^-}) \frac{\eta_8}{\sqrt{6}} K^+ \pi^- \right. \\ & + h_8 (\partial_{K^+} \partial_{\pi_8} - \partial_{K^+} \partial_{\pi^-}) \frac{\pi_8}{\sqrt{2}} \pi^- K^+ \\ & \left. + 3h_1 (\partial_{\eta_1} \partial_{K^+} - \partial_{\eta_1} \partial_{\pi^-}) \frac{\eta_1}{\sqrt{3}} \pi^- K^+ \right] + \text{h.c.} , \end{aligned} \quad (\text{D.37a})$$

$$\begin{aligned} \mathcal{L}_{K\pi\Phi}^{a\partial^2} = & -\frac{i\epsilon_{\text{EW}}}{4f_0} h_{27} \left[ (7\partial_{\pi_8} \partial_{K^+} - 5\partial_{\pi_8} \partial_{\pi^-} - 2\partial_{\pi^-} \partial_{K^+}) \frac{\pi_8}{\sqrt{2}} \pi^- K^+ \right. \\ & \left. - 3(3\partial_{\eta_8} \partial_{\pi^-} - 2\partial_{\pi^-} \partial_{K^+} - \partial_{\eta_8} \partial_{K^+}) \frac{\eta_8}{\sqrt{6}} \pi^- K^+ \right] + \text{h.c.} . \end{aligned} \quad (\text{D.37b})$$

Diagonalising the Lagrangian, one obtains the final interactions

$$\mathcal{L}_{K\pi\Phi} = \mathcal{L}_{K\pi\pi} + \mathcal{L}_{K\pi\eta} + \mathcal{L}_{K\pi\eta'} , \quad (\text{D.38})$$

where

$$\mathcal{L}_{K\pi\pi} = -\frac{i\epsilon_{\text{EW}}}{4f_0} [(h_8 + 7h_{27})\partial_{\pi^0}\partial_{K^+} - 5h_{27}\partial_{\pi^0}\partial_{\pi^-} - (h_8 + 2h_{27})\partial_{K^+}\partial_{\pi^-}] K^+\pi^-\frac{\pi^0}{\sqrt{2}}, \quad (\text{D.39a})$$

$$\mathcal{L}_{K\pi\eta} = -\frac{i\epsilon_{\text{EW}}}{4f_0} c_\eta [(3h_8 + 6h_{27})\partial_{K^+}\partial_{\pi^-} - (h_8 + 3\sqrt{2}t_\eta h_1 - 3h_{27})\partial_\eta\partial_{K^+} - (2h_8 - 3\sqrt{2}t_\eta h_1 + 9h_{27})\partial_\eta\partial_{\pi^-}] K^+\pi^-\frac{\eta}{\sqrt{6}}, \quad (\text{D.39b})$$

$$\mathcal{L}_{K\pi\eta'} = -\frac{i\epsilon_{\text{EW}}}{4f_0} s_\eta [(3h_8 + 6h_{27})\partial_{K^+}\partial_{\pi^-} - (h_8 - 3\sqrt{2}t_\eta^{-1}h_1 - 3h_{27})\partial_{\eta'}\partial_{K^+} - (2h_8 + 3\sqrt{2}t_\eta^{-1}h_1 + 9h_{27})\partial_{\eta'}\partial_{\pi^-}] K^+\pi^-\frac{\eta'}{\sqrt{6}}, \quad (\text{D.39c})$$

## References

- [1] J. C. Pati and A. Salam. ‘Lepton Number as the Fourth Color’. In: *Phys. Rev. D* 10 (1974), pp. 275–289. DOI: 10.1103/PhysRevD.10.275. №: IC-74-7. Erratum in: *Phys. Rev. D* 11 (1975), pp. 703–703. DOI: 10.1103/PhysRevD.11.703.2.
- [2] H. Georgi and S. L. Glashow. ‘Unity of All Elementary Particle Forces’. In: *Phys. Rev. Lett.* 32 (1974), pp. 438–441. DOI: 10.1103/PhysRevLett.32.438.
- [3] H. Georgi, H. R. Quinn, and S. Weinberg. ‘Hierarchy of Interactions in Unified Gauge Theories’. In: *Phys. Rev. Lett.* 33 (1974), pp. 451–454. DOI: 10.1103/PhysRevLett.33.451. №: PRINT-74-1122 REV. (HARVARD).
- [4] Y. A. Golfand and E. P. Likhtman. ‘Extension of the Algebra of Poincare Group Generators and Violation of  $p$  Invariance’. In: *JETP Lett.* 13 (1971), pp. 323–326.
- [5] J.-L. Gervais and B. Sakita. ‘Field Theory Interpretation of Supergauges in Dual Models’. In: *Nucl. Phys. B* 34 (1971). Ed. by K. Kikkawa, M. Virasoro, and S. R. Wadia, pp. 632–639. DOI: 10.1016/0550-3213(71)90351-8.
- [6] A. Neveu and J. H. Schwarz. ‘Factorizable dual model of pions’. In: *Nucl. Phys. B* 31 (1971), pp. 86–112. DOI: 10.1016/0550-3213(71)90448-2.
- [7] P. Ramond. ‘Dual Theory for Free Fermions’. In: *Phys. Rev. D* 3 (1971), pp. 2415–2418. DOI: 10.1103/PhysRevD.3.2415. №: FERMILAB-PUB-70-008-T and NAL-THY-8.
- [8] P. Minkowski. ‘ $\mu \rightarrow e\gamma$  at a Rate of One Out of  $10^9$  Muon Decays?’ In: *Phys. Lett. B* 67 (1977), pp. 421–428. DOI: 10.1016/0370-2693(77)90435-X. №: PRINT-77-0182 (BERN).
- [9] M. Gell-Mann, P. Ramond, and R. Slansky. ‘Complex Spinors and Unified Theories’. In: *Supergravity Workshop Stony Brook, New York, September 27-28, 1979*. Vol. C790927. 1979, pp. 315–321. arXiv: 1306.4669 [hep-th]. №: PRINT-80-0576.
- [10] J. Schechter and J. W. F. Valle. ‘Neutrino Masses in  $SU(2) \times U(1)$  Theories’. In: *Phys. Rev. D* 22 (1980), p. 2227. DOI: 10.1103/PhysRevD.22.2227. №: SU-4217-167 and COO-3533-167.

- [11] R. N. Mohapatra and G. Senjanovic. ‘Neutrino Mass and Spontaneous Parity Violation’. In: *Phys. Rev. Lett.* 44 (1980), p. 912. DOI: 10.1103/PhysRevLett.44.912. №: MDDP-TR-80-060, MDDP-PP-80-105, and CCNY-HEP-79-10.
- [12] T. Yanagida. ‘Horizontal Symmetry and Masses of Neutrinos’. In: *Prog. Theor. Phys.* 64 (1980), p. 1103. DOI: 10.1143/PTP.64.1103. №: TU-80-208.
- [13] J. Schechter and J. W. F. Valle. ‘Neutrino Decay and Spontaneous Violation of Lepton Number’. In: *Phys. Rev. D* 25 (1982), p. 774. DOI: 10.1103/PhysRevD.25.774. №: SU-4217-203 and COO-3533-203.
- [14] T. Asaka and M. Shaposhnikov. ‘The  $\nu$ MSM, dark matter and baryon asymmetry of the universe’. In: *Phys. Lett. B* 620 (2005), pp. 17–26. DOI: 10.1016/j.physletb.2005.06.020. arXiv: hep-ph/0505013 [hep-ph].
- [15] M. Shaposhnikov. ‘A Possible symmetry of the  $\nu$ MSM’. In: *Nucl. Phys. B* 763 (2007), pp. 49–59. DOI: 10.1016/j.nuclphysb.2006.11.003. arXiv: hep-ph/0605047 [hep-ph]. №: CERN-PH-TH-2006-079.
- [16] R. D. Peccei and H. R. Quinn. ‘Constraints Imposed by CP Conservation in the Presence of Instantons’. In: *Phys. Rev. D* 16 (1977), pp. 1791–1797. DOI: 10.1103/PhysRevD.16.1791. №: ITP-572-STANFORD.
- [17] R. D. Peccei and H. R. Quinn. ‘CP Conservation in the Presence of Instantons’. In: *Phys. Rev. Lett.* 38 (1977), pp. 1440–1443. DOI: 10.1103/PhysRevLett.38.1440. №: ITP-568-STANFORD.
- [18] S. Weinberg. ‘A New Light Boson?’ In: *Phys. Rev. Lett.* 40 (1978), pp. 223–226. DOI: 10.1103/PhysRevLett.40.223. №: HUTP-77/A074.
- [19] F. Wilczek. ‘Problem of Strong  $P$  and  $T$  Invariance in the Presence of Instantons’. In: *Phys. Rev. Lett.* 40 (1978), pp. 279–282. DOI: 10.1103/PhysRevLett.40.279. №: PRINT-77-0939 (COLUMBIA).
- [20] D. S. M. Alves and N. Weiner. ‘A viable QCD axion in the MeV mass range’. In: *JHEP* 07 (2018), p. 092. DOI: 10.1007/JHEP07(2018)092. arXiv: 1710.03764 [hep-ph]. №: LA-UR-17-29295.
- [21] N. Arkani-Hamed, A. G. Cohen, and H. Georgi. ‘Electroweak symmetry breaking from dimensional deconstruction’. In: *Phys. Lett. B* 513 (2001), pp. 232–240. DOI: 10.1016/S0370-2693(01)00741-9. arXiv: hep-ph/0105239. №: HUTP-01-A024, BUHEP-01-06, and UCB-PTH-01-15.
- [22] D. E. Kaplan and M. Schmaltz. ‘The Little Higgs from a simple group’. In: *JHEP* 10 (2003), p. 039. DOI: 10.1088/1126-6708/2003/10/039. arXiv: hep-ph/0302049. №: BUHEP-03-03.
- [23] S. Chang. ‘A ‘Littlest Higgs’ model with custodial  $SU(2)$  symmetry’. In: *JHEP* 12 (2003), p. 057. DOI: 10.1088/1126-6708/2003/12/057. arXiv: hep-ph/0306034.
- [24] C.-R. Chen, J. Hajer, T. Liu, I. Low, and H. Zhang. ‘Testing naturalness at 100 TeV’. In: *JHEP* 09 (2017), p. 129. DOI: 10.1007/JHEP09(2017)129. arXiv: 1705.07743 [hep-ph].

- [25] S. Weinberg. ‘Phenomenological Lagrangians’. In: *Physica A* 96.1-2 (1979). Ed. by S. Deser, pp. 327–340. DOI: 10.1016/0378-4371(79)90223-1. №: HUTP-78-A051A.
- [26] H. Leutwyler. ‘On the foundations of chiral perturbation theory’. In: *Annals Phys.* 235 (1994), pp. 165–203. DOI: 10.1006/aphy.1994.1094. arXiv: hep-ph/9311274. №: BUTP-93-24.
- [27] I. Brivio and M. Trott. ‘The Standard Model as an Effective Field Theory’. In: *Phys. Rept.* 793 (2019), pp. 1–98. DOI: 10.1016/j.physrep.2018.11.002. arXiv: 1706.08945 [hep-ph].
- [28] W. Buchmüller and D. Wyler. ‘Effective Lagrangian Analysis of New Interactions and Flavor Conservation’. In: *Nucl. Phys. B* 268 (1986), pp. 621–653. DOI: 10.1016/0550-3213(86)90262-2. №: CERN-TH.4254/85.
- [29] B. Grzadkowski, M. Iskrzynski, M. Misiak, and J. Rosiek. ‘Dimension-Six Terms in the Standard Model Lagrangian’. In: *JHEP* 10 (2010), p. 085. DOI: 10.1007/JHEP10(2010)085. arXiv: 1008.4884 [hep-ph]. №: IFT-9-2010 and TTP10-35.
- [30] D. Barducci et al. ‘Interpreting top-quark LHC measurements in the standard-model effective field theory’ (Feb. 2018). Ed. by J. A. Aguilar-Saavedra, C. Degrande, G. Durieux, F. Maltoni, E. Vryonidou, and C. Zhang. arXiv: 1802.07237 [hep-ph]. №: CERN-LPCC-2018-01.
- [31] J. Ellis, C. W. Murphy, V. Sanz, and T. You. ‘Updated Global SMEFT Fit to Higgs, Diboson and Electroweak Data’. In: *JHEP* 06 (2018), p. 146. DOI: 10.1007/JHEP06(2018)146. arXiv: 1803.03252 [hep-ph]. №: CAVENDISH-HEP-2018-06, DAMTP-2018-12, KCL-PH-TH/2018-12, CERN-PH-TH/2018-042, and CERN-TH-2018-042.
- [32] E. Slade. ‘Towards global fits in EFT’s and New Physics implications’. In: *PoS LHCP 2019* (2019). Ed. by P. Roig Garcés, I. Bautista Guzman, A. Fernández Téllez, and M. I. Martínez Hernández, p. 150. DOI: 10.22323/1.350.0150. arXiv: 1906.10631 [hep-ph].
- [33] F. Feruglio. ‘The Chiral approach to the electroweak interactions’. In: *Int. J. Mod. Phys. A* 8 (1993), pp. 4937–4972. DOI: 10.1142/S0217751X93001946. arXiv: hep-ph/9301281. №: DFPD-92-TH-50.
- [34] C. P. Burgess, J. Matias, and M. Pospelov. ‘A Higgs or not a Higgs? What to do if you discover a new scalar particle’. In: *Int. J. Mod. Phys. A* 17 (2002), pp. 1841–1918. DOI: 10.1142/S0217751X02009813. arXiv: hep-ph/9912459. №: CERN-TH-99-311, MCGILL-99-33, TPI-MINN-99-53, and UMN-TH-1828-99.
- [35] B. Grinstein and M. Trott. ‘A Higgs-Higgs bound state due to new physics at a TeV’. In: *Phys. Rev. D* 76 (2007), p. 073002. DOI: 10.1103/PhysRevD.76.073002. arXiv: 0704.1505 [hep-ph]. №: UCSD-PTH-07-03.
- [36] R. Barbieri, B. Bellazzini, V. S. Rychkov, and A. Varagnolo. ‘The Higgs boson from an extended symmetry’. In: *Phys. Rev. D* 76 (2007), p. 115008. DOI: 10.1103/PhysRevD.76.115008. arXiv: 0706.0432 [hep-ph].

- [37] E. Fermi. ‘Trends to a Theory of beta Radiation’. Italian. In: *Meeting of the Italian School of Physics and Weak Interactions Bologna, Italy, April 26-28, 1984*. Vol. 11. 535. 1934, pp. 1–19. DOI: 10.1007/BF02959820.
- [38] E. E. Jenkins, A. V. Manohar, and M. Trott. ‘Renormalization Group Evolution of the Standard Model Dimension Six Operators I: Formalism and lambda Dependence’. In: *JHEP* 10 (2013), p. 087. DOI: 10.1007/JHEP10(2013)087. arXiv: 1308.2627 [hep-ph].
- [39] E. E. Jenkins, A. V. Manohar, and M. Trott. ‘Renormalization Group Evolution of the Standard Model Dimension Six Operators II: Yukawa Dependence’. In: *JHEP* 01 (2014), p. 035. DOI: 10.1007/JHEP01(2014)035. arXiv: 1310.4838 [hep-ph].
- [40] R. Alonso, E. E. Jenkins, A. V. Manohar, and M. Trott. ‘Renormalization Group Evolution of the Standard Model Dimension Six Operators III: Gauge Coupling Dependence and Phenomenology’. In: *JHEP* 04 (2014), p. 159. DOI: 10.1007/JHEP04(2014)159. arXiv: 1312.2014 [hep-ph]. №: CERN-PH-TH-2013-305.
- [41] J. S. Schwinger. ‘Chiral dynamics’. In: *Phys. Lett. B* 24 (1967), pp. 473–476. DOI: 10.1016/0370-2693(67)90277-8.
- [42] J. A. Cronin. ‘Phenomenological model of strong and weak interactions in chiral  $U(3) \times U(3)$ ’. In: *Phys. Rev.* 161 (1967), pp. 1483–1494. DOI: 10.1103/PhysRev.161.1483.
- [43] J. Wess and B. Zumino. ‘Lagrangian method for chiral symmetries’. In: *Phys. Rev.* 163 (1967), pp. 1727–1735. DOI: 10.1103/PhysRev.163.1727.
- [44] S. Weinberg. ‘Dynamical approach to current algebra’. In: *Phys. Rev. Lett.* 18 (1967), pp. 188–191. DOI: 10.1103/PhysRevLett.18.188.
- [45] S. Weinberg. ‘Nonlinear realizations of chiral symmetry’. In: *Phys. Rev.* 166 (1968), pp. 1568–1577. DOI: 10.1103/PhysRev.166.1568.
- [46] R. F. Dashen and M. Weinstein. ‘Soft pions, chiral symmetry, and phenomenological lagrangians’. In: *Phys. Rev.* 183 (1969), pp. 1261–1291. DOI: 10.1103/PhysRev.183.1261.
- [47] S. Gasiorowicz and D. A. Geffen. ‘Effective Lagrangians and field algebras with chiral symmetry’. In: *Rev. Mod. Phys.* 41 (1969), pp. 531–573. DOI: 10.1103/RevModPhys.41.531. №: DESY-69-13.
- [48] M. A. Shifman and M. B. Voloshin. ‘On Production of  $d$  and  $D^*$  Mesons in  $B$  Meson Decays’. In: *Sov. J. Nucl. Phys.* 47 (1988). [Yad. Fiz. 47, 801], p. 511. №: ITEP-87-64.
- [49] N. Isgur and M. B. Wise. ‘Weak Decays of Heavy Mesons in the Static Quark Approximation’. In: *Phys. Lett. B* 232 (1989), pp. 113–117. DOI: 10.1016/0370-2693(89)90566-2. №: UTPT-89-27 and CALT-68-1585.
- [50] H. Georgi. ‘An Effective Field Theory for Heavy Quarks at Low-energies’. In: *Phys. Lett. B* 240 (1990), pp. 447–450. DOI: 10.1016/0370-2693(90)91128-X. №: HUTP-90/A007.
- [51] N. Isgur and M. B. Wise. ‘Weak Transition Form-Factors between Heavy Mesons’. In: *DPF Conf.1990:0459-464*. Vol. B237. 1990, pp. 527–530. DOI: 10.1016/0370-2693(90)91219-2. №: UTPT-90-01 and CALT-68-1608.

- [52] B. Grinstein. ‘The Static Quark Effective Theory’. In: *Nucl. Phys. B* 339 (1990), pp. 253–268. DOI: 10.1016/0550-3213(90)90349-I. №: HUTP-90/A002.
- [53] A. F. Falk, H. Georgi, B. Grinstein, and M. B. Wise. ‘Heavy Meson Form-factors From QCD’. In: *Nucl. Phys. B* 343 (1990), pp. 1–13. DOI: 10.1016/0550-3213(90)90591-Z. №: HUTP-90/A011 and CALT-68-1618.
- [54] W. E. Caswell and G. P. Lepage. ‘Effective Lagrangians for Bound State Problems in QED, QCD, and Other Field Theories’. In: *Phys. Lett. B* 167 (1986), pp. 437–442. DOI: 10.1016/0370-2693(86)91297-9. №: CLNS-85/641.
- [55] G. T. Bodwin, E. Braaten, and G. P. Lepage. ‘Rigorous QCD analysis of inclusive annihilation and production of heavy quarkonium’. In: *Phys. Rev. D* 51 (1995). [Erratum: *Phys. Rev. D* 55, 5853 (1997)], pp. 1125–1171. DOI: 10.1103/PhysRevD.55.5853. arXiv: hep-ph/9407339 [hep-ph]. №: ANL-HEP-PR-94-24, FERMILAB-PUB-94-073-T, and NUHEP-TH-94-5. Erratum in: *Phys. Rev. D* 55 (1997), p. 5853. DOI: 10.1103/PhysRevD.55.1125.
- [56] C. W. Bauer, S. Fleming, and M. E. Luke. ‘Summing Sudakov logarithms in  $B \rightarrow X(s\gamma)$  in effective field theory’. In: *Phys. Rev. D* 63 (2000), p. 014006. DOI: 10.1103/PhysRevD.63.014006. arXiv: hep-ph/0005275 [hep-ph]. №: UTPT-00-03.
- [57] C. W. Bauer, S. Fleming, D. Pirjol, and I. W. Stewart. ‘An Effective field theory for collinear and soft gluons: Heavy to light decays’. In: *Phys. Rev. D* 63 (2001), p. 114020. DOI: 10.1103/PhysRevD.63.114020. arXiv: hep-ph/0011336 [hep-ph]. №: UCSD-PTH-00-28.
- [58] C. W. Bauer and I. W. Stewart. ‘Invariant operators in collinear effective theory’. In: *Phys. Lett. B* 516 (2001), pp. 134–142. DOI: 10.1016/S0370-2693(01)00902-9. arXiv: hep-ph/0107001 [hep-ph]. №: UCSD-PTH-01-09.
- [59] C. W. Bauer and A. V. Manohar. ‘Shape function effects in  $B \rightarrow X(s)\gamma$  and  $B \rightarrow X(u)l\bar{\nu}$  decays’. In: *Phys. Rev. D* 70 (2004), p. 034024. DOI: 10.1103/PhysRevD.70.034024. arXiv: hep-ph/0312109 [hep-ph]. №: CALT-68-2465.
- [60] S. W. Bosch, B. O. Lange, M. Neubert, and G. Paz. ‘Factorization and shape function effects in inclusive  $B$  meson decays’. In: *Nucl. Phys. B* 699 (2004), pp. 335–386. DOI: 10.1016/j.nuclphysb.2004.07.041. arXiv: hep-ph/0402094 [hep-ph]. №: CLNS-04-1858.
- [61] M. Beneke, F. Campanario, T. Mannel, and B. D. Pecjak. ‘Power corrections to  $\bar{B} \rightarrow X(u)l\bar{\nu}(X(s)\gamma)$  decay spectra in the ‘shape-function’ region’. In: *JHEP* 06 (2005), p. 071. DOI: 10.1088/1126-6708/2005/06/071. arXiv: hep-ph/0411395 [hep-ph]. №: PITHA-04-18, SI-HEP-2004-12, and SFB-CPP-04-64.
- [62] C. W. Bauer, A. Hornig, and F. J. Tackmann. ‘Factorization for generic jet production’. In: *Phys. Rev. D* 79 (2009), p. 114013. DOI: 10.1103/PhysRevD.79.114013. arXiv: 0808.2191 [hep-ph].
- [63] S. Alekhin et al. ‘A facility to Search for Hidden Particles at the CERN SPS: the SHiP physics case’. In: *Rept. Prog. Phys.* 79.12 (2016), p. 124201. DOI: 10.1088/0034-4885/79/12/124201. arXiv: 1504.04855 [hep-ph]. №: CERN-SPSC-2015-017 and SPSC-P-350-ADD-1.

- [64] J. Beacham et al. ‘Physics Beyond Colliders at CERN: Beyond the Standard Model Working Group Report’. In: *J. Phys. G* 47.1 (2020), p. 010501. DOI: 10.1088/1361-6471/ab4cd2. arXiv: 1901.09966 [hep-ex]. №: CERN-PBC-REPORT-2018-007.
- [65] P. Agrawal et al. ‘Feebly-Interacting Particles: FIPs 2020 Workshop Report’ (Feb. 2021). arXiv: 2102.12143 [hep-ph].
- [66] CMS. ‘A search for pair production of new light bosons decaying into muons in proton-proton collisions at 13 TeV’. In: *Phys. Lett. B* 796 (2019), pp. 131–154. DOI: 10.1016/j.physletb.2019.07.013. arXiv: 1812.00380 [hep-ex]. №: CMS-HIG-18-003 and CERN-EP-2018-288.
- [67] CMS. ‘Search for Low-Mass Quark-Antiquark Resonances Produced in Association with a Photon at  $\sqrt{s}=13$  TeV’. In: *Phys. Rev. Lett.* 123.23 (2019), p. 231803. DOI: 10.1103/PhysRevLett.123.231803. arXiv: 1905.10331 [hep-ex]. №: CMS-EXO-17-027 and CERN-EP-2019-068.
- [68] CMS. ‘Data Scouting and Data Parking with the CMS High level Trigger’. In: *PoS EPS-HEP2019* (2020), p. 139. DOI: 10.22323/1.364.0139.
- [69] ATLAS. ‘Measurement of light-by-light scattering and search for axion-like particles with 2.2 nb<sup>-1</sup> of Pb+Pb data with the ATLAS detector’. In: *JHEP* 03 (2021), p. 243. DOI: 10.1007/JHEP03(2021)243. arXiv: 2008.05355 [hep-ex]. №: CERN-EP-2020-135.
- [70] LHCb. ‘Search for Dark Photons Produced in 13 TeV *pp* Collisions’. In: *Phys. Rev. Lett.* 120.6 (2018), p. 061801. DOI: 10.1103/PhysRevLett.120.061801. arXiv: 1710.02867 [hep-ex]. №: LHCb-PAPER-2017-038 and CERN-EP-2017-248.
- [71] LHCb. ‘Search for lepton-flavour-violating decays of Higgs-like bosons’. In: *Eur. Phys. J. C* 78.12 (2018), p. 1008. DOI: 10.1140/epjc/s10052-018-6386-8. arXiv: 1808.07135 [hep-ex]. №: CERN-EP-2018-210 and LHCb-PAPER-2018-030.
- [72] LHCb. ‘Search for  $A' \rightarrow \mu^+ \mu^-$  Decays’. In: *Phys. Rev. Lett.* 124.4 (2020), p. 041801. DOI: 10.1103/PhysRevLett.124.041801. arXiv: 1910.06926 [hep-ex]. №: LHCb-PAPER-2019-031 and CERN-EP-2019-212.
- [73] LHCb. ‘Searches for low-mass dimuon resonances’. In: *JHEP* 10 (2020), p. 156. DOI: 10.1007/JHEP10(2020)156. arXiv: 2007.03923 [hep-ex]. №: LHCb-PAPER-2020-013 and CERN-EP-2020-114.
- [74] M. Borsato et al. ‘Unleashing the full power of LHCb to probe Stealth New Physics’ (May 2021). arXiv: 2105.12668 [hep-ph].
- [75] LHCb. ‘Search for heavy neutral leptons in  $W^+ \rightarrow \mu^+ \mu^\pm \text{jet}$  decays’. In: *Eur. Phys. J. C* 81.3 (2021), p. 248. DOI: 10.1140/epjc/s10052-021-08973-5. arXiv: 2011.05263 [hep-ex]. №: LHCb-PAPER-2020-022 and CERN-EP-2020-194.
- [76] LHCb. ‘Search for long-lived particles decaying to  $e^\pm \mu^\mp \nu$ ’. In: *Eur. Phys. J. C* 81.3 (2021), p. 261. DOI: 10.1140/epjc/s10052-021-08994-0. arXiv: 2012.02696 [hep-ex]. №: LHCb-PAPER-2020-027 and CERN-EP-2020-212.

- [77] X. Cid Vidal et al. ‘Report from Working Group 3: Beyond the Standard Model physics at the HL-LHC and HE-LHC’. In: *CERN Yellow Rep. Monogr.* 7 (2019). Ed. by A. Dainese, M. Mangano, A. B. Meyer, A. Nisati, G. Salam, and M. A. Vesterinen, pp. 585–865. DOI: 10.23731/CYRM-2019-007.585. arXiv: 1812.07831 [hep-ph]. №: CERN-LPCC-2018-05.
- [78] NA62. ‘The Beam and detector of the NA62 experiment at CERN’. In: *JINST* 12.05 (2017), P05025. DOI: 10.1088/1748-0221/12/05/P05025. arXiv: 1703.08501 [physics.ins-det].
- [79] NA62. ‘Search for heavy neutral lepton production in  $K^+$  decays’. In: *Phys. Lett. B* 778 (2018), pp. 137–145. DOI: 10.1016/j.physletb.2018.01.031. arXiv: 1712.00297 [hep-ex]. №: CERN-EP-2017-311.
- [80] M. Drewes, J. Hajer, J. Klaric, and G. Lanfranchi. ‘NA62 sensitivity to heavy neutral leptons in the low scale seesaw model’. In: *JHEP* 07 (2018), p. 105. DOI: 10.1007/JHEP07(2018)105. arXiv: 1801.04207 [hep-ph].
- [81] NA62. ‘First search for  $K^+ \rightarrow \pi^+ \nu \bar{\nu}$  using the decay-in-flight technique’. In: *Phys. Lett. B* 791 (2019), pp. 156–166. DOI: 10.1016/j.physletb.2019.01.067. arXiv: 1811.08508 [hep-ex]. №: CERN-EP-2018-314.
- [82] NA62. ‘Search for production of an invisible dark photon in  $\pi^0$  decays’. In: *JHEP* 05 (2019), p. 182. DOI: 10.1007/JHEP05(2019)182. arXiv: 1903.08767 [hep-ex]. №: CERN-EP-2019-048.
- [83] NA62. ‘Search for heavy neutral lepton production in  $K^+$  decays to positrons’. In: *Phys. Lett. B* 807 (2020), p. 135599. DOI: 10.1016/j.physletb.2020.135599. arXiv: 2005.09575 [hep-ex]. №: CERN-EP-2020-089.
- [84] NA62. ‘Search for a feebly interacting particle  $X$  in the decay  $K^+ \rightarrow \pi^+ X$ ’. In: *JHEP* 03 (2021), p. 058. DOI: 10.1007/JHEP03(2021)058. arXiv: 2011.11329 [hep-ex]. №: CERN-EP-2020-227.
- [85] KOTO. ‘Search for the  $K_L \rightarrow \pi^0 \nu \bar{\nu}$  and  $K_L \rightarrow \pi^0 X^0$  decays at the J-PARC KOTO experiment’. In: *Phys. Rev. Lett.* 122.2 (2019), p. 021802. DOI: 10.1103/PhysRevLett.122.021802. arXiv: 1810.09655 [hep-ex].
- [86] SeaQuest. ‘The SeaQuest Spectrometer at Fermilab’. In: *Nucl. Instrum. Meth. A* 930 (2019), pp. 49–63. DOI: 10.1016/j.nima.2019.03.039. arXiv: 1706.09990 [physics.ins-det]. №: FERMILAB-PUB-17-209-E.
- [87] J. Alimena et al. ‘Searching for long-lived particles beyond the Standard Model at the Large Hadron Collider’. In: *J. Phys. G* 47.9 (2020), p. 090501. DOI: 10.1088/1361-6471/ab4574. arXiv: 1903.04497 [hep-ex].
- [88] D. Curtin et al. ‘Long-Lived Particles at the Energy Frontier: The MATHUSLA Physics Case’. In: *Rept. Prog. Phys.* 82.11 (2019), p. 116201. DOI: 10.1088/1361-6633/ab28d6. arXiv: 1806.07396 [hep-ph]. №: FERMILAB-PUB-18-264-T.
- [89] FASER. ‘FASER’s physics reach for long-lived particles’. In: *Phys. Rev. D* 99.9 (2019), p. 095011. DOI: 10.1103/PhysRevD.99.095011. arXiv: 1811.12522 [hep-ph]. №: UCI-TR-2018-19 and KYUSHU-RCAPP-2018-06.



- [90] V. V. Gligorov, S. Knapen, M. Papucci, and D. J. Robinson. ‘Searching for Long-lived Particles: A Compact Detector for Exotics at LHCb’. In: *Phys. Rev. D* 97.1 (2018), p. 015023. DOI: 10.1103/PhysRevD.97.015023. arXiv: 1708.09395 [hep-ph].
- [91] M. Duch, B. Grzadkowski, and J. Wudka. ‘Classification of effective operators for interactions between the Standard Model and dark matter’. In: *JHEP* 05 (2015), p. 116. DOI: 10.1007/JHEP05(2015)116. arXiv: 1412.0520 [hep-ph].
- [92] A. De Simone and T. Jacques. ‘Simplified models vs. effective field theory approaches in dark matter searches’. In: *Eur. Phys. J. C* 76.7 (2016), p. 367. DOI: 10.1140/epjc/s10052-016-4208-4. arXiv: 1603.08002 [hep-ph]. №: SISSA-21-2016-FISI.
- [93] I. Brivio, M. B. Gavela, L. Merlo, K. Mimasu, J. M. No, R. del Rey, and V. Sanz. ‘ALPs Effective Field Theory and Collider Signatures’. In: *Eur. Phys. J. C* 77.8 (2017), p. 572. DOI: 10.1140/epjc/s10052-017-5111-3. arXiv: 1701.05379 [hep-ph]. №: IFT-UAM-CSIC-16-141, KCL-PH-TH-2016-72, FTUAM-16-49, and CP3-17-04.
- [94] W. Dekens and P. Stoffer. ‘Low-energy effective field theory below the electroweak scale: matching at one loop’. In: *JHEP* 10 (2019), p. 197. DOI: 10.1007/JHEP10(2019)197. arXiv: 1908.05295 [hep-ph].
- [95] R. Contino, K. Max, and R. K. Mishra. ‘Searching for Elusive Dark Sectors with Terrestrial and Celestial Observations’ (Dec. 2020). arXiv: 2012.08537 [hep-ph].
- [96] V. Cirigliano, M. L. Graesser, and G. Ovanessian. ‘WIMP-nucleus scattering in chiral effective theory’. In: *JHEP* 10 (2012), p. 025. DOI: 10.1007/JHEP10(2012)025. arXiv: 1205.2695 [hep-ph].
- [97] A. L. Fitzpatrick, W. Haxton, E. Katz, N. Lubbers, and Y. Xu. ‘The Effective Field Theory of Dark Matter Direct Detection’. In: *JCAP* 02 (2013), p. 004. DOI: 10.1088/1475-7516/2013/02/004. arXiv: 1203.3542 [hep-ph].
- [98] M. Cirelli, E. Del Nobile, and P. Panci. ‘Tools for model-independent bounds in direct dark matter searches’. In: *JCAP* 10 (2013), p. 019. DOI: 10.1088/1475-7516/2013/10/019. arXiv: 1307.5955 [hep-ph]. №: CP3-ORIGINS-2013-014, DIAS-2013-14, and SACLAY-T13-022.
- [99] M. Hoferichter, P. Klos, and A. Schwenk. ‘Chiral power counting of one- and two-body currents in direct detection of dark matter’. In: *Phys. Lett. B* 746 (2015), pp. 410–416. DOI: 10.1016/j.physletb.2015.05.041. arXiv: 1503.04811 [hep-ph].
- [100] M. Hoferichter, P. Klos, J. Menéndez, and A. Schwenk. ‘Analysis strategies for general spin-independent WIMP-nucleus scattering’. In: *Phys. Rev. D* 94.6 (2016), p. 063505. DOI: 10.1103/PhysRevD.94.063505. arXiv: 1605.08043 [hep-ph]. №: INT-PUB-16-012.
- [101] F. Bishara, J. Brod, B. Grinstein, and J. Zupan. ‘Chiral Effective Theory of Dark Matter Direct Detection’. In: *JCAP* 02 (2017), p. 009. DOI: 10.1088/1475-7516/2017/02/009. arXiv: 1611.00368 [hep-ph]. №: DO-TH-16-28, OUTP-16-24P, and CERN-TH-2016-259.

- [102] F. Bishara, J. Brod, B. Grinstein, and J. Zupan. ‘From quarks to nucleons in dark matter direct detection’. In: *JHEP* 11 (2017), p. 059. DOI: 10.1007/JHEP11(2017)059. arXiv: 1707.06998 [hep-ph]. №: DO-TH-17-10, OUTP-17-07P, and CERN-TH-2017-157.
- [103] M. Hoferichter, P. Klos, J. Menéndez, and A. Schwenk. ‘Nuclear structure factors for general spin-independent WIMP-nucleus scattering’. In: *Phys. Rev. D* 99.5 (2019), p. 055031. DOI: 10.1103/PhysRevD.99.055031. arXiv: 1812.05617 [hep-ph]. №: INT-PUB-18-059.
- [104] J. C. Criado, A. Djouadi, M. Pérez-Victoria, and J. Santiago. ‘A complete Effective Field Theory for Dark Matter’ (Apr. 2021). arXiv: 2104.14443 [hep-ph].
- [105] J. Gasser and H. Leutwyler. ‘Chiral Perturbation Theory: Expansions in the Mass of the Strange Quark’. In: *Nucl. Phys. B* 250 (1985), pp. 465–516. DOI: 10.1016/0550-3213(85)90492-4. №: CERN-TH-3798.
- [106] H. Leutwyler and M. A. Shifman. ‘Light Higgs Particle in Decays of  $K$  and  $\eta$  Mesons’. In: *Nucl. Phys. B* 343 (1990), pp. 369–397. DOI: 10.1016/0550-3213(90)90475-S. №: BUTP-89/29-BERN.
- [107] A. Pich and E. de Rafael. ‘Four quark operators and nonleptonic weak transitions’. In: *Nucl. Phys. B* 358 (1991), pp. 311–382. DOI: 10.1016/0550-3213(91)90351-W. №: CERN-TH-5906-90 and CPT-90-P-2393.
- [108] A. Pich and E. de Rafael. ‘Weak  $K$  amplitudes in the chiral and  $1/n_c$  expansions’. In: *Phys. Lett. B* 374 (1996), pp. 186–192. DOI: 10.1016/0370-2693(96)00171-2. arXiv: hep-ph/9511465. №: CPT-95-P-3265, FTUV-95-56, and IFIC-95-58.
- [109] R. Kaiser and H. Leutwyler. ‘Large  $N_c$  in chiral perturbation theory’. In: *Eur. Phys. J. C* 17 (2000), pp. 623–649. DOI: 10.1007/s100520000499. arXiv: hep-ph/0007101. №: BUTP-00-19.
- [110] E. Pallante, A. Pich, and I. Scimemi. ‘The Standard model prediction for  $\epsilon'/\epsilon$ ’. In: *Nucl. Phys. B* 617 (2001), pp. 441–474. DOI: 10.1016/S0550-3213(01)00418-7. arXiv: hep-ph/0105011. №: IFIC-00-31, FTUV-01-0502, and SISSA-37-2001-EP.
- [111] V. Cirigliano, G. Ecker, H. Neufeld, and A. Pich. ‘Isospin breaking in  $K \rightarrow \pi\pi$  decays’. In: *Eur. Phys. J. C* 33 (2004), pp. 369–396. DOI: 10.1140/epjc/s2003-01579-3. arXiv: hep-ph/0310351. №: IFIC-03-39, UWTHPH-2003-17, and MAP-292.
- [112] J.-M. Gérard, C. Smith, and S. Trine. ‘Radiative kaon decays and the penguin contribution to the  $\Delta I = 1/2$  rule’. In: *Nucl. Phys. B* 730 (2005), pp. 1–36. DOI: 10.1016/j.nuclphysb.2005.09.040. arXiv: hep-ph/0508189 [hep-ph]. №: UCL-IPT-05-08.
- [113] J. Berges. ‘Introduction to nonequilibrium quantum field theory’. In: *AIP Conf. Proc.* 739.1 (2004). Ed. by M. Bracco, M. Chiapparini, E. Ferreira, and T. Kodama, pp. 3–62. DOI: 10.1063/1.1843591. arXiv: hep-ph/0409233.
- [114] J. Kambor, J. H. Missimer, and D. Wyler. ‘The Chiral Loop Expansion of the Nonleptonic Weak Interactions of Mesons’. In: *Nucl. Phys. B* 346 (1990), pp. 17–64. DOI: 10.1016/0550-3213(90)90236-7. №: PSI-PR-89-18 and ETH-TH-89-42.

- [115] J. F. Donoghue, E. Golowich, and B. R. Holstein. *Dynamics of the Standard Model*. Vol. 2. Cambridge Monographs on Particle Physics, Nuclear Physics and Cosmology. Cambridge University Press, 1992. DOI: 10.1017/CBO9780511524370.
- [116] G. Ecker, J. Kambor, and D. Wyler. ‘Resonances in the weak chiral Lagrangian’. In: *Nucl. Phys. B* 394 (1993), pp. 101–138. DOI: 10.1016/0550-3213(93)90103-V. №: CERN-TH-6610-92, TUM-T31-27-92, and ZU-TH-36-92.
- [117] A. J. Buras and J.-M. Gérard. ‘ $K \rightarrow \pi\pi$  and  $K - \pi$  Matrix Elements of the Chromomagnetic Operators from Dual QCD’. In: *JHEP* 07 (2018), p. 126. DOI: 10.1007/JHEP07(2018)126. arXiv: 1803.08052 [hep-ph].
- [118] G. ’t Hooft. ‘Dimensional regularization and the renormalization group’. In: *Nucl. Phys. B* 61 (1973), pp. 455–468. DOI: 10.1016/0550-3213(73)90376-3.
- [119] S. Weinberg. ‘New approach to the renormalization group’. In: *Phys. Rev. D* 8 (1973), pp. 3497–3509. DOI: 10.1103/PhysRevD.8.3497.
- [120] K. Maltman, D. Leinweber, P. Moran, and A. Sternbeck. ‘The Realistic Lattice Determination of  $\alpha_s(M_Z)$  Revisited’. In: *Phys. Rev. D* 78 (2008), p. 114504. DOI: 10.1103/PhysRevD.78.114504. arXiv: 0807.2020 [hep-lat].
- [121] PACS-CS. ‘Precise determination of the strong coupling constant in  $N_f = 2 + 1$  lattice QCD with the Schrödinger functional scheme’. In: *JHEP* 10 (2009), p. 053. DOI: 10.1088/1126-6708/2009/10/053. arXiv: 0906.3906 [hep-lat]. №: UTHERP-584 and UTCCS-P-54.
- [122] C. McNeile, C. T. H. Davies, E. Follana, K. Hornbostel, and G. P. Lepage. ‘High-Precision c and b Masses, and QCD Coupling from Current-Current Correlators in Lattice and Continuum QCD’. In: *Phys. Rev. D* 82 (2010), p. 034512. DOI: 10.1103/PhysRevD.82.034512. arXiv: 1004.4285 [hep-lat].
- [123] A. Bazavov, N. Brambilla, X. Garcia i Tormo, P. Petreczky, J. Soto, and A. Vairo. ‘Determination of  $\alpha_s$  from the QCD static energy: An update’. In: *Phys. Rev. D* 90.7 (2014), p. 074038. DOI: 10.1103/PhysRevD.90.074038. arXiv: 1407.8437 [hep-ph]. №: TUM-EFT-47-14, UB-ECM-PF-14-81, and ICCUB-14-055.
- [124] B. Chakraborty et al. ‘High-precision quark masses and QCD coupling from  $n_f = 4$  lattice QCD’. In: *Phys. Rev. D* 91.5 (2015), p. 054508. DOI: 10.1103/PhysRevD.91.054508. arXiv: 1408.4169 [hep-lat].
- [125] K. Nakayama, B. Fahy, and S. Hashimoto. ‘Short-distance charmonium correlator on the lattice with Möbius domain-wall fermion and a determination of charm quark mass’. In: *Phys. Rev. D* 94.5 (2016), p. 054507. DOI: 10.1103/PhysRevD.94.054507. arXiv: 1606.01002 [hep-lat]. №: KEK-CP-345.
- [126] ALPHA. ‘QCD Coupling from a Nonperturbative Determination of the Three-Flavor  $\Lambda$  Parameter’. In: *Phys. Rev. Lett.* 119.10 (2017), p. 102001. DOI: 10.1103/PhysRevLett.119.102001. arXiv: 1706.03821 [hep-lat]. №: CERN-TH-2017-129, DESY-17-088, and WUB-17-03.

- [127] S. Zafeiropoulos, P. Boucaud, F. De Soto, J. Rodríguez-Quintero, and J. Segovia. ‘Strong Running Coupling from the Gauge Sector of Domain Wall Lattice QCD with Physical Quark Masses’. In: *Phys. Rev. Lett.* 122.16 (2019), p. 162002. DOI: 10.1103/PhysRevLett.122.162002. arXiv: 1902.08148 [hep-ph].
- [128] *Flavour Lattice Averaging Group*. ‘FLAG Review 2019: Flavour Lattice Averaging Group (FLAG)’. In: *Eur. Phys. J. C* 80.2 (2020), p. 113. DOI: 10.1140/epjc/s10052-019-7354-7. arXiv: 1902.08191 [hep-lat]. №: FERMILAB-PUB-19-077-T.
- [129] H. K. Dreiner, H. E. Haber, and S. P. Martin. ‘Two-component spinor techniques and Feynman rules for quantum field theory and supersymmetry’. In: *Phys. Rept.* 494 (2010), pp. 1–196. DOI: 10.1016/j.physrep.2010.05.002. arXiv: 0812.1594 [hep-ph]. №: BN-TH-2008-12, SCIPP-08-08, and FERMILAB-PUB-09-855-T.
- [130] A. Bazavov et al. ‘Staggered chiral perturbation theory in the two-flavor case and SU(2) analysis of the MILC data’. In: *28th International Symposium on Lattice field theory (Lattice 2010)* (Villasimius, Italy, 14th–19th June 2010). Vol. LATTICE2010. 2010, p. 083. arXiv: 1011.1792 [hep-lat].
- [131] S. Borsanyi, S. Durr, Z. Fodor, S. Krieg, A. Schafer, E. E. Scholz, and K. K. Szabo. ‘SU(2) chiral perturbation theory low-energy constants from 2 + 1 flavor staggered lattice simulations’. In: *Phys. Rev. D* 88 (2013), p. 014513. DOI: 10.1103/PhysRevD.88.014513. arXiv: 1205.0788 [hep-lat].
- [132] C. McNeile, A. Bazavov, C. T. H. Davies, R. J. Dowdall, K. Hornbostel, G. P. Lepage, and H. D. Trotter. ‘Direct determination of the strange and light quark condensates from full lattice QCD’. In: *Phys. Rev. D* 87.3 (2013), p. 034503. DOI: 10.1103/PhysRevD.87.034503. arXiv: 1211.6577 [hep-lat].
- [133] *Budapest-Marseille-Wuppertal*. ‘Lattice QCD at the physical point meets SU(2) chiral perturbation theory’. In: *Phys. Rev. D* 90.11 (2014), p. 114504. DOI: 10.1103/PhysRevD.90.114504. arXiv: 1310.3626 [hep-lat]. №: CPT-P005-2013 and WUB-13-14.
- [134] P. A. Boyle et al. ‘Low energy constants of SU(2) partially quenched chiral perturbation theory from  $N_f = 2 + 1$  domain wall QCD’. In: *Phys. Rev. D* 93.5 (2016), p. 054502. DOI: 10.1103/PhysRevD.93.054502. arXiv: 1511.01950 [hep-lat].
- [135] G. Cossu, H. Fukaya, S. Hashimoto, T. Kaneko, and J.-I. Noaki. ‘Stochastic calculation of the Dirac spectrum on the lattice and a determination of chiral condensate in 2 + 1-flavor QCD’. In: *PTEP* 2016.9 (2016), 093B06. DOI: 10.1093/ptep/ptw129. arXiv: 1607.01099 [hep-lat]. №: KEK-CP-346 and OU-HET-898.
- [136] *JLQCD*. ‘Topological susceptibility of QCD with dynamical Möbius domain-wall fermions’. In: *PTEP* 2018.4 (2018), 043B07. DOI: 10.1093/ptep/pty041. arXiv: 1705.10906 [hep-lat]. №: OU-HET-937, KEK-CP-359, and YITP-17-51.
- [137] *HPQCD*. ‘Determination of the quark condensate from heavy-light current-current correlators in full lattice QCD’. In: *Phys. Rev. D* 100.3 (2019), p. 034506. DOI: 10.1103/PhysRevD.100.034506. arXiv: 1811.04305 [hep-lat].

- [138] J. A. M. Vermaseren, S. A. Larin, and T. van Ritbergen. ‘The four loop quark mass anomalous dimension and the invariant quark mass’. In: *Phys. Lett. B* 405 (1997), pp. 327–333. DOI: 10.1016/S0370-2693(97)00660-6. arXiv: hep-ph/9703284. №: UM-TH-97-03 and NIKHEF-97-012.
- [139] J. S. Bell and R. Jackiw. ‘A PCAC puzzle:  $\pi^0 \rightarrow \gamma\gamma$  in the  $\sigma$  model’. In: *Nuovo Cim. A* 60 (1969), pp. 47–61. DOI: 10.1007/BF02823296.
- [140] S. L. Adler. ‘Axial vector vertex in spinor electrodynamics’. In: *Phys. Rev.* 177 (1969), pp. 2426–2438. DOI: 10.1103/PhysRev.177.2426.
- [141] S. L. Adler and W. A. Bardeen. ‘Absence of higher order corrections in the anomalous axial vector divergence equation’. In: *Phys. Rev.* 182 (1969), pp. 1517–1536. DOI: 10.1103/PhysRev.182.1517.
- [142] G. ’t Hooft. ‘Computation of the Quantum Effects Due to a Four-Dimensional Pseudoparticle’. In: *Phys. Rev. D* 14 (1976). Ed. by M. A. Shifman, pp. 3432–3450. DOI: 10.1103/PhysRevD.14.3432. №: PRINT-76-0551 (HARVARD). Erratum in: *Phys. Rev. D* 18 (1978), p. 2199. DOI: 10.1103/PhysRevD.18.2199.3.
- [143] G. ’t Hooft. ‘Symmetry Breaking Through Bell-Jackiw Anomalies’. In: *Phys. Rev. Lett.* 37 (1976). Ed. by M. A. Shifman, pp. 8–11. DOI: 10.1103/PhysRevLett.37.8. №: PRINT-76-0254 (HARVARD).
- [144] *Particle Data Group*. ‘Review of Particle Physics’. In: *PTEP* 2020.8 (2020), p. 083C01. DOI: 10.1093/ptep/ptaa104.
- [145] W. A. Bardeen. ‘Anomalous Currents in Gauge Field Theories’. In: *Nucl. Phys. B* 75 (1974), pp. 246–258. DOI: 10.1016/0550-3213(74)90546-X. №: ITP-452-STANFORD.
- [146] A. Belavin, A. M. Polyakov, A. Schwartz, and Y. Tyupkin. ‘Pseudoparticle Solutions of the Yang-Mills Equations’. In: *Phys. Lett. B* 59 (1975). Ed. by J. Taylor, pp. 85–87. DOI: 10.1016/0370-2693(75)90163-X.
- [147] R. Crewther. ‘Chirality Selection Rules and the U(1) Problem’. In: *Phys. Lett. B* 70 (1977), pp. 349–354. DOI: 10.1016/0370-2693(77)90675-X. №: CERN-TH-2350.
- [148] T. Bhattacharya, V. Cirigliano, R. Gupta, E. Mereghetti, and B. Yoon. ‘Contribution of the QCD  $\Theta$ -term to nucleon electric dipole moment’ (Jan. 2021). arXiv: 2101.07230 [hep-lat]. №: LA-UR-20-30515.
- [149] P. Di Vecchia and G. Veneziano. ‘Chiral dynamics in the large  $N$  limit’. In: *Nucl. Phys. B* 171 (1980), pp. 253–272. DOI: 10.1016/0550-3213(80)90370-3. №: CERN-TH-2814.
- [150] H. Leutwyler and A. V. Smilga. ‘Spectrum of Dirac operator and role of winding number in QCD’. In: *Phys. Rev. D* 46 (1992), pp. 5607–5632. DOI: 10.1103/PhysRevD.46.5607. №: BUTP-92-10.
- [151] G. ’t Hooft. ‘A Planar Diagram Theory for Strong Interactions’. In: *Nucl. Phys. B* 72 (1974). Ed. by J. Taylor, p. 461. DOI: 10.1016/0550-3213(74)90154-0. №: CERN-TH-1786.
- [152] G. Veneziano. ‘U(1) Without Instantons’. In: *Nucl. Phys. B* 159 (1979), pp. 213–224. DOI: 10.1016/0550-3213(79)90332-8. №: CERN-TH-2651.

- [153] S. Coleman. *Aspects of Symmetry: Selected Erice Lectures*. Cambridge, U.K.: Cambridge University Press, 1985. ISBN: 978-0-521-31827-3. DOI: 10.1017/CBO9780511565045.
- [154] A. V. Manohar. ‘Large  $N$  QCD’. *Les Houches Summer School in Theoretical Physics, Session 68: Probing the Standard Model of Particle Interactions*. Feb. 1998, pp. 1091–1169. arXiv: [hep-ph/9802419](#). №: UCSD-PTH-98-06.
- [155] G. ’t Hooft. ‘Large  $N$ ’. *The Phenomenology of Large  $N_c$  QCD*. Apr. 2002, pp. 3–18. DOI: 10.1142/9789812776914\_0001. arXiv: [hep-th/0204069](#). №: SPIN-2002-08 and ITF-2002-14.
- [156] J. Callan Curtis G., S. R. Coleman, and R. Jackiw. ‘A New improved energy-momentum tensor’. In: *Annals Phys.* 59 (1970), pp. 42–73. DOI: 10.1016/0003-4916(70)90394-5.
- [157] P. Minkowski. ‘On the Anomalous Divergence of the Dilatation Current in Gauge Theories’ (1976). №: PRINT-76-0813 (BERN).
- [158] N. K. Nielsen. ‘The Energy Momentum Tensor in a Nonabelian Quark Gluon Theory’. In: *Nucl. Phys. B* 120 (1977), pp. 212–220. DOI: 10.1016/0550-3213(77)90040-2.
- [159] S. L. Adler, J. C. Collins, and A. Duncan. ‘Energy-Momentum-Tensor Trace Anomaly in Spin 1/2 Quantum Electrodynamics’. In: *Phys. Rev. D* 15 (1977), p. 1712. DOI: 10.1103/PhysRevD.15.1712. №: COO-2220-77-REV and COO-2220-77.
- [160] J. C. Collins, A. Duncan, and S. D. Joglekar. ‘Trace and Dilatation Anomalies in Gauge Theories’. In: *Phys. Rev. D* 16 (1977), pp. 438–449. DOI: 10.1103/PhysRevD.16.438. №: COO-2220-88.
- [161] A. J. Buras. ‘Weak Hamiltonian, CP violation and rare decays’. *Probing the Standard Model of Particle Interactions*. Les Houches Summer School in Theoretical Physics 68. June 1998, pp. 281–539. arXiv: [hep-ph/9806471](#). №: TUM-HEP-316-98.
- [162] V. M. Belyaev and B. L. Ioffe. ‘Determination of Baryon and Baryonic Resonance Masses from QCD Sum Rules. 1. Nonstrange Baryons’. In: *Sov. Phys. JETP* 56 (1982), pp. 493–501. №: ITEP-59-1982.
- [163] K. Aladashvili and M. Margvelashvili. ‘On the flavor dependence of the mixed quark-gluon condensate’. In: *Phys. Lett. B* 372 (1996), pp. 299–305. DOI: 10.1016/0370-2693(96)00043-3. arXiv: [hep-ph/9512261](#). №: TSU-HEPI-04-95.
- [164] V. M. Braun and A. Lenz. ‘On the SU(3) symmetry-breaking corrections to meson distribution amplitudes’. In: *Phys. Rev. D* 70 (2004), p. 074020. DOI: 10.1103/PhysRevD.70.074020. arXiv: [hep-ph/0407282](#).
- [165] P. Gubler and D. Satow. ‘Recent Progress in QCD Condensate Evaluations and Sum Rules’. In: *Prog. Part. Nucl. Phys.* 106 (2019), pp. 1–67. DOI: 10.1016/j.pnpnp.2019.02.005. arXiv: 1812.00385 [hep-ph].
- [166] T.-W. Chiu and T.-H. Hsieh. ‘Light quark masses, chiral condensate and quark gluon condensate in quenched lattice QCD with exact chiral symmetry’. In: *Nucl. Phys. B* 673 (2003), pp. 217–237. DOI: 10.1016/j.nuclphysb.2003.09.035. arXiv: [hep-lat/0305016](#). №: NTUTH-03-505C.

- [167] G. Altarelli and L. Maiani. ‘Octet Enhancement of Nonleptonic Weak Interactions in Asymptotically Free Gauge Theories’. In: *Phys. Lett. B* 52 (1974), pp. 351–354. DOI: 10.1016/0370-2693(74)90060-4. №: ISS-P-74-4.
- [168] M. K. Gaillard and B. W. Lee. ‘ $\Delta I = 1/2$  Rule for Nonleptonic Decays in Asymptotically Free Field Theories’. In: *Phys. Rev. Lett.* 33 (1974), p. 108. DOI: 10.1103/PhysRevLett.33.108. №: NAL-PUB-74-034-THY, NAL-PUB-74-34-THY, and FERMILAB-PUB-74-034-T.
- [169] A. I. Vainshtein, V. I. Zakharov, and M. A. Shifman. ‘A Possible mechanism for the  $\Delta T = 1/2$  rule in nonleptonic decays of strange particles’. In: *JETP Lett.* 22 (1975), pp. 55–56. Original in: *Pisma Zh. Eksp. Teor. Fiz.* 22 (1975), p. 123.
- [170] M. A. Shifman, A. I. Vainshtein, and V. I. Zakharov. ‘Light Quarks and the Origin of the  $\Delta I = 1/2$  Rule in the Nonleptonic Decays of Strange Particles’. In: *Nucl. Phys. B* 120 (1977), pp. 316–324. DOI: 10.1016/0550-3213(77)90046-3. №: ITEP-59-1975.
- [171] V. Cirigliano, G. Ecker, H. Neufeld, A. Pich, and J. Portoles. ‘Kaon Decays in the Standard Model’. In: *Rev. Mod. Phys.* 84 (2012), p. 399. DOI: 10.1103/RevModPhys.84.399. arXiv: 1107.6001 [hep-ph]. №: FTUV-11-0729, IFIC-11-02, and UWTHPH-2011-25.
- [172] B. J. Kavanagh, P. Panci, and R. Ziegler. ‘Faint Light from Dark Matter: Classifying and Constraining Dark Matter-Photon Effective Operators’. In: *JHEP* 04 (2019), p. 089. DOI: 10.1007/JHEP04(2019)089. arXiv: 1810.00033 [hep-ph]. №: CERN-TH-2018-200.
- [173] C. Arina, A. Cheek, K. Mimasu, and L. Pagani. ‘Light and Darkness: consistently coupling dark matter to photons via effective operators’. In: *Eur. Phys. J. C* 81.3 (2021), p. 223. DOI: 10.1140/epjc/s10052-021-09010-1. arXiv: 2005.12789 [hep-ph]. №: CP3-20-22.
- [174] C. Mariani. ‘Review of Reactor Neutrino Oscillation Experiments’. In: *Mod. Phys. Lett. A* 27 (2012), p. 1230010. DOI: 10.1142/S0217732312300108. arXiv: 1201.6665 [hep-ex].
- [175] A. Manohar and H. Georgi. ‘Chiral Quarks and the Nonrelativistic Quark Model’. In: *Nucl. Phys. B* 234 (1984), pp. 189–212. DOI: 10.1016/0550-3213(84)90231-1. №: HUTP-83/A042A.
- [176] E. E. Jenkins, A. V. Manohar, and M. Trott. ‘Naive Dimensional Analysis Counting of Gauge Theory Amplitudes and Anomalous Dimensions’. In: *Phys. Lett. B* 726 (2013), pp. 697–702. DOI: 10.1016/j.physletb.2013.09.020. arXiv: 1309.0819 [hep-ph]. №: CERN-PH-TH-2013-213.
- [177] B. Gavela, E. Jenkins, A. Manohar, and L. Merlo. ‘Analysis of General Power Counting Rules in Effective Field Theory’. In: *Eur. Phys. J. C* 76.9 (2016), p. 485. DOI: 10.1140/epjc/s10052-016-4332-1. arXiv: 1601.07551 [hep-ph]. №: CERN-TH-2016-015, FTUAM-16-2, and IFT-UAM-CSIC-16-006.
- [178] A. V. Manohar. ‘Introduction to Effective Field Theories’. *Les Houches summer school: EFT in Particle Physics and Cosmology*. Apr. 2018. arXiv: 1804.05863 [hep-ph].

- [179] G. Buchalla, A. J. Buras, and M. E. Lautenbacher. ‘Weak decays beyond leading logarithms’. In: *Rev. Mod. Phys.* 68 (1996), pp. 1125–1144. DOI: 10.1103/RevModPhys.68.1125. arXiv: hep-ph/9512380. №: SLAC-PUB-7009, SLAC-PUB-95-7009, MPI-PH-95-104, TUM-T31-100-95, and FERMILAB-PUB-95-305-T.
- [180] Y. Nambu. ‘Quasiparticles and Gauge Invariance in the Theory of Superconductivity’. In: *Phys. Rev.* 117 (1960). Ed. by J. Taylor, pp. 648–663. DOI: 10.1103/PhysRev.117.648.
- [181] J. Goldstone. ‘Field Theories with Superconductor Solutions’. In: *Nuovo Cim.* 19 (1961), pp. 154–164. DOI: 10.1007/BF02812722.
- [182] J. Goldstone, A. Salam, and S. Weinberg. ‘Broken Symmetries’. In: *Phys. Rev.* 127 (1962), pp. 965–970. DOI: 10.1103/PhysRev.127.965.
- [183] P. Herrera-Siklody, J. I. Latorre, P. Pascual, and J. Taron. ‘Chiral effective Lagrangian in the large  $N_c$  limit: The Nonet case’. In: *Nucl. Phys. B* 497 (1997), pp. 345–386. DOI: 10.1016/S0550-3213(97)00260-5. arXiv: hep-ph/9610549. №: UB-ECM-PF-96-16.
- [184] A. Pich. ‘Chiral perturbation theory’. In: *Rept. Prog. Phys.* 58 (1995), pp. 563–610. DOI: 10.1088/0034-4885/58/6/001. arXiv: hep-ph/9502366. №: FTUV-95-4 and IFIC-95-4.
- [185] S. Scherer. ‘Introduction to chiral perturbation theory’. In: *Adv. Nucl. Phys.* 27 (2003). Ed. by J. W. Negele and E. Vogt, p. 277. arXiv: hep-ph/0210398. №: MKPH-T-02-09.
- [186] A. Pich. ‘Introduction to chiral perturbation theory’. In: *Proceedings, 5th Mexican School of Particles and Fields* (Guanajuato, Mexico, 29th Nov.–11th Dec. 1992). Vol. 317. 1994, pp. 95–140. DOI: 10.1063/1.46859. arXiv: hep-ph/9308351 [hep-ph]. №: CERN-TH-6978-93.
- [187] G. Ecker. ‘Chiral perturbation theory’. *Hadron Physics*. June 1996, pp. 125–167. arXiv: hep-ph/9608226. №: UWTHPH-1996-34.
- [188] J. Bijnens and M. B. Wise. ‘Electromagnetic Contribution to  $\epsilon'/\epsilon$ ’. In: *Phys. Lett. B* 137 (1984), pp. 245–250. DOI: 10.1016/0370-2693(84)90238-7. №: CALT-68-1074.
- [189] A. J. Buras and J. M. Gerard. ‘Isospin Breaking Contributions to  $\epsilon'/\epsilon$ ’. In: *Phys. Lett. B* 192 (1987), pp. 156–162. DOI: 10.1016/0370-2693(87)91159-2. №: MPI-PAE/PTH-7/87.
- [190] G. Ecker, J. Gasser, A. Pich, and E. de Rafael. ‘The Role of Resonances in Chiral Perturbation Theory’. In: *Nucl. Phys. B* 321 (1989), pp. 311–342. DOI: 10.1016/0550-3213(89)90346-5. №: CERN-TH-5185/88, UWTHPH-1988-29, BUTP-88/18, and CPT-88/PE-2158.
- [191] R. Urech. ‘Virtual photons in chiral perturbation theory’. In: *Nucl. Phys. B* 433 (1995), pp. 234–254. DOI: 10.1016/0550-3213(95)90707-N. arXiv: hep-ph/9405341. №: BUTP-94-9.
- [192] G. Ecker, G. Isidori, G. Muller, H. Neufeld, and A. Pich. ‘Electromagnetism in non-leptonic weak interactions’. In: *Nucl. Phys. B* 591 (2000), pp. 419–434. DOI: 10.1016/S0550-3213(00)00568-X. arXiv: hep-ph/0006172. №: UWTHPH-2000-17, LNF-00-016-P, FTUV-00-0614, and IFIC-00-29.



- [193] M. Knecht, H. Neufeld, H. Rupertsberger, and P. Talavera. ‘Chiral perturbation theory with virtual photons and leptons’. In: *Eur. Phys. J. C* 12 (2000), pp. 469–478. DOI: 10.1007/s100529900265. arXiv: hep-ph/9909284. №: CPT-99-P-3884, UWTHPH-1999-51, and LU-TP-99-17.
- [194] A. J. Buras and J. M. Gerard. ‘ $\epsilon'/\epsilon$  in the Standard Model’. In: *Phys. Lett. B* 203 (1988), pp. 272–278. DOI: 10.1016/0370-2693(88)90551-5. №: MPI-PAE/PTH-84/87.
- [195] G. Buchalla, A. J. Buras, and M. K. Harlander. ‘The Anatomy of  $\epsilon'/\epsilon$  in the Standard Model’. In: *Nucl. Phys. B* 337 (1990), pp. 313–362. DOI: 10.1016/0550-3213(90)90275-I. №: MPI-PAE/PTH-63/89 and TUM-T31-3/89.
- [196] J. Aebischer, C. Bobeth, and A. J. Buras. ‘ $\epsilon'/\epsilon$  in the Standard Model at the Dawn of the 2020s’. In: *Eur. Phys. J. C* 80.8 (2020), p. 705. DOI: 10.1140/epjc/s10052-020-8267-1. arXiv: 2005.05978 [hep-ph]. №: AJB-20-1 and TUM-HEP-1261/20.
- [197] J. Bijnens. ‘Chiral perturbation theory beyond one loop’. In: *Prog. Part. Nucl. Phys.* 58 (2007), pp. 521–586. DOI: 10.1016/j.ppnp.2006.08.002. arXiv: hep-ph/0604043. №: LU-TP-06-16.
- [198] J. Wess and B. Zumino. ‘Consequences of anomalous Ward identities’. In: *Phys. Lett. B* 37 (1971), pp. 95–97. DOI: 10.1016/0370-2693(71)90582-X.
- [199] E. Witten. ‘Global Aspects of Current Algebra’. In: *Nucl. Phys. B* 223 (1983), pp. 422–432. DOI: 10.1016/0550-3213(83)90063-9. №: PRINT-83-0262 (PRINCETON).
- [200] H. Kawai and S. H. H. Tye. ‘Chiral Anomalies, Effective Lagrangian and Differential Geometry’. In: *Phys. Lett. B* 140 (1984), pp. 403–407. DOI: 10.1016/0370-2693(84)90780-9. №: CLNS-84/595.
- [201] K.-c. Chou, H.-y. Guo, K. Wu, and X.-c. Song. ‘On the Gauge Invariance and Anomaly Free Condition of Wess-Zumino-witten Effective Action’. In: *Phys. Lett. B* 134 (1984), pp. 67–69. DOI: 10.1016/0370-2693(84)90986-9. №: AS-ITP-83-027.
- [202] J. L. Manes. ‘Differential Geometric Construction of the Gauged Wess-Zumino Action’. In: *Nucl. Phys. B* 250 (1985), pp. 369–384. DOI: 10.1016/0550-3213(85)90487-0. №: LBL-17318.
- [203] O. Cata and V. Mateu. ‘Chiral perturbation theory with tensor sources’. In: *JHEP* 09 (2007), p. 078. DOI: 10.1088/1126-6708/2007/09/078. arXiv: 0705.2948 [hep-ph]. №: FTUV-07-05-21 and IFIC-07-23.
- [204] M. A. Shifman, A. I. Vainshtein, and V. I. Zakharov. ‘Remarks on Higgs Boson Interactions with Nucleons’. In: *Phys. Lett. B* 78 (1978), pp. 443–446. DOI: 10.1016/0370-2693(78)90481-1. №: ITEP-22-1978.
- [205] W. A. Bardeen, A. J. Buras, and J. M. Gerard. ‘A Consistent Analysis of the  $\Delta I = 1/2$  Rule for  $K$  Decays’. In: *Phys. Lett. B* 192 (1987), pp. 138–144. DOI: 10.1016/0370-2693(87)91156-7. №: FERMILAB-PUB-87-088-T and MPI-PAE-PTH-55-86.
- [206] A. J. Buras, J.-M. Gérard, and W. A. Bardeen. ‘Large  $N$  Approach to Kaon Decays and Mixing 28 Years Later:  $\Delta I = 1/2$  Rule,  $\hat{B}_K$  and  $\Delta M_K$ ’. In: *Eur. Phys. J. C* 74 (2014), p. 2871. DOI: 10.1140/epjc/s10052-014-2871-x. arXiv: 1401.1385 [hep-ph]. №: FLAVOUR(267104)-ERC-60, CP3-14-01, and FERMILAB-PUB-14-001-T.

- [207] M. A. Shifman, A. I. Vainshtein, and V. I. Zakharov. ‘Nonleptonic Decays of K Mesons and Hyperons’. In: *Sov. Phys. JETP* 45 (1977), p. 670. №: ITEP-64-1976 and ITEP-63-1976.
- [208] J. C. Collins. *Renormalization: An Introduction to Renormalization, The Renormalization Group, and the Operator Product Expansion*. Vol. 26. Cambridge Monographs on Mathematical Physics. Cambridge: Cambridge University Press, 1986. ISBN: 978-0-521-31177-9. DOI: 10.1017/CBO9780511622656.
- [209] G. Ecker. ‘Chiral perturbation theory’. In: *Prog. Part. Nucl. Phys.* 35 (1995), pp. 1–80. DOI: 10.1016/0146-6410(95)00041-G. arXiv: hep-ph/9501357. №: UWTHPH-1994-49.
- [210] M. B. Voloshin and V. I. Zakharov. ‘Measuring QCD Anomalies in Hadronic Transitions Between Onium States’. In: *Phys. Rev. Lett.* 45 (1980), p. 688. DOI: 10.1103/PhysRevLett.45.688. №: DESY-80-28.
- [211] V. A. Novikov and M. A. Shifman. ‘Comment on the  $\psi' \rightarrow J/\psi \pi \pi$  Decay’. In: *Z. Phys. C* 8 (1981), p. 43. DOI: 10.1007/BF01429829. №: ITEP-93-1980.
- [212] W. A. Bardeen, A. J. Buras, and J. M. Gerard. ‘The  $\Delta I = 1/2$  Rule in the Large  $N$  Limit’. In: *Phys. Lett. B* 180 (1986), pp. 133–140. DOI: 10.1016/0370-2693(86)90150-4. №: MPI-PAE/PTH 37/86.
- [213] W. A. Bardeen, A. J. Buras, and J. M. Gerard. ‘The  $K \rightarrow \pi \pi$  Decays in the Large  $n$  Limit: Quark Evolution’. In: *Nucl. Phys. B* 293 (1987), pp. 787–811. DOI: 10.1016/0550-3213(87)90091-5. №: MPI-PAE/PTH-45/86.
- [214] G. Amelino-Camelia et al. ‘Physics with the KLOE-2 experiment at the upgraded DAΦNE’. In: *Eur. Phys. J. C* 68 (2010), pp. 619–681. DOI: 10.1140/epjc/s10052-010-1351-1. arXiv: 1003.3868 [hep-ex]. №: CAFPE-141-10 and UG-FT-271-10.
- [215] T. Kitahara, T. Okui, G. Perez, Y. Soreq, and K. Tobioka. ‘New physics implications of recent search for  $K_L \rightarrow \pi^0 \nu \bar{\nu}$  at KOTO’. In: *Phys. Rev. Lett.* 124.7 (2020), p. 071801. DOI: 10.1103/PhysRevLett.124.071801. arXiv: 1909.11111 [hep-ph]. №: KEK-TH-2157 and CERN-TH-2019-151.
- [216] J. McDonald. ‘Thermally generated gauge singlet scalars as selfinteracting dark matter’. In: *Phys. Rev. Lett.* 88 (2002), p. 091304. DOI: 10.1103/PhysRevLett.88.091304. arXiv: hep-ph/0106249 [hep-ph].
- [217] M. Pospelov, A. Ritz, and M. B. Voloshin. ‘Secluded WIMP Dark Matter’. In: *Phys. Lett. B* 662 (2008), pp. 53–61. DOI: 10.1016/j.physletb.2008.02.052. arXiv: 0711.4866 [hep-ph].
- [218] L. J. Hall, K. Jedamzik, J. March-Russell, and S. M. West. ‘Freeze-In Production of FIMP Dark Matter’. In: *JHEP* 03 (2010), p. 080. DOI: 10.1007/JHEP03(2010)080. arXiv: 0911.1120 [hep-ph]. №: OUTP-09-18-P and UCB-PTH-09-32.
- [219] M. Battaglieri et al. ‘New Ideas in Dark Matter 2017: Community Report’. *U.S. Cosmic Visions*. July 2017. arXiv: 1707.04591 [hep-ph]. №: FERMILAB-CONF-17-282-AE-PPD-T.

- [220] N. Bernal, M. Heikinheimo, T. Tenkanen, K. Tuominen, and V. Vaskonen. ‘The Dawn of FIMP Dark Matter: A Review of Models and Constraints’. In: *Int. J. Mod. Phys. A* 32.27 (2017), p. 1730023. DOI: 10.1142/S0217751X1730023X. arXiv: 1706.07442 [hep-ph]. №: PI-UAN-2017-602FT, HIP-2017-08-TH, PI-UAN-2017-602FT, and HIP-2017-08-TH.
- [221] A. Goudelis, K. A. Mohan, and D. Sengupta. ‘Clockworking FIMPs’. In: *JHEP* 10 (2018), p. 014. DOI: 10.1007/JHEP10(2018)014. arXiv: 1807.06642 [hep-ph].
- [222] F. Bezrukov and D. Gorbunov. ‘Light inflaton after LHC8 and WMAP9 results’. In: *JHEP* 07 (2013), p. 140. DOI: 10.1007/JHEP07(2013)140. arXiv: 1303.4395 [hep-ph]. №: RBRC-1012.
- [223] G. Ballesteros, J. Redondo, A. Ringwald, and C. Tamarit. ‘Unifying inflation with the axion, dark matter, baryogenesis and the seesaw mechanism’. In: *Phys. Rev. Lett.* 118.7 (2017), p. 071802. DOI: 10.1103/PhysRevLett.118.071802. arXiv: 1608.05414 [hep-ph]. №: DESY-16-049 and IPPP-16-25.
- [224] P. W. Graham, D. E. Kaplan, and S. Rajendran. ‘Cosmological Relaxation of the Electroweak Scale’. In: *Phys. Rev. Lett.* 115.22 (2015), p. 221801. DOI: 10.1103/PhysRevLett.115.221801. arXiv: 1504.07551 [hep-ph].
- [225] B. Batell, G. F. Giudice, and M. McCullough. ‘Natural Heavy Supersymmetry’. In: *JHEP* 12 (2015), p. 162. DOI: 10.1007/JHEP12(2015)162. arXiv: 1509.00834 [hep-ph]. №: CERN-PH-TH-2015-215 and PITT-PACC-1512.
- [226] K. Choi and S. H. Im. ‘Realizing the relaxion from multiple axions and its UV completion with high scale supersymmetry’. In: *JHEP* 01 (2016), p. 149. DOI: 10.1007/JHEP01(2016)149. arXiv: 1511.00132 [hep-ph]. №: CTPU-15-16.
- [227] D. E. Kaplan and R. Rattazzi. ‘Large field excursions and approximate discrete symmetries from a clockwork axion’. In: *Phys. Rev. D* 93.8 (2016), p. 085007. DOI: 10.1103/PhysRevD.93.085007. arXiv: 1511.01827 [hep-ph].
- [228] T. Flacke, C. Frugiuele, E. Fuchs, R. S. Gupta, and G. Perez. ‘Phenomenology of relaxion-Higgs mixing’. In: *JHEP* 06 (2017), p. 050. DOI: 10.1007/JHEP06(2017)050. arXiv: 1610.02025 [hep-ph]. №: CTPU-16-25.
- [229] G. F. Giudice and M. McCullough. ‘A Clockwork Theory’. In: *JHEP* 02 (2017), p. 036. DOI: 10.1007/JHEP02(2017)036. arXiv: 1610.07962 [hep-ph]. №: CERN-TH-2016-223.
- [230] J. P. Derendinger, L. E. Ibanez, and H. P. Nilles. ‘On the Low-Energy Limit of Superstring Theories’. In: *Nucl. Phys. B* 267 (1986), pp. 365–414. DOI: 10.1016/0550-3213(86)90396-2. №: CERN-TH-4228-85.
- [231] G. Lazarides, C. Panagiotakopoulos, and Q. Shafi. ‘Phenomenology and Cosmology With Superstrings’. In: *Phys. Rev. Lett.* 56 (1986), p. 432. DOI: 10.1103/PhysRevLett.56.432. №: RU85/B/135.
- [232] S. B. Giddings and A. Strominger. ‘Axion Induced Topology Change in Quantum Gravity and String Theory’. In: *Nucl. Phys. B* 306 (1988), pp. 890–907. DOI: 10.1016/0550-3213(88)90446-4. №: HUTP-87-A067.

- [233] H. Georgi, D. B. Kaplan, and L. Randall. ‘Manifesting the Invisible Axion at Low-energies’. In: *Phys. Lett. B* 169 (1986), pp. 73–78. DOI: 10.1016/0370-2693(86)90688-X. №: HUTP-86/A004.
- [234] K. Choi, K. Kang, and J. E. Kim. ‘Effects of  $\eta'$  in Low-energy Axion Physics’. In: *Phys. Lett. B* 181 (1986), pp. 145–149. DOI: 10.1016/0370-2693(86)91273-6. №: BROWN-HET-593 and SNUHE 86/05.
- [235] A. Salvio, A. Strumia, and W. Xue. ‘Thermal axion production’. In: *JCAP* 1401 (2014), p. 011. DOI: 10.1088/1475-7516/2014/01/011. arXiv: 1310.6982 [hep-ph]. №: FTUAM-13-29 and IFT-UAM-CSIC-13-113.
- [236] M. Bauer, M. Neubert, and A. Thamm. ‘Collider Probes of Axion-Like Particles’. In: *JHEP* 12 (2017), p. 044. DOI: 10.1007/JHEP12(2017)044. arXiv: 1708.00443 [hep-ph]. №: MITP-17-047.
- [237] H. Primakoff. ‘Photoproduction of neutral mesons in nuclear electric fields and the mean life of the neutral meson’. In: *Phys. Rev.* 81 (1951), p. 899. DOI: 10.1103/PhysRev.81.899.
- [238] R. N. Lerner and J. McDonald. ‘Gauge singlet scalar as inflaton and thermal relic dark matter’. In: *Phys. Rev. D* 80 (2009), p. 123507. DOI: 10.1103/PhysRevD.80.123507. arXiv: 0909.0520 [hep-ph].
- [239] D. E. Morrissey, T. Plehn, and T. M. P. Tait. ‘Physics searches at the LHC’. In: *Phys. Rept.* 515 (2012), pp. 1–113. DOI: 10.1016/j.physrep.2012.02.007. arXiv: 0912.3259 [hep-ph]. №: ANL-HEP-PR-09-114, UCI-TR-2009-17, and NUHEP-TH-09-19.
- [240] R. Barbieri, L. J. Hall, and V. S. Rychkov. ‘Improved naturalness with a heavy Higgs: An Alternative road to LHC physics’. In: *Phys. Rev. D* 74 (2006), p. 015007. DOI: 10.1103/PhysRevD.74.015007. arXiv: hep-ph/0603188. №: UCB-PTH-06-04 and LBNL-59894.
- [241] G. C. Branco, P. M. Ferreira, L. Lavoura, M. N. Rebelo, M. Sher, and J. P. Silva. ‘Theory and phenomenology of two-Higgs-doublet models’. In: *Phys. Rept.* 516 (2012), pp. 1–102. DOI: 10.1016/j.physrep.2012.02.002. arXiv: 1106.0034 [hep-ph].
- [242] L. Lopez Honorez, E. Nezri, J. F. Oliver, and M. H. G. Tytgat. ‘The Inert Doublet Model: An Archetype for Dark Matter’. In: *JCAP* 02 (2007), p. 028. DOI: 10.1088/1475-7516/2007/02/028. arXiv: hep-ph/0612275. №: ULB-TH-06-27.
- [243] J. E. Kim. ‘Effects of decay of scalar partner of axion on cosmological bounds of axion supermultiplet properties’. In: *Phys. Rev. Lett.* 67 (1991), pp. 3465–3468. DOI: 10.1103/PhysRevLett.67.3465. №: SNUTP-91-27-REV and SNUTP-91-27.
- [244] J. Abdallah et al. ‘Simplified Models for Dark Matter Searches at the LHC’. In: *Phys. Dark Univ.* 9-10 (2015), pp. 8–23. DOI: 10.1016/j.dark.2015.08.001. arXiv: 1506.03116 [hep-ph]. №: FERMILAB-PUB-15-283-CD and CERN-PH-TH-2015-139.
- [245] J. McDonald. ‘Gauge singlet scalars as cold dark matter’. In: *Phys. Rev. D* 50 (1994), pp. 3637–3649. DOI: 10.1103/PhysRevD.50.3637. arXiv: hep-ph/0702143. №: IFM-13-93.

- [246] C. P. Burgess, M. Pospelov, and T. ter Veldhuis. ‘The Minimal model of nonbaryonic dark matter: A Singlet scalar’. In: *Nucl. Phys. B* 619 (2001), pp. 709–728. DOI: 10.1016/S0550-3213(01)00513-2. arXiv: hep-ph/0011335. №: TPI-MINN-00-46, UMN-TH-1922-00, MCGILL-00-31, and IASSNS-HEP-00-83.
- [247] G. Bélanger, K. Kannike, A. Pukhov, and M. Raidal. ‘Minimal semi-annihilating  $\mathbb{Z}_N$  scalar dark matter’. In: *JCAP* 06 (2014), p. 021. DOI: 10.1088/1475-7516/2014/06/021. arXiv: 1403.4960 [hep-ph]. №: LAPTH-017-14.
- [248] E. Berti et al. ‘Testing General Relativity with Present and Future Astrophysical Observations’. In: *Class. Quant. Grav.* 32 (2015), p. 243001. DOI: 10.1088/0264-9381/32/24/243001. arXiv: 1501.07274 [gr-qc].
- [249] X.-G. He, J. Tandean, and G. Valencia. ‘Light Higgs production in hyperon decay’. In: *Phys. Rev. D* 74 (2006), p. 115015. DOI: 10.1103/PhysRevD.74.115015. arXiv: hep-ph/0610274.
- [250] S. Dawson. ‘Light Higgs Production in a two Higgs Doublet Model’. In: *Nucl. Phys. B* 339 (1990), pp. 19–37. DOI: 10.1016/0550-3213(90)90531-H. №: PRINT-90-0061 (BNL) and 43777.
- [251] R. M. Barnett, G. Senjanovic, and D. Wyler. ‘Tracking Down Higgs Scalars With Enhanced Couplings’. In: *Phys. Rev. D* 30 (1984), p. 1529. DOI: 10.1103/PhysRevD.30.1529. №: NSF-ITP-84-45.
- [252] M. E. Lautenbacher. ‘Can One Exclude a Light Neutral Scalar in a Two Higgs Doublet Model’. In: *Nucl. Phys. B* 347 (1990), pp. 120–148. DOI: 10.1016/0550-3213(90)90554-Q. №: TUM-T31-6/90.
- [253] S. Andreas, O. Lebedev, S. Ramos-Sanchez, and A. Ringwald. ‘Constraints on a very light CP-odd Higgs of the NMSSM and other axion-like particles’. In: *JHEP* 08 (2010), p. 003. DOI: 10.1007/JHEP08(2010)003. arXiv: 1005.3978 [hep-ph]. №: DESY-10-069.
- [254] U. Ellwanger and C. Hugonie. ‘A 750 GeV Diphoton Signal from a Very Light Pseudo-scalar in the NMSSM’. In: *JHEP* 05 (2016), p. 114. DOI: 10.1007/JHEP05(2016)114. arXiv: 1602.03344 [hep-ph]. №: LPT-ORSAY-16-07 and LUPM:16-004.
- [255] R. S. Gupta, Z. Komargodski, G. Perez, and L. Ubaldi. ‘Is the Relaxion an Axion?’ In: *JHEP* 02 (2016), p. 166. DOI: 10.1007/JHEP02(2016)166. arXiv: 1509.00047 [hep-ph].
- [256] J. Alexander et al. ‘Dark Sectors 2016 Workshop: Community Report’. Aug. 2016. arXiv: 1608.08632 [hep-ph]. №: FERMILAB-CONF-16-421.
- [257] A. Brignole, F. Feruglio, and F. Zwirner. ‘Four-fermion interactions and sgoldstino masses in models with a superlight gravitino’. In: *Phys. Lett. B* 438 (1998), pp. 89–95. DOI: 10.1016/S0370-2693(98)00974-5. arXiv: hep-ph/9805282 [hep-ph]. №: CERN-TH-98-149 and DFPD-98-TH-20.
- [258] D. S. Gorbunov. ‘Light sgoldstino: Precision measurements versus collider searches’. In: *Nucl. Phys. B* 602 (2001), pp. 213–237. DOI: 10.1016/S0550-3213(01)00122-5. arXiv: hep-ph/0007325 [hep-ph].

- [259] D. S. Gorbunov and V. A. Rubakov. ‘Kaon physics with light sgoldstinos and parity conservation’. In: *Phys. Rev. D* 64 (2001), p. 054008. DOI: 10.1103/PhysRevD.64.054008. arXiv: hep-ph/0012033 [hep-ph].
- [260] D. S. Gorbunov and V. A. Rubakov. ‘On sgoldstino interpretation of HyperCP events’. In: *Phys. Rev. D* 73 (2006), p. 035002. DOI: 10.1103/PhysRevD.73.035002. arXiv: hep-ph/0509147 [hep-ph].
- [261] I. Antoniadis and D. M. Ghilencea. ‘Low-scale SUSY breaking and the (s)goldstino physics’. In: *Nucl. Phys. B* 870 (2013), pp. 278–291. DOI: 10.1016/j.nuclphysb.2013.01.015. arXiv: 1210.8336 [hep-th]. №: CERN-PH-TH-2012-231.
- [262] E. Dudas, C. Petersson, and P. Tziveloglou. ‘Low Scale Supersymmetry Breaking and its LHC Signatures’. In: *Nucl. Phys. B* 870 (2013), pp. 353–383. DOI: 10.1016/j.nuclphysb.2013.02.001. arXiv: 1211.5609 [hep-ph]. №: CERN-PH-TH-2012-317.
- [263] K. Astapov and D. Gorbunov. ‘Sgoldstino rate estimates in the SHiP’. In: *19th International Seminar on High Energy Physics (Quarks)* (Pushkin, Russia, 29th May–4th June 2016). Vol. 125. 2016, p. 02003. DOI: 10.1051/epjconf/201612502003.
- [264] K. O. Astapov and D. V. Kirpichnikov. ‘Prospects of models with light sgoldstino in electron beam dump experiment at CERN SPS’ (2016). arXiv: 1612.02813 [hep-ph]. №: INR-TH-2016-048.
- [265] L. E. Ibanez. ‘The Scalar Neutrinos as the Lightest Supersymmetric Particles and Cosmology’. In: *Phys. Lett. B* 137 (1984), pp. 160–164. DOI: 10.1016/0370-2693(84)90221-1. №: FTUAM-83-28-REV and FTUAM-83-28.
- [266] J. S. Hagelin, G. L. Kane, and S. Raby. ‘Perhaps Scalar Neutrinos Are the Lightest Supersymmetric Partners’. In: *Nucl. Phys. B* 241 (1984), pp. 638–652. DOI: 10.1016/0550-3213(84)90064-6. №: LA-UR-83-3711.
- [267] C. Arina and N. Fornengo. ‘Sneutrino cold dark matter, a new analysis: Relic abundance and detection rates’. In: *JHEP* 11 (2007), p. 029. DOI: 10.1088/1126-6708/2007/11/029. arXiv: 0709.4477 [hep-ph]. №: DFTT-17-2007.
- [268] S. Bobrovskiy, W. Buchmüller, J. Hajer, and J. Schmidt. ‘Broken R-Parity in the Sky and at the LHC’. In: *JHEP* 10 (2010), p. 061. DOI: 10.1007/JHEP10(2010)061. arXiv: 1007.5007 [hep-ph]. №: DESY-10-068.
- [269] G. Alonso-Álvarez, G. Elor, A. E. Nelson, and H. Xiao. ‘A Supersymmetric Theory of Baryogenesis and Sterile Sneutrino Dark Matter from *B* Mesons’. In: *JHEP* 03 (2020), p. 046. DOI: 10.1007/JHEP03(2020)046. arXiv: 1907.10612 [hep-ph].
- [270] U. Ellwanger, C. Hugonie, and A. M. Teixeira. ‘The Next-to-Minimal Supersymmetric Standard Model’. In: *Phys. Rept.* 496 (2010), pp. 1–77. DOI: 10.1016/j.physrep.2010.07.001. arXiv: 0910.1785 [hep-ph]. №: LPT-ORSAY-09-76, CFTP-09-032, and LPTA-09-066.
- [271] S. P. Martin. ‘TASI 2011 lectures notes: two-component fermion notation and supersymmetry’. *Theoretical Advanced Study Institute in Elementary Particle Physics: The Dark Secrets of the Terascale*. 2013, pp. 199–258. DOI: 10.1142/9789814390163\_0005. arXiv: 1205.4076 [hep-ph].

- [272] M. Drewes. ‘The Phenomenology of Right Handed Neutrinos’. In: *Int. J. Mod. Phys. E* 22 (2013), p. 1330019. DOI: 10.1142/So218301313300191. arXiv: 1303.6912 [hep-ph]. №: TUM-HEP-881-13.
- [273] J. Hisano, T. Moroi, K. Tobe, M. Yamaguchi, and T. Yanagida. ‘Lepton flavor violation in the supersymmetric standard model with seesaw induced neutrino masses’. In: *Phys. Lett. B* 357 (1995), pp. 579–587. DOI: 10.1016/0370-2693(95)00954-J. arXiv: hep-ph/9501407. №: TU-476.
- [274] S. F. King. ‘Neutrino mass models’. In: *Rept. Prog. Phys.* 67 (2004), pp. 107–158. DOI: 10.1088/0034-4885/67/2/R01. arXiv: hep-ph/0310204. №: SHEP-03-15.
- [275] C. Arina, F. Bazzocchi, N. Fornengo, J. C. Romao, and J. W. F. Valle. ‘Minimal supergravity sneutrino dark matter and inverse seesaw neutrino masses’. In: *Phys. Rev. Lett.* 101 (2008), p. 161802. DOI: 10.1103/PhysRevLett.101.161802. arXiv: 0806.3225 [hep-ph]. №: DFTT-11-2008 and IFIC-08-31.
- [276] S. M. Boucenna, S. Morisi, and J. W. F. Valle. ‘The low-scale approach to neutrino masses’. In: *Adv. High Energy Phys.* 2014 (2014), p. 831598. DOI: 10.1155/2014/831598. arXiv: 1404.3751 [hep-ph].
- [277] M. Lindner, M. Platscher, and F. S. Queiroz. ‘A Call for New Physics: The Muon Anomalous Magnetic Moment and Lepton Flavor Violation’. In: *Phys. Rept.* 731 (2018), pp. 1–82. DOI: 10.1016/j.physrep.2017.12.001. arXiv: 1610.06587 [hep-ph].
- [278] K. Rajagopal, M. S. Turner, and F. Wilczek. ‘Cosmological implications of axinos’. In: *Nucl. Phys. B* 358 (1991), pp. 447–470. DOI: 10.1016/0550-3213(91)90355-2. №: IASSNS-HEP-90-79, PUPT-1227, and FERMILAB-PUB-90-243-A.
- [279] L. Covi, H.-B. Kim, J. E. Kim, and L. Roszkowski. ‘Axinos as dark matter’. In: *JHEP* 05 (2001), p. 033. DOI: 10.1088/1126-6708/2001/05/033. arXiv: hep-ph/0101009. №: CERN-TH-2000-378, DESY-00-193, and SNUTP-00-034.
- [280] G. A. Gómez-Vargas, D. E. López-Fogliani, C. Muñoz, and A. D. Perez. ‘MeV–GeV  $\gamma$ -ray telescopes probing axino LSP/gravitino NLSP as dark matter in the  $\mu\nu$ SSM’. In: *JCAP* 01 (2020), p. 058. DOI: 10.1088/1475-7516/2020/01/058. arXiv: 1911.03191 [hep-ph].
- [281] X. G. He, G. C. Joshi, H. Lew, and R. R. Volkas. ‘New  $Z'$  Phenomenology’. In: *Phys. Rev. D* 43 (1991), pp. 22–24. DOI: 10.1103/PhysRevD.43.R22. №: UM-P-90/42 and OZ-P-90/16.
- [282] X.-G. He, G. C. Joshi, H. Lew, and R. R. Volkas. ‘Simplest  $Z'$  model’. In: *Phys. Rev. D* 44 (1991), pp. 2118–2132. DOI: 10.1103/PhysRevD.44.2118. №: CERN-TH-6084-91, UM-P-91-32, and OZ-91-07.
- [283] S. Baek, N. G. Deshpande, X. G. He, and P. Ko. ‘Muon anomalous  $g - 2$  and gauged  $L_\mu - L_\tau$  models’. In: *Phys. Rev. D* 64 (2001), p. 055006. DOI: 10.1103/PhysRevD.64.055006. arXiv: hep-ph/0104141. №: KAIST-TH-2001-08.

- [284] E. Ma, D. P. Roy, and S. Roy. ‘Gauged  $L_\mu - L_\tau$  with large muon anomalous magnetic moment and the bimaximal mixing of neutrinos’. In: *Phys. Lett. B* 525 (2002), pp. 101–106. DOI: 10.1016/S0370-2693(01)01428-9. arXiv: hep-ph/0110146. №: UCRHEP-T320 and TIFR-TH-01-39.
- [285] E. Salvioni, A. Strumia, G. Villadoro, and F. Zwirner. ‘Non-universal minimal  $Z'$  models: present bounds and early LHC reach’. In: *JHEP* 03 (2010), p. 010. DOI: 10.1007/JHEP03(2010)010. arXiv: 0911.1450 [hep-ph]. №: CERN-PH-TH-2009-212 and DFPD-09-TH-22.
- [286] J. Heeck and W. Rodejohann. ‘Gauged  $L_\mu - L_\tau$  Symmetry at the Electroweak Scale’. In: *Phys. Rev. D* 84 (2011), p. 075007. DOI: 10.1103/PhysRevD.84.075007. arXiv: 1107.5238 [hep-ph].
- [287] M. Fabbrichesi, E. Gabrielli, and G. Lanfranchi. ‘The Dark Photon’ (May 2020). DOI: 10.1007/978-3-030-62519-1. arXiv: 2005.01515 [hep-ph].
- [288] L. B. Okun. ‘Limits of Electrodynamics: Paraphotons?’ In: *Sov. Phys. JETP* 56 (1982), p. 502. №: ITEP-48-1982.
- [289] B. Holdom. ‘Searching for  $\epsilon$  Charges and a New  $U(1)$ ’. In: *Phys. Lett. B* 178 (1986), pp. 65–70. DOI: 10.1016/0370-2693(86)90470-3. №: UTPT-86-03.
- [290] E. Stückelberg. ‘Interaction energy in electrodynamics and in the field theory of nuclear forces’. In: *Helv. Phys. Acta* 11 (1938), pp. 225–244. DOI: 10.5169/seals-110852.
- [291] B. Kors and P. Nath. ‘Aspects of the Stückelberg extension’. In: *JHEP* 07 (2005), p. 069. DOI: 10.1088/1126-6708/2005/07/069. arXiv: hep-ph/0503208. №: DESY-05-044, MIT-CTP-3612, and NUB-TH-3254.
- [292] *LHCb*. ‘Test of lepton universality in beauty-quark decays’ (Mar. 2021). arXiv: 2103.11769 [hep-ex]. №: LHCb-PAPER-2021-004 and CERN-EP-2021-042.
- [293] A. Alloul, N. D. Christensen, C. Degrande, C. Duhr, and B. Fuks. ‘FeynRules 2.0: A complete toolbox for tree-level phenomenology’. In: *Comput. Phys. Commun.* 185 (2014), pp. 2250–2300. DOI: 10.1016/j.cpc.2014.04.012. arXiv: 1310.1921 [hep-ph]. №: CERN-PH-TH-2013-239, MCNET-13-14, IPPP-13-71, DCPT-13-142, and PITT-PACC-1308.
- [294] J. Alwall et al. ‘The automated computation of tree-level and next-to-leading order differential cross sections, and their matching to parton shower simulations’. In: *JHEP* 07 (2014), p. 079. DOI: 10.1007/JHEP07(2014)079. arXiv: 1405.0301 [hep-ph]. №: CERN-PH-TH-2014-064, CP3-14-18, LPN14-066, MCNET-14-09, and ZU-TH-14-14.
- [295] F. Ambrogio et al. ‘MadDM v.3.0: a Comprehensive Tool for Dark Matter Studies’. In: *Phys. Dark Univ.* 24 (2019), p. 100249. DOI: 10.1016/j.dark.2018.11.009. arXiv: 1804.00044 [hep-ph]. №: CP3-18-26 and MCNET-18-07.
- [296] C. Arina, J. Heisig, F. Maltoni, L. Mantani, D. Massaro, O. Mattelaer, and G. Mohlabeng. ‘Studying dark matter with MadDM 3.1: a short user guide’. *Tools for High Energy Physics and Cosmology*. Dec. 2020. arXiv: 2012.09016 [hep-ph]. №: CP3-20-62 and MCNET-20-26.



- [297] L. Buonocore, C. Frugiuele, F. Maltoni, O. Mattelaer, and F. Tramontano. ‘Event generation for beam dump experiments’. In: *JHEP* 05 (2019), p. 028. DOI: 10.1007/JHEP05(2019)028. arXiv: 1812.06771 [hep-ph]. №: CP3-18-70.
- [298] M. Fierz. ‘Zur Fermischen Theorie des  $\beta$ -Zerfalls’. In: *Zeitschrift für Physik* 104 (1937), pp. 553–565. DOI: 10.1007/BF01330070.
- [299] C. Nishi. ‘Simple derivation of general Fierz-like identities’. In: *Am. J. Phys.* 73 (2005), pp. 1160–1163. DOI: 10.1119/1.2074087. arXiv: hep-ph/0412245.
- [300] P. Klose. ‘Aspects of Bottom-up Hidden Sector Models’. PhD thesis. Louvain U., 2020.
- [301] C. Arzt. ‘Reduced effective Lagrangians’. In: *Phys. Lett. B* 342 (1995), pp. 189–195. DOI: 10.1016/0370-2693(94)01419-D. arXiv: hep-ph/9304230. №: UM-TH-92-28.
- [302] S. Scherer and M. R. Schindler. ‘A Chiral perturbation theory primer’ (May 2005). arXiv: hep-ph/0505265. №: MKPH-T-05-08.
- [303] J. R. Ellis, K. Enqvist, and D. V. Nanopoulos. ‘A Very Light Gravitino in a No Scale Model’. In: *Phys. Lett. B* 147 (1984), pp. 99–102. DOI: 10.1016/0370-2693(84)90600-2. №: CERN-TH-3890.
- [304] J. R. Ellis, K. Enqvist, and D. V. Nanopoulos. ‘Non-compact supergravity solves problems’. In: *Phys. Lett. B* 151 (1985), pp. 357–362. DOI: 10.1016/0370-2693(85)91654-5. №: CERN-TH-4036/84.
- [305] W. Buchmüller, M. Endo, and T. Shindou. ‘Superparticle Mass Window from Leptogenesis and Decaying Gravitino Dark Matter’. In: *JHEP* 11 (2008), p. 079. DOI: 10.1088/1126-6708/2008/11/079. arXiv: 0809.4667 [hep-ph]. №: DESY-08-127.
- [306] S. Bobrovskiy, W. Buchmüller, J. Hajer, and J. Schmidt. ‘Quasi-stable neutralinos at the LHC’. In: *JHEP* 09 (2011), p. 119. DOI: 10.1007/JHEP09(2011)119. arXiv: 1107.0926 [hep-ph]. №: DESY-11-077.
- [307] S. Bobrovskiy, J. Hajer, and S. Rydbeck. ‘Long-lived higgsinos as probes of gravitino dark matter at the LHC’. In: *JHEP* 02 (2013), p. 133. DOI: 10.1007/JHEP02(2013)133. arXiv: 1211.5584 [hep-ph]. №: DESY-12-175.
- [308] N. Arkani-Hamed, S. Dimopoulos, and G. R. Dvali. ‘The Hierarchy problem and new dimensions at a millimeter’. In: *Phys. Lett. B* 429 (1998), pp. 263–272. DOI: 10.1016/S0370-2693(98)00466-3. arXiv: hep-ph/9803315 [hep-ph]. №: SLAC-PUB-7769 and SU-ITP-98-13.
- [309] N. Arkani-Hamed, S. Dimopoulos, and G. R. Dvali. ‘Phenomenology, astrophysics and cosmology of theories with submillimeter dimensions and TeV scale quantum gravity’. In: *Phys. Rev. D* 59 (1999), p. 086004. DOI: 10.1103/PhysRevD.59.086004. arXiv: hep-ph/9807344 [hep-ph]. №: SLAC-PUB-7864, SU-ITP-98-142, and IC-98-44.
- [310] T. Han, J. D. Lykken, and R.-J. Zhang. ‘On Kaluza-Klein states from large extra dimensions’. In: *Phys. Rev. D* 59 (1999), p. 105006. DOI: 10.1103/PhysRevD.59.105006. arXiv: hep-ph/9811350 [hep-ph]. №: MADPH-98-1092 and FERMILAB-PUB-98-364.
- [311] L. Randall and R. Sundrum. ‘A Large mass hierarchy from a small extra dimension’. In: *Phys. Rev. Lett.* 83 (1999), pp. 3370–3373. DOI: 10.1103/PhysRevLett.83.3370. arXiv: hep-ph/9905221 [hep-ph]. №: MIT-CTP-2860, PUPT-1860, and BUHEP-99-9.

- [312] J. Murata and S. Tanaka. ‘A review of short-range gravity experiments in the LHC era’. In: *Class. Quant. Grav.* 32.3 (2015), p. 033001. DOI: 10.1088/0264-9381/32/3/033001. arXiv: 1408.3588 [hep-ex].
- [313] CMS. ‘Search for high-mass resonances in dilepton final states in proton-proton collisions at  $\sqrt{s} = 13$  TeV’. In: *JHEP* 06 (2018), p. 120. DOI: 10.1007/JHEP06(2018)120. arXiv: 1803.06292 [hep-ex]. №: CMS-EXO-16-047 and CERN-EP-2018-027.
- [314] ATLAS. ‘Search for Higgs boson pair production in the  $b\bar{b}WW^*$  decay mode at  $\sqrt{s} = 13$  TeV with the ATLAS detector’. In: *JHEP* 04 (2019), p. 092. DOI: 10.1007/JHEP04(2019)092. arXiv: 1811.04671 [hep-ex]. №: CERN-EP-2018-237.
- [315] G. Das, C. Degrande, V. Hirschi, F. Maltoni, and H.-S. Shao. ‘NLO predictions for the production of a spin-two particle at the LHC’. In: *Phys. Lett. B* 770 (2017), pp. 507–513. DOI: 10.1016/j.physletb.2017.05.007. arXiv: 1605.09359 [hep-ph]. №: CERN-TH-2016-122, CP3-16-25, IPPP-16-42, MCNET-16-17, and SLAC-PUB-16528.
- [316] S. Kraml, U. Laa, K. Mawatari, and K. Yamashita. ‘Simplified dark matter models with a spin-2 mediator at the LHC’. In: *Eur. Phys. J. C* 77.5 (2017), p. 326. DOI: 10.1140/epjc/s10052-017-4871-0. arXiv: 1701.07008 [hep-ph]. №: OCHA-PP-345.
- [317] H. M. Lee, M. Park, and V. Sanz. ‘Gravity-mediated (or Composite) Dark Matter’. In: *Eur. Phys. J. C* 74 (2014), p. 2715. DOI: 10.1140/epjc/s10052-014-2715-8. arXiv: 1306.4107 [hep-ph]. №: CERN-PH-TH-2013-143 and KIAS-P13032.
- [318] S. F. Hassan and R. A. Rosen. ‘Bimetric Gravity from Ghost-free Massive Gravity’. In: *JHEP* 02 (2012), p. 126. DOI: 10.1007/JHEP02(2012)126. arXiv: 1109.3515 [hep-th].
- [319] A. Schmidt-May and M. von Strauss. ‘Recent developments in bimetric theory’. In: *J. Phys. A* 49.18 (2016), p. 183001. DOI: 10.1088/1751-8113/49/18/183001. arXiv: 1512.00021 [hep-th].
- [320] L. Marzola, M. Raidal, and F. R. Urban. ‘Oscillating Spin-2 Dark Matter’. In: *Phys. Rev. D* 97.2 (2018), p. 024010. DOI: 10.1103/PhysRevD.97.024010. arXiv: 1708.04253 [hep-ph].
- [321] X. Chu and C. Garcia-Cely. ‘Self-interacting Spin-2 Dark Matter’. In: *Phys. Rev. D* 96.10 (2017), p. 103519. DOI: 10.1103/PhysRevD.96.103519. arXiv: 1708.06764 [hep-ph].
- [322] N. González Alborno, A. Schmidt-May, and M. von Strauss. ‘Dark matter scenarios with multiple spin-2 fields’. In: *JCAP* 01 (2018), p. 014. DOI: 10.1088/1475-7516/2018/01/014. arXiv: 1709.05128 [hep-th].
- [323] J. E. Juknevich, D. Melnikov, and M. J. Strassler. ‘A Pure-Glue Hidden Valley I. States and Decays’. In: *JHEP* 07 (2009), p. 055. DOI: 10.1088/1126-6708/2009/07/055. arXiv: 0903.0883 [hep-ph]. №: RUNHETC-2008-18, TAUP-2890-08, and ITEP-TH-45-08.
- [324] J. E. Juknevich. ‘Pure-glue hidden valleys through the Higgs portal’. In: *JHEP* 08 (2010), p. 121. DOI: 10.1007/JHEP08(2010)121. arXiv: 0911.5616 [hep-ph]. №: RUNHETC-2009-25.

- [325] J. Bijnens and J. Prades. ‘Electromagnetic corrections for pions and kaons: Masses and polarizabilities’. In: *Nucl. Phys. B* 490 (1997), pp. 239–271. DOI: 10.1016/S0550-3213(97)00107-7. arXiv: hep-ph/9610360. №: FTUV-96-69, IFIC-96-78, and NORDITA-96-70-N-P.
- [326] J. Bijnens and I. Jemos. ‘A new global fit of the  $L_i^r$  at next-to-next-to-leading order in Chiral Perturbation Theory’. In: *Nucl. Phys. B* 854 (2012), pp. 631–665. DOI: 10.1016/j.nuclphysb.2011.09.013. arXiv: 1103.5945 [hep-ph]. №: LU-TP-11-14.
- [327] L. Gan, B. Kubis, E. Passemar, and S. Tulin. ‘Precision tests of fundamental physics with  $\eta$  and  $\eta'$  mesons’ (July 2020). arXiv: 2007.00664 [hep-ph]. №: JLAB-THY-20-3219.